

Glycosylation Site Occupancy Heterogeneity in Chinese Hamster Ovary Cell Culture

by

Gregg B. Nyberg

B.S. Chemical Engineering and Petroleum Refining
Colorado School of Mines, 1992

SUBMITTED TO THE DEPARTMENT OF CHEMICAL ENGINEERING
IN PARTIAL FULFILLMENT OF THE REQUIREMENTS FOR THE DEGREE OF

DOCTOR OF PHILOSOPHY
at the
MASSACHUSETTS INSTITUTE OF TECHNOLOGY

June, 1998

©1998 Gregg B. Nyberg. All rights reserved.

The author hereby grants to MIT permission to reproduce and to distribute publicly
paper and electronic copies of this thesis document in whole or in part.

Signature of Author: _____
Department of Chemical Engineering
April 6, 1998

Certified by: _____
Daniel I. C. Wang
Institute Professor
Thesis Supervisor

Accepted by: _____
Robert E. Cohen
St. Laurent Professor of Chemical Engineering
Chairman, Committee for Graduate Students

MASSACHUSETTS INSTITUTE
OF TECHNOLOGY

JUL 09 1998

LIBRARIES

ARCHIVES

Glycosylation Site Occupancy Heterogeneity in Chinese Hamster Ovary Cell Culture

by
Gregg B. Nyberg

Submitted to the Department of Chemical Engineering on April 6, 1998
in Partial Fulfillment of the Requirements for the Degree of
Doctor of Philosophy in Chemical Engineering

Abstract

Asparagine linked (N-linked) glycosylation is an important secondary modification of recombinant proteins. Oligosaccharide chains can significantly influence glycoprotein properties such as specific activity, solubility, thermal stability and clearance rate in the blood stream. Despite the importance of glycosylation, it is an inherently variable process, and not all potential glycosylation sites are occupied with oligosaccharide. Furthermore, glycosylation characteristics can change with time in batch and fed-batch cultures. To investigate the interaction between cellular metabolism and glycosylation site occupancy heterogeneity, we studied how central carbon metabolism influences the availability of the nucleotide sugars which serve as sugar donors in glycosylation.

We were able to characterize metabolism and glycosylation through a series of continuous culture (chemostat) experiments with Chinese hamster ovary cells producing recombinant human gamma interferon. Nutrient uptake and byproduct formation data obtained in chemostats were used to solve material balances for a biochemical network model of central carbon metabolism. From data obtained in glucose limited chemostats, we found that glycosylation correlated with TCA cycle activity, but not glycolysis. This finding led to the hypothesis that nucleotide sugar formation is influenced more by nucleoside triphosphate availability than hexose availability. Nucleotide and nucleotide sugar measurements from these and subsequent experiments confirmed that the primary determinants of nucleotide sugar concentrations during exponential growth are nucleoside triphosphate levels and, in the case of amino sugars such as N-acetylglucosamine, amino sugar formation.

Understanding how to manipulate nucleotide sugar concentrations allowed us to investigate how glycosylation site occupancy is influenced by nucleotide sugars in batch and fed-batch experiments. The data indicate that nucleotide sugars primarily influence glycosylation during periods of glucose or glutamine starvation. Under starvation conditions nucleotide sugar levels drop and glycosylation site occupancy decreases. Nucleotide sugar concentrations can be increased by feeding nucleotide precursors, but this leads to only modest improvement in glycosylation site occupancy. Thus nucleotide

sugar deprivation has a much larger influence than nucleotide sugar expansion. Furthermore, a gradual decline in glycosylation observed during fed-batch exponential growth is caused by a step downstream of nucleotide sugar formation, as nucleotide sugars actually increase during this time.

Thesis Supervisor: Dr. Daniel I. C. Wang

Title: Institute Professor

Acknowledgments

At times Ph.D. graduate work can seem very isolating. Freedom to pursue ideas can not only be exhilarating, but it can also be overwhelming. Looking back on my time at MIT, I really appreciate the support and guidance from those around me, who helped keep my research on track and my sanity intact. Too often we take people for granted, and do not thank them for their contributions to our lives. I am grateful for this opportunity, so that I may attempt to express my gratitude to those who made this thesis possible.

My thesis advisor, Professor Daniel Wang, deserves much of the credit for keeping my research on track. Dr. Wang kept me focused on the important issues, and I learned to appreciate his direct, honest advice. As my career develops, I can only hope to emulate his intellectual integrity. Professor Gregory Stephanopoulos also deserves special mention, especially for his support and guidance on the “Chemostat Project.” Dr. Stephanopoulos always made me feel welcome in his research group and provided me with useful advice. I am also indebted to the other members of my thesis committee, Professors Harvey Lodish, Douglas Lauffenburger and Linda Griffith, for their comments and suggestions.

One of the primary reasons I came to MIT was for the interaction with other graduate students. My fellow graduate students at BPEC not only contributed to my research, but they made my graduate career enjoyable. They taught me cell culture, biology and laboratory techniques. They also taught me Sheepshead, darts and poker. The political and philosophical discussions at lunch gave me things to think about other than research. Thank you to David Chang, Keqin Chen, John Chung, Peter Frier, Joydeep Goswami, Bryan Harmon, Brian Kelley, Dan Lasko, Kai-Chee Loh, Gautam Nayar, Jörg Neermann, Chandra Papudesu, Martin Reinecke, Cliff Rutt, Eric Scharin, Marc Shelikoff, Troy Simpson, Rahul Singhvi, Araba Lamousé-Smith, Dave Stevenson, Inn Yuk, Liangzhi Xie, Jifeng Zhang and Craig Zupke. I would like to express special thanks to Brian Follstad and Robert Balcarcel (members of the Chemostat Team who worked with me on the experiments described in Chapter 5), Sherry Gu (my fellow IFN- γ glycosylation researcher—I forgive her for arriving after me and graduating before me) and Steve Meier (classmate turned friend and colleague—I look forward to future poker games).

The opportunity to supervise research assistants was an added bonus in my education. Much of the research described in this thesis was done with their help. Thank you to Jessica Oleson, Allen Wong, Shawn Brennan, Shital Shah, Brad Gray and Alethia de León; I hope you learned as much from me as I learned from you.

I would also like to express my appreciation to the BPEC staff including Audrey Childs, Sonia Foster, Lynne Lenker, Joya Gargano, James Leung, John Galvin, Darlene Ray, Lorraine Cable and Sara Puffer. With my duties as “Technical Coordinator” I worked especially closely with the administrative staff, and I am grateful for their help.

Having saved the best for last, I would like to thank my family for their love and support. My mother inspired me by getting her own Ph.D., and she did her best to help guide me through the graduate school process. Her caring and love will always be appreciated. Although I will never be able to duplicate my father's tireless work ethic and sense of duty, his example helped get me through the difficult times. I just wish he would take a break occasionally. My sister has always offered me her love and support, and I hope I can do the same for her as she works to finish her schooling and start a new career. Finally, I would like to thank my best friend and wonderful wife, Gina. Gina's encouragement and unconditional love gave me the strength to persevere, and I know she will continue to be there as we start a new chapter in our life together.

Table of Contents

ABSTRACT	3
ACKNOWLEDGMENTS	5
TABLE OF CONTENTS.....	7
LIST OF FIGURES.....	11
LIST OF TABLES	17
1. INTRODUCTION.....	19
1.1 Background.....	19
1.2 Motivation.....	20
1.3 Thesis Objectives	21
1.4 Thesis Organization.....	21
2. LITERATURE REVIEW	23
2.1 Overview of N-linked Glycosylation.....	23
2.2 Implications of N-linked Glycosylation.....	29
2.2.1 Implications for Protein Folding.....	29
2.2.2 Implications for Targeting and Secretion.....	32
2.2.3 Implications for Glycoprotein Biochemical Properties.....	33
2.2.4 Implications for Circulatory Half-Life	35
2.3 Factors Influencing N-linked Glycosylation Site Occupancy Heterogeneity	38
2.3.1 Lipid-Linked Oligosaccharide Precursor Formation.....	38
2.3.2 Oligosaccharyltransferase Activity	50
2.3.3 Substrate Amino Acid Sequence.....	51
2.3.4 Competition with Protein Folding.....	55
2.3.5 Cell Culture Environment.....	56
2.4 Model System: Recombinant Human Gamma Interferon Production in Chinese Hamster Ovary Cells.....	59

3. MATERIALS AND METHODS.....	65
3.1 Cell Culture.....	65
3.1.1 Cell Line.....	65
3.1.2 Chaperone Protein (BiP) Levels in T-flask Cultures.....	65
3.1.3 T-flask Cultures Treated with Tunicamycin.....	66
3.1.4 Adaption to Suspension Culture.....	66
3.1.5 Low-Serum Culture	67
3.1.6 Serum-Free Culture.....	67
3.1.7 Culture Maintenance	69
3.2 Pulse-Chase Radiolabeling Experiment.....	69
3.3 Pulse Radiolabeling Experiments.....	70
3.3.1 Monitoring Secreted Protein Glycosylation with Radiolabeling.....	70
3.3.2 Batch Culture.....	70
3.3.3 Fed Batch Culture.....	71
3.3.4 Sugar Precursor Fed Cultures	71
3.3.5 Nucleotide Precursor Fed Cultures.....	72
3.3.6 Glucosamine and Uridine Fed Cultures.....	73
3.3.7 Uridine Fed Batch Culture.....	74
3.4 Continuous Culture Experiments	75
3.4.1 Continuous Culture Media.....	75
3.4.2 Bioreactor Operation.....	75
3.4.3 Oxygen Uptake Rate	76
3.4.4 Carbon Dioxide Evolution Rate.....	77
3.5 Analytical Methods.....	78
3.5.1 Cell Number, Viability and Dry Cell Weight.....	78
3.5.2 Sugar and Lactate Assays.....	79
3.5.3 Amino Acid Analysis.....	79
3.5.4 Measuring Amino Acids in Peptides.....	80
3.5.5 Nucleotide and Nucleotide Sugar Analysis.....	82
3.5.6 Determination of IFN- γ Concentration.....	87
3.5.7 Radiolabeled IFN- γ Glycosylation Site Occupancy Analysis.....	87
3.5.8 Accumulated IFN- γ Glycosylation Site Occupancy Analysis.....	88
3.5.9 Quantitative Western Blot for BiP	90
3.5.10 Total Protein Assay	92
3.6 Material Balancing for Intracellular Flux Analysis.....	93
3.6.1 Biochemical Network	93
3.6.2 Calculation of Fluxes	97
3.6.3 Redundancy and Consistency	98

4. IFN-γ GLYCOSYLATION SITE OCCUPANCY IN BATCH AND FED-BATCH CULTURES.	101
4.1 Glycosylation Site Occupancy Monitoring with Radiolabeling.....	102
4.2 Batch Culture Glycosylation Site Occupancy	108
4.3 Fed-Batch Culture Glycosylation Site Occupancy	113
4.3.1 Transient Starvation Impacts Glycosylation	114
4.3.2 Glycosylation During Non-Starved Fed-Batch Intervals	120
5. CENTRAL CARBON METABOLISM AND GLYCOSYLATION: CONTINUOUS CULTURE EXPERIMENTS.....	125
5.1 Glycosylation Site Occupancy in Continuous Culture.....	126
5.1.1 Glycosylation at Steady State.....	126
5.1.2 Glycosylation Site Occupancy and Nucleotide Sugars	128
5.2 Metabolic Flux Analysis	130
5.2.1 Redundancy Analysis: Predictions of Oxygen Uptake and Carbon Dioxide Evolution	136
5.2.2 Redundancy Analysis using a Statistical Consistency Index	138
5.2.3 Estimated Metabolic Fluxes	140
5.3 Nucleotide Sugars, Glycosylation and Metabolism	141
5.3.1 Reaction Yields Correlated with Glycosylation Site Occupancy.....	141
5.3.2 Nucleoside Triphosphates and Nucleotide Sugars in Chemostat Cultures	144
5.3.3 Nucleoside Triphosphates and Nucleotide Sugars in Batch and Fed-Batch Cultures.....	145
5.4 Discussion	148
5.5 Conclusions	154
6. THE INFLUENCE OF NUCLEOTIDE SUGARS ON IFN-γ GLYCOSYLATION SITE OCCUPANCY	157
6.1 Sugar Precursor Feeding.....	158
6.1.1 Alternative Carbon Sources.....	158
6.1.2 The Influence of Glucosamine On Nucleotide Sugars and Glycosylation Site Occupancy.....	161
6.1.3 Discussion	165
6.2 Nucleotide Precursor Feeding.....	167
6.2.1 Altered Nucleotide Levels and Glycosylation Site Occupancy with Exposure to Nucleotide Precursors	167
6.2.2 Uridine Feeding in Fed-Batch Culture.....	170
6.2.3 Discussion	181
6.3 Conclusions	186

7. QUALITY CONTROL OF SECRETED GLYCOPROTEINS VIA MOLECULAR CHAPERONES	189
7.1 Background.....	190
7.2 Model Development.....	192
7.2.1 Model Structure.....	192
7.2.2 Parameter Estimation.....	196
7.3 Model Results	200
7.4 Discussion	204
7.5 The Feasibility of Improving IFN- γ Quality Through BiP Overexpression in γ -CHO Cells	206
7.6 Conclusions	206
8. CONCLUSIONS AND RECOMMENDATIONS.....	209
8.1 Conclusions	209
8.2 Recommendations.....	212
REFERENCES.....	215

List of Figures



Figure 2-1.	Schematic of the N-linked glycosylation pathway in the endoplasmic reticulum: formation of the oligosaccharide precursor, transfer to protein and initial sugar trimming.....	24
Figure 2-2.	Schematic of the oligosaccharide processing pathway in the endoplasmic reticulum and compartments of the Golgi apparatus (derived from Kornfeld and Kornfeld, 1985).....	26
Figure 2-3.	Structures representing the major classes of N-linked oligosaccharides. Abbreviations are: GlcNAc, N-acetylglucosamine; Man, mannose; Gal, galactose; Fuc, fucose; NeuNAc, sialic acid.....	28
Figure 2-4.	Biosynthesis of common nucleotide sugars.....	39
Figure 2-5.	The chemical structure of dolichol (n=17 to 21 for mammalian cells).....	43
Figure 2-6.	The proposed biochemical pathway for dolichol synthesis	44
Figure 2-7.	A reaction mechanism proposed by Imperiali et al. (1992b) for the oligosaccharyltransferase reaction (Figure reproduced from Silberstein and Gilmore, 1996).....	54
Figure 2-8.	The amino acid sequence of mature human interferon- γ (after signal peptide cleavage). Glycosylation sites are indicated by 	62
Figure 2-9.	Schematic drawings of <i>E. Coli</i> derived recombinant human interferon- γ dimers (from Ealick <i>et al.</i> , 1991). (A) Ribbon drawing approximately parallel to the dimer twofold axis. (B) The α helices are represented as cylinders, while nonhelical regions are tubes. (C) α helices are represented by circles, with the N-terminal end darkened. Glycosylation sites are indicated by 	63
Figure 3-1.	Example chromatogram for a 150 μ l injection of CHO cell PCA extract analyzed with pH=6.0 buffers. A. Entire chromatogram. B. Detail of nucleotide sugar region.....	84
Figure 3-2.	Example chromatogram for a 150 μ l injection of CHO cell PCA extract analyzed with pH = 5.0 buffers. A. Entire chromatogram. B. Detail of UTP and GTP separation.....	86

Figure 3-3. Schematic diagram of a simplified biochemical reaction network describing central carbon metabolism.	94
Figure 4-1. Glycoform distribution of radiolabeled IFN- γ secreted during the chase period following a pulse of ^{35}S labeled methionine.....	103
Figure 4-2. Glycoform distribution of radiolabeled IFN- γ secreted following a step pulse of ^{35}S labeled methionine into medium containing 0.1 mM of non-labeled methionine.	106
Figure 4-3. Overview of the pulse radiolabeling technique for monitoring differential product glycosylation site occupancy.....	107
Figure 4-4. Viable and total γ -CHO cell numbers during batch suspension culture in low-serum medium.	108
Figure 4-5. Glucose consumption and lactate production during low-serum batch culture of γ -CHO cells.	109
Figure 4-6. Differentially produced IFN- γ glycosylation site occupancy monitored with pulse radiolabeling in low-serum batch culture of γ -CHO cells.....	110
Figure 4-7. Specific glucose consumption rate in low-serum batch culture of γ -CHO cells.....	111
Figure 4-8. Normalized intracellular concentration of the molecular chaperone BiP during low-serum batch culture of γ -CHO cells.....	113
Figure 4-9. Viable γ -CHO cell densities in batch and fed-batch serum-free, suspension cultures.	115
Figure 4-10. Glucose concentration and lactate production during batch and fed-batch serum-free cultures of γ -CHO cells.....	116
Figure 4-11. Glutamine concentration and ammonia accumulation during fed-batch serum-free culture of γ -CHO cells.	117
Figure 4-12. Differentially produced IFN- γ glycosylation site occupancy monitored with pulse radiolabeling in batch serum-free culture of γ -CHO cells.....	118
Figure 4-13. Cell growth in serum-free fed-batch cultures of γ -CHO cells transfected with the Bcl-2 anti-death gene and control transfected γ -CHO cells.	121

Figure 4-14. Differentially produced IFN-g glycosylation site occupancy monitored with pulse radiolabeling in fed-batch culture of γ -CHO cells transfected with the Bcl-2 anti-death gene and control transfected γ -CHO cells. Glycosylation was monitored between feeding times with four hour pulses of radioactive methionine.	123
Figure 5-1. The relationship between glycosylation site occupancy and intracellular UDP-GNAc concentration in glucose and glutamine limited chemostat cultures.	130
Figure 5-2. Schematic diagram of a simplified biochemical reaction network describing central carbon metabolism.	131
Figure 5-3. Peptide bound amino acids in the feed and reactor effluent for glucose limited steady state 4.	133
Figure 5-4. Measured specific carbon dioxide evolution rate in glucose limited chemostats (○) compared to calculated based upon free amino acid data only (◆) and calculated based upon total (peptide + free) amino acids (⊕).	136
Figure 5-5. Measured specific oxygen uptake rate in glucose limited chemostats (○) compared to calculated based upon free amino acid data only (◆) and calculated based upon total (peptide + free) amino acids (⊕).	138
Figure 5-6. Reaction yields correlated to glycosylation site occupancy heterogeneity in glucose limited chemostat cultures. Site occupancy correlated with the yield of the pyruvate to acetyl CoA reaction (◆) and the reactions of the TCA cycle such as oxaloacetate to α -ketoglutarate (■) and α -ketoglutarate to succinyl CoA (⊕).	143
Figure 5-7. The relationship between intracellular UDP-GNAc concentration and UTP in glucose and glutamine limited chemostat cultures.	145
Figure 5-8. The correlation between intracellular UDP-GNAc and UTP during exponential growth in batch, fed-batch and chemostat cultures. Symbols indicate results from various independent experiments.	146
Figure 5-9. Reduced UDP-GNAc formation under glutamine limitation: the relationship between UDP-GNAc and UTP during glutamine limitation (◆) compared to exponential growth in batch, fed-batch and chemostat cultures (⊕).	147
Figure 5-10. Synthesis of UDP-GlcNAc under glucose and glutamine limitation. During glucose starvation, nucleoside triphosphates including UTP are depleted, which limits nucleotide sugar formation. In contrast, glutamine starvation limits UDP-GlcNAc synthesis by preventing amino sugar formation.	149

Figure 6-1.	Biosynthesis of common nucleotide sugars from various carbon sources (Schachter, 1978).....	159
Figure 6-2.	Glycosylation site occupancy of IFN- γ produced in the presence of various sugars.....	160
Figure 6-3.	The influence of glucosamine on IFN- γ glycosylation site occupancy.....	162
Figure 6-4.	The relationship between IFN- γ glycosylation site occupancy and intracellular UDP-GNac with glucosamine and uridine feeding.	164
Figure 6-5.	Differentially produced IFN- γ glycosylation site occupancy monitored with pulse radiolabeling in fed-batch culture of γ -CHO cells with and without uridine supplementation.....	172
Figure 6-6.	Percentage of IFN- γ two-site glycosylated (monitored with pulse radiolabeling) during fed-batch culture of γ -CHO cells with and without uridine supplementation.....	173
Figure 6-7.	Viable γ -CHO cell densities during fed-batch culture with and without uridine supplementation.....	174
Figure 6-8.	Gamma interferon productivity during fed-batch culture of γ -CHO cells with and without uridine supplementation.	175
Figure 6-9.	Changes in intracellular UDP-GNac concentration during fed-batch culture of γ -CHO cells with and without uridine supplementation.....	176
Figure 6-10.	Changes in intracellular UDP-Glc+GDP-Man concentration during fed-batch culture of γ -CHO cells with and without uridine supplementation.....	177
Figure 6-11.	Glucose concentration during fed-batch culture of γ -CHO cells with and without uridine supplementation.	179
Figure 6-12.	Glutamine concentration during fed-batch culture of γ -CHO cells with and without uridine supplementation.	180
Figure 6-13.	Conceptual schematic of the initial N-linked glycosylation steps. The nucleotide sugar pool is considered as a liquid in a tank, with the height corresponding to the nucleotide sugar concentration.....	182
Figure 6-14.	The relationship between glycosylation site occupancy and intracellular UDP-GNac concentration during fed-batch exponential growth of γ -CHO cells with and without uridine supplementation. Data is grouped by sample time.	184

Figure 6-15. The relationship between glycosylation site occupancy and intracellular UDP-GNAc concentration during fed-batch exponential growth of γ -CHO cells with and without uridine supplementation. Data is grouped by supplemental uridine concentration..... 185

Figure 7-1. Schematic of a single species model for BiP mediated protein folding, secretion and degradation (B = BiP; P = unfolded polypeptide; BP = BiP/unfolded polypeptide complex; F = folded polypeptide; A = unfolded polypeptide aggregates; D = degradation products)..... 193

Figure 7-2. Model simulation of total BiP concentration versus oligosaccharyltransferase (OST) efficiency in a wild-type cell maintaining a constant level of uncomplexed BiP..... 201

Figure 7-3. Experimental data for the induction of BiP synthesis in γ -CHO cells in the presence of the glycosylation inhibitor tunicamycin (10 μ g/ml)..... 201

Figure 7-4. Model simulation of BiP overexpression: secreted product glycosylation vs. oligosaccharyltransferase (OST) efficiency with varying total BiP concentrations..... 202

Figure 7-5. Model simulation of BiP overexpression: amount of glycosylated product secreted vs. oligosaccharyltransferase (OST) efficiency with varying total BiP concentrations. As the total concentration of BiP increases, more of the desired product is degraded along with the underglycosylated species..... 203

Figure 8-1. Interactions between metabolism, nucleotide sugar formation and glycosylation site occupancy. 211

List of Tables

Table 3-1.	Listing of reactions included in the simplified biochemical reaction network describing central carbon metabolism.	95
Table 3-2.	Biomass synthesis requirements for central carbon metabolism intermediates. Requirements (in mmol/gram dry cell weight) were calculated as described in Zupke and Stephanopoulos (1995). Positive values indicate the intermediate is consumed in biomass synthesis. Amino acid requirements for protein synthesis were accounted for separately.....	96
Table 4-1.	Differentially produced IFN- γ glycosylation site occupancy monitored with pulse radiolabeling in fed-batch serum-free culture of γ -CHO cells: the impact of periodic feeding.	119
Table 5-1.	Glucose and glutamine limited steady states achieved in continuous culture.	126
Table 5-2.	Glycosylation site occupancy for four glucose limited and one glutamine limited steady state cultures.....	127
Table 5-3.	Cell mass-specific nucleotide concentrations (μ mole/g viable dry cell weight) measured in perchloric acid extracts.	129
Table 5-4.	Rates of peptide amino acid consumption in steady state chemostat cultures (mmol/g DCW/d).	134
Table 5-5.	Measured metabolite production rates (r) for steady state chemostat cultures (mmol/g DCW/d). Amino acid production rates include peptide derived amino acids and are the net catabolic rates after accounting for biomass synthesis.....	135
Table 5-6.	Consistency indices, h , for steady state data analyzed with a metabolic network including two redundant measurements. Glucose limited chemostat data were analyzed based upon either free amino acid measurements only or on total (free + peptide) amino acid measurements.....	139
Table 5-7.	Estimated central carbon metabolism reaction yields (mmole/g viable dry cell weight) for chemostat steady state cultures.	142
Table 6-1.	The effects of uridine (5 mM) and glucosamine (2 mM) on intracellular nucleotide levels (μ mol/g viable dry cell weight).....	163
Table 6-2.	The effects of various nucleotide precursors on intracellular nucleotide levels (μ mol/g viable dry cell weight).	168

Table 6-3. The effects of various nucleotide precursors on secreted IFN- γ glycosylation site occupancy. 170

Table 6-4. Site-specific oligosaccharide microheterogeneity of IFN- γ secreted during fed-batch culture of γ -CHO cells with and without uridine supplementation. 181

1. Introduction

1.1 Background

Biological systems have been used by man for thousands of years. Even before microorganisms were discovered, fermentations were used to produce intoxicating drinks and to age food. With Pasteur's discovery in the mid 1800's that alcoholic fermentations and certain diseases were caused by living organisms, the science of microbiology was born. Initial industrial uses of microorganisms were to produce small molecules such as ethanol, acetone and citric acid. As the field of microbiology advanced, the products became more complicated. World War II brought the development of biological fermentations to produce antibiotics such as penicillin and streptomycin. Advances in biochemistry had revealed that chemical reactions were catalyzed by proteins, and naturally occurring enzymes were soon being produced as another major product from microorganisms. Unfortunately many proteins of pharmaceutical or industrial interest were not produced in sufficient quantities in their natural hosts, and this limited the number of proteins which could be produced.

With the development of molecular biology in the 1960's and 1970's, it became possible to produce large quantities of proteins that were difficult or impossible to isolate from natural sources. Recombinant DNA technology made it possible to produce proteins in virtually any cell line once the gene had been isolated. In 1982 human insulin became the first recombinant pharmaceutical product approved for use in the United States. Rather than being isolated from pig pancreas, insulin was then produced in a recombinant *Escherichia coli* cell line. Today recombinant proteins produced in yeast, bacteria and animal cells are sold for billions of dollars annually.

1.2 Motivation

Recombinant proteins are typically produced in animal cell culture when the protein is not adequately processed by faster growing and more easily manipulated organisms such as bacteria and yeast. Animal cells are able to correctly fold and covalently modify proteins, and this post-translational processing can significantly impact protein properties. The most extensive covalent modification performed by eukaryotic cells is glycosylation, which is the attachment of sugars to the polypeptide chain. Glycosylation is especially important for therapeutic proteins, because the oligosaccharides can significantly impact biological activity and circulatory half-life within the body. Thus the quality of recombinant product can depend upon the extent of glycosylation.

Despite its importance, glycosylation is an inherently variable process. Potential glycosylation sites are not always occupied with oligosaccharide (site occupancy heterogeneity) and the composition of attached oligosaccharides can vary (microheterogeneity). Furthermore glycosylation characteristics can vary with time during batch culture and with changes in the culture environment. Consistently producing high quality biopharmaceuticals requires an understanding of the factors which influence glycosylation heterogeneity. This thesis research analyzed a specific type of glycosylation heterogeneity: N-linked glycosylation site occupancy heterogeneity. N-linked glycosylation occurs at an asparagine residue, and it constitutes the majority of secreted protein glycosylation. The initial steps of N-linked glycosylation involve the formation of an oligosaccharide precursor which is bound to the membrane of the endoplasmic reticulum. The precursor oligosaccharide is subsequently transferred to a nascent polypeptide, typically as the polypeptide is translocated into the lumen of the endoplasmic reticulum. The transfer of oligosaccharide precursor does not always proceed to completion; a given protein may be produced as a heterogeneous population with potential N-linked glycosylation sites variably occupied.

1.3 Thesis Objectives

The goals of this thesis were to monitor N-linked glycosylation site occupancy heterogeneity during batch and fed-batch cultures, to determine how site occupancy is influenced by cell culture conditions and to develop strategies for improving site occupancy. This thesis focused in particular on the role of central carbon metabolism in providing the sugar precursors for glycosylation. Recombinant human gamma interferon (IFN- γ) produced in Chinese hamster ovary (CHO) cell culture served as the model system for this study. IFN- γ was a good model protein for this study, because it has two potential glycosylation sites which are variably occupied.

1.4 Thesis Organization

This thesis is organized into eight chapters. The first chapter introduced the research topic and outlined the specific objectives of the thesis. A more detailed review of relevant background information is included in Chapter 2. Chapter 3 provides a complete description of the experimental methods described in the thesis, including cell culturing protocols, glycosylation monitoring techniques, analytical procedures and metabolic flux analysis methodologies. Chapter 4 describes results of radiolabeling experiments which studied how glycosylation site occupancy varied in batch and fed-batch cultures. The continuous culture experiments described in Chapter 5 analyzed the relationship between central carbon metabolism and glycosylation in more detail than was possible in batch experiments. Based upon the results of Chapter 5, Chapter 6 explores the feasibility of improving glycosylation site occupancy by increasing nucleotide sugar concentrations. Chapter 6 also examines whether sugar precursors are responsible for glycosylation changes in fed-batch culture, such as the changes described in Chapter 4. Chapter 7 suggests an alternative method for influencing site occupancy. A mathematical modeling analysis is presented for how the intracellular chaperone BiP might be used to selectively retain underglycosylated proteins as a quality control mechanism. Finally, Chapter 8 summarizes important conclusions and presents suggestions for future work.

2. Literature Review

Most proteins secreted by mammalian cells, including many with pharmaceutical applications, have sugars covalently attached to their polypeptide backbones (i.e. they are glycoproteins). The sugars are important because they can significantly impact the properties of secreted proteins, such as biological activity and circulatory half-life within the body. The process of sugar attachment, referred to as glycosylation, typically leads to heterogeneous products. Potential glycosylation sites are not always occupied with oligosaccharide (site occupancy heterogeneity) and the composition of attached oligosaccharides can vary (microheterogeneity). This thesis focused on a specific type of glycosylation heterogeneity: N-linked glycosylation site occupancy heterogeneity. N-linked glycosylation occurs at an asparagine residue, and it constitutes the majority of secreted protein glycosylation. This chapter provides background information on N-linked glycosylation which will be useful for subsequent chapters in this thesis.

2.1 Overview of N-linked Glycosylation

The pathway of N-linked glycosylation has been well established (see reviews in Hirschberg and Snider, 1987; Kornfeld and Kornfeld, 1985). N-glycosylation occurs as a series of enzyme catalyzed reactions in the endoplasmic reticulum and Golgi apparatus of eukaryotic cells. The initial steps involve the formation of a precursor oligosaccharide which is bound to the membrane of the endoplasmic reticulum via a pyrophosphate linkage to the lipid dolichol (Dol). The precursor is formed through step-wise addition of activated sugar monomers. Figure 2-1 illustrates that the first seven sugars (two N-acetylglucosamine and five mannose) are added directly from nucleotide sugars while the precursor faces the cytosol (Abeijon and Hirschberg, 1990; Abeijon and Hirschberg, 1992; Kean, 1991b; Orlean, 1992). This precursor is subsequently flipped to face the lumen of

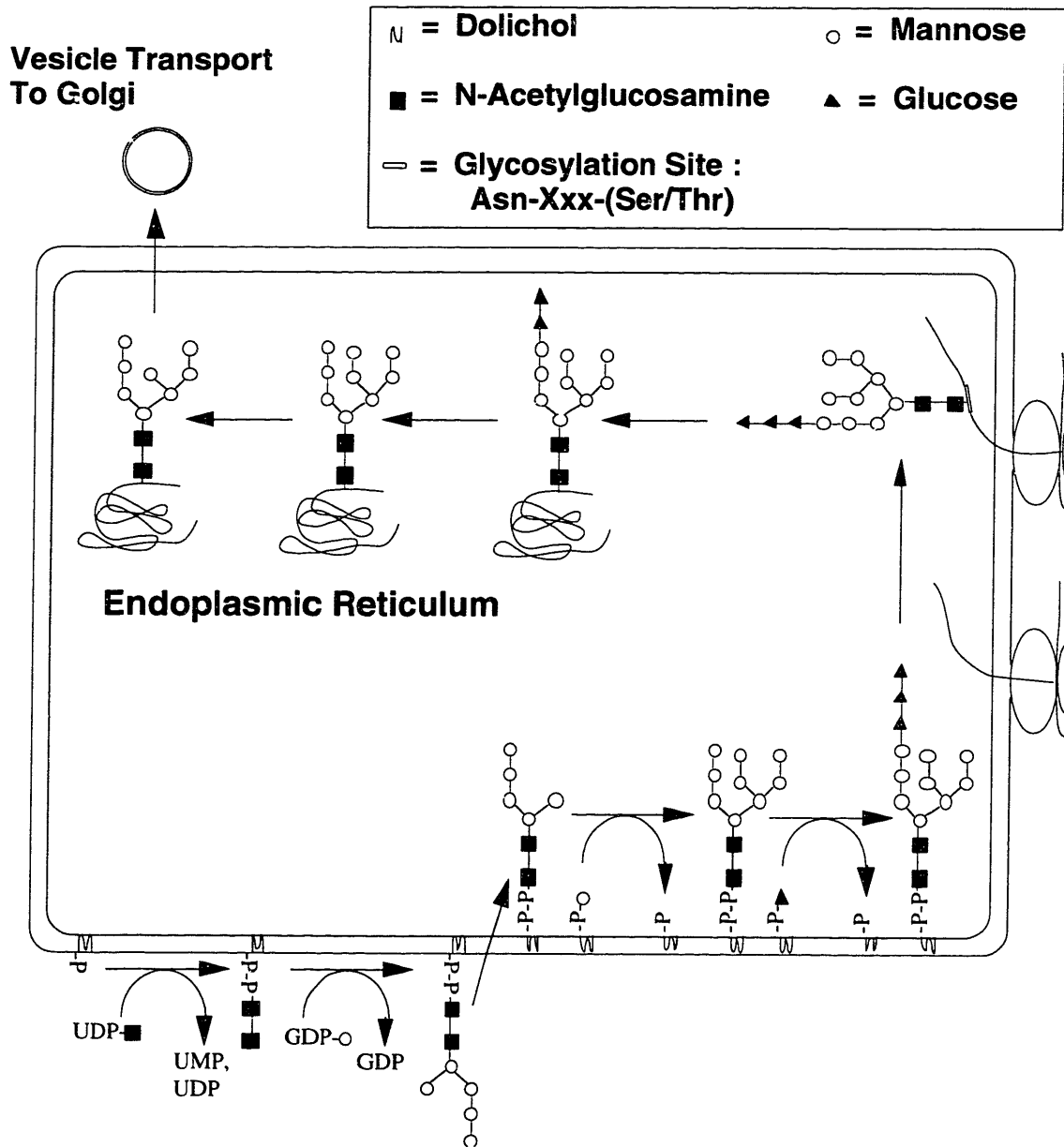


Figure 2-1. Schematic of the N-linked glycosylation pathway in the endoplasmic reticulum: formation of the oligosaccharide precursor, transfer to protein and initial sugar trimming.

the ER where the next seven sugars (four mannose and three glucose) are added from dolichol linked sugars (dolichol-P-mannose and dolichol-P-glucose). The dolichol linked sugars are formed from dolichol-P and nucleotide sugars. Dolichol-P-mannose is synthesized on the cytosolic side of the membrane and subsequently translocated to the lumen. Protease sensitivity assays with intact microsomes suggest that dolichol-P-glucose is synthesized in a similar fashion (Abeijon and Hirschberg, 1992). Thus nucleotide sugar transport into the endoplasmic reticulum may not be necessary for synthesis of the $\text{Glc}_3\text{Man}_9\text{GlcNAc}_2\text{-P-P-Dol}$ precursor. Although sugar transporters for the nucleotide sugars UDP-glucose (UDP-Glc) and UDP-N-acetylglucosamine (UDP-GlcNAc) have been identified, these transporters may be necessary for other glycosylation reactions such as O-linked glycosylation, phosphatidylinositol (GPI)-anchored glycosylation and for transient reglucosylation of N-linked oligosaccharides after they have been added to protein and trimmed (Abeijon and Hirschberg, 1992). The mechanisms of Dol-sugar and $\text{Man}_5\text{GlcNAc}_2\text{-P-P-Dol}$ translocation across the ER membrane are not known. Dolichol has been shown to induce destabilization of phospholipid bilayers, and this property may play a role in a protein-mediated translocation process (Abeijon and Hirschberg, 1992).

Once the $\text{Glc}_3\text{Man}_9\text{GlcNAc}_2\text{-P-P-Dol}$ precursor has been formed, it is transferred onto a nascent polypeptide chain, where it forms an amide bond to an asparagine residue that is part of the tripeptide recognition sequence Asn-Xxx-Ser/Thr (Xxx is any amino acid except proline). Oligosaccharyltransferase catalyzes this transfer, typically cotranslationally as the polypeptide is translocated into the lumen of the endoplasmic reticulum (Rothman and Lodish, 1977), although post-translational glycosylation can also occur (Sareneva et al., 1994). Following some initial sugar trimming reactions in the ER, the protein is transported via vesicles to the Golgi apparatus. Figure 2-2 illustrates that the protein is transferred through the compartments of the Golgi (again via vesicles), where the oligosaccharide undergoes various enzyme catalyzed sugar transfer and trimming reactions. These modifications create the high mannose, complex and hybrid

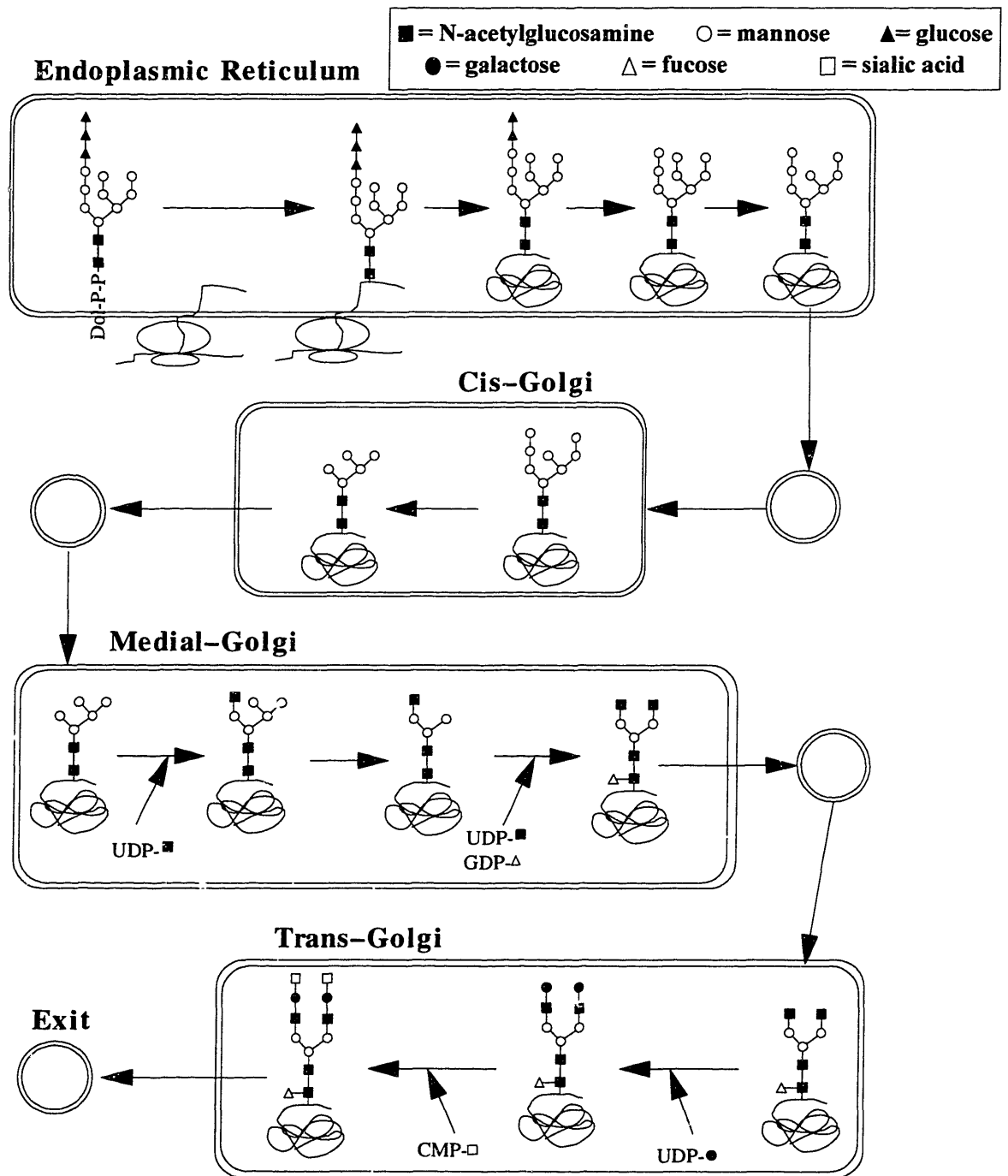


Figure 2-2. Schematic of the oligosaccharide processing pathway in the endoplasmic reticulum and compartments of the Golgi apparatus (derived from Kornfeld and Kornfeld, 1985).

type oligosaccharides depicted in Figure 2-3. All N-linked oligosaccharides contain a core of $\text{Man}_3\text{GlcNAc}_2\text{-Asn}$, and it is the composition of the outer branches which determine whether the oligosaccharide is classified as high mannose, complex or hybrid. High mannose oligosaccharides have only mannose residues on the outer branches, while complex structures have N-acetylglucosamine and galactose residues. Hybrids have at least one complex branch and at least one high mannose branch. Up to four branches can be attached to the core oligosaccharide. Additional heterogeneity can arise from terminal sialic acid groups which may be added to the galactose of complex branches. The core oligosaccharide may also be modified through the addition of fucose or a bisecting GlcNAc as shown in Figure 2-3.

The compartmentalized, enzyme catalyzed reactions comprising the N-glycosylation pathway result in heterogeneous glycoproteins. The first potential source of heterogeneity is the transfer of the $\text{Glc}_3\text{Man}_9\text{GlcNAc}_2$ oligosaccharide precursor to the nascent polypeptide. This reaction does not always proceed to completion, and asparagines that are potential glycosylation sites may not have oligosaccharides attached. This type of heterogeneity is referred to as site occupancy heterogeneity or macroheterogeneity. A second type of heterogeneity, called microheterogeneity, arises from the myriad sugar trimming and addition reactions which may occur once the oligosaccharides are attached to protein. The sequence or extent of reactions may vary as proteins move through the compartments of the Golgi, causing the attached oligosaccharides to vary in composition from molecule to molecule. Because of macro- and microheterogeneity, glycoproteins are usually expressed as sets of glycoforms which share a common amino acid sequence but have different glycosylation characteristics. Glycoforms can have varying functional properties, and so it is desirable to produce therapeutic glycoproteins as reproducible sets of glycoforms. This thesis focuses in particular on site occupancy heterogeneity.

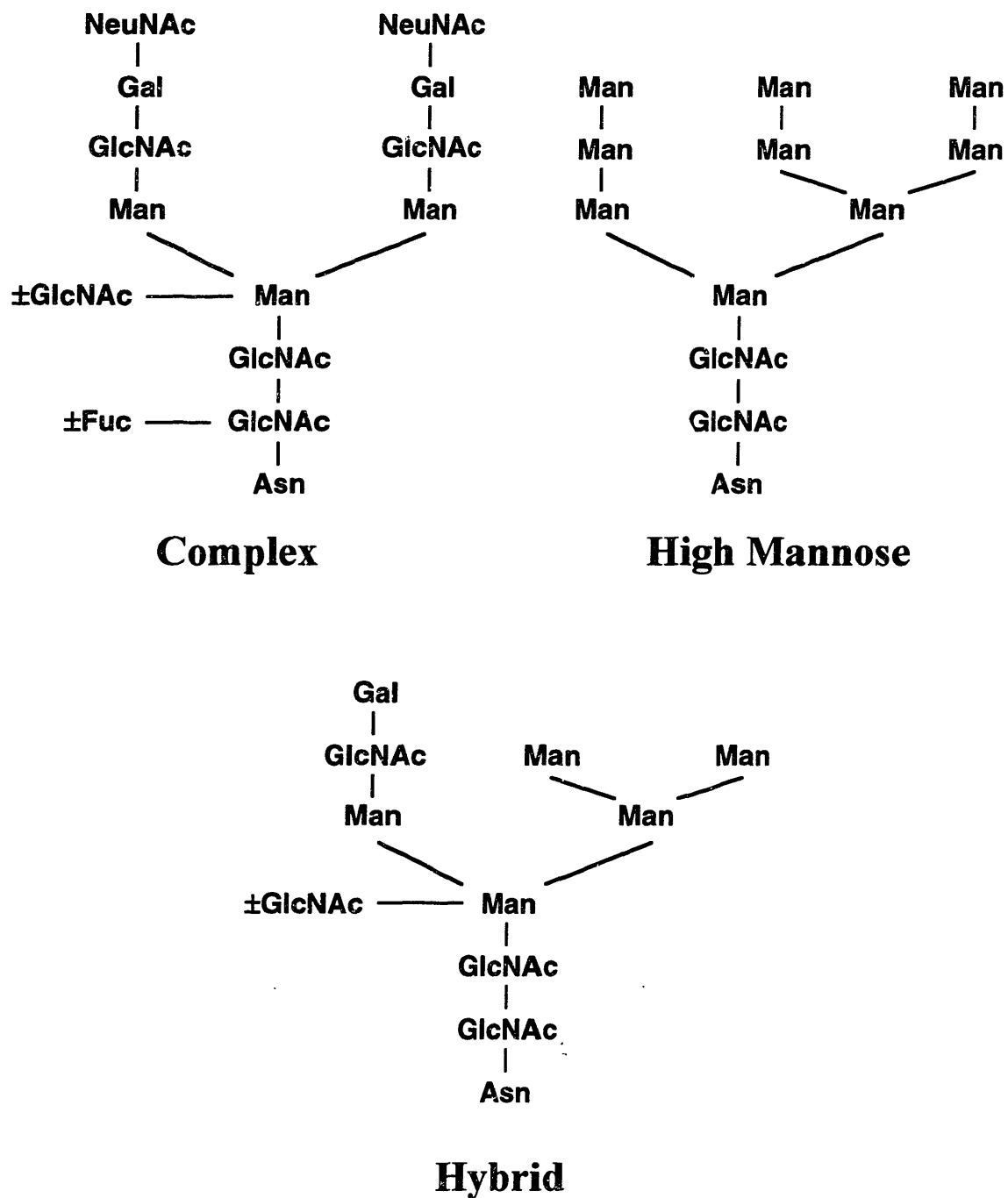


Figure 2-3. Structures representing the major classes of N-linked oligosaccharides. Abbreviations are: GlcNAc, N-acetylglucosamine; Man, mannose; Gal, galactose; Fuc, fucose; NeuNAc, sialic acid.

2.2 Implications of N-linked Glycosylation

2.2.1 Implications for Protein Folding

The oligosaccharides attached to nascent polypeptides can make an immediate impact by influencing protein folding. When glycosylation is inhibited (either through chemical inhibitors such as tunicamycin or through elimination of glycosylation sites through site directed mutagenesis), many proteins fail to fold correctly (Dorner et al., 1987; Gallagher et al., 1992; Riederer and Hinnen, 1991; Sareneva et al., 1994). The underglycosylated proteins often form aggregates which are noncovalently associated with BiP, an abundant ER resident chaperone protein that binds to hydrophobic regions of incompletely folded proteins (Gething et al., 1994). The BiP-bound, misfolded proteins are prevented from secretion and are targeted for eventual degradation (Knittler et al., 1995; Schmitz et al., 1995). Thus the first important function of N-glycosylation is to aid in the proper folding of nascent polypeptides.

N-linked oligosaccharides can influence protein folding in multiple ways. The oligosaccharides enhance the solubility of folding intermediates, stabilize folding domains and enable the interaction between unfolded protein and lectin-chaperones such as calnexin (Helenius, 1994). *In vitro* protein refolding experiments have demonstrated the influence that oligosaccharides can have on solubility and folding kinetics. A number of glycoproteins have been shown to refold more slowly and/or to aggregate during refolding after their carbohydrates have been removed (Kern et al., 1992; Schülke and Schmid, 1988; Strickland et al., 1985). The hydrophilic nature of the attached carbohydrates helps to solubilize the folding intermediates and prevent interactions which would otherwise lead to aggregation. Glycosylation may also help establish folding domains early in the folding process, because the hydrophilicity of attached oligosaccharides will orient them to the protein surface, where they will reside in the mature glycoprotein. It should be noted that oligosaccharides are not always critical for folding. For example, the refolding

of ribonucleases is independent of glycosylation (Krebs et al., 1983), which illustrates that folding can be independent of the presence of oligosaccharides for proteins with a robust folding pathway.

More recently another role has been identified for oligosaccharides in the folding process. Lectin-like chaperones have been identified which interact with the oligosaccharides of glycoproteins and are believed to play a role in protein folding. *In vivo* protein folding varies significantly from *in vitro* refolding because the *in vivo* process can be initiated cotranslationally (Chen et al., 1995; Fedorov and Baldwin, 1995), and *in vivo* folding is aided by proteins which act as catalysts and chaperones (Gething and Sambrook, 1992; Hartl et al., 1992). Current evidence suggests that *in vivo* protein folding occurs in an assisted self-assembly process, where various proteins catalyze isomerization reactions (foldases) while others reduce the probability of unproductive interactions (chaperones). The final protein configuration is believed to be determined by free energy minimization (Anfinsen, 1973), so that foldases and chaperones facilitate rather than determine protein folding (i.e. proteins that can refold *in vitro* will achieve the same final configuration as *in vivo* folded proteins). Some examples of foldases in the endoplasmic reticulum include protein disulfide isomerase (PDI), which catalyzes thiol/disulfide interchanges, and peptidyl prolyl *cis-trans* isomerase (PPIase), which catalyzes isomerizations of peptide bonds involving proline. Chaperone proteins of the ER include BiP (GRP78), endoplasmin (GRP94) and the lectin-like chaperones calnexin and calreticulin. BiP is the most studied ER chaperone, and it normally functions by binding hydrophobic regions of unfolded proteins which might otherwise associate with other nascent polypeptides and lead to aggregation (Gething et al., 1994). BiP undergoes a series of binding and release which requires ATP hydrolysis. Once the protein folds correctly, the hydrophobic sequences are buried in the core of the protein and are no longer available for BiP binding.

The chaperones calnexin and calreticulin are unique, because they recognize their substrates through interactions with glycoprotein carbohydrate. Calnexin is also unique

because it is a type I integral membrane protein, while calreticulin is soluble like most chaperones which have been identified. Calnexin and calreticulin act as lectins with affinity for glycoprotein $\text{Glc}_1\text{Man}_9\text{GlcNAc}_2$ oligosaccharide (Spiro et al., 1996; Ware et al., 1995). After the initial $\text{Glc}_3\text{Man}_9\text{GlcNAc}_2$ precursor is transferred to protein, the glucose residues are trimmed from the core oligosaccharide within minutes by the enzymes glucosidase I, which trims the initial glucose, and glucosidase II, which can remove the final two glucose residues. The oligosaccharides of unfolded proteins are typically maintained in a monoglucosylated state by the action of the enzyme UDP-glucose:glycoprotein glucosyltransferase. This glucosyltransferase, which transfers a glucose onto $\text{Man}_9\text{GlcNAc}_2$ oligosaccharides, only uses unfolded glycoproteins as substrates (Sousa et al., 1992). Because of deglucosylation by glucosidase II and reglucosylation by the glucosyltransferase, unfolded glycoproteins typically have rapid turnover of the single glucose residue on the $\text{Glc}_1\text{Man}_9\text{GlcNAc}_2$ oligosaccharide. Once the nascent glycoprotein folds correctly, the glucose is removed by glucosidase II and the glycoprotein is no longer a substrate for the glucosyltransferase, calnexin or calreticulin. Thus the oligosaccharide mediates the interaction between nascent glycoproteins and the chaperones calnexin and calreticulin.

Calnexin and calreticulin act as chaperones by promoting proper folding, preventing premature oligomerization, inhibiting degradation and mediating quality control (Tatu and Helenius, 1997). Interaction with these chaperones appears important for the proper folding of several proteins. If glucosidase I or II is inhibited, the $\text{Glc}_1\text{Man}_9\text{GlcNAc}_2$ oligosaccharide can not be formed, and interaction with calnexin and calreticulin is prevented. Under such conditions, nascent glycoprotein folding and transport is often perturbed (Chen et al., 1995; Helenius, 1994). Calnexin has been shown to bind cotranslationally to hemagglutinin (Chen et al., 1995), which illustrates that it acts early in the folding process. The exact mechanisms of action are unclear, but direct interaction with the polypeptide chain is likely. Ware et al. (1995) have demonstrated that interaction with the oligosaccharide is critical for initial calnexin binding, but that once the

complex is formed the oligosaccharide does not contribute significantly to the interaction. It is not known whether folding occurs while the polypeptide is complexed with calnexin, or if it occurs during cycles of binding and release similar to the chaperone BiP (Ware et al., 1995).

In summary, glycosylation can be critical for proper folding because oligosaccharides can enhance the solubility of folding intermediates, stabilize folding domains and enable the interaction between unfolded protein and lectin-chaperones. Sugar trimming and addition reactions in the ER function as a quality control mechanism for monitoring and mediating protein folding.

2.2.2 Implications for Targeting and Secretion

As mentioned above, N-glycosylation can impact protein secretion by influencing folding and hence exit from the endoplasmic reticulum. Proper folding has been identified as a prerequisite for transport from the ER to the Golgi (Gething et al., 1986; Helenius, 1994). Chaperone proteins such as BiP and calnexin are believed to play a central role in mediating the interaction between folding and transport. Stable association of unfolded proteins with BiP has been correlated to reduced secretion efficiency (Dorner et al., 1987; Dorner et al., 1993). There is evidence that the degree of association with BiP can depend upon the ER BiP concentration, so that secretion of proteins which transiently associate with BiP can be enhanced by reducing BiP (Dorner et al., 1988) and inhibited by elevating BiP (Dorner et al., 1992). Since they typically fold more slowly, underglycosylated proteins are more likely to associate with BiP and be retained in the ER. Exit from the ER may therefore represent a site of “quality control”, where underglycosylated proteins may be selectively retained. Chapter 7 considers the relationship between glycosylation and secretion in greater detail and explores the possibility of using BiP overexpression to selectively retain underglycosylated proteins.

Glycosylation can also impact other intracellular trafficking and secretion events. The most extensively studied example of oligosaccharide mediated protein sorting is the targeting of lysosomal enzymes to the endocytic pathway (Fielder and Simons, 1995; Kornfeld and Mellman, 1989). Lysosomal proteins are recognized in the Golgi by a specific UDP-GlcNAc phosphotransferase, which catalyzes the transfer of GlcNAc-P to a mannose of the core oligosaccharide. This enzyme only recognizes native lysosomal proteins. A second enzyme subsequently cleaves off the GlcNAc, generating an oligosaccharide with a mannose-6-P marker which can bind to mannose-6-P receptors in the *trans*-Golgi network. The receptors thus sort out proteins which are bound for lysosomes. Another example of oligosaccharide mediated trafficking is the asymmetric sorting of proteins to the plasma membrane of epithelial cells (Fielder and Simons, 1995). For example, there is experimental evidence for the involvement of carbohydrate in apical secretion by Madin-Darby Canine Kidney (MDCK) cells (Kitagawa et al., 1994). Other roles for N-glycans in protein trafficking have been speculated (Fielder and Simons, 1995), but experimental evidence is lacking.

2.2.3 Implications for Glycoprotein Biochemical Properties

Oligosaccharides normally constitute a significant fraction of a glycoprotein's mass, and they can be important contributors to the protein's biochemical properties (see reviews in Cumming, 1991; Goochee et al., 1991; Goochee et al., 1992; Jenkins and Curling, 1994). For example, glycosylation can influence the solubility of glycoproteins. Proteins such as EPO and fibrinogen are more susceptible to aggregation when they are deglycosylated (Dordal et al., 1985; Langer et al., 1988). As discussed above, the solubility of denatured glycoproteins can also be influenced by oligosaccharides (Kern et al., 1992; Schülke and Schmid, 1988; Strickland et al., 1985). The oligosaccharides are believed to enhance solubility by contributing a strong hydrophilic component to the glycoprotein, and by masking the protein surface to prevent intramolecular polypeptide interactions (Goochee et al., 1992).

Fully glycosylated proteins are typically more stable than their non-glycosylated counterparts. Several proteins are more susceptible to thermal inactivation upon oligosaccharide removal, although it is not always clear whether the effect is due to thermal instability or reduced solubility of the denatured protein (Goochee et al., 1992). For example carbohydrates protect thermally denatured yeast invertase from aggregation, but they apparently do not influence the thermal denaturation process (Schülke and Schmid, 1988). The *in vivo* stability of a glycoprotein can also be a function of susceptibility to protease attack. There are many documented cases of oligosaccharides protecting proteins from proteases. The glycans at Asn-25 in human interferon- γ , for example, protect the protein from degradation by elastase, cathepsin G, plasmin and crude granulocyte protease (Sareneva et al., 1995). Similarly, the carbohydrates of porcine pancreatic ribonuclease protect the protein from degradation by trypsin and subtilisin (Wang and Hirs, 1977). The oligosaccharides may protect the polypeptide from proteases by sterically blocking potential cleavage sites.

The oligosaccharides of glycoproteins can also impact biological activity. For example, the glycans of the human interferon- γ receptor are required for proper ligand binding (Fischer et al., 1990). Carbohydrates have also been found to affect the specific activity of immunoglobulins, due to glycosylation in both the heavy chain and variable regions (reviewed in Goochee et al., 1992). In contrast to these examples, biological activity of other glycoproteins can be unaffected or even negatively impacted by oligosaccharides. Human interferon- γ (IFN- γ) *in vitro* activity is not affected by glycosylation; *E. coli* derived IFN- γ has full anti-viral and anti-proliferative activity *in vitro* (Rinderknecht et al., 1984). Tissue-type plasminogen activator (t-PA) is an example where specific activity is negatively impacted by increased extent of glycosylation. t-PA is produced as two forms because of variable glycosylation at Asn-184: type I has three N-linked oligosaccharides, whereas type II has only two. The oligosaccharide at Asn-184 inhibits the proteolytic conversion of single chain t-PA to two chain t-PA (Wittwer and Howard, 1990). The two chain form of t-PA has a higher catalytic activity (Berg et al., 1993), and

so type II t-PA is more effective than type I. Rademacher et al. (1988) suggest that variable glycosylation may confer greater sensitivity to tPA-mediated thrombolysis, by providing both fast and slow acting forms.

A recurring theme that emerges from the above discussion is that oligosaccharides influence glycoprotein properties in a very protein specific manner. While glycosylation may be critical for folding or activity of one protein, it may be irrelevant for another. The impact of glycosylation must be determined on a case by case basis. However it is clear that in many instances carbohydrates play an important role in determining glycoprotein properties.

2.2.4 Implications for Circulatory Half-Life

Oligosaccharides are of critical importance in determining the *in vivo* circulatory half-life of glycoproteins in the blood stream. Proteins are cleared from the blood by a variety of mechanisms, and the *in vivo* activity of an injected therapeutic protein can depend upon how long it is able to remain in circulation.

One mechanism of glycoprotein removal is by receptors which recognize specific terminal monosaccharides of glycoprotein carbohydrates. Once glycoproteins are bound by the receptors, they enter the cell and are degraded in lysosomes. The steps of the endocytic pathway are: concentration of receptor-ligand complexes in coated pits, internalization, pH mediated dissociation of receptor-ligand in the CURL (compartment of uncoupling of receptor and ligand), segregation, transport of ligand to lysosomes and recycling of the receptor (Darnell et al., 1990). Examples of glycosylation-specific receptors include the asialoglycoprotein receptor (ASGP-R) present on hepatocytes and the mannose receptor found on tissue resident macrophages. The ASGP-R recognizes oligosaccharides with terminal galactose or N-acetylgalactose residues, including under-sialylated and desialylated complex N-glycans (Monroe and Huber, 1994; Weiss and Ashwell, 1989). Glycoproteins with terminal mannose, N-acetylglucosamine or fucose residues are

recognized by the mannose receptor (Ezekowitz and Stahl, 1988). The receptor mediated clearance mechanisms serve to eliminate abnormal or foreign glycoproteins from circulation. The majority of human plasma N-glycoproteins carry complex-type oligosaccharides with terminal sialic acid residues. In contrast, mannose is a common component of bacterial pathogens, parasites, yeasts and the envelope glycoprotein of certain viruses (Ezekowitz and Stahl, 1988).

A less specific mechanism of protein clearance occurs in the kidney. The renal glomerulus acts as an ultrafiltration device, allowing small molecules to pass through to the urinary (Bowman's) space, while almost completely restricting the passage of molecules the size of plasma albumin or larger (Kanwar, 1984). The permeability of a given molecule has an inverse relationship with its effective hydrodynamic radius, so that larger molecules are more likely to be retained. In addition, permeability is influenced by the molecule's configuration and net electrical charge. The more positively charged a molecule is, the more likely it will pass through to the urinary space. Thus, small positively charged molecules are likely to be cleared by the kidney, while large negatively charged molecules will remain in circulation. It is important to note that oligosaccharides can significantly increase the size of a glycoprotein, and attached sialic acid groups contribute negative charges. Therefore glycosylation can prevent small proteins from being cleared by the kidney.

Studies of glycoprotein persistence in the blood stream have identified each of the mechanisms described above as potentially important determinants of *in vivo* half life. For example, Flesher et al. (1995) found that clearance of a CTLA4 fusion protein could be correlated to sialic acid content. This is consistent with hepatic clearance of asialoglycoproteins by the ASGP-R. Similarly, removal of terminal sialic acid residues from erythropoietin (EPO) results in rapid ASGP-R mediated clearance from the blood stream (Spivak and Hogans, 1989). EPO is a particularly interesting protein, because it also appears to be partially cleared by the kidney. EPO with biantennary

oligosaccharides was found to be cleared by the kidney more rapidly than EPO with predominantly tetraantennary structures (Misaizu et al., 1995). EPO is a relatively small protein, with carbohydrate accounting for 40% of its 30 kDa molecular weight. Extra carbohydrate branching provides EPO with a greater mass and more negative charge (due to additional sialic acid residues), and hence reduces the likelihood that it will be cleared by the kidney. Low molecular weight secretory proteins from rat liver have also been shown to be protected from renal clearance by complex carbohydrates (Gross et al., 1988; Gross et al., 1989). When the carbohydrates were of the high mannose type, the rat liver glycoproteins were rapidly cleared via the mannose receptor pathway (Gross et al., 1988; Gross et al., 1989).

The examples discussed above illustrate that effective therapeutic glycoproteins must not only be glycosylated, but they must be glycosylated correctly. In fact improper glycosylation is worse than lack of glycosylation, because improperly glycosylated proteins are rapidly removed through receptor-mediated mechanisms. For this reason, Chinese hamster ovary (CHO) cells have emerged as the most widely used cell line for producing recombinant human therapeutic glycoproteins. CHO cells are able to closely mimic human *in vivo* glycosylation characteristics, perhaps even more closely than some human cell lines of tumor origin (Goochee et al., 1992). Although the glycosylation fidelity is not perfect (for example CHO cells synthesize α 2,3-linked terminal sialic acids exclusively, while humans synthesize α 2,6 and α 2,3-linked sialic acids), CHO cells are more effective than most other cell lines (Jenkins et al., 1996). Simpler organisms are typically unable to create the required complex carbohydrates (see reviews in Goochee et al., 1991; Jenkins et al., 1996). For example, bacteria can not N-glycosylate proteins, while yeast attach high mannose glycans, plants do not add sialic acids and insect cells typically produce simpler oligomannose oligosaccharides.

2.3 Factors Influencing N-linked Glycosylation Site Occupancy Heterogeneity

More than twenty individual enzymes are involved in the conversion of glucose to protein bound carbohydrate, not including the sugar trimming and addition reactions which occur in the Golgi. The reactions which these enzymes catalyze rely on an adequate supply of sugar and activated carrier molecules such as nucleoside triphosphates and dolichol phosphate. In principle, any of the enzymes or substrates might limit transfer of oligosaccharide to protein. This section reviews the features of the glycosylation pathway which are most likely to influence glycosylation site occupancy.

2.3.1 Lipid-Linked Oligosaccharide Precursor Formation

An obvious potential cause of unoccupied glycosylation sites is a lack of oligosaccharide precursor. If the lipid-bound precursor is not available to the oligosaccharyltransferase enzyme, the glycosylation reaction can not occur. There are several potential bottlenecks to synthesis of the precursor oligosaccharide, including nucleotide sugar availability, dolichol availability and the activity of the various glycosyltransferase enzymes which catalyze the synthesis.

2.3.1.1 Nucleotide Sugar Availability

All sugars added to protein in glycosylation are ultimately derived from nucleotide sugar intermediates. Figure 2-4 illustrates how the nucleotide sugars are formed from various carbon sources (Schachter, 1978). All of the nucleotide sugars may be formed from a fructose-6-P or glucose-6-P intermediate. These intermediates undergo enzyme catalyzed isomerization reactions to the appropriate hexose-1-P, and then they react with nucleoside triphosphates to form nucleotide sugars. The activated sugars can then serve directly as donors in glycosylation reactions or be used to form dolichol-sugars. The role

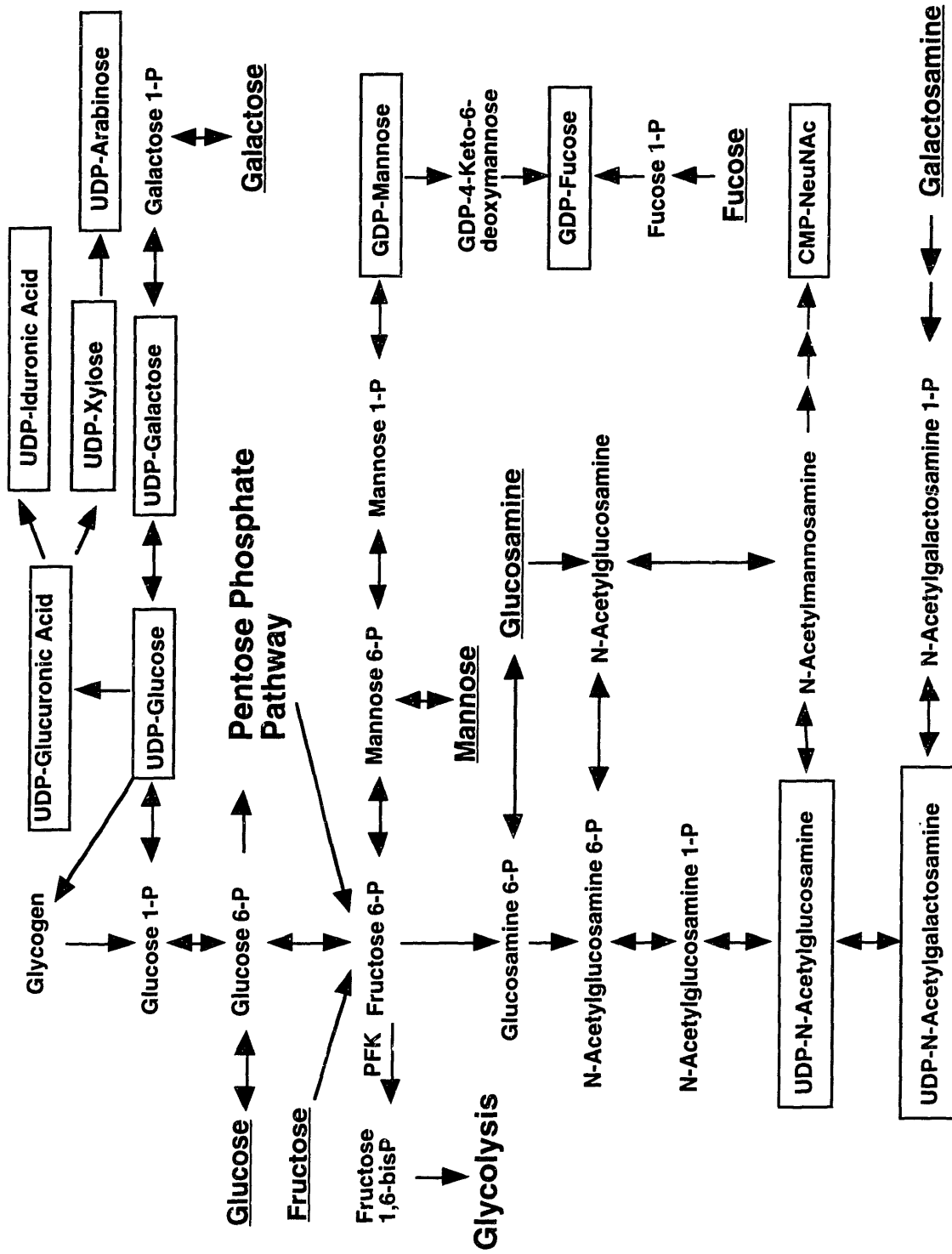


Figure 2-4. Biosynthesis of common nucleotide sugars.

that nucleotide sugars play in glycosylation has primarily been studied under conditions of glucose starvation or during feeding of specific nucleotide sugar precursors.

Numerous studies have examined the effects of glucose starvation on glycosylation (Baumann and Jahreis, 1983; Chapman and Calhoun, 1988; Gershman and Robbins, 1981; Rearick et al., 1981; Stark and Heath, 1979; Turco, 1980). These studies have generally concluded that glucose starvation leads to accumulation of truncated oligosaccharides bound to lipid, along with transfer of smaller oligosaccharides to proteins. Glucose fed cells synthesize predominantly $\text{Glc}_3\text{Man}_9\text{GlcNAc}_2\text{-P-P-Dol}$, while starved cells synthesize $\text{Man}_2\text{GlcNAc}_2\text{-P-P-Dol}$, $\text{Man}_5\text{GlcNAc}_2\text{-P-P-Dol}$ and $\text{Glc}_3\text{Man}_5\text{GlcNAc}_2\text{-P-P-Dol}$ (Chapman and Calhoun, 1988; Gershman and Robbins, 1981; Rearick et al., 1981). The truncated $\text{Glc}_3\text{Man}_5\text{GlcNAc}_2\text{-P-P-Dol}$ species can be transferred to protein, although with a much lower efficiency than the normal precursor. This leads to decreased glycosylation site occupancy of some proteins. The glucose starvation response can be reversed by adding exogenous glucose or mannose (and to a smaller extent galactose), but adding pyruvate, glutamine, glycine, inositol, fructose, ribose, N-acetylglucosamine or glycerol is not effective (Gershman and Robbins, 1981; Turco, 1980). Nucleotide sugar depletion has also been observed in glucose starved cultures (Chapman and Calhoun, 1988; Ullrey and Kalckar, 1979), and it is often cited as the likely cause of truncated precursor synthesis. Proposed explanations for nucleotide sugar depletion during glucose starvation have generally focused on supply of hexose phosphates, leading to the suggestion that glycosylation may be sensitive to cellular glucose-6-P pools and thus the metabolic state of the cell (Turco, 1980).

Some nucleotide sugars can be formed from carbohydrate sources other than glucose, mannose and galactose. For example, GDP-Fucose can be formed from fucose with minimal catabolism or conversion to other sugars (Beeley, 1985). Similarly the amino sugars glucosamine and galactosamine can be used to form UDP-N-acetylglucosamine (UDP-GlcNAc), UDP-N-acetylgalactosamine (UDP-GalNAc) and CMP-N-

acetylneuraminic acid (CMP-NeuNAc or CMP-sialic acid). N-acetylmannosamine is another example of a specific sugar precursor, and it is used to synthesize CMP-NeuNAc almost exclusively (Gu, 1997). Low concentrations of these sugar precursors are commonly used in radiolabeling experiments to label glycoproteins or specific types of glycoproteins (Beeley, 1985). Feeding millimolar amounts of glucosamine, galactosamine and N-acetylmannosamine leads to accumulation of specific nucleotide sugars and perturbations in glycosylation. N-acetylmannosamine feeding, for example, results in elevated CMP-NeuNAc and increased sialylation (Gu, 1997). In terms of glycosylation site occupancy, glucosamine and galactosamine are more important, because they cause accumulation of UDP-GlcNAc (Kornfeld and Ginsburg, 1966; Pels Rijcken et al., 1995a), which is used to synthesize the lipid-linked precursor oligosaccharide.

Following their entry into the cell, glucosamine and galactosamine are converted into hexosamine phosphates, acetylated, and reacted with UTP to make UDP-GlcNAc and UDP-GalNAc (the sum is referred to as UDP-GNAc). UDP-GlcNAc and UDP-GalNAc can be interconverted readily by UDP-GalNAc 4-epimerase, and the two species were present at the equilibrium ratio in glucosamine fed HeLa cells (Kornfeld and Ginsburg, 1966). The amino sugars are not converted to other sugars, because the formation of glucosamine-6-P from fructose-6-P is normally not reversible (Beeley, 1985). Despite the fact that UDP-GlcNAc and UDP-GalNAc are most likely in equilibrium, feeding glucosamine affects glycosylation much differently than feeding galactosamine. Glucosamine feeding causes a reduction in glycosylation (Datema and Schwarz, 1979; Elbein, 1987; Koch et al., 1979; Pan and Elbein, 1982), while rat hepatocytes fed galactosamine slightly increased mannosylation of proteins and increased sialylation by a factor of 2.5 (Pels Rijcken et al., 1995a). Five mM glucosamine caused truncated precursor oligosaccharide synthesis in MDCK cells, while the same concentration of galactosamine did not influence precursor synthesis or glycosylation (Pan and Elbein, 1982). The effect of glucosamine on glycosylation may be due to glucosamine itself rather than the nucleotide sugar. Koch et al. (1979) demonstrated that the negative impact

of glucosamine on glycosylation was rapidly reversible, and that reversibility correlated to depletion of glucosamine itself and not any of its metabolites. The concentration of UDP-Glc, UDP-GlcNAc and GDP-Man did not change significantly, while glucosamine levels declined and glycosylation ability was recovered.

The impact of nucleotide sugars on glycosylation has also been studied by altering nucleoside triphosphate levels. Pels Rijcken et al. (1995b) found that treating rat hepatocytes with 0.5 mM uridine or cytidine led to large increases in UTP (6.7 fold increase after 40 h) and UDP-sugars (2.5 to 4.6 fold increases after 40 h). The nucleotide precursor treatment also led to changes in glycosylation: incorporation of N-acetylhexosamine into cell-associated and secreted glycoconjugates increased, while sialylation decreased. The authors suggested that increased UDP-GNAc was responsible for both of the observed effects. UDP-GNAc was suggested to impair the transport of CMP-NeuNAc into the Golgi, thus reducing sialylation. However, similar increases in UDP-GNAc observed during treatment with galactosamine did not impair sialylation; in contrast sialylation increased by a factor of 2.5 in these cells (Pels Rijcken et al., 1995a). Pels Rijcken et al. (1995a) suggest that the apparent contradiction may be due to different compartmentation of the UDP-GNAc made with uridine feeding versus galactosamine feeding. Alternatively other UDP-sugars or uridine metabolites may be responsible for the reduction in sialylation observed with uridine feeding. On an equimolar basis, UDP-Gal is a more potent inhibitor of *in vitro* CMP-NeuNAc transport than UDP-GlcNAc (Carey et al., 1980), which supports the hypothesis that other UDP-sugars may be influencing CMP-NeuNAc transport.

The glucose starvation, sugar precursor feeding and nucleotide precursor feeding experiments demonstrate that nucleotide sugars can influence glycosylation. However, the impact of nucleotide sugars under normal growth conditions is less clear. Furthermore the effects of precursor feeding are often ambiguous, since the precursors may influence multiple metabolic pathways or produce metabolites which impact glycosylation in

unexpected ways. Galactosamine feeding versus glucosamine feeding illustrates the second point; despite the fact that both precursors lead to similar alterations in nucleotide sugar levels, glycosylation is impacted very differently. The results described in subsequent chapters of this thesis help to elucidate how normal cellular metabolism influences nucleotide sugar levels and glycosylation site occupancy.

2.3.1.2 Dolichol Availability

In addition to nucleotide sugars, proper glycosylation depends upon an adequate supply of dolichol phosphate, the membrane lipid which is the anchor of the precursor oligosaccharide. Dolichols are actually a class of related polyprenols in which the final (alpha) isoprene unit is saturated (see Figure 2-5). In mammalian cells, dolichol typically contains 17-21 isoprenyl units, with the 19 unit isomer the most prevalent in Chinese hamster ovary cells (Kaiden and Krag, 1992). Dolichol is formed from farnesyl pyrophosphate and isopentenyl pyrophosphate, intermediates which are also part of the cholesterol biosynthesis pathway. Although there is still some debate about how dehydrodolichol pyrophosphate is converted to dolichol phosphate, Figure 2-6 illustrates what is currently believed to be the dolichol biosynthesis pathway (Sagami et al., 1996; Sagami et al., 1993). The activities of important enzymes downstream of 3-hydroxy-3-methylglutaryl CoA (HMG CoA) synthesis have been isolated in the microsomal fractions of mammalian cells, including HMG CoA reductase, *cis*-Isoprenyltransferase

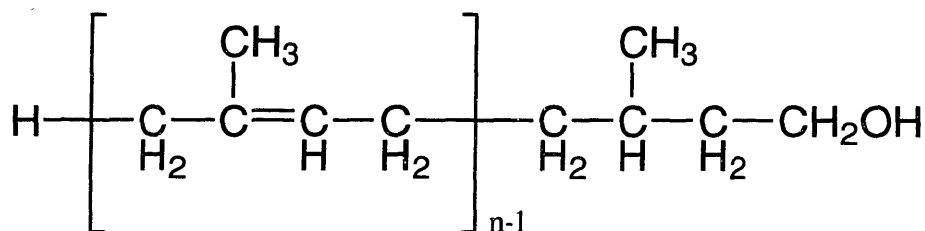


Figure 2-5. The chemical structure of dolichol (n=17 to 21 for mammalian cells).

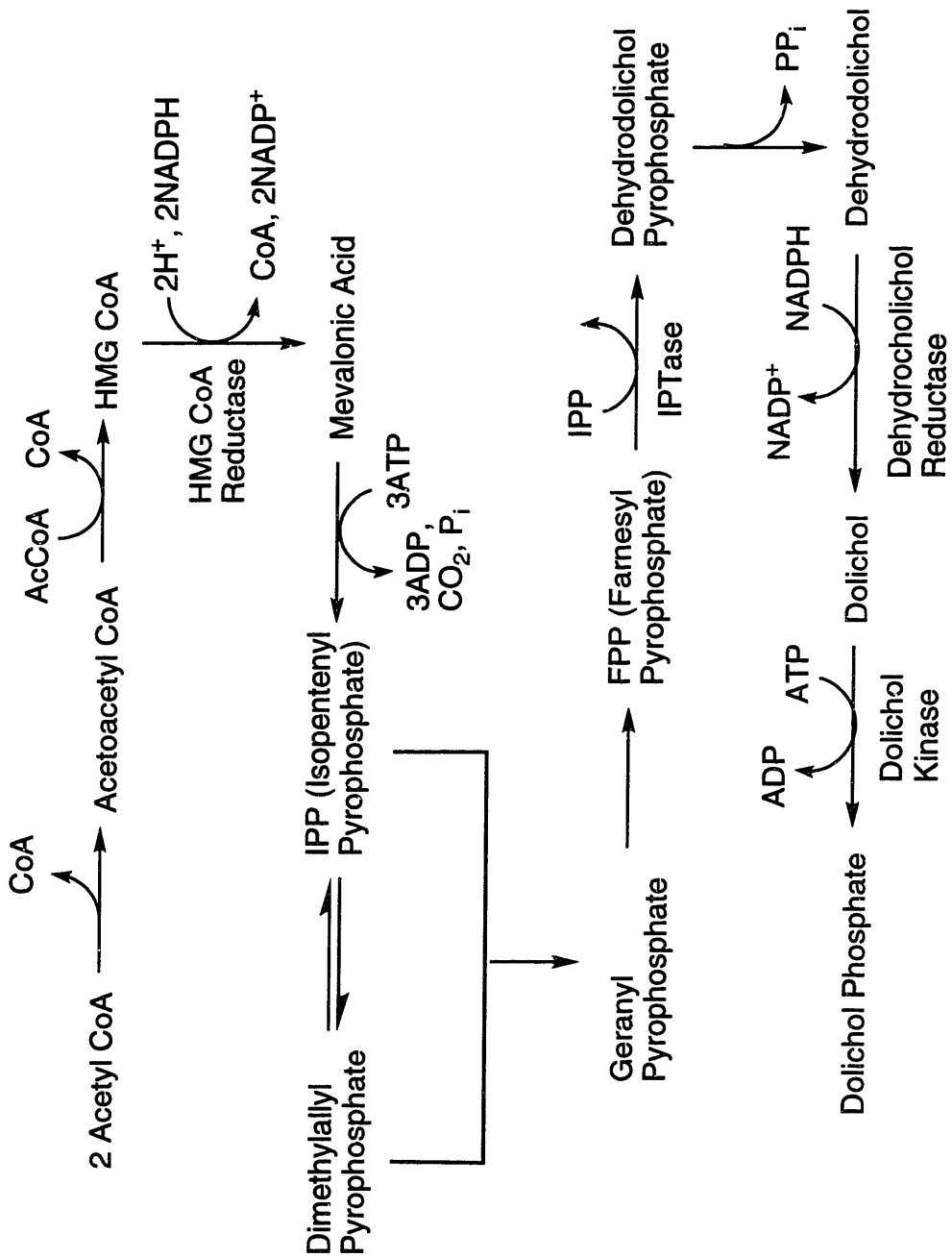


Figure 2-6. The proposed biochemical pathway for dolichol synthesis .

(also known as IPTase or dehydrodolichyl pyrophosphate synthase) and dehydrodolichol reductase.

A number of studies have related dolichol-P levels to the formation of lipid-linked oligosaccharide precursors. For example, exogenous Dol-P added to the culture medium increased the rate of oligosaccharide-P-P-dolichol synthesis and protein N-glycosylation in embryonic rat brain cells (Crick and Waechter, 1994). There is increasing evidence that cells use dolichol-P synthesis to modulate N-glycosylation capacity. Induction of dolichol synthesis has been correlated to increased oligosaccharide-P-P-dolichol synthesis and N-glycosylation in several cell lines, including during cell cycle dependent regulation in rat 3Y1 cells (Fukushima et al., 1997), mitogenic response regulation in mouse B cells (Crick et al., 1994) and developmental regulation in embryonic rat brain cells (Crick and Waechter, 1994). Dolichol synthesis appears to be regulated separately from cholesterol synthesis, because the rate of cholesterol synthesis was not accelerated during the expansion of Dol-P and oligosaccharide-P-P-Dol (Crick and Waechter, 1994). Consistent with this hypothesis is the finding that HMG CoA reductase was not up-regulated under any of the conditions described above, while IPTase, which is specific to the dolichol pathway, was induced. In addition, when 0.5 μM lovastatin was added to partially inhibit HMG CoA reductase, cholesterol synthesis was suppressed, while dolichol synthesis was slightly enhanced (Crick et al., 1994). A higher concentration (3 μM) of lovastatin was found to inhibit dolichol-P synthesis and N-glycosylation in the human melanoma cell line SK-MEL-2, which illustrates that a partially functioning HMG CoA reductase is required to supply the necessary mevalonate (Carlberg et al., 1996). Under normal conditions, however, mevalonate does not appear to be limiting for dolichol synthesis in a variety of cell lines.

Deficiencies in dolichol synthesis have been shown to negatively impact oligosaccharide-P-P-dolichol synthesis and protein N-glycosylation. It has recently been found that the congenital disorder known as carbohydrate-deficient glycoprotein (CDG) syndrome type

I can be caused by deficient dehydrodolichol reductase enzyme (Ohkura et al., 1997). Primary fibroblast cultures established from skin biopsies of patients with this deficiency accumulated dehydrodolichol and had less dolichol. The cells synthesized the normal $\text{Glc}_3\text{Man}_9\text{GlcNAc}_2\text{-P-P-Dol}$ precursor, although in smaller amounts. It has been shown that N-glycoproteins from patients with CDG syndrome type I are underglycosylated. The importance of dolichol synthesis in glycosylation was also demonstrated with a Chinese hamster ovary mutant which had a severe defect in the dehydrodolichol reductase enzyme (Stoll and Krag, 1988). The mutant F2A8 synthesized dehydrodolichol to dolichol in a ratio of 100:1, while the ratio in control cells was 0.4:1. The mutant synthesized oligosaccharide precursors which were similar to the parental cell line, except that a significant fraction were synthesized on dehydrodolichol while control cells utilized dolichol almost exclusively (Stoll et al., 1988). The unsaturated polyprenol was not as effective in glycosylation reactions, and the mutant cells were unable to synthesize the lipid-precursor effectively, which led to under utilization of potential glycosylation sites (Stoll and Krag, 1988).

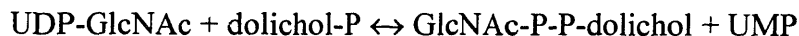
The evidence suggests that dolichol-P synthesis is an important regulator of oligosaccharide-P-P-dolichol synthesis. Defects in dolichol-P synthesis cause underglycosylation of proteins, while increased dolichol-P levels correlate with a higher glycosylation capacity. Control of dolichol-P synthesis appears to reside with enzymes such as IPTase and dehydrodolichol reductase. In some tissues dolichol kinase may play an important role, although the pool of free dolichol in CHO cells is small, which suggests that kinase activity is not limiting (Stoll et al., 1988).

2.3.1.3 Glycosyltransferase Activities

The $\text{Glc}_3\text{Man}_9\text{GlcNAc}_2\text{-P-P-Dol}$ precursor is synthesized in a series of enzyme catalyzed reactions. Theoretically any of the glycosyltransferase enzymes involved in the dolichol-oligosaccharide synthesis pathway could limit precursor synthesis and hence influence

glycosylation site occupancy. Indeed a number of mutants with specific enzyme inactivations have been isolated which synthesize abnormal dolichol-linked oligosaccharide precursors (Brändli, 1991; Lehrman and Zeng, 1989; Stanley, 1983; Stoll and Krag, 1988). Most of these cell lines were generated by selecting for mutants resistant to cytotoxic lectins or glycoprotein processing inhibitors, and they have proved quite useful in elucidating the N-glycosylation pathway. Such cell lines produce truncated oligosaccharide precursors which are typically transferred to protein with lower efficiency than the normal precursor. Under normal conditions, however, Glc₃Man₉GlcNAc₂-P-P-Dol is the dominant lipid-linked oligosaccharide species, with smaller amounts of Glc_{1,2}Man₉GlcNAc₂-P-P-Dol and Man₅GlcNAc₂-P-P-Dol usually detectable (Fukushima et al., 1997; Gershman and Robbins, 1981; Ohkura et al., 1997; Rearick et al., 1981). Hence the activities of intermediate glycosyltransferase enzymes do not normally limit the formation of the oligosaccharide precursor, and so the enzymes involved in the initial steps of the pathway have received the most attention as potential sites of control.

The first glycosyltransferase in the Glc₃Man₉GlcNAc₂-P-P-Dol synthesis pathway is UDP-GlcNAc:dolichol-P GlcNAc-1-P transferase (GPT), which catalyzes the reaction



This enzyme is inhibited by tunicamycin, a specific and reversible inhibitor which is thought to be a substrate-product transition state analogue (Elbein, 1987). Experiments utilizing tunicamycin have illustrated the importance of GPT in the N-linked glycosylation pathway. Cells treated with tunicamycin are unable to synthesize the lipid-linked oligosaccharide precursor, and N-linked glycosylation is inhibited. Chinese hamster ovary cells selected for resistance to tunicamycin were found to have elevated GPT activities and phenotypes consistent with gene amplification (Waldman et al., 1987; Zhu et al., 1992). Zhu et al. (1992) demonstrated that the elevated GPT activity was due to an unusually high copy number of a gene which was found to encode GPT. When grown in the absence of tunicamycin, cell lines overexpressing GPT (selected mutants and

cells transfected with the GPT gene) had 10 to 15-fold higher GPT activity than control cells (Waldman et al., 1987; Zhu et al., 1992). GPT overexpression did not, however, lead to enhanced glycosylation. In contrast, cells overexpressing GPT were found to accumulate the truncated oligosaccharide precursor $\text{Man}_5\text{GlcNAc}_2\text{-P-P-Dol}$. Similar to the case of glucose starvation (see the section on Nucleotide Sugar Availability), accumulation of the truncated oligosaccharide precursor resulted in reduced incorporation into protein.

Though caused by very different phenomena, glucose starvation and GPT overexpression may share a common mechanism which leads to truncated precursor synthesis: depletion of dolichol linked sugars. The truncated $\text{Man}_5\text{GlcNAc}_2\text{-P-P-Dol}$ precursor is synthesized directly from nucleotide sugars; the four mannoses and three glucoses which are normally added to complete the precursor are added from dolichol linked sugars. The dolichol linked sugars mannose-P-Dol and glucose-P-Dol were depleted in cells overexpressing GPT, due to excessive accumulation of oligosaccharide-P-P-Dol (primarily $\text{Man}_5\text{GlcNAc}_2\text{-P-P-Dol}$) (Rosenwald et al., 1990). The enzymes catalyzing dolichol sugar formation (Man-P-Dol synthase and Glc-P-Dol synthase) compete with GPT for a common pool of dolichol-P, and overexpression of GPT depletes the dolichol-P needed for dolichol sugar formation. The activities of GPT, Man-P-Dol synthase and Glc-P-Dol synthase must be balanced to produce the proper oligosaccharide precursor. When one of the activities is altered, the distribution between Man-P-Dol, Glc-P-Dol and oligosaccharide-P-P-Dol shifts accordingly, with little impact on total dolichol or dolichol-P levels. For example a Man-P-Dol synthase mutant had lower Man-P-Dol and correspondingly higher oligosaccharide-P-P-Dol (the truncated precursor), while cells treated with tunicamycin to inhibit GPT had reduced oligosaccharide-P-P-Dol and elevated Man-P-Dol and Glc-P-Dol (Rosenwald et al., 1990).

With their importance in the oligosaccharide-P-P-Dol pathway, one would expect the activities of enzymes such as GPT, Man-P-Dol synthase and Glc-P-Dol synthase to be

tightly regulated. GPT is the most thoroughly studied, and indeed it is thought to be under several types of control. For example, Mota et al. (1994) found that hamster GPT activity paralleled transcript abundance, and that the gene was differentially expressed during development and in differentiated adult tissues. Similarly, GPT was found to be developmentally and hormonally regulated in mouse mammary gland (Ma et al., 1996). In addition to transcriptional controls, GPT activity can be modulated by post-translational means. Recent evidence suggests that GPT forms dimers, and dimer formation may play a role in *in vivo* activity (Dan and Lehrman, 1997). The finding that Man-P-Dol is an allosteric activator of GPT may indicate that the activities of GPT, Man-P-Dol synthase and Glc-P-Dol synthase are coordinately modulated through feed-back mechanisms (Kean, 1991a).

Less is known about the other glycosyltransferases involved in the oligosaccharide precursor biosynthetic pathway, although a few have been cloned. Several of these genes have been shown to be essential for viability in yeast, including the genes for the enzymes catalyzing the first (ALG7 which corresponds to the mammalian gene for GPT), third (ALG1) and fifth (ALG2) steps in $\text{Glc}_3\text{Man}_9\text{GlcNAc}_2\text{-P-P-Dol}$ synthesis (Lennon et al., 1995). The enzymes appear to share similar membrane-spanning regions which have been suggested as dolichol recognition sequences (Orlean, 1992). Genes for several enzymes in the dolichol pathway have been shown to display characteristics of early growth response genes in yeast (Lennon et al., 1995).

Since $\text{Glc}_3\text{Man}_9\text{GlcNAc}_2\text{-P-P-Dol}$ is the dominant lipid-linked oligosaccharide species, the glycosyltransferases downstream of GPT do not normally limit precursor formation. During glucose starvation or overexpression of GPT, however, downstream steps can limit precursor formation at the $\text{Man}_5\text{GlcNAc}_2\text{-P-P-Dol}$ species. Therefore of the enzymes directly involved in oligosaccharide precursor synthesis, the most important for glycosylation site occupancy are GPT, Dol-P-Man synthase (and translocase), Dol-P-Glc synthase (and translocase), Dol-P-Man: $\text{Man}_5\text{GlcNAc}_2\text{-P-P-Dol}$ Man-1-P transferase and

the enzyme catalyzing the translocation of the $\text{Man}_5\text{GlcNAc}_2\text{-P-P-Dol}$ precursor from the cytosol to the lumen of the ER.

2.3.2 Oligosaccharyltransferase Activity

Even if sufficient oligosaccharide-P-P-Dol precursor is available, the N-glycosylation reaction could be limited by the activity of the oligosaccharyltransferase (OST) enzyme which catalyzes the transfer of the oligosaccharide to the polypeptide acceptor. OST has recently been isolated in a number of species, and is found as a heteroligomeric complex of between three and six polypeptides (Silberstein and Gilmore, 1996). OST activity for several mammalian cell types has been co-purified with a heterotrimeric complex composed of 66, 63 and 48 kDa subunits. Based upon amino acid sequence and protease accessibility studies, the three subunits are believed to be type I integral membrane proteins with large amino-terminal luminal domains and short carboxy-terminal cytoplasmic domains (Silberstein and Gilmore, 1996).

The 66 and 63 kDa subunits of OST were found to be identical to the previously identified proteins ribophorin I and ribophorin II, respectively (Kelleher et al., 1992). The ribophorins were initially identified as components of the rough endoplasmic reticulum (RER) which were associated with bound ribosomes. The ribophorins were found to be present in approximately equimolar amounts relative to the number of bound ribosomes on the RER (Marcantonio et al., 1984). Ribophorins, while not believed to be directly responsible for ribosome binding, are apparently closely related to the translocon apparatus. Antibodies to ribophorins I and II were able to inhibit translocation, presumably by sterically inhibiting ribosome targeting to the ER membrane (Yu et al., 1990). Such an intimate and stoichiometric association with bound ribosomes suggests that the amounts of ribophorins are not limiting for co-translational OST activity. Further evidence suggests that the 48 kDa unit is probably not limiting either. The yeast homolog to the mammalian 48 kDa OST component is the protein WBP1 (Silberstein et

al., 1992), and overexpression of WBP1 did not lead to increased OST activity in yeast (te Heesen et al., 1992). WBP1 was shown to be an essential yeast protein; depletion of WBP1 led to underglycosylation and eventual cell death. Thus the evidence suggests that co-translational glycosylation site occupancy is not modulated by the amount of OST enzyme complex.

Although the amount of OST probably does not limit glycosylation, it is possible that the activity of the enzyme complex could vary. For example, Oda-Tamai et al. (1985) present evidence that changes in OST activity cause a decrease in glycosylation in regenerating rat liver. The altered glycosylation site occupancy was apparently unrelated to oligosaccharide precursor availability. Changes in membrane composition and fluidity are also associated with rat liver regeneration, and these changes may have played a role in modulating OST activity. *In vitro* studies have shown that OST activity has a stringent requirement for phospholipid, with phosphatidylcholine being much more effective than other naturally occurring phosphoglycerides (Chalifour and Spiro, 1988). Microsomes from vitamin A deficient rat livers also show a radically altered lipid composition and reduced OST activity (Chan and Wolf, 1987). Thus membrane composition is a possible modulator of enzyme activity. Some biochemical factors are also known to influence OST activity in *in vitro* assays. The OST activity is stimulated by bivalent metal ions, with Mn^{2+} being the most effective (Bause and Legler, 1981). OST is maximal at a neutral pH, with activity dropping off quickly below pH 6.5 (Bause and Legler, 1981). In summary, several biochemical factors may affect oligosaccharyltransferase activity, but the amount of the enzyme is probably not limiting.

2.3.3 Substrate Amino Acid Sequence

The extent to which a potential glycosylation site is utilized can depend upon the amino acid sequence of the substrate. Early analysis of glycoprotein amino acid sequences identified the consensus recognition sequence Asn-Xxx-Ser/Thr (where Xxx is any amino

acid) as a requirement for N-linked glycosylation. As more protein sequences have become available, the consensus sequence has been generally confirmed, although rare exceptions have been identified (Gavel and von Heijne, 1990). Surveys of protein data bases have found that the tripeptide sequences Asn-Xxx-Thr and Asn-Xxx-Ser appear with equal frequency, but that sequences containing Thr are two to three times more likely to be glycosylated than sites containing Ser (Gavel and von Heijne, 1990; Kaplan et al., 1987). This conclusion is consistent with the finding that hexapeptides with Asn-Xxx-Thr were forty-fold better acceptors than peptides with Asn-Xxx-Ser when assayed *in vitro* (Bause and Legler, 1981). Although the *in vitro* results exaggerate the *in vivo* differences, recent experiments with specific model proteins have confirmed that threonine is the more effective hydroxy amino acid in the glycosylation sequon (Holst et al., 1996; Kasturi et al., 1995).

The amino acid in the Xxx position of the recognition sequence has also been shown to influence glycosylation site occupancy. From analysis of protein data bases, it was found that certain amino acids such as Cys, Trp and Pro were very rare in the Xxx position of glycosylated proteins (Kaplan et al., 1987). A recent study used site-directed mutagenesis to substitute each of the 20 common amino acids for the Xxx position of an Asn-Xxx-Ser sequon of a cell surface glycoprotein (Shakin-Eshleman et al., 1996). This study found that glycosylation site occupancy varied significantly depending upon the identity of Xxx. A Pro substituted mutant was not glycosylated at all, while mutants substituted with large hydrophobic amino acids (e.g. Trp, Leu, Phe and Tyr) were glycosylated inefficiently. It also appeared that negatively charged amino acids (Asp and Glu) inhibited glycosylation, while positively charged amino acids (Lys, Arg and His) were efficiently glycosylated.

The amino acid sequence specificity of the glycosylation reaction is likely related to the reaction mechanism. The transferase reaction is interesting because it involves the nucleophilic displacement of dolichol pyrophosphate from the donor oligosaccharide by

the primary amide nitrogen of an asparagine. Asparagine is not a particularly reactive nucleophile, and so the reaction mechanism presumably involves an activation of the primary amide (Silberstein and Gilmore, 1996). Initial proposed mechanisms for the transferase reaction suggested that the asparagine amide is activated through hydrogen bond interactions involving the hydroxy amino acid in the Asn-Xxx-Ser/Thr recognition sequence (Bause and Legler, 1981; Marshall, 1972). The secondary structure of the polypeptide acceptor was also believed to be important, based upon the observation that utilized glycosylation sites frequently have a high probability of forming a β -turn conformation (Avanov, 1991). The relevance of secondary structure to the transferase reaction was later refined based upon experiments with conformationally constrained cyclic peptide substrates (Imperiali et al., 1992a). These experiments demonstrated that, rather than a β -turn, glycosylation sites adopt an asparagine-turn conformation. The asparagine-turn is stabilized by hydrogen bond interactions between the carboxamide oxygen of asparagine, an amide from the polypeptide backbone and the hydroxyl group of the recognition site Ser/Thr. Based upon this evidence, the revised reaction mechanism presented Figure 2-7 in has been proposed (Imperiali et al., 1992b). According to this mechanism, the hydroxy amino acid of the acceptor site stabilizes an asparagine-turn conformation and is involved in the formation of an imidate tautomer, which is formed when a base from the oligosaccharyltransferase active site abstracts a hydrogen from the asparagine amide. The imidate tautomer is a competent nucleophile to displace dolichol pyrophosphate from the oligosaccharide precursor. This mechanism would explain the pH dependence of the transferase reaction and the importance of the Xxx amino acid. A low pH would interfere with hydrogen bonding, while bulky Xxx side chains and proline might interfere with the asparagine-turn conformation.

In addition to the local amino acid sequence and secondary structure, the position of the glycosylation sequon in the polypeptide chain is important. The oligosaccharyltransferase (OST) enzyme complex is membrane bound and the substrate must reach the active site for glycosylation to occur. Experiments with membrane

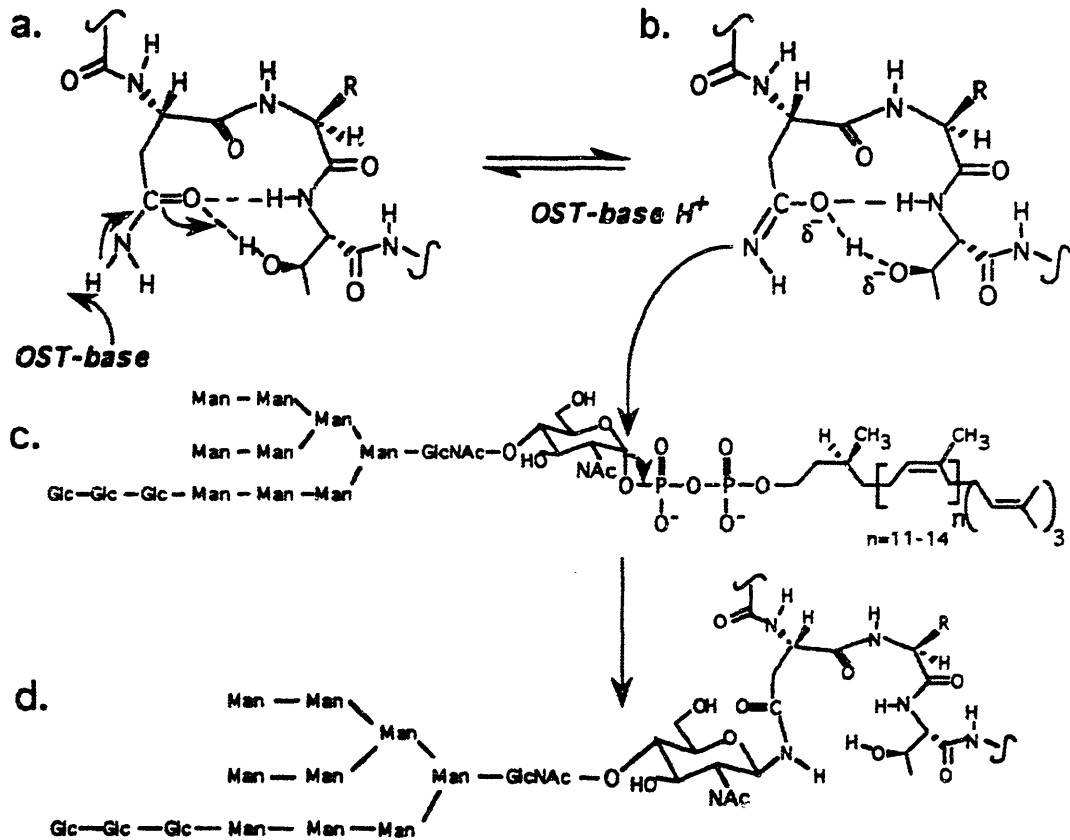


Figure 2-7. A reaction mechanism proposed by Imperiali et al. (1992b) for the oligosaccharyltransferase reaction (Figure reproduced from Silberstein and Gilmore, 1996).

proteins have determined that the acceptor must be located a minimum of 12–14 residues either upstream or downstream from the nearest transmembrane segment (Nilsson and von Heijne, 1993; Popov et al., 1997). These results refined the previous estimate that 30 amino acids must have exited the ribosomal cleft upstream of a potential glycosylation site before glycosylation could occur (Glabe et al., 1980). The precise distance required for glycosylation suggests that OST's active site is located 30–40 Å above the endoplasmic reticulum membrane surface. The membrane bound nature of the OST

enzyme complex means that there is a defined spatial “window” in which glycosylation may occur (Shelikoff et al., 1996). The polypeptide must be in close proximity to the membrane, and yet must extend at least 30 Å from the membrane surface. This stringent spatial requirement may partially explain the observation that glycosylation sites are less likely to be occupied the closer they are to the carboxy-terminus (Gavel and von Heijne, 1990). Nascent proteins are held in close proximity to the ER membrane as long as the polypeptide chain is still attached to the ribosome; once the carboxy-terminus is completed, the nascent polypeptide can move away from the membrane. Therefore glycosylation sites located closer to the amino-terminus would be expected to spend more time in the vicinity of the OST. Another possible explanation for less glycosylation towards the carboxy-terminus is that more polypeptide is available for competing folding reactions. The influence of protein folding on the transferase reaction is discussed in the next section.

2.3.4 Competition with Protein Folding

An adequate polypeptide substrate, plenty of precursor oligosaccharide and an active oligosaccharyltransferase (OST) still do not guarantee that a potential glycosylation site will be occupied. The Asn-Xxx-Ser/Thr recognition sequence must be accessible to the membrane-bound OST enzyme or the reaction will not proceed. Because glycosylation typically occurs cotranslationally, the polypeptide is only accessible to the OST for a limited time. Protein folding events also occur cotranslationally (Chen et al., 1995; Fedorov and Baldwin, 1995), and if they render the glycosylation site inaccessible, then glycosylation may not occur. The complex spatial and temporal relationship between folding and glycosylation has recently been modeled (Shelikoff et al., 1996). This model suggests that competition between folding and glycosylation may influence site occupancy heterogeneity.

There is some experimental evidence to support the concept of protein folding events interfering with glycosylation. By altering the redox potential in a cell-free transcription and translation system, Bulleid et al. (1992) demonstrated that an inverse relationship existed between disulfide bond formation and glycosylation of t-PA. Under conditions where disulfide bond formation was inhibited, glycosylation site occupancy at Asn-184 increased. The *in vitro* results were later confirmed *in vivo* by culturing recombinant CHO cells in the presence of the reducing agent dithiothreitol (DTT) to prevent co-translational disulfide bond formation in the endoplasmic reticulum (Allen et al., 1995). In accordance with *in vitro* results, inhibiting disulfide bond formation led to complete glycosylation of the otherwise partially glycosylated Asn-184. Similarly, DTT treatment of *Saccharomyces cerevisiae* has been shown to increase site occupancy of a novel glycosylation site added via mutagenesis to carboxypeptidase Y (Holst et al., 1996). In this study, similar effects were observed when *in vivo* folding was disrupted by deleting a section of the polypeptide that was known to influence folding. Hence the change in glycosylation site occupancy could be directly attributed to changes in folding, and not to a secondary effect of DTT.

2.3.5 Cell Culture Environment

This literature review has so far focused on specific mechanisms for influencing glycosylation site occupancy. A number of studies have also been published which report alterations in glycosylation in response to changes in culture environment, without identifying specific causes for the observed effects. Culture environment changes can potentially impact site occupancy through any of the mechanisms described in the preceding sections. This section briefly reviews the influence of culture environment and discusses the likely causes for observed glycosylation changes.

Several investigators have noted that ammonia can influence glycosylation. Ammonia has been shown to reduce the extent of sialylation of N-linked (Gawlitzek et al., 1995b; Kopp

et al., 1995; Thorens and Vassalli, 1986) and O-linked (Anderson and Goochee, 1995) glycoproteins. In addition, ammonia negatively impacted glycosylation site occupancy of recombinant mouse placental lactogen-I produced by CHO cells (Borys et al., 1994a). Borys et al. (1994a) demonstrated that the negative impact of ammonium chloride correlated with the concentration of the unprotonated ammonia species (NH_3) and was thus pH dependent. The uncharged species can freely diffuse across membranes, whereas the charged species (NH_4^+) must be transported through ion-transport systems. Once across the plasma membrane, ammonia may influence glycosylation by altering the intracellular pH. Sialylation in particular might be influenced by changes in pH, since the normal trans-Golgi is slightly acidic and ammonia has been shown to collapse the Golgi-cytosol pH gradient (Anderson and Goochee, 1995). The O-linked sialyltransferase from CHO cells has an approximately twofold decrease in activity as the pH is raised from 6.75 to 7.0 (Anderson and Goochee, 1995). Changes in Golgi pH could potentially cause changes in N-linked sialylation as well, assuming the N-linked sialyltransferase has a similar pH dependence. An alternative mechanism for ammonia's influence is buildup of intracellular UDP-GlcNAc + UDP-GalNAc (UDP-GNAc). Ryll et al. (1994) found that ammonium treatment leads to accumulation of UDP-GNAc, apparently due to enzymatic action of glucosamine-6-P deaminase. Normally amino sugars are formed using glutamine as the ammonia donor in a reaction catalyzed by glutamine:fructose-6-P amidotransferase (GFAT), but apparently accumulation of ammonia can lead to amino sugar formation using ammonia directly. Excessive UDP-GNAc may negatively impact glycosylation reactions.

In addition to mediating the toxicity of ammonia by altering its extent of protonation, extreme variations in culture pH have been reported to influence glycosylation in the absence of ammonia buildup (Borys et al., 1993). Borys et al. (1993) found that glycosylation of mouse placental lactogen-I by CHO cells did not vary significantly between pH 6.9 to 8.2, as determined by western blot molecular weight distributions. At lower or higher pH values, more low molecular weight species were produced,

presumably due to lower glycosylation site occupancy. The mechanism of pH disruption of glycosylation is not clear. It may be related to variations in glycosylation enzyme activities due to changes in intracellular and intracompartamental pH, since glycosylation was fairly constant within a range of external pH over which CHO cells were reported to maintain fairly constant intracellular pH (Borys et al., 1993). Alternatively, extreme pH values may disrupt cellular metabolism, which would influence the availability of sugar precursors and activated carrier molecules such as nucleoside triphosphates and dolichol phosphate.

Lipid supplements have been shown to influence glycosylation site occupancy of IFN- γ produced by CHO cells (Jenkins et al., 1994). Lipids could be expected to influence glycosylation site occupancy through at least two mechanisms. Lipids supplements could alter the activity of the oligosaccharyltransferase (OST) enzyme due to changes in the composition of the ER membrane (as discussed above in the section Oligosaccharyltransferase Activity). Alternatively, the lipid supplements may influence the availability of dolichol phosphate, thereby changing the amount of precursor oligosaccharide.

Substantial changes in glycosylation have also been observed when cells are cultured in serum-free versus serum-containing medium (Gawlitzeck et al., 1995a; Jenkins et al., 1996). In several cases cells cultured in serum-free medium had higher levels of terminal sialylation. Gawlitzeck et al. (1995a) also found that cells grown in serum-free medium had a higher glycosylation site occupancy. The effects of serum on glycosylation might be partially related to the lipid effects described above. In addition, hormones can impact glycosylation (Goochee and Monica, 1990; Konrad and Merz, 1994), and serum content will vary growth factor/hormone levels. Many hormonal and growth factor effects are mediated by cyclic AMP, and Konrad and Merz (1994) have demonstrated that cAMP stimulates lipid-linked oligosaccharide precursor synthesis in JEG-3 choriocarcinoma cells. Hormonally induced oligosaccharide precursor synthesis may be a result of

increased activity of glycosyltransferase enzymes such as UDP-GlcNAc:dolichol-P GlcNAc-1-P transferase (GPT) (Ma et al., 1996) or due to increased dolichol synthesis (Crick and Waechter, 1994). Because of the complex and undefined nature of serum, it is difficult to determine which factors are most responsible for alterations in glycosylation.

Variations in glycosylation have been noted with time during batch and fed-batch culture (Curling et al., 1990; Robinson et al., 1994; Xie et al., 1997) and with changes in culture characteristics such as extent of aggregation (Borys et al., 1994b; Coppen et al., 1995). Such changes may be due to many of the factors discussed above, including changes in pH, ammonia, lipids, etc. A further complication is that many culture environment changes would be expected to impact central carbon metabolism, and the influence of metabolism on glycosylation is not well understood. Metabolism would be expected to impact availability of sugar precursors and activated carrier molecules such as nucleoside triphosphates and dolichol phosphate. The results described in subsequent chapters of this thesis help to elucidate how normal cellular metabolism influences glycosylation site occupancy.

2.4 Model System: Recombinant Human Gamma Interferon Production in Chinese Hamster Ovary Cells

In this research, glycosylation site occupancy was analyzed for recombinant human gamma interferon (IFN- γ) produced in Chinese hamster ovary cell culture. Natural human IFN- γ is a secretory glycoprotein produced by activated T lymphocytes and natural killer cells in response to various mitogenic stimuli (Devos et al., 1982). IFN- γ is a potent member of the cytokine family with antiviral, antiproliferative and immunomodulatory activities (Farrar and Schreiber, 1993). A recombinant form of IFN- γ is sold under the trade name Actimmune by Genentech as a treatment for Chronic Granulomatous Disease (CGD) (Physicians' Desk Reference, 1996). CGD is an inherited

disorder characterized by deficient phagocyte oxidative metabolism, and IFN- γ treatment is able to stimulate phagocyte function.

Natural IFN- γ is a partially glycosylated, dimeric protein (Rinderknecht et al., 1984). The monomer has two potential N-linked glycosylation sites, and these sites are variably occupied which results in a mixture of proteins with two sites (Asn-25 and Asn-97), one site (Asn-25 only) or zero sites glycosylated (James et al., 1995). When analyzed by sodium dodecyl sulfate polyacrylamide gel electrophoresis (SDS-PAGE), IFN- γ migrates as three major bands at 16, 20 and 24 kDa corresponding to the zero, one and two site glycosylated species, respectively. IFN- γ derived from cultured leucocytes was found to be 52% two site, 39% one site and 9% zero site glycosylated, with dimers formed randomly from the variously glycosylated monomers (Sareneva et al., 1995). Natural IFN- γ also exhibits heterogeneity at the carboxy terminus due to variable proteolytic processing (Rinderknecht et al., 1984).

Human IFN- γ cDNA has been cloned (Devos et al., 1982) and expressed in several recombinant expression systems including Chinese hamster ovary cells (Scahill et al., 1983), *Escherichia coli* (Arakawa et al., 1985; Zhang et al., 1992), insect cells (James et al., 1995; Sareneva et al., 1994) and transgenic mice (James et al., 1995). Of these various expression systems, the Chinese hamster ovary (CHO) cells produce a product which most closely resembles natural human IFN- γ . CHO cell derived IFN- γ has glycosylation site occupancy heterogeneity and variable carboxy terminal processing similar to the natural product (Curling et al., 1990). Natural human IFN- γ and recombinant CHO IFN- γ also have similar site specific glycosylation characteristics. The carbohydrates of recombinant CHO IFN- γ were characterized initially by $^1\text{H-NMR}$ (Mutsaers et al., 1986) and later by matrix-assisted laser desorption/time-of-flight (MALDI/TOF) mass spectrometry (Gu et al., 1997; Harmon et al., 1996; James et al., 1995). The carbohydrates of natural IFN- γ were recently determined with MALDI/TOF (Mørtz et al., 1996), and similar structures were found. The oligosaccharides at Asn-25 are

predominantly core fucosylated complex biantennary structures, with lesser amounts of tri- and tetraantennary complex oligosaccharides. Asn-97 oligosaccharides are not core fucosylated, and they are generally less branched. Similar to the Asn-25 glycans, Asn-97 oligosaccharides are primarily complex biantennary structures, but there are fewer tri- and tetraantennary glycans and more high mannose and hybrid structures. In comparison, glycosylation of insect cell and transgenic mouse derived IFN- γ differs significantly from natural human IFN- γ (James et al., 1995). Insect cells attached mainly truncated mannose oligosaccharides, while transgenic mice produced high mannose carbohydrates at the Asn-97 site.

The site occupancy heterogeneity of IFN- γ produced in recombinant CHO cells is largely due to variable occupation of the Asn-97 glycosylation site (James et al., 1995). Typically 10% or less of the protein is non-glycosylated, while the remaining 90+% contains oligosaccharide at Asn-25. The Asn-97 site is occupied to a lesser extent, which gives rise to a significant fraction of protein glycosylated at only the Asn-25 site. Virtually no Asn-97 one site glycosylated protein is detected. There are several possible explanations for the preference of Asn-25 over Asn-97. The Asn-25 is part of an Asn-Gly-Thr recognition sequence, while Asn-97 is part of Asn-Tyr-Ser. As discussed above (see Substrate Amino Acid Sequence), threonine is a more effective hydroxy amino acid in the Asn-Xxx-Ser/Thr glycosylation sequon (Kasturi et al., 1995), and glycine would be expected to be better than the bulky aromatic tyrosine in the Xxx position (Shakin-Eshleman et al., 1996). Thus the Asn-25 is part of a more effective glycosylation sequon. Furthermore the Asn-97 residue is closer to the carboxy terminus, and, as noted previously (see Substrate Amino Acid Sequence), asparagines towards the carboxy terminus are less likely to be glycosylated than those near the amino terminus (Gavel and von Heijne, 1990). In addition the Asn-25 may be more accessible, because it is located on a random coil structure, while Asn-97 is located at the end of an alpha helix (see Figure 2-8). It is also possible that glycosylation at Asn-25 facilitates glycosylation at Asn-97. Pulse-chase radiolabeling studies with insect cells producing recombinant IFN- γ indicate

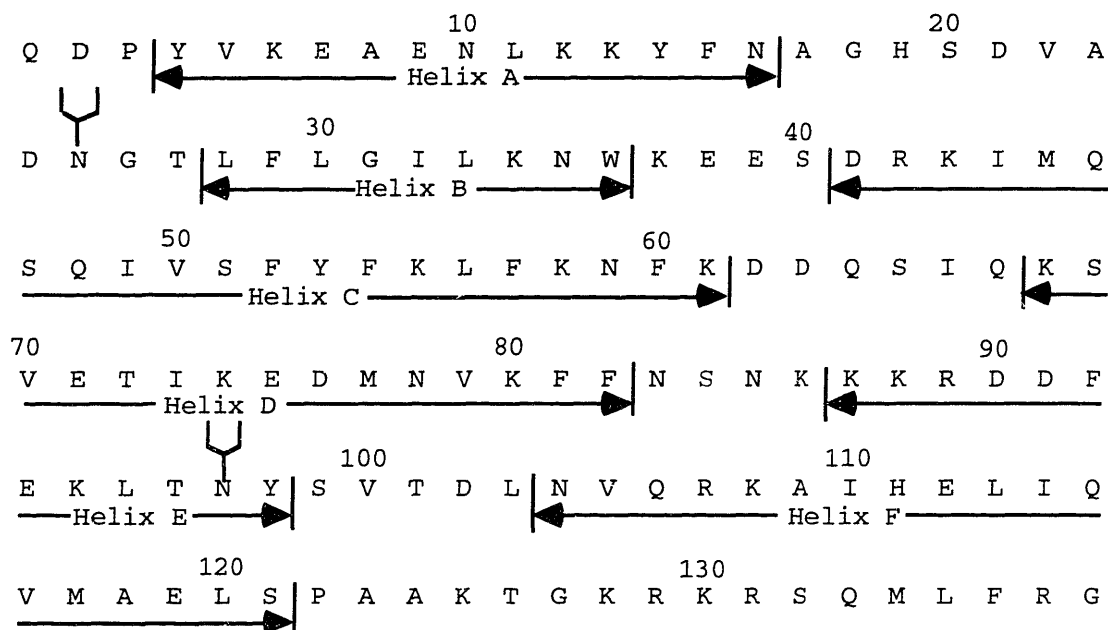



Figure 2-8. The amino acid sequence of mature human interferon- γ (after signal peptide cleavage). Glycosylation sites are indicated by .

that the Asn-25 glycans are added cotranslationally, while core glycosylation of Asn-97 occurs largely post-translationally (Sareneva et al., 1994). Glycosylation at Asn-25 would promote interaction of IFN- γ with calnexin, a membrane-bound lectin chaperone (see Implications for Protein Folding). Calnexin would keep the protein in close proximity to the membrane, making post-translational glycosylation by the membrane-bound oligosaccharyltransferase more probable.

The oligosaccharides of IFN- γ can impact the protein in many of the ways discussed previously (see Implications of N-linked Glycosylation). Glycosylation appears to be important for the correct folding and dimerization of IFN- γ , with glycosylation at Asn-25 being especially critical (Sareneva et al., 1994). When the Asn-25 glycosylation site was

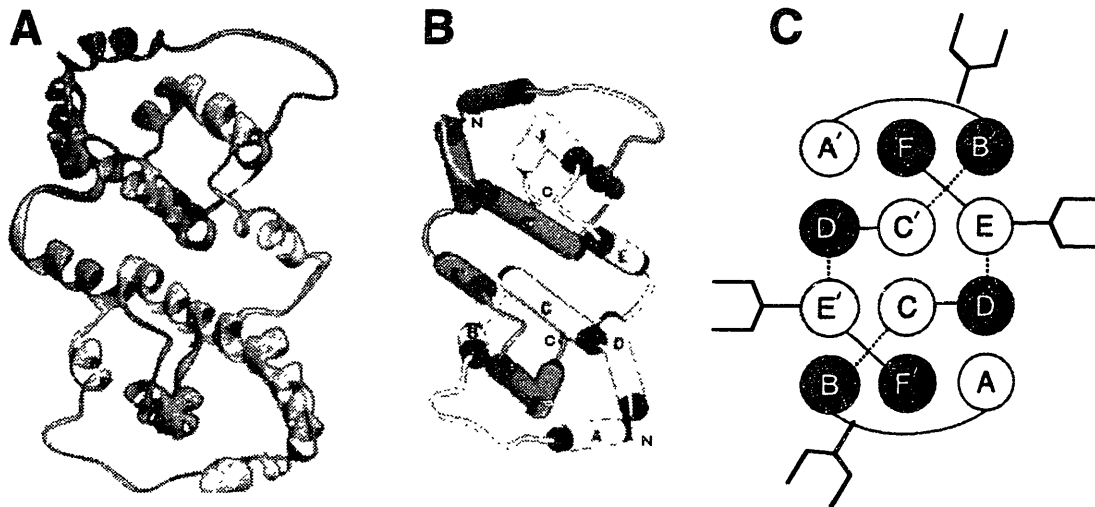
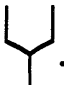


Figure 2-9. Schematic drawings of *E. Coli* derived recombinant human interferon- γ dimers (from Ealick *et al.*, 1991). (A) Ribbon drawing approximately parallel to the dimer twofold axis. (B) The α helices are represented as cylinders, while nonhelical regions are tubes. (C) α helices are represented by circles, with the N-terminal end darkened. Glycosylation sites are indicated by .

eliminated through site directed mutagenesis, dimerization was less efficient and protein secretion dropped by more than 90%. IFN- γ was observed in insoluble aggregates which were hypothesized to be misfolded material tightly bound to chaperone proteins. Inefficient folding of non-glycosylated protein might explain why *E. coli* produce recombinant IFN- γ as inclusion bodies (Arakawa *et al.*, 1985; Zhang *et al.*, 1992). IFN- γ from inclusion bodies can be refolded from 7 M urea or guanidine hydrochloride, although there is typically loss of protein due to aggregation (Arakawa *et al.*, 1985; Zhang *et al.*, 1992). Re-folded *E. coli* derived IFN- γ forms a dimer, and the crystal structure for the dimer has been solved (Ealick *et al.*, 1991). The dimer is non-covalently associated, as IFN- γ does not contain any cysteine residues or disulfide bonds. Figure 2-9 illustrates

that the dimeric structure is stabilized by intertwining of alpha helices across the subunit interface, and these interactions are believed to be essential for proper tertiary structure (Dudich et al., 1992). Natural glycosylated IFN- γ is believed to adopt a similar configuration, and the glycosylation sites are on the surface of the dimer.

In addition to aiding *in vivo* protein folding, the oligosaccharides of IFN- γ impact other protein properties. The oligosaccharides have been shown to protect the polypeptide from proteolysis by elastase, cathepsin G and plasmin (Sareneva et al., 1995). The N-linked glycans can also be important for pharmacokinetics. Naturally glycosylated IFN- γ has a longer circulatory half-life than both non-glycosylated and recombinant insect cell glycosylated IFN- γ (Sareneva et al., 1993). The glycosylated insect cell product was eliminated the most rapidly. Insect cells are known to attach primarily truncated mannose oligosaccharides to IFN- γ (James et al., 1995), and so rapid clearance of insect glycosylated IFN- γ was likely due to uptake via mannose receptors on tissue resident macrophages (see Implications for Circulatory Half-Life). This illustrates that improper glycosylation can be worse than lack of glycosylation. Proper glycosylation, on the other hand, may help IFN- γ avoid clearance in the kidney. The non-glycosylated IFN- γ dimer has a mass of around 34 kDa and is positively charged (Farrar and Schreiber, 1993). As discussed above, small positively charged molecules are likely to be cleared by the kidney. Full glycosylation increases the mass of the dimer to ~50 kDa and sialic acid residues contribute negative charges. Both of these changes may help prevent renal clearance. This hypothesis is supported by evidence that *E. coli* derived IFN- γ was cleared by perfused rabbit liver and kidney more rapidly than glycosylated IFN- γ from CHO cells (Bocci et al., 1985). A longer circulatory half-life could potentially make the CHO cell derived interferon a more effective pharmaceutical, despite the fact that glycosylated and non-glycosylated interferon have similar *in vitro* activity (Rinderknecht et al., 1984). The product sold by Genentech is derived from *E. coli*, and it is rapidly cleared from circulation when administered intravenously (Physicians' Desk Reference, 1996).

3. Materials and Methods

3.1 Cell Culture

3.1.1 Cell Line

A Chinese hamster ovary cell line producing recombinant human gamma interferon (γ -CHO) was obtained from Dr. Walter Fiers at the University of Ghent, Belgium (Scahill et al., 1983). The γ -CHO cell line was created from a dihydrofolate reductase deficient (DHFR⁻) CHO cell line by co-transfecting the cells with genes for DHFR and human gamma interferon (IFN- γ). DHFR⁻ cells require added ribonucleosides to survive, while transformed cells are able to produce their own ribonucleosides. The cells were selected for growth in 0.25 μ M methotrexate, which is a competitive inhibitor of the DHFR enzyme. Methotrexate selection leads to amplification of the DHFR gene and adjacent DNA (Kaufman and Sharp, 1982), which increases the copy number of genes co-transfected with DHFR (IFN- γ in our case). The cell line was originally grown in the presence of serum, and was anchorage dependent. To maintain selection pressure, the cells were grown in ribonucleoside-free medium with dialyzed serum and 0.25 μ M methotrexate.

3.1.2 Chaperone Protein (BiP) Levels in T-flask Cultures

Lysates were collected from the γ -CHO cell line and two other CHO cell lines to determine whether overexpression of IFN- γ affects intracellular concentrations of the chaperone protein BiP. CHO-K1 (CCL-61) and CHO/DHFR⁻ (CRL-9096) cell lines were obtained from the American Type Culture Collection (ATCC, Rockville, MD). The cell lines were all adapted to growth in RPMI-1640 medium (Sigma, St. Louis, MO) supplemented with 5% dialyzed fetal bovine serum (Sigma), 10,000 units/l penicillin (Sigma) and 10 mg/l streptomycin (Sigma). Hypoxanthine at 0.1 mM (Sigma) and 0.01 mM thymidine (Sigma) were added to the medium for the CRL-9096 cells, because the

cell line is deficient in dihydrofolate reductase and therefore requires added ribonucleosides. Cells were grown anchorage dependent in T-flasks maintained at 37°C with a 10% carbon dioxide overlay. Cell lysates were collected during the exponential growth phase and analyzed as described in Quantitative Western Blot for BiP (page 90).

3.1.3 T-flask Cultures Treated with Tunicamycin

Anchorage dependent γ -CHO cells were grown in T-25 flasks in an incubator maintained at 37°C with a 10% carbon dioxide overlay. The medium was DMEM/F12 (Sigma) supplemented with 5% dialyzed fetal bovine serum (Sigma), 0.25 μ M methotrexate (Sigma), 10,000 units/l penicillin (Sigma) and 10 mg/l streptomycin (Sigma). Cell lysates were collected from control and 10 μ g/ml tunicamycin (Sigma) treated cultures 17 hours, 24 hours and 48 hours after exposure to tunicamycin. Lysates were collected and analyzed as described in Quantitative Western Blot for BiP (page 90).

3.1.4 Adaption to Suspension Culture

The γ -CHO cell line was adapted from serum-containing medium and anchorage dependence to serum-free, suspension culture. These growth conditions were selected in order to provide a defined environment, free of serum composition variations and surface morphological effects. Cells growing in Dulbecco's Modified Eagle's Medium (Sigma, St. Louis, MO) with 10% serum (Sigma) were trypsinized from T-flasks and suspended at 3×10^5 cells/ml. Twenty ml aliquots were placed into 50 ml shake flasks, which were agitated at 70 rpm in an incubator maintained at 37°C with a 10% carbon dioxide overlay. Every 3-5 days the cells were counted and resuspended at $\sim 3 \times 10^5$ cells/ml in fresh medium. The serum-containing medium was gradually replaced by a commercial serum free medium, CHO-S-SFM (Gibco, Gaithersburg, MD) supplemented with 0.25 μ M methotrexate (Sigma), 10,000 units/l penicillin (Sigma) and 10 mg/l streptomycin (Sigma). Serum-content was reduced stepwise (5.00%, 3.75%, 2.50%, 1.25%, 0% dFBS) over a period of several weeks. As serum-free medium replaced the serum-containing medium,

clumping and wall growth gradually subsided. Cells growing on walls were avoided when transferring cells to fresh medium and flasks. The cells were completely adapted to serum-free, suspension growth after about 3.5 months. Cells seeded at 3×10^5 cells/ml typically grew to $\sim 1.8 \times 10^6$ cells/ml with a doubling time of 26 hours.

3.1.5 Low-Serum Culture

Although the γ -CHO cells grew well in CHO-S-SFM, the medium was a proprietary formulation and therefore unsuitable for experiments which required detailed knowledge of medium composition. We attempted to develop a non-proprietary serum-free medium based upon published formulations (Hamilton and Ham, 1977; Hayter et al., 1992; Jenkins, 1991). Our initial serum-free medium was an RPMI-1640 base supplemented with 10 mg/l insulin, 10 mg/l transferrin, 0.5 g/l albumin, 0.1 wt% Pluronic F-68, 1 mM sodium pyruvate, 0.1 mM alanine, 1 μ M putrescine, 11 mg/l choline chloride, 100 μ M ethanolamine, 1.5 μ M linoleic acid, 0.25 μ M methotrexate, 10,000 units/l penicillin, 10 mg/l streptomycin and trace elements according to Hamilton and Ham (1977). All medium components were obtained from Sigma (St. Louis, MO). Although the cells were able to survive in this medium, the growth rate was quite slow (~ 38 h doubling) and the maximum cell density was low ($\sim 7 \times 10^5$ cells/ml). We found that adding low concentrations of serum (0.75% dialyzed fetal bovine serum) improved the growth rate to 24 hour doubling and the maximum cell density increased to $\sim 1.5 \times 10^6$ cells/ml. “Low-serum” experiments were performed using this medium.

3.1.6 Serum-Free Culture

In order to improve growth in serum-free media, many formulations include low molecular weight digests of biological material such as yeast extracts and plant or animal tissue hydrolysates (Bonarius et al., 1996; Keen and Rapson, 1995; Schumpp and Schlaeger, 1990; Velez et al., 1986). Such additives provide sources of free amino acids, peptides, vitamins, minerals and undefined components. We tested hydrolysates from wheat, rice,

soy, and animal tissue (supplied by Quest International, Norwich, NY) at 2.5 g/l with our preliminary serum-free medium formulation to see if we could get acceptable performance without adding serum. The animal tissue hydrolysate Primatone RL (Quest International) was found to provide the best improvement.

We also found that the high concentration (0.5 g/l) of albumin in our initial serum-free medium formulation could be replaced by including 0.4 g/l 2-hydroxypropyl- β -cyclodextrin (Sigma). Cyclodextrins can act as carriers for hydrophobic molecules such as lipids and vitamins (Keen and Rapson, 1995), which is one of the primary roles for albumin. Other medium improvements included reducing insulin and transferrin concentrations, including EDTA to complex trace minerals and switching from ferrous sulfate to ferric citrate. The final serum-free medium, designated RPMI-SFM, consisted of RPMI-1640 supplemented with 2.5 g/l Primatone RL, 0.4 g/l 2-hydroxypropyl- β -cyclodextrin, 1 g/l (0.1%) Pluronic F-68, 5 mg/l insulin, 5 mg/l transferrin, 1 mM sodium pyruvate, 1 μ M putrescine, 11 mg/l choline chloride, 100 μ M ethanolamine, 1.5 μ M linoleic acid, 0.25 μ M methotrexate, 10,000 units/l penicillin, 10 mg/l streptomycin, 6.3 mg/l EDTA and trace minerals (10 nM sodium selenite, 1 nM manganese sulfate, 10 nM molybdic acid, 10 nM ammonium metavanadate, 10 nM cupric sulfate, 3 μ M zinc sulfate and 5 μ M ferric citrate). For experiments which involved 35 S methionine radiolabeling, methionine-free RPMI-1640 was used to increase the specific activity of the radiolabel. Primatone RL at 2.5 g/l contains 150 to 200% of the methionine normally supplied by RPMI-1640, and therefore ample methionine was present to support cell growth even when methionine-free RPMI-1640 was used. Cell growth was identical whether or not methionine was included in the RPMI-1640 base. In batch culture, the cells doubled every ~21 hours and reached maximum cell densities of $\sim 2 \times 10^6$ cells/ml when seeded at 2×10^5 cells/ml.

3.1.7 Culture Maintenance

Cultures were routinely maintained in shake flasks agitated at 70 rpm on an orbital shaker (Bellco, Vineland, NJ) placed in a 37°C incubator with a 5-10% carbon dioxide overlay. Every 2-4 days, cells were resuspended in fresh medium at 2×10^5 cells/ml. Frozen stocks were prepared from cells with viabilities $\geq 95\%$ by centrifuging the cells at 800 rpm for 7 minutes and resuspending the cells at 7×10^6 cells/ml in freezing medium (7.5% DMSO, 46.3% fresh medium and 46.3% conditioned medium). Vials containing 1 ml of the cell suspension were placed into a cryogenic 1°C/min freezing container (Cole-Parmer, Niles, IL) which was placed into a -70 °C freezer over-night. Cells were later transferred to a liquid nitrogen cell bank for long term storage. New cultures were started by quickly thawing the frozen cells and placing them directly into 20 ml of fresh medium in a shake flask. The following day the cells were resuspended at 2×10^5 cells/ml in fresh medium to remove the DMSO. Cells were re-suspended every 2–4 days until the viability was $\geq 95\%$, at which time experiments were initiated.

3.2 Pulse-Chase Radiolabeling Experiment

The kinetics of IFN- γ secretion were measured in a pulse-chase radiolabeling experiment. Cells growing in low-serum (0.75% dialyzed fetal bovine serum) suspension culture were collected and washed twice in phosphate buffered saline. The cells were then suspended at 7×10^5 cells/ml in 50 ml of methionine-free, low-serum medium. After a 30 minute pre-starvation period, a 5.0 mCi pulse of ^{35}S labeled methionine was added (0.1 mCi/ml final concentration). Following a 30 minute exposure to the labeled amino acid, the cells were transferred to chase medium containing excess (0.1 mM) non-labeled (“cold”) methionine. Samples (8 ml) were collected 0.5, 1.0, 1.5, 2.0 and 3.5 hours after adding the [^{35}S]methionine pulse. The samples were centrifuged for 4 minutes at $200 \times g$ to remove the cells, and the supernatants were stored at -70°C for later analysis. The radiolabeled IFN- γ was analyzed as described in Radiolabeled IFN-g Glycosylation Site Occupancy Analysis on page 87.

3.3 Pulse Radiolabeling Experiments

3.3.1 Monitoring Secreted Protein Glycosylation with Radiolabeling

To study how protein glycosylation varied with changes in culture environment, we developed a sensitive radiolabeling assay. Previously it was necessary to differentiate accumulated product data to determine glycosylation characteristics of proteins being produced at specific times during batch or fed-batch culture. Radiolabeling enabled essentially differential data to be obtained directly, and it overcame detection limit problems with methods such as western blot and silver stain. A 3 ml sample was removed from the flask to be tested and placed into a 25 ml shake flask. Between 0.5 and 1.0 mCi of ³⁵S labeled methionine was then added and the flask was incubated for 3–5 hours. No washing or media change steps were involved in the procedure, and the methionine was added from between 17 and 27 μ l of concentrated stock. This procedure allowed us to radiolabel proteins produced during a defined time interval, while introducing minimal perturbations in the cell culture environment. After the 3–5 hour incubation, the supernatant was collected and stored at -70°C for later analysis. The radiolabeled IFN- γ was analyzed as described in Radiolabeled IFN-g Glycosylation Site Occupancy Analysis on page 87.

3.3.2 Batch Culture

Glycosylation site occupancy and the concentration of the intracellular chaperone protein BiP were monitored in low-serum (0.75% dFBS) batch culture. A 500 ml spinner flask was seeded at 1.5×10^5 cells/ml and agitated at approximately 75 rpm in a 37°C incubator with a 5% carbon dioxide atmosphere. Every eight hours, a 3 ml sample was taken from the spinner flask and radiolabeled in a 25 ml shake flask with between 0.5 and 1.0 mCi of ³⁵S methionine. More radioactivity was used for early samples to compensate for the higher concentration of unlabeled methionine and the lower cell density. The radiolabel incubation lasted 3 hours. During the incubation period, the cell number and viability in

the spinner flask were determined using the trypan blue exclusion method with a hemacytometer. Samples containing 2.5×10^6 cells were then collected from the spinner flask, and the cells were lysed in 2 ml of lysis buffer (see Quantitative Western Blot for BiP on page 90). Radiolabeled supernatants were collected and analyzed for glycosylation site occupancy heterogeneity, and cell lysates were analyzed for intracellular BiP concentrations.

3.3.3 Fed Batch Culture

Fed batch cultures were performed in spinner flasks using the stoichiometric feeding technique developed at MIT (Xie et al., 1997; Xie and Wang, 1994a; Xie and Wang, 1994b). Agitation was set at 100 rpm, and the flasks were placed in a 37°C incubator with a 5% carbon dioxide atmosphere. Cultures were inoculated at $2-5 \times 10^5$ cells/ml in initial medium containing 3 mM glucose and 0.5 mM glutamine. The initial medium was either a stoichiometrically designed medium (Xie et al., 1997), or RPMI-SFM with reduced glucose and glutamine and enhanced buffer capacity. The buffer capacity of RPMI-1640 was enhanced by adding 2.09 g/l of MOPS (Sigma) and 6.50 g/l HEPES sodium salt (Sigma). To maintain proper osmolarity when the extra buffers were added, the sodium chloride concentration was reduced from 6 g/l to 2 g/l. Choice of initial medium had little impact on culture performance; similar results were obtained with the stoichiometrically designed medium and the modified RPMI-SFM. Feeding was performed with a stoichiometrically designed supplemental medium as described in Xie et al. (1997). Cell counts and feeding were performed every 12 hours. Samples were withdrawn periodically to monitor glycoform secretion with radiolabeling and to collect supernatant for later analysis.

3.3.4 Sugar Precursor Fed Cultures

The potential impact of hexose carbon on glycosylation site occupancy was studied by feeding various sugars which could be converted to oligosaccharide sugars. Cells were

pre-treated for two days in glucose-containing RPMI-SFM supplemented with 5 mM mannose (Sigma), 5 mM galactose (Sigma), 5 mM fructose (Sigma) or 2 mM glucosamine (Sigma). In addition, combinations of sugars were tested including 5 mM mannose + 5 mM galactose, 2 mM glucosamine + 5 mM mannose, 2 mM glucosamine + 5 mM galactose, 2 mM glucosamine + 5 mM fructose and 2 mM glucosamine + 5 mM pyruvate. Following the two day pretreatment, cells were resuspended in fresh media at 7.25×10^5 cells/ml with the same additives used for pretreating. Three ml samples were removed from each flask and radiolabeled with 0.5 mCi of ^{35}S methionine for 3 hours. Radiolabeled samples were analyzed for glycosylation site occupancy heterogeneity.

The influence of glucosamine feeding on site occupancy was further studied in a dose-response experiment. Cells were suspended at 1.0×10^6 cells/ml in RPMI-SFM supplemented with 0, 0.5, 1.0, 2.0 or 5.0 mM glucosamine. 4 ml samples were radiolabeled with 0.5 mCi of ^{35}S methionine for 5 hours. Radiolabeled samples were analyzed for glycosylation site occupancy heterogeneity.

3.3.5 Nucleotide Precursor Fed Cultures

Glycosylation site occupancy was studied in the presence of the nucleotide precursors uridine, orotic acid, adenosine and guanosine in 20 ml shake flask cultures. A 100 mM stock of uridine (Sigma) and 2 mM stocks of orotic acid (Sigma), adenosine (Sigma) and guanosine (Sigma) were prepared in RPMI-SFM and sterile filtered (Millex-GV, Millipore, Bedford, MA) (guanosine was not very soluble in RPMI-SFM or water, and so the final concentration after filtering may have been less than 2 mM). Each 20 ml flask was prepared by blending the appropriate concentrated precursor stock, RPMI-SFM and a concentrated cell suspension so that the initial cell density was 2.5×10^5 cells/ml. Nucleotide precursor stocks were added so that the final concentrations tested were 0.5 mM orotic acid, 1.0 mM orotic acid, 0.5 mM uridine, 1.0 mM uridine, 1.0 mM adenosine and 1.0 mM guanosine. The flasks were incubated at 37°C in a 5% CO_2 atmosphere for 2

days. On the second day, 3 ml samples were removed from each flask and radiolabeled with 0.5 mCi of ^{35}S methionine for 5 hours. During the radiolabel incubation, the cell number and size was determined for each flask using a Coulter Counter (Coulter Electronics, Hialeah, FL). Cell numbers and viabilities were also obtained using the trypan blue exclusion method with a hemacytometer. Samples containing 5×10^6 cells were then collected from each flask, and the cells were extracted with perchloric acid (see Nucleotide and Nucleotide Sugar Analysis on page 82). The radiolabeled supernatant was analyzed to determine glycosylation site occupancy of secreted protein, and the perchloric acid extracts were used to determine nucleotide concentrations.

3.3.6 Glucosamine and Uridine Fed Cultures

An experiment was designed to study the interaction between glucosamine feeding, nucleotide sugar formation, UTP depletion and glycosylation site occupancy. Cells growing in RPMI-SFM were fed 2 mM glucosamine and 5 mM uridine alone and in combination. Fifteen ml cultures were seeded in the various media at 1.0×10^6 cells/ml in 50 ml shake flasks. Following a 3 hour pre-treatment, 3 ml samples were removed from each flask and radiolabeled with 0.5 mCi of ^{35}S methionine for 5 hours. During the radiolabeling period, the cell number and size was determined for each non-radioactive flask using a Coulter Counter (Coulter Electronics, Hialeah, FL). Cell numbers and viabilities were also obtained using the trypan blue exclusion method with a hemacytometer. Samples containing 5×10^6 cells were then collected from the original flasks, and the cells were extracted with perchloric acid (see Nucleotide and Nucleotide Sugar Analysis on page 82). The radiolabeled supernatant was analyzed to determine glycosylation site occupancy of secreted protein, and the perchloric acid extracts were used to determine nucleotide concentrations.

3.3.7 Uridine Fed Batch Culture

Nucleotide sugars and glycosylation site occupancy were studied in fed batch cultures which contained uridine. The fed batch protocol described above (see Fed Batch Culture) was performed with uridine added to the initial medium. The initial medium was a modified RPMI-SFM with 3 mM glucose, 0.5 mM glutamine, 2.09 g/l of MOPS, 6.50 g/l HEPES sodium salt and 2 g/l sodium chloride. A concentrated 100 mM stock of uridine was prepared in the initial medium, and this stock was blended with initial medium and a concentrated seed culture to give 100 ml spinner flasks containing 4.5×10^5 cells/ml and uridine at 2.5 mM or 10.0 mM. Two control flasks were also analyzed: a fed batch without added uridine, and a non-fed batch with 2 mM glutamine and 11 mM glucose in the initial medium. The flasks were seeded with equal volumes from a common concentrated seed culture. Feeding was performed with a stoichiometrically designed supplemental medium as described in Xie et al. (1997). Cell counts and feeding were performed every 12 hours. At 75 hours an additional 1 mM uridine was added to the uridine containing flasks to account for expected consumption.

Every 24 hours samples were collected for radiolabeling and perchloric acid extraction. The samples were taken between feeding times to avoid transiently starved or over-fed cultures. Three ml samples were removed from each flask and radiolabeled with 0.5 mCi of ^{35}S methionine for 4 hours. During the radiolabel incubation, the cell number and size was determined for each flask using a Coulter Counter (Coulter Electronics, Hialeah, FL). Cell numbers and viabilities were also obtained using the trypan blue exclusion method with a hemacytometer. Cell aggregation (clumping) was significant for the final sample, and so cells were trypsinized before counting this sample. Two ml of sample was centrifuged at 800 rpm for 7 minutes, and the supernatant was removed. The pellet was suspended in 0.5 ml of 0.5 g/l porcine trypsin + 0.2 g/l EDTA•4Na (Sigma) by pipeting the mixture repeatedly for two minutes. Trypsin was then neutralized by adding the suspension to 1.5 ml of 1 mg/ml soybean trypsin inhibitor (Sigma). The trypsinized

sample was then counted using both the Coulter Counter and hemacytometer methods. Following cell counts, fresh samples containing 5×10^6 cells were collected from each flask, and the cells were extracted with perchloric acid (see Nucleotide and Nucleotide Sugar Analysis on page 82). The radiolabeled supernatant was analyzed to determine glycosylation site occupancy of secreted protein, and the perchloric acid extracts were used to determine intracellular nucleotide concentrations.

3.4 Continuous Culture Experiments

3.4.1 Continuous Culture Media

The media used for continuous culture experiments were slightly modified versions of the RPMI-SFM serum-free medium described above (Serum-Free Culture on page 67). Concentrations of glucose and glutamine were varied so that either glucose or glutamine was the limiting nutrient. For glucose limited continuous culture, glucose-free RPMI-1640 was supplemented with 0.5 g/l glucose (2.78 mM = 25% of normal RPMI-1640), and glutamine was added to a final concentration of 0.45 g/l (3.08 mM = 150% of normal RPMI-1640). Similarly for glutamine limited chemostats, glutamine-free RPMI-1640 was supplemented with 75 mg/l glutamine (0.51 mM = 25% of normal RPMI-1640) and 2.0 g/l glucose (11.11 mM = 100% of normal RPMI-1640).

3.4.2 Bioreactor Operation

Continuous cultures were carried out in a 2 liter Applikon (Foster City, CA) reactor with a 1.2 liter working volume. A heated water jacket maintained the temperature at 37 °C, and agitation was set at 200 rpm. The pH was controlled at $7.20 \pm .05$ by addition upon demand of 320 mM HCl or a solution of 6.2 g/l NaOH and 0.4 g/l KOH. Carbon dioxide was not included in the pH control loop so that the carbon dioxide evolution rate could be more accurately measured (see below). Oxygen was supplied via surface aeration by mixing air with either nitrogen or oxygen so that the reactor dissolved oxygen was

maintained at 45% of air saturation, with the gas flow rate controlled by a mass flow controller at 35 mol/day (~0.05 VVM). An ML-4100 multi-loop processor controller (New Brunswick Scientific, Edison, NJ) was used for the pH and oxygen control. Process data were logged through the ML-4100 controller to a computer using the AFS software from New Brunswick Scientific (Edison, NJ).

Reactor seed cultures were grown in 250 ml spinner flasks (Bellco, Vineland, NJ), and reactors were seeded at approximately 4×10^5 cells/ml. After 24 hours the feed and waste pumps were started to initiate continuous culture. Following 5 residence times, time invariance of the following variables was assumed to indicate a steady state: total cell density, viability as measured by trypan blue exclusion, glucose concentration, lactate concentration and oxygen uptake. When these parameters were steady within a 10% range for 48 hours, the system was assumed to be at steady state.

3.4.3 Oxygen Uptake Rate

The oxygen uptake rate (OUR) was obtained from the mass balance for oxygen in the liquid phase of the reactor at steady state:

$$\text{OUR} = k_L a (C^* - C_R) + D(C_F - C_R) \quad (1)$$

where $k_L a \equiv$ liquid phase mass transfer coefficient for oxygen

$C^* \equiv$ liquid phase concentration of oxygen at equilibrium with the gas phase

$C_R \equiv$ concentration of oxygen in the liquid phase of the reactor

$D \equiv$ dilution rate

$C_F \equiv$ concentration of oxygen in the liquid feed

The first term on the right hand side represents oxygen transport across the gas-liquid interface. The second term accounts for the net inflow of oxygen with the liquid streams. Liquid concentrations of oxygen in the reactor and the feed were measured with a blood gas analyzer (Ciba Corning Diagnostics, Medfield, MA). The equilibrium concentration, C^* , was calculated based on the gas phase oxygen concentration at the exit of the reactor, which was determined with a gas analyzer containing a paramagnetic oxygen sensor

(Columbus Instruments, Columbus, OH). The partial pressures of oxygen, obtained from either the blood gas analyzer or the gas analyzer, were converted to liquid concentrations using Henry's Law ($C_{O_2} = P_{O_2}/H_{O_2}$). The Henry's constant for our serum free medium at 37 °C was estimated as $H_{O_2} = 9.99 \times 10^7$ Pa mol/l based upon correlations presented by Schumpe et al. (1982) for correcting gas solubilities to account for medium composition.

3.4.4 Carbon Dioxide Evolution Rate

The carbon dioxide evolution rate (CER) was determined from a mass balancing approach similar to that of Bonarius et al. (1995), except that liquid phase carbon dioxide levels were measured rather than calculated. A mass balance for carbon dioxide over the entire reactor at steady state yields:

$$\text{CER} = \frac{\dot{n}_g}{V_R} (y_{CO_2}^R - y_{CO_2}^F) + D(C_A^R - C_A^F) \quad (2)$$

where $\dot{n}_g \equiv$ molar gas flowrate to the reactor

$V_R \equiv$ liquid volume of the reactor

$y_{CO_2}^R \equiv$ mole fraction of CO₂ in reactor headspace

$y_{CO_2}^F \equiv$ mole fraction of CO₂ in the feed gas

$D \equiv$ dilution rate

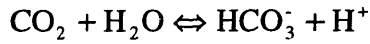
$C_A^R \equiv$ concentration of CO₂ and bicarbonate in the liquid phase of the reactor

$C_A^F \equiv$ concentration of CO₂ and bicarbonate in the liquid feed

The first term on the right hand side represents the net inflow of CO₂ between the entering and exiting gas streams. The mole fractions of CO₂ in gas streams were measured with a gas analyzer containing an IR CO₂ sensor (Columbus Instruments, Columbus, OH). To allow for more accurate determination of $(y_{CO_2}^R - y_{CO_2}^F)$, CO₂ was omitted from the feed gas ($y_{CO_2}^F < 10$ ppm).

The second term on the right hand side of equation 2 represents the net inflow of CO₂ with the liquid streams. A 250 ml pre-mixing vessel was used to equilibrate the feed liquid with air containing 12% CO₂ in order to eliminate variation in the feed CO₂ levels due to loss of CO₂ from the feed bottle. The amount of CO₂ in a particular liquid stream,

present mainly as dissolved CO₂ and bicarbonate, was determined by measuring the partial pressure of CO₂ (P_{CO_2}) and the pH using a blood gas analyzer (Ciba Corning Diagnostics, Medfield, MA). The partial pressure of CO₂ is related to the dissolved CO₂ concentration through Henry's law. The bicarbonate concentration can then be determined by assuming the simplified equilibrium relationship



which has an apparent equilibrium constant $K' = \frac{C_{HCO_3} a_H}{C_{CO_2}}$ (Putnam and Roos, 1991).

Thus measuring the partial pressure of CO₂ and the pH allows the total dissolved carbon dioxide plus bicarbonate concentration to be calculated from

$$C_A = C_{CO_2} + C_{HCO_3} = \frac{P_{CO_2}}{H_{CO_2}} \left(1 + \frac{K'}{10^{-pH}} \right) \quad (3).$$

Based on the correlations presented by Schumpe et al. (1982), the Henry's law constant for our serum free medium at 37 °C was estimated as $H_{CO_2} = 4.20 \times 10^6$ Pa mol/l, which is very close to the value (4.19×10^6 Pa mol/l) for cerebrospinal fluid at 37°C and pH = 7.20 (Severinghaus, 1965). Since both the Henry's law and equilibrium constants are functions of ionic strength, one would expect aqueous solutions with similar Henry's constants to have similar equilibrium constants. Therefore we estimated the apparent equilibrium constant as $pK' = -\log(K') = 6.138$, which is the measured value for cerebrospinal fluid at 37°C and pH = 7.20 (Severinghaus, 1965).

3.5 Analytical Methods

3.5.1 Cell Number, Viability and Dry Cell Weight

Cell number and viability were determined using a hemacytometer and microscope after staining the sample with trypan blue. Viable cells exclude the dye, while non-viable cells have lost membrane integrity and are stained blue. Total cell number was also determined using a Coulter electronic particle counter (Coulter Electronics, Hialeah, FL) after diluting

samples in an isotonic saline solution. Dry cell weight was determined by drying samples in a vacuum drying oven. One hundred ml reactor samples were collected and centrifuged at $250 \times g$ for 10 minutes, and the supernatant was removed. The cells were washed twice in phosphate buffered saline and centrifuged. After carefully removing the supernatant, cells were suspended in purified water and transferred to dried, pre-weighed aluminum weigh boats. Samples were dried to constant weights in a vacuum drying oven set at $60\text{ }^{\circ}\text{C}$.

3.5.2 Sugar and Lactate Assays

Suspension culture samples were centrifuged at $200 \times g$ for 8 minutes to remove the cells, and the supernatant was frozen at -20°C until ready for analysis. Three-hundred and forty μl of thawed sample was deproteinated before performing the lactate and sugar assays by adding 100 μl of 20% m/v trichloroacetic acid. Two-hundred μl of deproteinated sample was then neutralized with 50 μl of 25% m/v potassium bicarbonate. Enzymatic glucose and lactate assays were performed according to the 16-UV and 826-UV Sigma assay protocols (Sigma, St. Louis, MO), respectively. Enzymatic assays for fructose and mannose were performed according to kit 139-106 from Boehringer Mannheim (Indianapolis, IN). Galactose was measured using enzymatic kit 176-303 from Boehringer Mannheim. The amino sugar glucosamine was quantified using the amino acid HPLC measurement protocol described below (the amino group of glucosamine was derivitized along with the amino acids). The peak corresponding to glucosamine was determined by running spiked samples. A linear calibration was determined by running glucosamine standards.

3.5.3 Amino Acid Analysis

Samples for amino acid analysis were thawed and diluted between 1.5 and 3.5 times, so that the maximum expected amino acid concentration was less than 1 mM (the upper limit of calibration). The internal standards norvaline and sarcosine were added during dilution,

so that they were both present at a final concentration of 0.5 mM. Samples were then deproteinated using Ultrafree-MC 5,000 MW cut-off ultrafilters (Millipore, Bedford, MA). Amino acids were analyzed using the AminoQuant protocol on an HP 1090 HPLC (Hewlett Packard, Palo Alto, CA). This protocol uses pre-column derivitization with ortho-phthalaldehyde (OPA) for detection of primary amino acids and 9-fluorenylmethyl chloroformate (FMOC) for detection of secondary amino acids (AminoQuant Series II Operator's Handbook, Hewlett Packard part # 01090-90025). Separation was achieved on a C18 reverse phase column (Hewlett Packard, Palo Alto, CA).

3.5.4 Measuring Amino Acids in Peptides

Amino acids present in peptides can be quantified by first deproteinating the sample and then acid hydrolyzing the peptides into individual amino acids. By measuring the free amino acid concentration before and after hydrolysis, the amount of amino acids present in peptides can be calculated:

$$\text{Peptide amino acids} = (\text{post-hydrolysis amino acids}) - (\text{pre-hydrolysis amino acids})$$

The internal standards norvaline and sarcosine were added to samples so that their final concentrations after hydrolysis and neutralization would be 0.5 mM. Samples were then deproteinated using pre-rinsed Ultrafree-MC 5,000 MW cut-off ultrafilters (Millipore, Bedford, MA). It was important to pre-rinse the filters with water before use, because the filters contain extractable triethylene glycol that is present as a humectant. If this triethylene glycol is not flushed from the membrane, then a brown precipitate will form during the hydrolysis step. Following deproteination the samples were dried in microcentrifuge tubes in a Speed-Vac (Savant Instruments, Farmingdale, NY).

Samples were hydrolyzed using constant boiling (6 N) hydrochloric acid according to the method of Chiou and Wang (1989). Reusable Pyrex hydrolysis tubes as described in Chiou and Wang (1988) were ordered from the Custom Glass Shop, which is a division of the Kontes Glass Company (Vineland, NJ). Before each use the tubes were cleaned with

a 2:1 nitric to sulfuric acid mixture, and then rinsed with purified water and dried. The deproteinated, dried reactor samples were dissolved in 6 N HCl (Pierce, Rockford, IL), and then 200 μ l of each reconstituted sample was added to separate hydrolysis tubes. The tubes were purged of oxygen by alternately flowing nitrogen and pulling a vacuum for 15 second intervals over 2 minutes while gently agitating the tubes. The tubes were sealed while nitrogen flowed over the openings. The samples were hydrolyzed individually in a microwave at 80% of full power (approximately 1200 W) for 4 minutes each. Four minutes was established as an appropriate time by hydrolyzing chicken egg white lysozyme (Sigma, St. Louis, MO) for various times and comparing actual amino acid recoveries to theoretical recovery based upon the amino acid sequence. Four minutes provided good recovery for most amino acids, with less destruction of labile amino acids such as serine and threonine (data not shown). Hydrolyzed samples were cooled in ice water to condense volatilized HCl, and then 100 μ l of sample was neutralized with 75 μ l of 8 M NaOH and 25 μ l of 0.4 N borate buffer. Amino acids were then analyzed using the AminoQuant procedure described above. Each sample was hydrolyzed in quadruplicate, with amino acid measurements for each hydrolysis in duplicate.

The hydrolysis procedure described above causes extensive degradation of tryptophan, and glutamine and asparagine are deamidated to glutamate and aspartate, respectively. Of these amino acids, glutamine and asparagine are important in terms of central carbon metabolism. If peptide glutamate+glutamine (glx) or aspartate+asparagine (asx) are consumed by the cells, then the consumption of each of these individual amino acids must be estimated. For the experiments described here, there was no significant uptake of glutamine or glutamate from peptides (i.e. glx measured in peptides was the same in the feed and reactor samples within experimental error). Significant peptide asx uptake was detected, however, and so the asx was assumed to be 48% asparagine and 52% aspartate, based upon a measured amino acid composition for animal cell protein (Xie and Wang, 1994a).

3.5.5 Nucleotide and Nucleotide Sugar Analysis

Analysis of nucleotides and nucleotide sugars was performed based upon the methods of Ryll and Wagner (1991). Cells were extracted using perchloric acid (PCA), and neutralized extracts were analyzed with ion-pair reverse phase HPLC. Some modifications in the ion-pair HPLC buffers and gradients were required to obtain adequate separation of the desired nucleotides and nucleotide sugars.

3.5.5.1 Extraction of Cells

Approximately 5×10^6 cells were removed from the reactor and immediately centrifuged at 0°C and $190 \times g$ for 3 minutes. After discarding the supernatant, 500 μl of ice-cold 0.5 M perchloric acid (Mallinckrodt, Paris, KY) was added and the sample was vortexed vigorously. The sample placed on ice for 2 minutes before centrifuging at 4°C and $10,000 \times g$ for 3 minutes. The supernatant was placed on ice and the insoluble pellet was extracted a second time with 500 μl of ice-cold 0.5 M PCA. Following another centrifugation at 4°C and $10,000 \times g$ for 3 minutes, the supernatants from the first and second extractions were combined. Eight-hundred μl of the combined extract was then neutralized with 200 μl of ice-cold 2.5 M KOH (Mallinckrodt) in 1.5 M K_2HPO_4 (Sigma, St. Louis, MO). After sitting on ice for 2 minutes, the neutralized sample was centrifuged at 4°C and $10,000 \times g$ for 3 minutes to remove the potassium perchlorate precipitate. The supernatant was filtered using a 0.2 μm syringe filter (Acrodisc, Gelman Sciences, Ann Arbor, MI), and the samples were stored at -70°C prior to HPLC analysis.

3.5.5.2 Ion-Pair High Performance Liquid Chromatography

In order to obtain acceptable separation of the desired nucleotides and nucleotide sugars from the cell extracts, we found it necessary to slightly modify the buffer pH's and gradients reported by Ryll and Wagner (1991). Two separate analyses with different buffer pH's and gradients were required to quantify all of the desired compounds. For both analyses the buffer compositions were the same; buffer A was 100 mM potassium

phosphate buffer (Sigma) + 8 mM tetrabutylammonium hydrogen sulfate (Sigma), and buffer B was 70% buffer A plus 30% methanol (EM Science, Gibbstown, NJ). Buffers were prepared with HPLC grade water (EM Science) and were filtered (0.45 μ m Durapore filter, Millipore, Bedford, MA) and degassed before use. Chromatography was performed using an HP 1090 HPLC (Hewlett Packard, Palo Alto, CA). Separation was achieved on a Supelcosil LC-18-T column (150 mm long \times 4.6 mm inside diameter, 3 μ m particle size) equipped with a guard column (Supelco, Bellefonte, PA). Sample detection by a diode array detector was at 254 nm, referenced to the 390 nm wavelength.

Nucleotide sugars and all nucleoside phosphates except UTP and GTP could be resolved using buffers A and B at pH = 6.0. Buffers were pH adjusted with 4 M phosphoric acid (Sigma) and 4 M KOH (Mallinckrodt). The gradient used was 0% buffer B for 7 minutes followed by a 0–40% buffer B linear gradient over 5 minutes, a 40–100% buffer B linear gradient over 6 minutes, a hold at 100% buffer B for 5 minutes, a switch from 100–0% buffer B in 1 minute and finally a hold at 0% B for 6 minutes to equilibrate the column for the next sample. The flow rate was 1.5 ml/min, and the column temperature was controlled at 40°C. Figure 3-1 shows a typical chromatogram for a 150 μ l injection of CHO cell perchloric acid extract analyzed using this method. Under these chromatographic conditions UTP and GTP co-eluted, but these two nucleotides could be resolved by switching to pH = 5.0 buffers. The nucleotide sugars UDP-glucose (UDP-Glc) and GDP-mannose (GDP-Man) also co-eluted, as did UDP-N-acetylglucosamine (UDP-GlcNAc) and UDP-N-acetylgalactosamine (UDP-GalNAc). These nucleotide sugars co-eluted under all conditions tested with PCA cell extracts, and so the composite UDP-Glc+GDP-Man and UDP-GNAc (UDP-GlcNAc+UDP-GalNAc) are reported here. UDP-GlcNAc and UDP-GalNAc can be interconverted readily by UDP-GalNAc 4-epimerase, and the two species were present at the equilibrium ratio in glucosamine fed HeLa cells (Kornfeld and Ginsburg, 1966). Therefore, the composite UDP-GNAc is expected to indicate relative UDP-GlcNAc abundance.

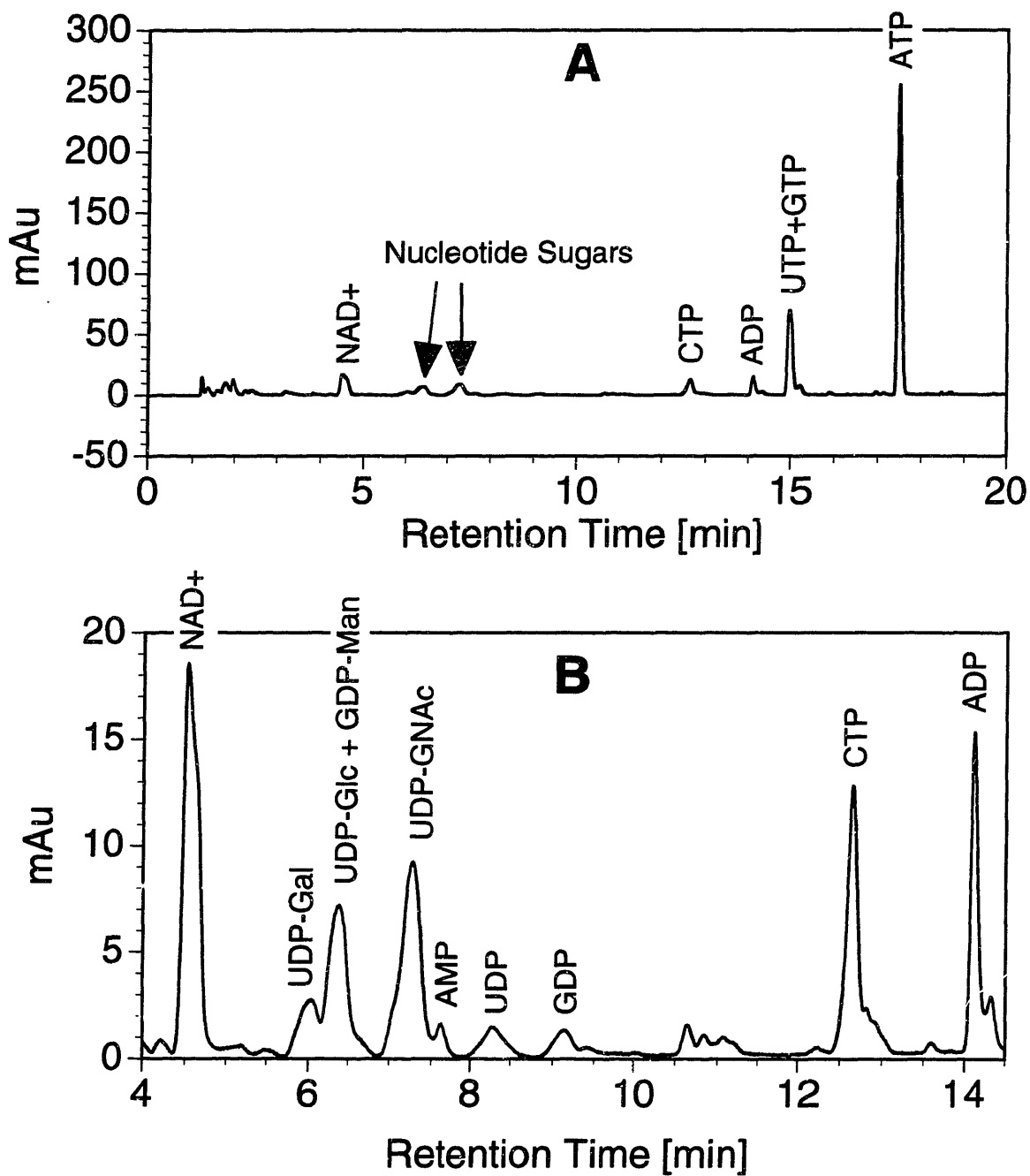


Figure 3-1. Example chromatogram for a 150 μ l injection of CHO cell PCA extract analyzed with pH=6.0 buffers. A. Entire chromatogram. B. Detail of nucleotide sugar region.

Switching buffers A and B to pH = 5.0 provided resolution between UTP and GTP, but the retention times of UDP and GDP also shifted. When PCA cell extracts were analyzed, the UDP and GDP peaks overlapped with nucleotide sugar peaks to such an extent that they were difficult to quantify. For this reason samples were run with pH = 6.0 buffers to quantify all nucleotide sugars and nucleotides except for UTP and GTP. At a pH of 5.0, it was possible to quantify UTP and GTP, and to obtain additional measurements for ATP, ADP and CTP. The gradient used with pH = 5.0 buffers was a 0–25% buffer B linear gradient over the first 22.5 minutes followed by a 25–100% buffer B linear gradient over 3.5 minutes, a hold at 100% buffer B for 6 minutes, a switch from 100–0% buffer B in 1 minute and finally a hold at 0% buffer B for 7 minutes to equilibrate the column for the next sample. The flow rate was 1.5 ml/min, and the column temperature was set at 40°C. Figure 3-2 shows a typical chromatogram for a 150 µl injection of CHO cell PCA extract analyzed with pH 5.0 buffers.

Chromatogram peaks were identified by comparing retention times and by analyzing samples spiked with standards (nucleotide and nucleotide sugar standards were obtained from Sigma), and these results agreed with the elution order and peak designations reported by Ryll and Wagner (1991). Integrated peak areas were used for quantification. Peak areas were related to concentration via standard curves which were obtained by running standards at concentrations between 100 and 10,000 pmol. Concentration was linearly related to peak area over this range.

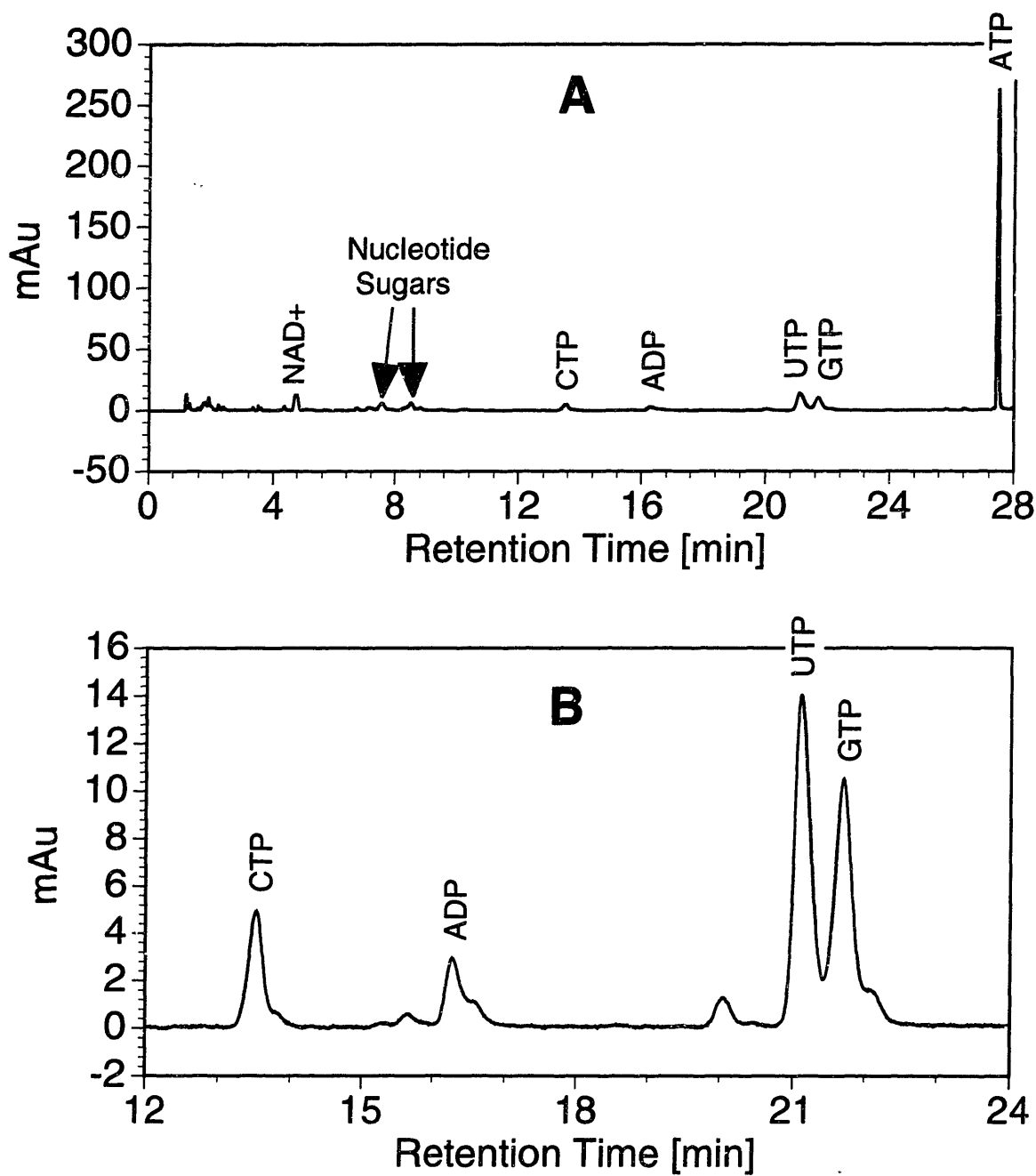


Figure 3-2. Example chromatogram for a 150 μ l injection of CHO cell PCA extract analyzed with pH = 5.0 buffers. A. Entire chromatogram. B. Detail of UTP and GTP separation.

3.5.6 Determination of IFN- γ Concentration

Gamma interferon concentrations were measured using a commercially available ELISA kit (Endogen, Inc., Cambridge, MA). Prior to analysis, samples were diluted to less than 1 $\mu\text{g/l}$ IFN- γ (the maximum standard concentration) in a 10 g/l solution of bovine serum albumin in phosphate buffered saline (Pierce, Rockford, IL). It was important to include BSA in the dilution buffer to avoid loss of IFN- γ due to non-specific adsorption to tube walls. The assay was performed according to the manufacturer's protocol.

3.5.7 Radiolabeled IFN- γ Glycosylation Site Occupancy Analysis

Glycosylation site occupancy of labeled IFN- γ in radioactive supernatants was determined by immunoprecipitating the IFN- γ , separating the glycoforms based on molecular weight using gel electrophoresis, and then analyzing the dried gels using autoradiography. Immunoprecipitation was carried out with 1.4 ml of labeled supernatant added to 1 ml of IP reaction buffer (50 mM Tris-HCl pH=8.2, 5 mM EDTA, 5 mM EGTA). Thirty μl of a 1:1 suspension of phosphate buffered saline:IgG antibody-sepharose complex (Reselute- γ affinity chromatography medium, Celltech Ltd., Slough, UK) was added to each sample. Samples were incubated with agitation for at least 3 hours at 4°C. Following incubation the sample was centrifuged 1 minute at 200 \times g, and the pellet was washed twice with wash buffer I (0.5% nonidet P40, 50 mM Tris-HCl, 500 mM NaCl, 5 mM EDTA, 1 g/l bovine serum albumin, pH=8.0), twice with wash buffer II (0.5% nonidet P40, 50 mM Tris-HCl, 5 mM EDTA, pH=8.0) and once with water. Samples were eluted by boiling for 5 minutes in 60 μl of 2X non-reducing SDS-PAGE sample buffer (125 mM Tris-HCl pH=6.8, 20% v/v glycerol, 4% w/v SDS, 0.0025% w/v bromophenol blue).

Five μl of the eluted sample was used for scintillation counting (LS6500, Beckman Instruments, Inc., Fullerton, CA) to determine the activity of precipitated interferon. Equal amounts of radioactivity (10,000 to 15,000 dpm) were loaded per lane onto 12%

polyacrylamide gels for sodium dodecyl sulfate polyacrylamide gel electrophoresis (SDS-PAGE) in the Bio-Rad Mini-Protean II electrophoresis system (Bio-Rad, Hercules, CA). The gels were run at a constant voltage of 130 V until the bromophenol blue dye front had migrated to the bottom of the gel (1.2 to 1.5 hours). Following electrophoresis the gels were treated with Entensify autoradiography enhancer (DuPont NEN, Boston, MA) and dried. The dried gels were either exposed to pre-flashed X-ray film (X-OMAT AR, Eastman Kodak Co., Rochester, NY) or a phosphor screen (Molecular Dynamics, Sunnyvale, CA). The amount of each glycoform was determined from films using densitometry (Molecular Dynamics) or from phosphor screens using a PhosphorImager (Molecular Dynamics).

3.5.8 Accumulated IFN- γ Glycosylation Site Occupancy Analysis

Glycosylation site occupancy heterogeneity of total accumulated IFN- γ was analyzed by immunoprecipitating IFN- γ from culture supernatants and analyzing the purified product using micellar electrokinetic capillary chromatography (MECC). Following immunoprecipitation, the IFN- γ was directly eluted into the MECC running buffer. This procedure provided more reproducible glycosylation site occupancy results than when IFN- γ was purified with affinity chromatography followed by a low pH (pH=2–3) elution. Purifications that involved a low pH elution yielded non-reproducible fractions of non-glycosylated protein (data not shown). Non-glycosylated gamma interferon is known to unfold at low pH and aggregate in the presence of salts. This aggregation has been suggested as the reason IFN- γ activity is unstable in an acid environment (Arakawa and Hsu, 1987). Furthermore the Asn-25 glycan of glycosylated IFN- γ has been shown to play an important role in folding and dimerization (Sareneva et al., 1994). We hypothesize that non-reproducible results obtained using low pH elution may have been due to aggregation of non-glycosylated IFN- γ , while the glycans of glycosylated IFN- γ may have prevented or reduced aggregation loss.

3.5.8.1 Immunoprecipitation

Samples containing approximately 10 µg of IFN-γ (between 4 and 8 ml of chemostat steady state samples) were filtered (0.22 µm Millex-GV, Millipore, Bedford, MA) and mixed 2:1 with IP reaction buffer (50 mM tris-HCl, 5 mM EDTA, 5 mM EGTA, pH = 8.2). Thirty-five µl of a 1:1 suspension of phosphate buffered saline:IgG antibody (anti-IFN-γ)-sepharose complex (Reselute-γ, Celltech Ltd., Slough, UK) was added to each sample. Samples were incubated at 4 °C with agitation overnight. Following incubation samples were centrifuged for 1 minute at 200 × g, and the pellet was washed twice with wash buffer I (0.5% nonidet P40, 50 mM tris-HCl, 500 mM NaCl, 5 mM EDTA, 1 g/l bovine serum albumin, pH = 8.0), twice with wash buffer II (0.5% nonidet P40, 50 mM tris-HCl, 5 mM EDTA, pH = 8.0) and once with water. Samples were eluted directly into 35 µl of filtered (0.45 µm Durapore filter, Millipore), degassed MECC running buffer (20 mM sodium borate, 20 mM boric acid, 100 mM SDS, pH = 8.2). The samples were incubated at room temperature for 5 minutes after adding the MECC running buffer, and then vortexed, centrifuged for 1 minute at 200 × g and the supernatants transferred to 0.5 ml micro-centrifuge tubes for MECC analysis. All buffer components were from Sigma (St. Louis, MO).

3.5.8.2 Micellar Electrokinetic Capillary Chromatography (MECC)

The immunoprecipitated IFN-γ was analyzed using MECC based upon the method described by James et al. (1994). An analytical capillary electrophoresis system (Model 270A, Applied Biosystems, Foster City, CA) was equipped with a 75 µm inside diameter × 70 cm long (50 cm to detector) neutral hydrophilic bonded silica capillary (CElect P175, Supelco, Bellefonte, PA). New capillaries were conditioned by washing with 0.1 M KOH (Mallinckrodt) for 10 minutes, followed by 1 hour of MECC running buffer. Between each separation the capillary was rinsed with 0.1 M KOH for 2 minutes and then MECC running buffer for 5 minutes. Samples were vacuum injected over 3 seconds, and then a 17 kV voltage was applied to the capillary. The separation was

performed at 30 °C, and the detection wavelength was set to 200 nm. The separate peaks for 2-site, 1-site and non-glycosylated IFN- γ eluted within 25 minutes, with glycoform migration time inversely related to extent of glycosylation. Chromatograms were exported from the System Gold software used for data acquisition (Beckman Instruments, Fullerton, CA) and were analyzed using the GS370 peak integration software (version 3.0, Hoefer Scientific Instruments, San Francisco, CA).

3.5.9 Quantitative Western Blot for BiP

3.5.9.1 Cell Lysis

Intracellular BiP concentrations were determined by analyzing cell lysates with a quantitative western blot. Cells were detergent lysed in a buffer containing 0.5% Triton X-100, 150 mM NaCl, 10 mM Tris-HCl (pH = 8.0) and 0.025% sodium azide. Immediately prior to use, protease inhibitors were added to the following final concentrations: 2 mM EDTA, 100 mg/l PMSF, 1 μ M pepstatin A and 10 mg/l aprotinin. Protease inhibitors were added from 100x concentrated stocks prepared in water (EDTA), isopropanol (PMSF), methanol (pepstatin A) or phosphate buffered saline (aprotinin). All buffer components were from Sigma. Approximately 1 ml of lysis buffer was used per 1.25×10^6 cells, which ensured efficient extraction (we were we were able to lyse up to 2×10^7 cells/ml without losing total protein extraction efficiency).

Anchorage dependent cells were lysed in T-flasks after removing the medium and washing the cells twice with phosphate buffered saline (PBS). Ice cold lysis buffer was added and the flask was incubated on ice for 30 minutes. Following the first incubation, the T-flask was shaken vigorously to free residual cells from the walls and then incubated another 30 minutes on ice. The lysate was collected and centrifuged at $10,000 \times g$ at 4°C for 10 minutes, and the clarified supernatant was stored at -20°C until ready for western blot analysis. Suspension cells were lysed in a similar fashion after spinning the cells down at $200 \times g$ for 7 minutes and removing the supernatant. Cells were washed in PBS,

centrifuged and then suspended in ice-cold lysis buffer. The suspension was vortexed and placed on ice for 30 minutes before vortexing a second time. After another 15 to 30 minute incubation on ice, the lysate was collected and centrifuged at $10,000 \times g$ at 4°C for 10 minutes, and the clarified supernatant was stored at -20°C .

3.5.9.2 *Quantitative Western Blot*

Lysates were prepared for western blot analysis by mixing them 1:1 with 2x SDS-PAGE sample buffer (125 mM Tris-HCl pH=6.8, 80 mM dithiothreitol, 20% v/v glycerol, 4% w/v SDS, 0.0025% w/v bromophenol blue) before heating the samples in boiling water for 5 minutes. BiP standards were prepared from recombinant hamster BiP produced in *E. coli* (Stressgen, Victoria, BC, Canada). The standards were diluted in lysis buffer, mixed 1:1 with 2x SDS-PAGE sample buffer and heated in boiling water for 5 minutes. Four standards were loaded on each gel at between 0.2 and 0.02 $\mu\text{g}/\text{lane}$ to produce a standard curve. Ten μl of each sample was loaded per lane onto 12% polyacrylamide gels for sodium dodecyl sulfate polyacrylamide gel electrophoresis (SDS-PAGE) in the Bio-Rad Mini-Protean II electrophoresis system (Bio-Rad, Hercules, CA). The gels were run at a constant voltage of 130 V for 1.25 hours.

Following electrophoresis, the gels were incubated in transfer buffer (25 mM tris base and 14.4 g/l glycine in a 20% methanol solution) at 4°C for 15 minutes. Proteins were then transferred from the gels onto nitrocellulose membranes in the Mini Trans-Blot Electrophoretic Transfer Cell (Bio-Rad) set at a constant 100 V for 45-60 minutes. Following the transfer, the membranes were rinsed in TBST, a tris buffered saline solution containing the detergent Tween-20 (10 mM Tris-HCl, 150 mM NaCl, 0.05% Tween-20, pH=8.0). The rinsed membranes were soaked two hours in a blocking buffer which contained 5% non-fat dry milk in TBST to saturate the nitrocellulose non-specific protein binding capacity. The blocked membranes were then rinsed 3x5 minutes in TBST before adding the primary antibody solution (30 μl of rabbit-derived polyclonal anti-BiP

antibody solution (Stressgen) in 40 ml of 2% non-fat dry milk in TBST). After a one hour incubation in the primary antibody solution, the membranes were again washed 3x5 minutes in TBST. The next step was a 1 hour incubation in the secondary antibody solution (15 μ l of horseradish peroxidase conjugated goat anti-rabbit IgG antibody solution (Bio-Rad) in 45 ml of 2% non-fat dry milk in TBST). In preparation for the development step, the membranes were rinsed 3x5 minutes in TBS (TBST without Tween-20). The membranes were developed using the Renaissance Enhanced Chemiluminescence kit (DuPont NEN, Boston, MA), and the results were recorded by exposing the membranes to pre-flashed X-ray film (X-OMAT AR, Eastman Kodak Co., Rochester, NY) for exposure times ranging from 5 seconds to 5 minutes. Films were developed in a film processor (Eastman Kodak Co.), and the results were quantified using a laser densitometer (Molecular Dynamics, Sunnyvale, CA). Standard curves were prepared from the integrated band intensities of standards run on the same gel as the unknowns.

3.5.10 Total Protein Assay

Total protein concentrations in cell lysates were determined using the Bio-Rad DC Protein Assay (Bio-Rad, Hercules, CA). The DC Protein Assay is compatible with ionic and non-ionic detergents, and therefore can be used with detergent-lysed cells. Bovine gamma globulin (Bio-Rad) was used as a standard. The standard was prepared in the same buffer used for cell lysis at the following concentrations: 0.1, 0.3, 0.5, 0.7 and 0.9 mg/ml. The assay was performed according to the instructions provided by the manufacturer, and unknown protein concentrations were determined from a linear standard curve.

3.6 Material Balancing for Intracellular Flux Analysis

3.6.1 Biochemical Network

The simplified biochemical reaction network considered here is depicted in Figure 3-3 and listed in Table 3-1. The network includes the reactions of central carbon metabolism which have been identified as important for producing biomass and energy (Bonarius et al., 1996; Savinell and Palsson, 1992; Stryer, 1988; Xie and Wang, 1996b; Zupke and Stephanopoulos, 1995). Groups of serial reactions were lumped into single reactions, and only pathways carrying significant flux were included. Production of recombinant protein represented less than 0.4% of biomass production, and so was neglected. Consumption of network intermediates for biosynthesis was treated as described in Zupke and Stephanopoulos (1995). The composition of CHO cells used for deriving the biomass requirements was estimated from measured values for hybridoma cells (Xie and Wang, 1994a). The estimated biosynthesis demands are listed in Table 3-2.

In this simplified network, flux through the pentose phosphate pathway is estimated from the biosynthetic demand for ribose-5-P in nucleotide synthesis. There is no accounting for recycling in the pentose phosphate pathway (PPP). NADPH production cannot unambiguously be used to calculate the pentose phosphate recycle because of uncertain transhydrogenase activity linking NADH and NADPH, and the fact that the malic enzyme can use either NAD⁺ or NADP⁺ as a cofactor (Eigenbrodt et al., 1985). In this analysis we lump NADH and NADPH into a single NAD(P)H pool of reducing power, and this NAD(P)H pool is related to both biomass synthesis and oxygen uptake. Under these assumptions, recycle in the pentose phosphate pathway and recycle in the citric acid (TCA) cycle are indistinguishable; in both cases 2 equivalents of reducing power are generated per carbon dioxide evolved. The inability to distinguish between TCA and PPP recycle makes networks incorporating PPP recycle and lumped NAD(P)H effectively singular. Thus our estimate for the TCA cycle flux may be an overestimate that also includes PPP recycle.

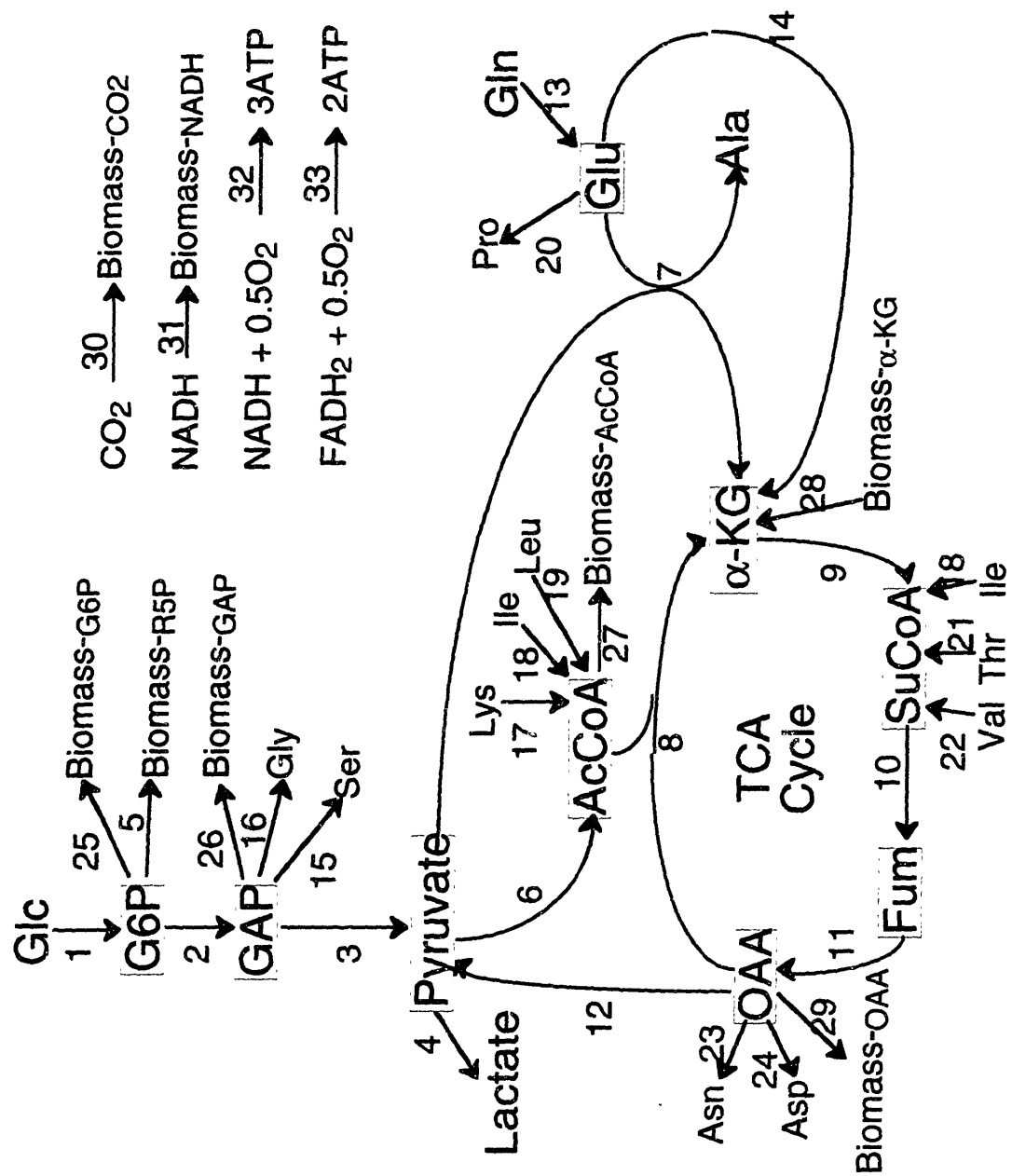


Figure 3-3. Schematic diagram of a simplified biochemical reaction network describing central carbon metabolism.

Table 3-1. Listing of reactions included in the simplified biochemical reaction network describing central carbon metabolism.

1	glucose + ATP → glucose-6-P + ADP
2	glucose-6-P + ATP → 2 glyceraldehyde-3-phosphate + ADP
3	glyceraldehyde-3-phosphate+2ADP+NAD ⁺ → pyruvate+2ATP+NADH
4	pyruvate + NADH → lactate + NAD ⁺
5	glucose-6-P + 2 NADP ⁺ → Biomass_R5P + CO ₂ + 2 NADPH
6	pyruvate + CoA + NAD ⁺ → acetyl CoA + CO ₂ + NADH
7	pyruvate + glutamate ↔ α-ketoglutarate + alanine
8	oxaloacetate + acetyl CoA + NAD ⁺ → α-ketoglutarate + CO ₂ + NADH
9	α-ketoglutarate + CoA + NAD ⁺ → succinyl CoA + CO ₂ + NADH
10	succinyl CoA + GDP + FAD → fumarate + CoA + GTP + FADH ₂
11	fumarate + NAD(P) ⁺ → oxaloacetate + NAD(P)H
12	oxaloacetate → pyruvate + CO ₂
13	glutamine + H ₂ O → glutamate + NH ₄ ⁺
14	glutamate + NAD ⁺ → α-ketoglutarate + NH ₄ ⁺ + NADH
15	glyceraldehyde-3-phosphate + glutamate + 2 NAD ⁺ → serine + α-ketoglutarate + 2 NADH
16	glyceraldehyde-3-phosphate + glutamate + 2 NAD ⁺ → glycine + α-ketoglutarate + 2 NADH
17	lysine+CoA+FAD+5NAD ⁺ → 2AcCoA+2CO ₂ +2NH ₄ ⁺ +FADH ₂ +5NADH
18	isoleucine + 2 CoA + ATP + FAD + 3 NAD ⁺ → acetyl CoA + succinyl CoA + ADP + NH ₄ ⁺ + FADH ₂ + 3 NADH
19	leucine + 2 ATP + FAD + 2 NAD ⁺ → 3 acetyl CoA + 2 ADP + NH ₄ ⁺ + FADH ₂ + 2 NADH
20	glutamate + ATP + 2 NADPH → proline + ADP + 2 NADP ⁺
21	threonine + CoA+ATP+NAD ⁺ → succinyl CoA+ADP+NH ₄ ⁺ +NADH
22	valine + CoA + ATP + FAD + 4 NAD ⁺ → succinyl CoA + ADP + CO ₂ + NH ₄ ⁺ + FADH ₂ + 4 NADH
23	oxaloacetate + glutamine → asparagine + α-ketoglutarate
24	oxaloacetate + glutamate → aspartate + α-ketoglutarate
25	glucose-6-P → Biomass_G6P
26	glyceraldehyde-3-phosphate → Biomass_GAP
27	acetyl CoA → Biomass_AcCoA
28	Biomass_AKG → α-ketoglutarate
29	oxaloacetate → Biomass_OAA
30	CO ₂ → Biomass_CO ₂
31	NADH → Biomass_NADH + NAD ⁺
32	0.5 O ₂ + 3 ADP + NADH → 3 ATP + NAD ⁺
33	0.5 O ₂ + 2 ADP + FADH ₂ → 2 ATP + FAD

Table 3-2. Biomass synthesis requirements for central carbon metabolism intermediates. Requirements (in mmol/gram dry cell weight) were calculated as described in Zupke and Stephanopoulos (1995). Positive values indicate the intermediate is consumed in biomass synthesis. Amino acid requirements for protein synthesis were accounted for separately.

<u>Building Block</u>	<u>Biomass Requirement (mmole/g DCW)</u>
Acetyl CoA	4.296
Glutamine	0.376
Glutamate	-0.022
Glucose-6-P	0.248
α -ketoglutarate	-0.354
Oxaloacetate	0.094
Ribose-5-P	0.188
Glyceraldehyde-3-phosphate	0.226
ATP	27.359
NADH	-0.346
NADPH	5.911
CO ₂	-0.035

3.6.2 Calculation of Fluxes

Letting x_i represent the flux (mmole/(g DCW*d)) of reaction i , α_{ij} represent the stoichiometric coefficient of metabolite j in reaction i and r_j represent the rate of accumulation of metabolite j , a series of mass balances for each metabolite can be written based upon the stoichiometry of the reactions presented in Table 3-1:

$$r_j = \sum_i \alpha_{i,j} x_i \quad (4)$$

The resulting set of material balance equations can be expressed in matrix notation as

$$\mathbf{Ax} = \mathbf{r} \quad (5)$$

where \mathbf{A} is the matrix of stoichiometric coefficients, \mathbf{x} is the unknown vector of reaction fluxes and \mathbf{r} is the vector of metabolite production. The \mathbf{A} matrix is determined by the stoichiometry of the assumed biochemistry, and has dimensions of $m \times n$, where m is the number of metabolites in the network and n is the number of reactions. The metabolite production vector, \mathbf{r} , consists of the actual measured production rates for extracellular metabolites, while production is assumed to be zero for intracellular metabolites based upon the pseudo-steady-state (PSS) approximation. The PSS assumption is considered reasonable, because the fluxes consuming and producing internal metabolites are much larger than their expected maximum rates of concentration change (Zupke and Stephanopoulos, 1995).

The unknown fluxes can be determined from equation (5) using simple matrix inversion if \mathbf{A} is square ($m = n$). In general \mathbf{A} will not be square, since it is desirable to include redundant information so that the consistency of the data and assumed biochemistry can be analyzed. In this case $m > n$ and the fluxes can be determined via the method of weighted least squares (Strang, 1988):

$$\mathbf{x} = (\mathbf{A}^T \boldsymbol{\Psi}^{-1} \mathbf{A})^{-1} \mathbf{A}^T \boldsymbol{\Psi}^{-1} \mathbf{r} \quad (6)$$

where $\boldsymbol{\Psi}$ is the variance-covariance matrix of the measurement vector, \mathbf{r} . Equation (6) can be used to give reliable estimates for \mathbf{x} assuming the matrix \mathbf{A} is of full rank and is reasonably well conditioned. A poorly conditioned matrix will be very sensitive to slight

changes in the measurements, and hence will not give reliable flux estimates. A measure of this sensitivity is given by the condition number, $c(\mathbf{A})$, defined as:

$$c(\mathbf{A}) = \|\mathbf{A}\| \bullet \|\mathbf{A}^{-1}\| \quad (7)$$

where $\|\ \|$ indicates a matrix norm. $c(\mathbf{A})$ serves as an upper bound to the relative error magnification inherent in solving $\mathbf{Ax}=\mathbf{r}$. There are a number of ways for estimating the norm of a matrix when calculating the condition number, but the 2-norm (also called the spectral norm) provides the smallest upper bound on the potential error magnification (Gerald and Wheatley, 1994). The 2-norm condition number can be calculated from the singular value decomposition of \mathbf{A} given that:

$$\|\mathbf{A}\|_2 = \sqrt{\text{largest eigenvalue of } \mathbf{A}^T \mathbf{A}} = \text{largest singular value of } \mathbf{A} \quad (8)$$

$$\|\mathbf{A}^{-1}\|_2 = 1/\sqrt{\text{smallest eigenvalue of } \mathbf{A}^T \mathbf{A}} = 1/\text{smallest singular value of } \mathbf{A} \quad (9)$$

(Maron and Lopez, 1991). The system can be considered well posed if $c(\mathbf{A})$ is small (<100), while a large $c(\mathbf{A})$ (>1000) indicates that sensitivity problems exist. As mentioned above, our network including PPP recycle and lumped NAD(P)H is effectively singular, because recycle in the PPP and TCA cycle are indistinguishable. The 2-norm condition number for this network is 535,602, which indicates that reliable estimates of PPP recycle are not possible. The modified network neglecting PPP recycle has a condition number of 69.

3.6.3 Redundancy and Consistency

Redundant data are necessary for testing the consistency of measurements and assumed biochemistry. A systematic method for analyzing data consistency was presented by Romagnoli and Stephanopoulos (1981), and this approach has been applied to fermentation data (Wang and Stephanopoulos, 1983) and flux analysis (Vallino and Stephanopoulos, 1990; Zupke and Stephanopoulos, 1995). The method is based upon statistical hypothesis testing to determine whether redundancies are satisfied to within

expected experimental error. The reader is referred to the original references for detailed descriptions of the methodology; only a brief outline will be presented here.

The first step in the redundancy analysis is to extract the redundant equations from the stoichiometry matrix, \mathbf{A} , and then place these equations in the form

$$\mathbf{E}\mathbf{r} = \mathbf{0} \quad (10)$$

where \mathbf{E} is the matrix of redundant equations and \mathbf{r} is the vector of metabolite accumulation as defined above. Zupke and Stephanopoulos (1995) provide an illustration of these manipulations. If the assumed stoichiometry is correct and the measurement rate vector, \mathbf{r} , contains no errors, then equation (10) will be satisfied exactly. In reality the product $\mathbf{E}\mathbf{r}$ will deviate from $\mathbf{0}$, and statistical hypothesis testing can be used to judge whether the deviation can be attributed to expected random measurement error in \mathbf{r} . The hypothesis test is performed by calculating a consistency index, h , defined as

$$h = \boldsymbol{\varepsilon}^T \boldsymbol{\varphi}^{-1} \boldsymbol{\varepsilon} \quad (11)$$

where

$$\boldsymbol{\varepsilon} = -\mathbf{E}\mathbf{r} \quad (12)$$

$$\boldsymbol{\varphi} = \mathbf{E}^T \boldsymbol{\psi} \mathbf{E} \quad (13)$$

and $\boldsymbol{\psi}$ is the variance-covariance matrix of the measurements contained in \mathbf{r} . Wang and Stephanopoulos (1983) demonstrated that h follows a χ^2 distribution with the number of redundant equations determining the degrees of freedom. h can be used to determine whether the residuals of equation (10) deviate beyond their expected distribution around zero for a specified significance (confidence level). If a given \mathbf{r} fails the consistency check (i.e. $h > \chi^2$), then there is a (confidence level)% chance that either \mathbf{r} contains gross measurement errors or the assumed biochemistry is incorrect. With more than one redundant measurement, suspect measurements can be identified by eliminating measurements one at a time and recalculating h . If elimination of a particular measurement dramatically decreases h , then it is likely that either the measurement is in error, or the assumed biochemical pathways involving the particular metabolite are incorrect.

4. IFN- γ Glycosylation Site Occupancy in Batch and Fed-Batch Cultures

Determining how cell culture parameters influence glycosylation site occupancy in batch and fed-batch cultures requires a sensitive assay for measuring changes in glycosylation. Typically, glycosylation of the accumulated product is analyzed by techniques such as western blot, silver stain or capillary electrophoresis. Because the environment is continually changing in batch and fed-batch cultures, the secreted product which accumulates in the media is the combined product from cells growing under a range of different conditions. To determine how culture conditions at a specific instant are influencing glycosylation, it is necessary to consider only the product being produced at that instant. For sufficiently large changes in glycosylation, it is possible to determine instantaneous glycosylation characteristics by differentiating accumulated product data. However, differentiation of data tends to magnify experimental errors, and accurately determining differential glycosylation requires large changes in the accumulated product. Furthermore, differentiation can be problematic for late times in a batch culture, when even large changes in the freshly secreted product will have little impact on the accumulated product.

This chapter presents an alternative method for monitoring glycosylation site occupancy heterogeneity with time in batch and fed-batch cultures. A sensitive radiolabeling assay was used to analyze product made during defined time intervals. Product glycosylation was determined by pulsing culture samples with ^{35}S labeled methionine for three to five hours and then collecting the supernatant. The product was immunoprecipitated from the supernatant and the glycoforms were separated by SDS-PAGE. The various glycoforms were then detected and quantified by autoradiography. By analyzing only the radioactive product, differential glycosylation data was collected directly. This technique was

applied to analyze glycosylation site occupancy of recombinant gamma interferon (IFN- γ) produced at various times during batch and fed-batch cultures of Chinese hamster ovary (CHO) cells.

4.1 Glycosylation Site Occupancy Monitoring with Radiolabeling

In order to obtain accurate “snap-shots” of secreted product glycosylation site occupancy, it was necessary to develop a method for selectively analyzing proteins synthesized during defined time intervals. A protocol was developed which allowed site occupancy to be determined for proteins produced during three hour labeling periods. The method was designed to introduce minimal disturbances so that the analyzed product would accurately reflect glycosylation in an undisturbed culture. By adding pulses of a radioactive amino acid, very small quantities of labeled protein could be analyzed while introducing a minimal disturbance. Applying this method to analysis of glycosylation required the determination of appropriate labeling conditions, including which radioactive amino acid to use, how much to use and what labeling protocol to follow.

The most commonly used radioactive amino acid for labeling proteins is [^{35}S]methionine (Harlow and Lane, 1988). The ^{35}S isotope is generally preferred over ^3H and ^{14}C because it is easier to detect. Furthermore, ^{35}S has a much shorter half-life and therefore the radioactive waste decays more rapidly. The model protein for this study, IFN- γ , has three or four methionine residues, depending upon carboxy-terminal proteolytic processing. Since IFN- γ does not have any cysteine residues, [^{35}S]cysteine is not an appropriate label. Thus [^{35}S]methionine was chosen as the radiolabeled amino acid for this work.

It is desirable to minimize the radiolabeling period so that the labeling time is essentially differential when compared to the total culture time. On the other hand, the labeling must be long enough so that detectable quantities of protein are produced at a steady state

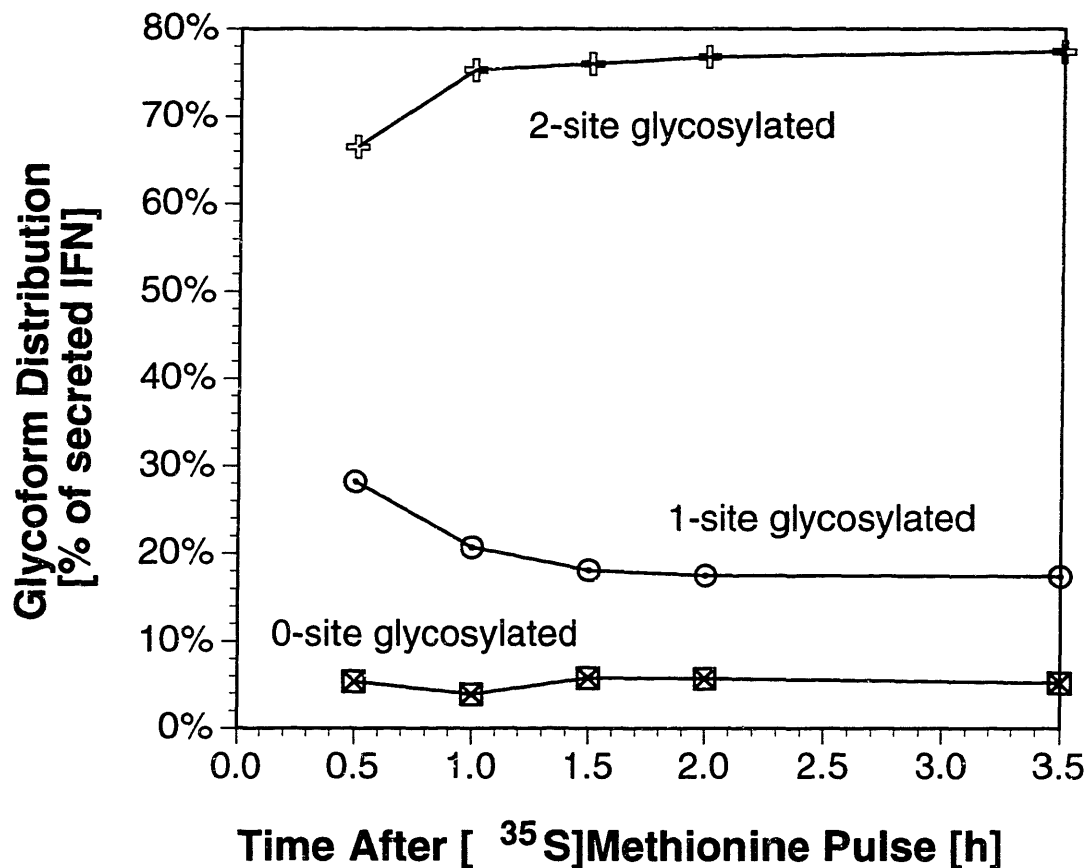


Figure 4-1. Glycoform distribution of radiolabeled IFN- γ secreted during the chase period following a pulse of ^{35}S labeled methionine.

glycoform distribution. The steady state criteria becomes important if the various glycoforms are synthesized or secreted at different rates. In order to determine the secretion kinetics of IFN- γ glycoforms, a pulse-chase experiment was performed. Cells growing in low-serum (0.75% dialyzed fetal bovine serum), suspension culture were placed in methionine-free media for 30 minutes before adding a pulse of [^{35}S]methionine at 0.1 mCi/ml. Following a 30 minute exposure to the labeled amino acid, the cells were transferred to chase media containing excess (0.1 mM) non-labeled (“cold”) methionine. The glycoform distribution of secreted product was analyzed with time beginning 30 minutes after initiating the labeling pulse, and the results are presented in Figure 4-1.

While the percentage of secreted IFN- γ which was non-glycosylated was rather constant with time, the fraction of one-site glycosylated IFN- γ decreased with time as more two-site glycosylated protein was secreted. Two hours after the [³⁵S]methionine pulse (1.5 hours after initiating the chase) the secreted product was approaching its final glycoform distribution.

The most likely explanation for the observed pulse-chase behavior is post-translational glycosylation of one-site glycosylated protein in the endoplasmic reticulum. Pulse-chase radiolabeling studies with insect cells producing recombinant IFN- γ indicated that the Asn-25 glycans are added co-translationally, while core glycosylation at Asn-97 occurs largely post-translationally (Sareneva et al., 1994). Virtually all of the one-site glycosylated IFN- γ is glycosylated at only Asn-25 (James et al., 1995), which suggests that non-glycosylated IFN- γ is a poor substrate for post-translational glycosylation. This explains why non-glycosylated IFN- γ does not vary with time during the pulse-chase experiment, while one-site glycosylated protein is apparently converted to two-site glycosylated protein with time during the chase. As was mentioned in the Literature Review, glycosylation at Asn-25 may be critical for post-translational glycosylation at Asn-97, because the glycans at Asn-25 should promote interaction of IFN- γ with calnexin, a membrane-bound lectin chaperone. Calnexin-complexed proteins are kept in close proximity to the ER membrane, which might facilitate post translational glycosylation by the membrane-bound oligosaccharyltransferase. Interferon secreted early in the chase period is less likely to be post-translationally glycosylated, because the protein spent less time in the vicinity of the oligosaccharyltransferase. Since the rate-limiting step for secretion of most proteins is transport from the endoplasmic reticulum to the Golgi (Dorner et al., 1993; Lodish et al., 1983), proteins which are secreted late in the chase period are expected to have spent more time in the ER. Post-translational glycosylation thus explains all of the observed pulse-chase behavior.

The pulse-chase experiment illustrated the importance of waiting for a steady state glycoform distribution when pulsing [³⁵S]methionine to determine differential secreted product glycosylation. Another consideration when monitoring batch cultures is that the labeling procedure must introduce a minimal perturbation, and so medium changes should be avoided. To determine whether sufficient labeled protein could be produced when the radiolabel is added directly to batch samples, a pulse labeling experiment was performed by adding [³⁵S]methionine to medium containing 0.1 mM cold methionine. The experiment was also designed to determine the time required to reach steady state labeling with a radiation pulse (no chase). A pulse of [³⁵S]methionine at 0.06 mCi/ml was added to γ -CHO cells growing in low-serum (0.75% dFBS), suspension culture, and samples were collected with time (Figure 4-2). Detectable quantities of labeled proteins were produced, although in future experiments the activity of [³⁵S]methionine was increased to reduce film development time. Figure 4-2 illustrates that steady state labeling was achieved within 3 to 5 hours. Significant changes in glycosylation were not observed between 3 and 19 hours.

Based upon the pulse-chase and pulse experiments described above, a radiolabeling protocol was developed for monitoring glycosylation at various times during batch culture. A schematic overview of the technique is presented in Figure 4-3. A 3 ml sample is removed from the culture being analyzed and placed into a shake flask along with a small quantity of [³⁵S]methionine. Typically 0.5 to 1.0 mCi of [³⁵S]methionine was added per 3 ml sample. The radiolabel was added from less than 35 μ l of an aqueous [³⁵S]methionine stock which had an activity of 1110 Ci/mmol. Therefore less than 0.3 μ M of [³⁵S]methionine was added per radiolabel, which amounts to less than 0.3% of the methionine concentration found in RPMI-1640. The minimal changes in methionine concentration and culture volume are expected to have no significant impact on the cell culture environment. The sample is next incubated for 3-5 hours under the same conditions as the parent culture. Following the incubation, the product is immunoprecipitated from the supernatant and the glycoforms are separated by SDS-

PAGE. The various glycoforms are then detected and quantified by autoradiography. This radiolabeling technique was applied to the analysis of glycosylation site occupancy in batch and fed-batch cultures.

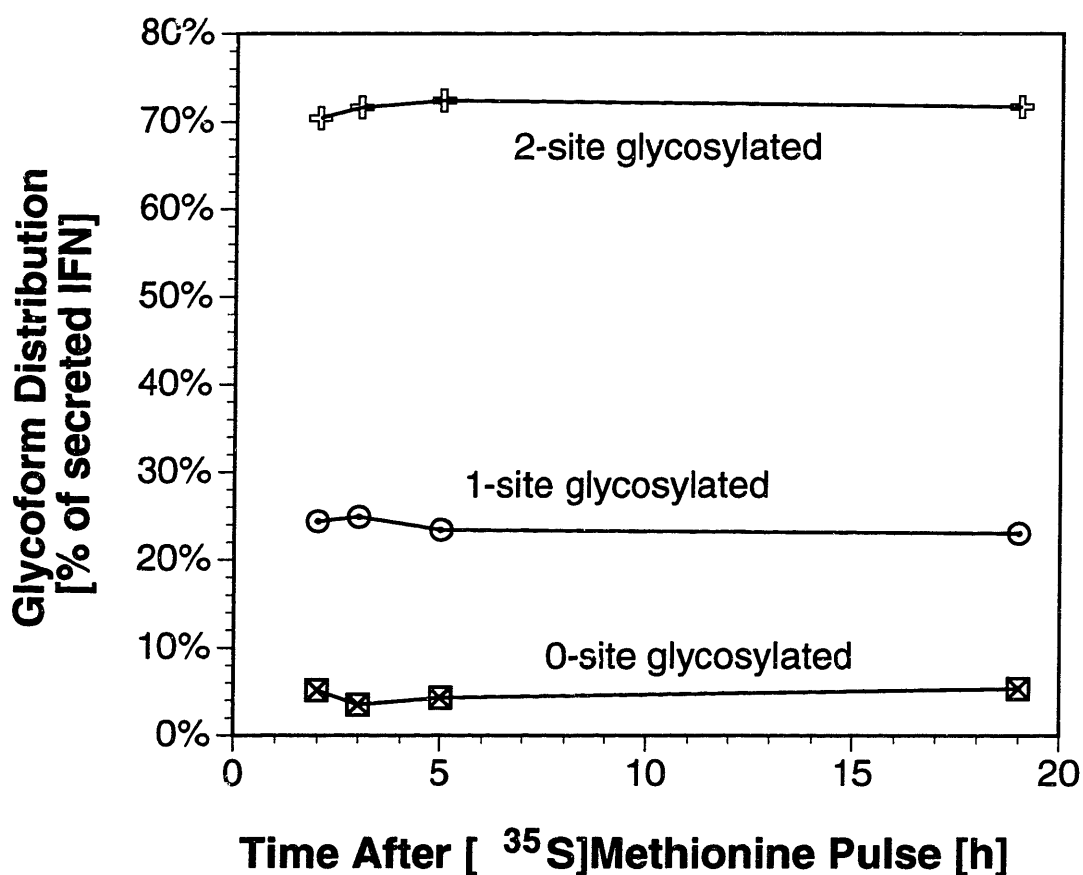


Figure 4-2. Glycoform distribution of radiolabeled IFN- γ secreted following a step pulse of ^{35}S labeled methionine into medium containing 0.1 mM of non-labeled methionine.

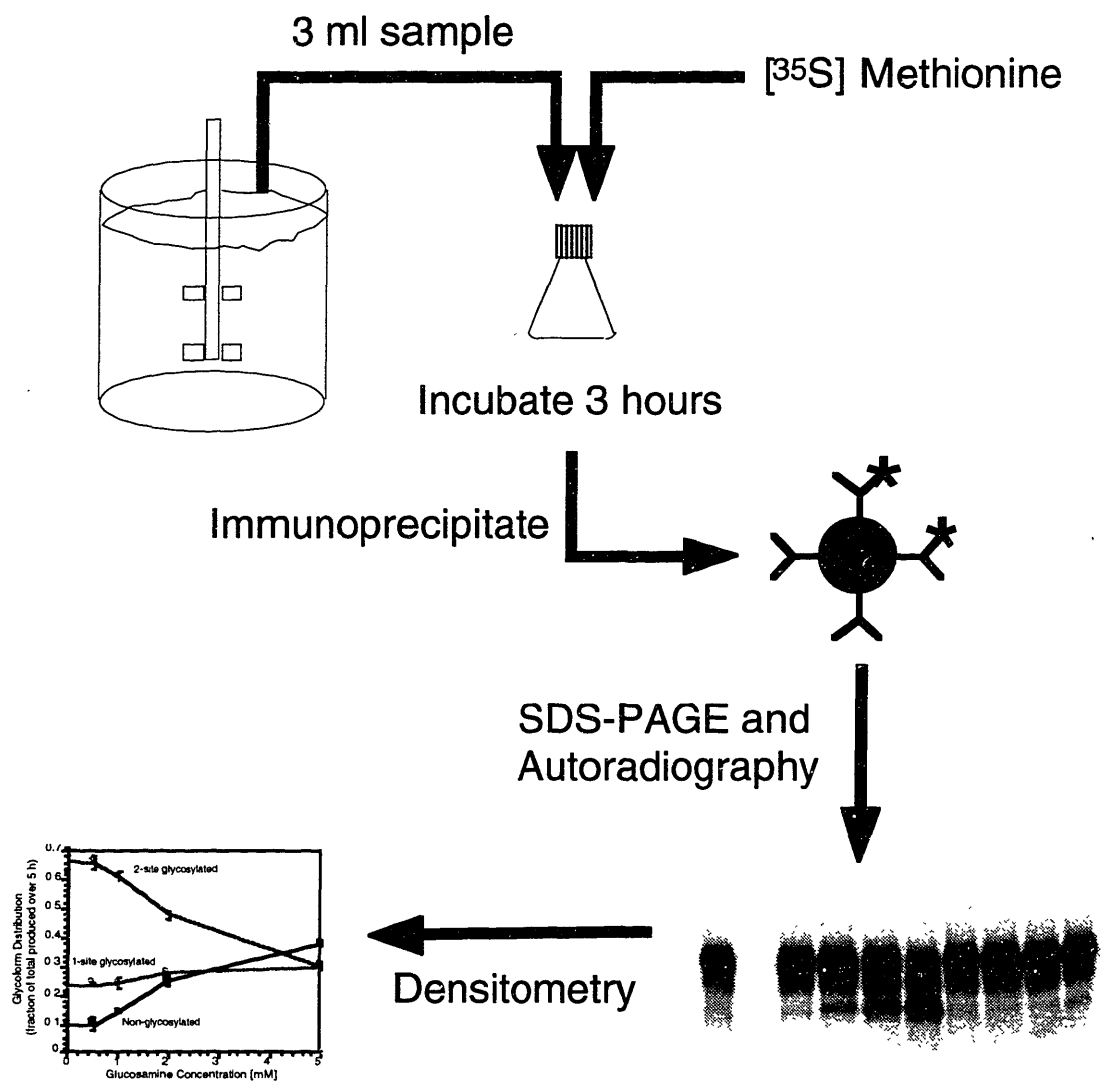


Figure 4-3. Overview of the pulse radiolabeling technique for monitoring differential product glycosylation site occupancy.

4.2 Batch Culture Glycosylation Site Occupancy

Recombinant IFN- γ glycosylation site occupancy was monitored in low-serum (0.75% dFBS) batch culture of γ -CHO cells. The suspension batch was performed in a 500 ml spinner flask, and samples were taken every eight hours. At each sample time, a three ml aliquot was removed for radiolabeling with [35 S]methionine and a second sample was collected for analysis of intracellular proteins. Figure 4-4 shows the cell growth during the batch culture. The cells grew exponentially for the first 80-90 hours, and then cell growth ceased. Shortly thereafter cell death initiated. Figure 4-5 shows that by the very end of the batch, glucose was depleted and the cells had begun to consume lactate.

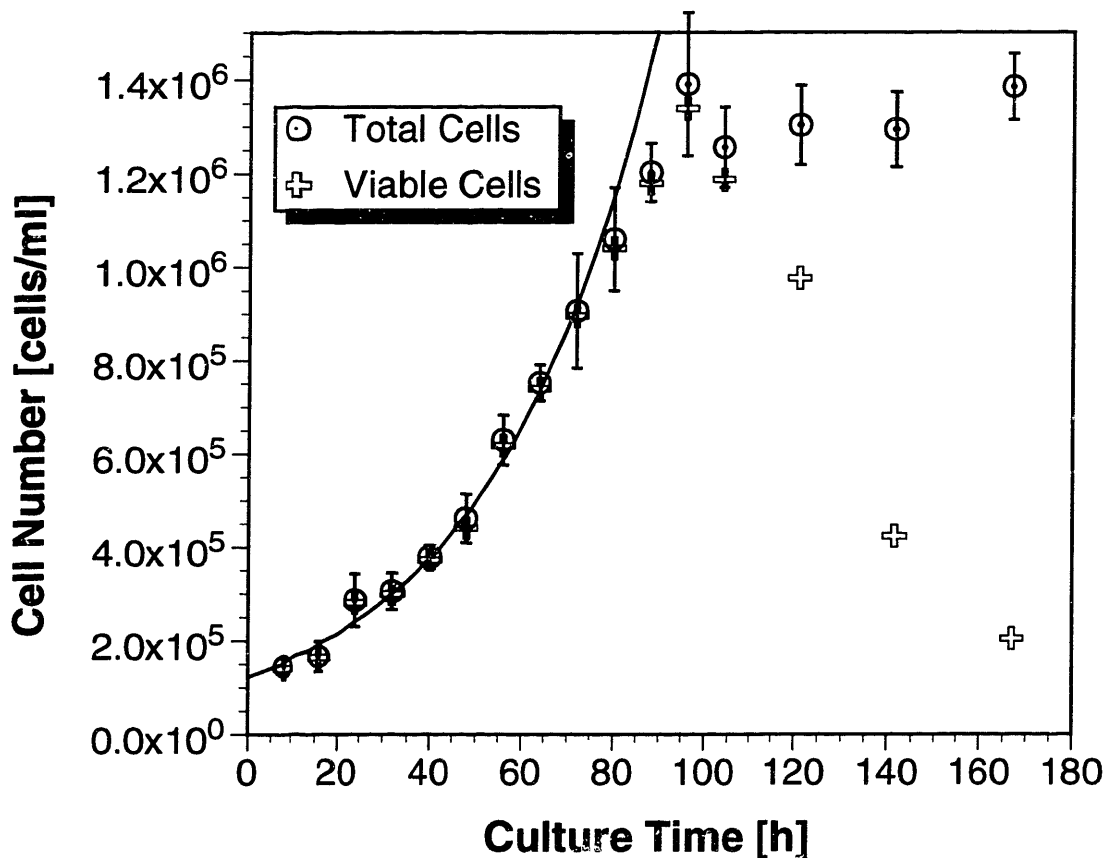


Figure 4-4. Viable and total γ -CHO cell numbers during batch suspension culture in low-serum medium.

The glycosylation site occupancy of product secreted at different times during the batch was determined from radiolabeled samples, and the results are plotted in Figure 4-6. The relative secretion of two-site glycosylated product gradually decreased during the exponential growth phase (from 69% down to 55%), while the relative proportions of one-site and non-glycosylated product increased (from 23% to 31% and from 8% to 14%, respectively). This trend is similar to the decreases in IFN- γ glycosylation observed during batch culture of a different CHO cell line by Jenkins and co-workers (Curling et al.,

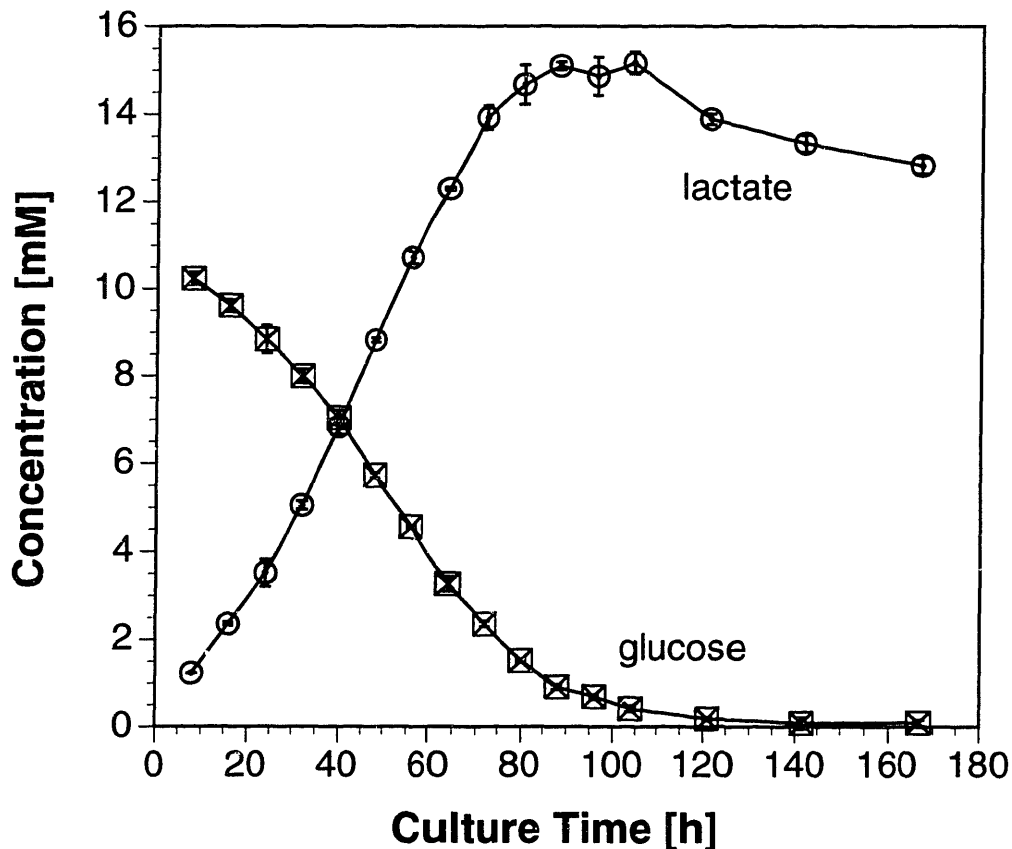


Figure 4-5. Glucose consumption and lactate production during low-serum batch culture of γ -CHO cells.

1990; Jenkins et al., 1994), except that the changes we observed were less pronounced. At the conclusion of exponential growth, the IFN- γ being secreted abruptly changed within 15 hours back to 69% two-site, 23% one-site and 8% non-glycosylated. A similar shift in glycosylation was not detected by Jenkins and co-workers, most likely because they were analyzing accumulated product via silver staining. The differential radiolabeling technique allows this shift to be detected, even though changes in accumulated IFN- γ would have been very subtle. By the end of the batch when glucose was essentially used up, glycosylation fell quickly to 50% two-site, 27% one-site and 23% non-glycosylated protein.

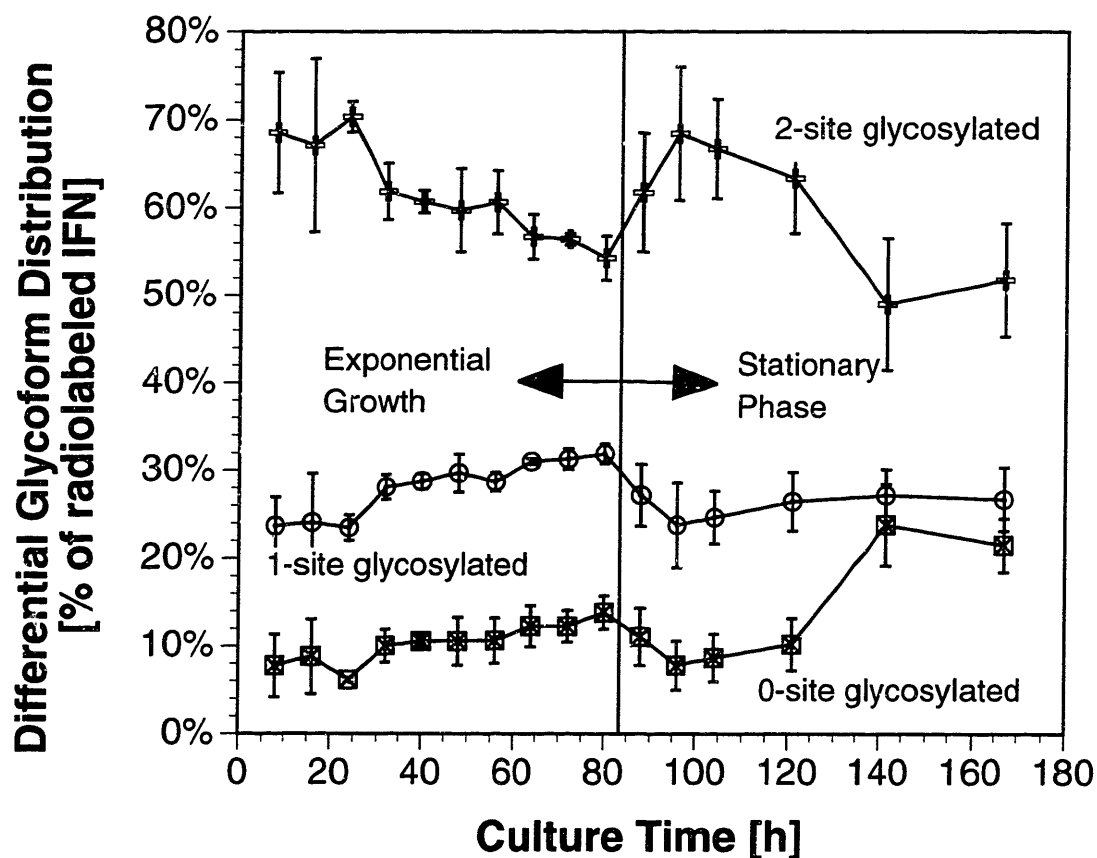


Figure 4-6. Differentially produced IFN- γ glycosylation site occupancy monitored with pulse radiolabeling in low-serum batch culture of γ -CHO cells.

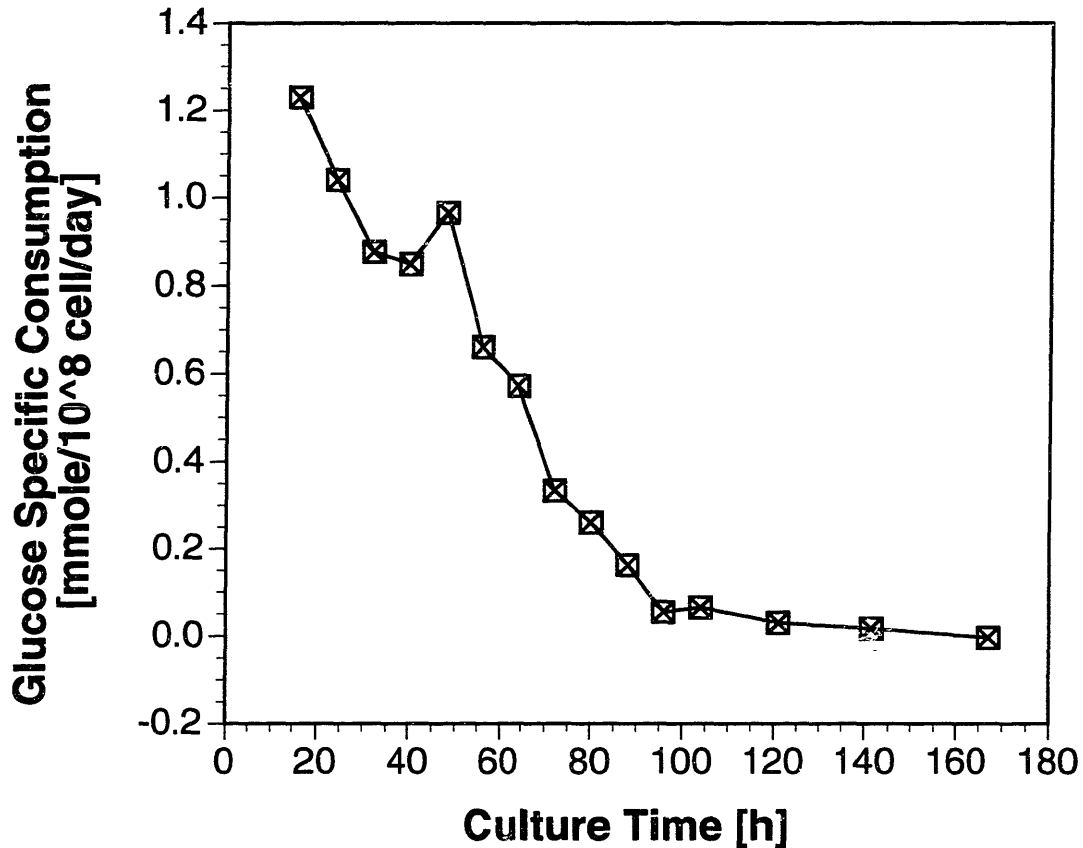


Figure 4-7. Specific glucose consumption rate in low-serum batch culture of γ -CHO cells.

The reason for the decline in glycosylation during exponential growth is not clear. The specific glucose consumption rate also declines during exponential growth (see Figure 4-7), which at first glance tends to implicate sugar metabolism. However, Curling et al. (1990) found that a similar decline in site occupancy was observed even when glucose was maintained above 6 mM. It is possible that glucose metabolism shifts during exponential growth independent of external glucose concentration. In this hypothesis central carbon metabolism may be shifting and causing the decline in glycosylation. The fed-batch experiments described in this chapter and experiments described in Chapters 5 and 6 explore this hypothesis in more detail. The rapid increase in glycosylation at the

onset of the stationary phase could be related to changes in central carbon metabolism as biosynthesis is shut down. Alternatively, reduced biosynthesis may simply decrease the consumption of oligosaccharides for cellular glycoproteins, leading to increased precursor availability for IFN- γ .

If sugar availability were to severely limit glycosylation, then the cells would be expected to respond by inducing synthesis of glucose regulated proteins such as GRP78 (BiP) (Beckmann et al., 1990; Sciandra and Subject, 1983). BiP synthesis is induced under conditions such as glucose starvation that lead to severe underglycosylation of proteins (see Chapters 2 and 7). Cell lysates from the batch culture were analyzed using quantitative western blots to determine BiP concentration, and the results are shown in Figure 4-8. The results are normalized, because absolute BiP concentrations varied depending upon which antibody was used for detection. A polyclonal primary antibody yielded an initial BiP concentration of ~2-3% of total cellular protein, while a monoclonal antibody western blot indicated that BiP constituted ~7% of total protein. Both estimates seem high, and so normalized results are presented here. Figure 4-8 shows that BiP levels remained relatively constant during exponential growth. Glucose regulated protein synthesis was not induced by the gradual decline in glycosylation during exponential growth. In contrast, BiP synthesis was induced more than 2 fold at the end of the batch when glycosylation efficiency had declined to low levels and glucose was essentially depleted. The final decline in glycosylation is typical of glucose starvation.

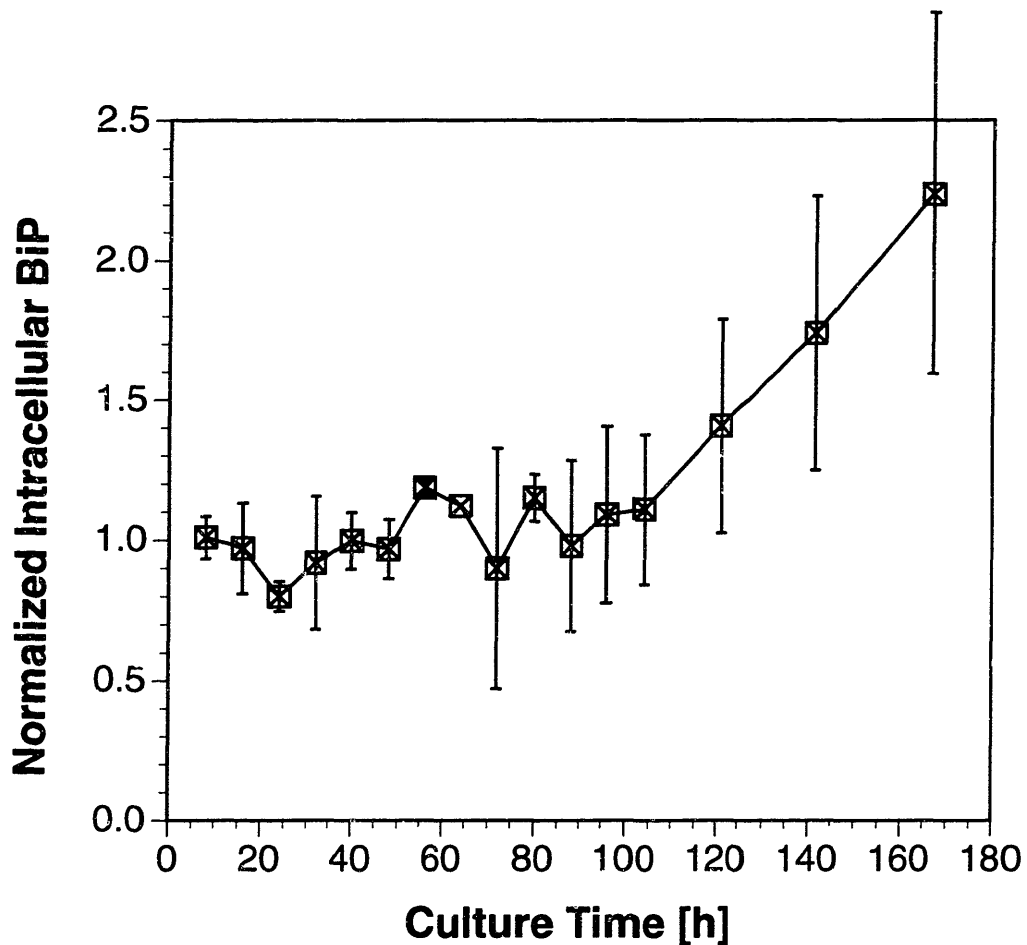


Figure 4-8. Normalized intracellular concentration of the molecular chaperone BiP during low-serum batch culture of γ -CHO cells.

4.3 Fed-Batch Culture Glycosylation Site Occupancy

If changes in glucose metabolism were responsible for the gradual decline in glycosylation observed during batch exponential growth, then improving the consistency of metabolism would be expected to improve glycosylation consistency. A stoichiometric fed-batch technique was recently proposed for improving the consistency of animal cell metabolism (Xie et al., 1997; Xie and Wang, 1994a; Xie and Wang, 1994b; Xie and Wang, 1994c). Nutrients such as glucose and amino acids are maintained at low levels and fed based upon

calculated stoichiometric demand. In this manner by-product formation is reduced and the nutritional environment is maintained relatively constant. This fed-batch technique was applied to the γ -CHO cell line and glycosylation was monitored with radiolabeling to determine whether consistent glycosylation could be obtained by maintaining a consistent nutritional environment.

4.3.1 Transient Starvation Impacts Glycosylation

A fed-batch, suspension culture was performed in a spinner flask using a stoichiometrically designed initial medium as described in Materials and Methods. The medium was serum-free, but contained the animal tissue hydrolysate Primatone RL at 2 g/l. Cell counts and feeding were performed manually every 12 hours. The maximum viable cell density in the fed-batch culture was 5.0×10^6 cells/ml as compared to 2.4×10^6 cells/ml in a control batch culture (Figure 4-9). Based upon the stoichiometric feeding strategy, glucose was maintained at low concentration in the fed-batch culture to reduce lactate formation (Xie and Wang, 1996a). Figure 4-10 illustrates that glucose was indeed maintained at low levels, and lactate formation was reduced compared to batch culture (specific lactate production in the fed batch was $0.024 \text{ mmole}/10^9 \text{ cells/h}$ versus $0.15 \text{ mmole}/10^9 \text{ cells/h}$ in the batch). The stoichiometric feeding strategy is also designed to maintain low concentrations of amino acids such as glutamine to limit amino acid metabolism and ammonia production (Xie and Wang, 1996a). The stoichiometric feeding was not perfect, however, which led to accumulation of amino acids such as glutamine (Figure 4-11). Overfeeding of amino acids may have been caused by not accounting for the amino acids supplied by Primatone RL.

Glycosylation was monitored periodically during the course of the experiment using [^{35}S]methionine radiolabeling. The serum-free batch culture had glycosylation characteristics similar to the low-serum batch culture described previously. Figure 4-12 shows that glycosylation site occupancy in the batch culture declined during the

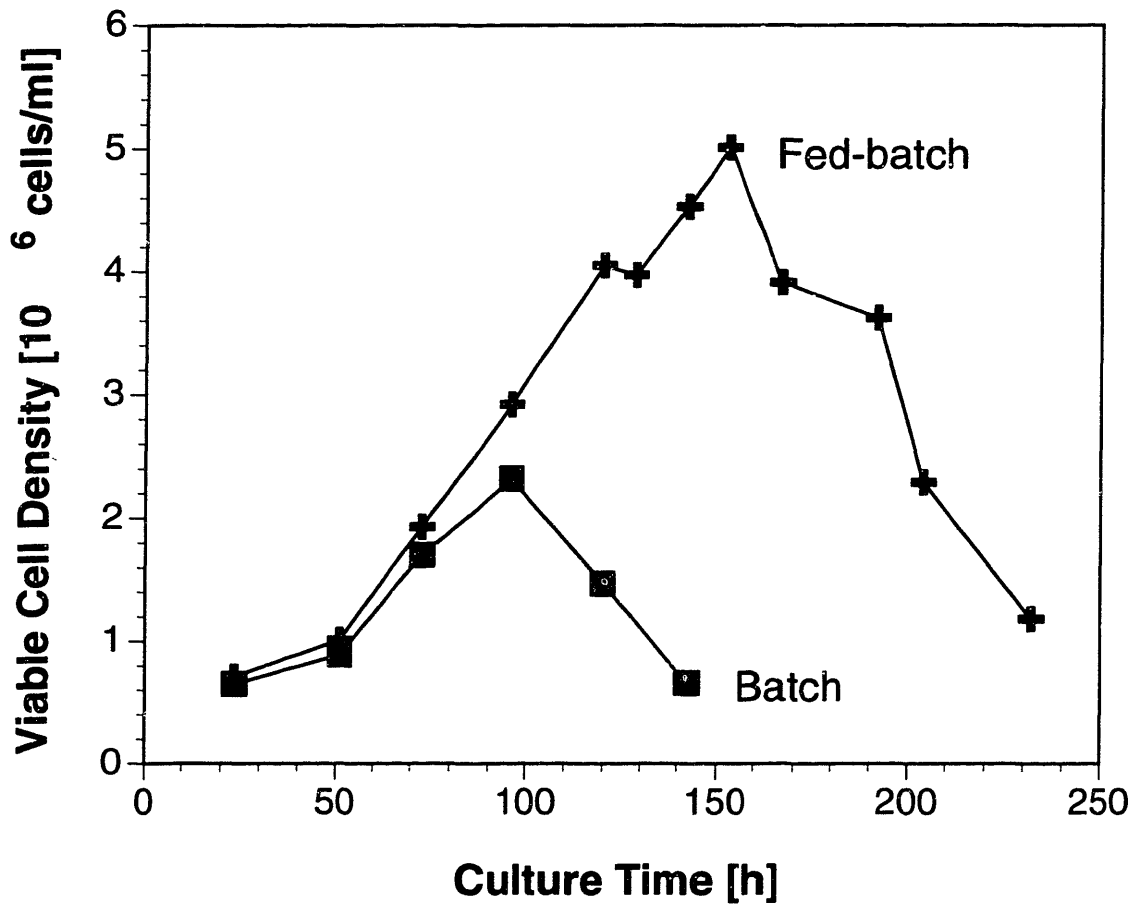


Figure 4-9. Viable γ -CHO cell densities in batch and fed-batch serum-free, suspension cultures.

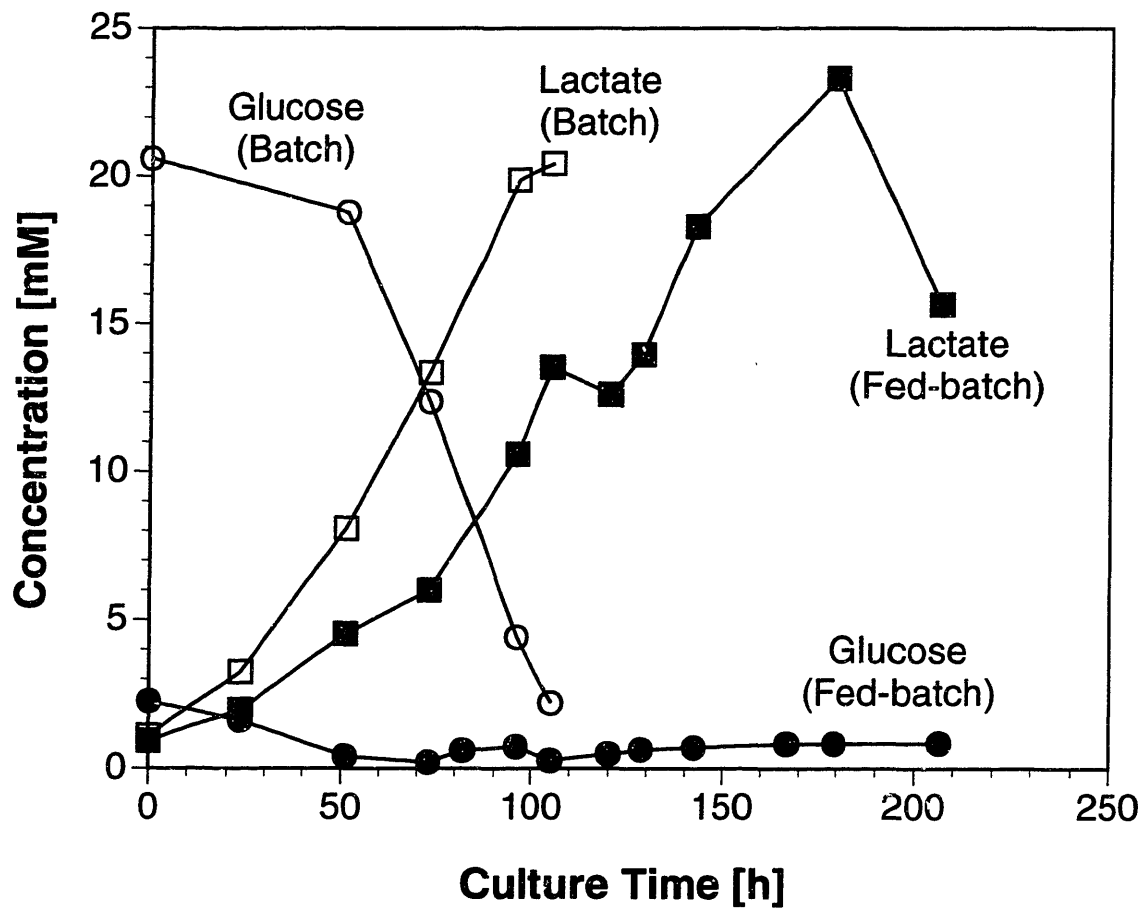


Figure 4-10. Glucose concentration and lactate production during batch and fed-batch serum-free cultures of γ -CHO cells.

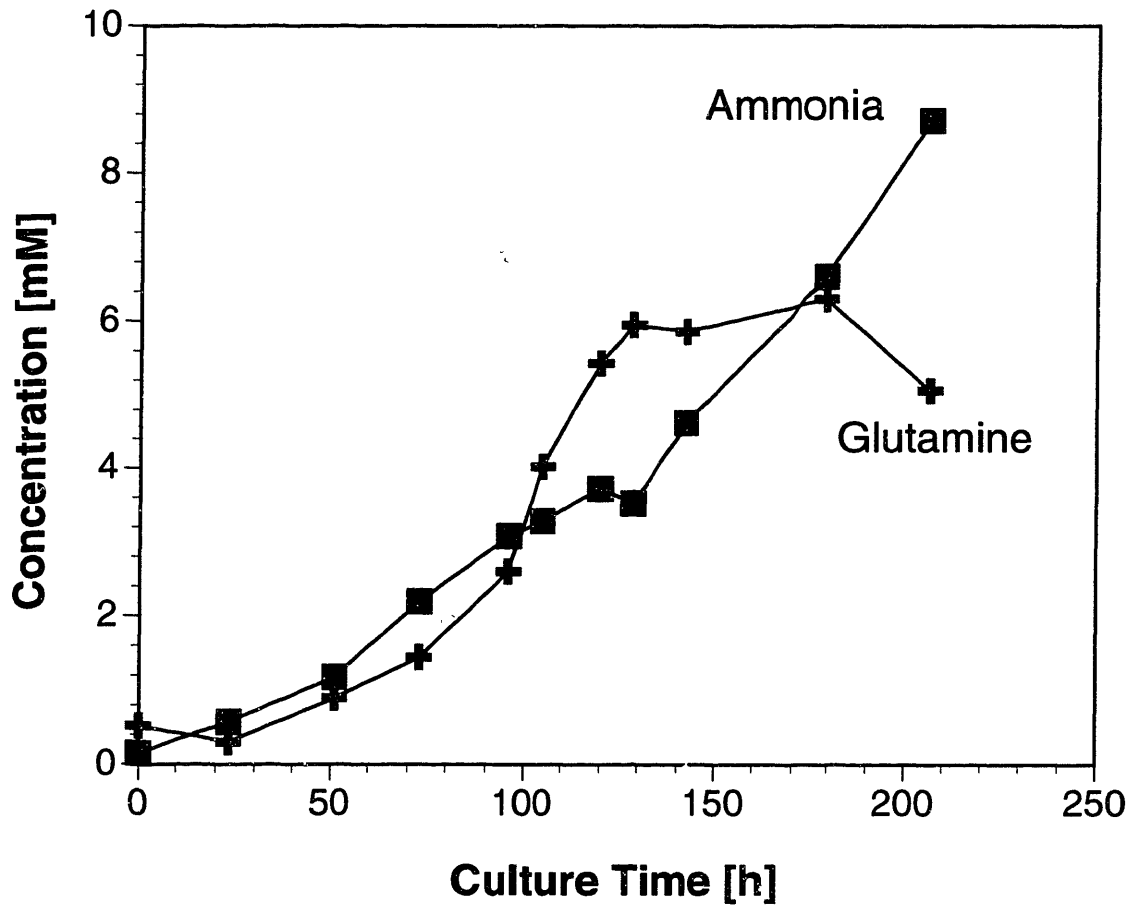


Figure 4-11. Glutamine concentration and ammonia accumulation during fed-batch serum-free culture of γ -CHO cells.

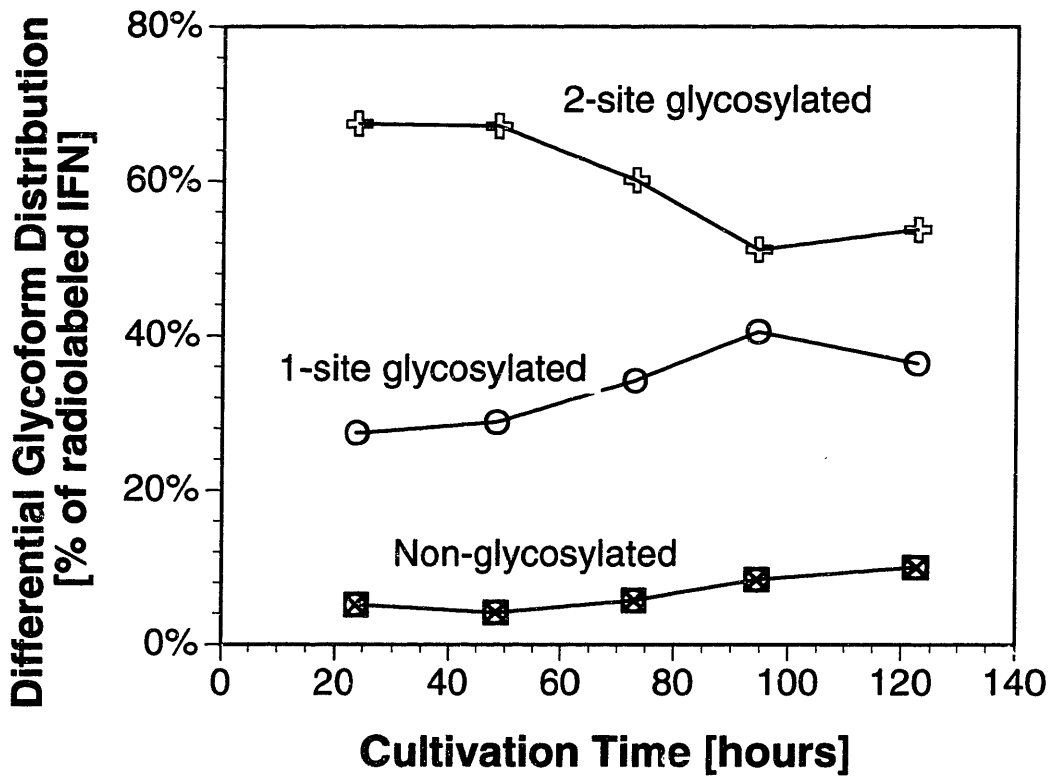


Figure 4-12. Differentially produced IFN- γ glycosylation site occupancy monitored with pulse radiolabeling in batch serum-free culture of γ -CHO cells.

exponential growth phase before increasing again at the onset of the stationary phase. The results demonstrate that similar behavior is observed in batch culture with serum-free and low-serum media.

The fed-batch culture was also monitored with radiolabeling, and the results are presented in Table 4-1. The wide variations in glycosylation site occupancy from sample to sample illustrate that periodic feeding impacted glycosylation. Several of the radiolabeling samples were taken just prior to the periodic feeding time, and so variations in glycosylation are apparently the result of transient starvation between feedings. The most likely components to limit glycosylation are glucose and glutamine (glutamine is

Table 4-1. Differentially produced IFN- γ glycosylation site occupancy monitored with pulse radiolabeling in fed-batch serum-free culture of γ -CHO cells: the impact of periodic feeding.

Time ^a [h]	Glucose ^b [mM]	0-site [%]	1-site [%]	2-site [%]
23.8	3.1	5.3	27	68
48.5	0.6	38	27	35
73.0	0.2	68	19	13
94.5	0.7	67	21	12
97.8	3.3	5.8	36	58
122.5	3.3	8.2	35	57
165.5	0.9	64	26	10
188.5	3.0	73	21	5.8

^aCulture time when a 3 mL sample was withdrawn and pulsed with [³⁵S]methionine.

^bEstimated glucose concentration at the beginning of the 3 hour pulse radiolabeling assay.

required for amino sugar formation as discussed in Chapter 2). Since glutamine was in excess throughout the culture (Figure 4-11), glycosylation patterns were presumably influenced by changes in glucose concentration. Table 4-1 lists the estimated glucose concentration at the beginning of each radiolabeling period. It should be kept in mind that the labeling lasted three hours, and so the glucose concentration continually decreased during the assay based upon the viable cell density of the sample. When the glucose concentration at the beginning of the radiolabel was low (below ~1 mM), glycosylation site occupancy was extremely poor. It is interesting to note that glycosylation at 23.8 hours was identical in the fed-batch and batch cultures, despite the fact that the glucose concentrations were approximately 3.1 mM and 20 mM, respectively. Glycosylation could be maintained over wide variations in glucose concentration, as long as the cultures were not starved. The influence of starvation between periodic feedings is most clearly illustrated by comparing results from the 94.5 h and 97.8 h sample times (Table 4-1). At 94.5 h glucose had dropped to 0.7 mM, and glycosylation site occupancy was extremely low (67% of the IFN- γ being secreted was non-glycosylated). By the 97.8 h sample time, which was taken only 20 minutes after feeding had elevated the glucose concentration to more than 4 mM, glycosylation had fully recovered. The results demonstrate that the effects of short term starvation were rapidly reversible, which agrees with previous studies of glycosylation and glucose starvation (Gershman and Robbins, 1981; Turco, 1980).

4.3.2 Glycosylation During Non-Starved Fed-Batch Intervals

The fed-batch experiment described above illustrated that transient starvation due to manual periodic feeding negatively impacted glycosylation. However, the extent to which glycosylation varied during non-starved periods was not clear. Another set of fed-batch experiments were performed to answer this question. In these experiments, glycosylation site occupancy was monitored with [^{35}S]methionine radiolabeling at the mid-point between feedings so that periods of transient starvation would be avoided. Experiments

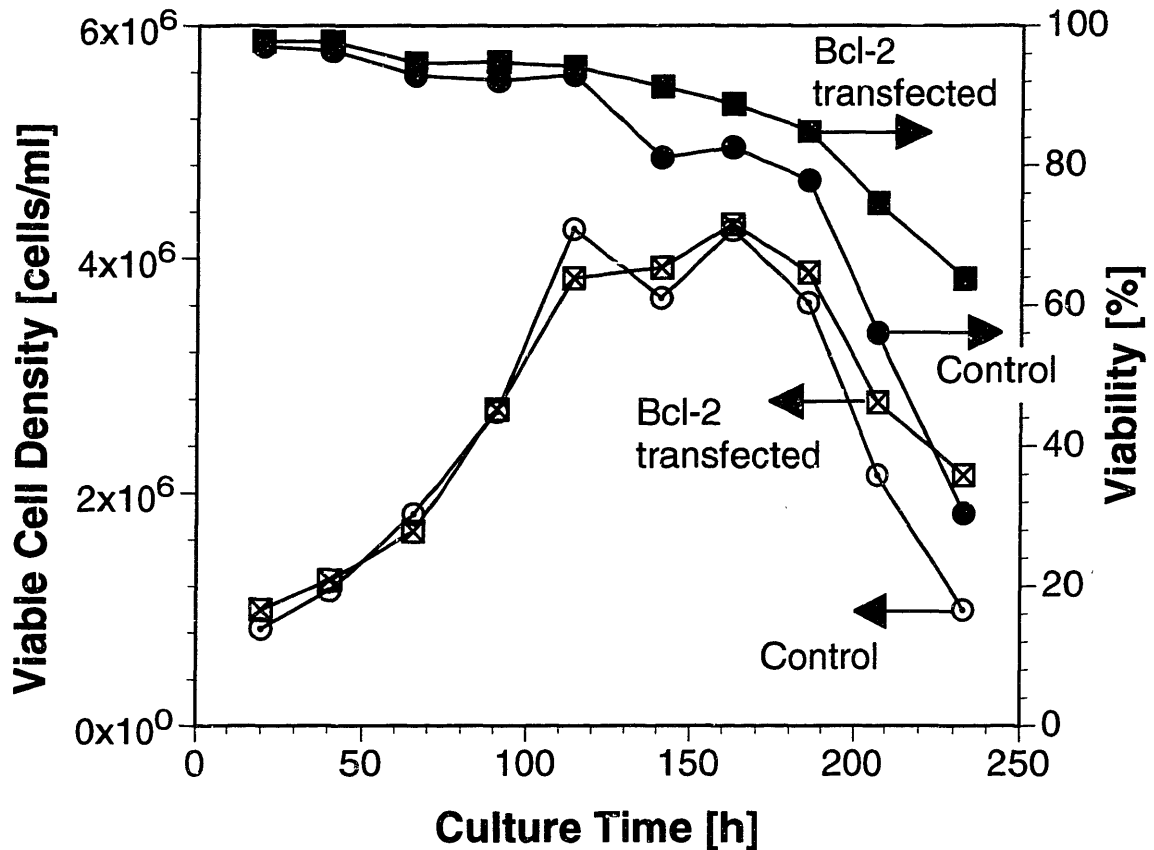


Figure 4-13. Cell growth in serum-free fed-batch cultures of γ -CHO cells transfected with the Bcl-2 anti-death gene and control transfected γ -CHO cells.

were performed in serum-free, suspension culture with γ -CHO cells which had been transfected with the anti-apoptosis gene Bcl-2 and control cells transfected with a similar plasmid without the Bcl-2 gene (Goswami et al., 1998). The fed-batch was performed using the stoichiometric fed-batch technique with a modified RPMI-SFM initial medium as described in Materials and Methods (Chapter 3).

The cell growth of the Bcl-2 transfected and control transfected γ -CHO cells was very similar (Figure 4-13). The viable cell densities in both fed-batches exceeded 4.2×10^6 cells/ml, although severe clumping at densities above 4.0×10^6 cells/ml precluded accurate

determination of the time of growth cessation and the final cell numbers. Dry cell weight measurements indicated that significant numbers of cells were adhered to the flask walls and were in clumps too large to be counted with a hemacytometer. The viability of the Bcl-2 transfected cells was consistently higher than the control cells, and this difference became especially apparent at the end of the fed-batch. The Bcl-2 transfected cells maintained a higher viability because they underwent less apoptosis (Goswami et al., 1998).

Figure 4-14 shows that glycosylation site occupancy of secreted IFN- γ was identical for the two cell lines. The remarkable agreement demonstrates the reproducibility of the [³⁵S]methionine radiolabeling technique for monitoring instantaneous glycosylation site occupancy. Furthermore, by labeling at the mid-point between feedings, periods of transient starvation were avoided. The changes in glycosylation with time were very reminiscent of the changes observed during batch culture. Site occupancy continually declined during the exponential growth period, before improving during the stationary phase. Glycosylation declined slightly at the onset of massive cell death. Although the cause of cell death was not clear in these experiments (nutrients such as glucose and amino acids were not limiting), excessive osmolality was believed to be partially responsible.

The similar changes observed in glycosylation site occupancy in batch and fed-batch cultures indicate that controlling glucose and amino acid concentrations was not sufficient to maintain consistent glycosylation. Although periodic feeding in the fed-batches led to some fluctuations in nutrient concentrations, the changes were much smaller than changes in batch culture. Alterations in glycosylation site occupancy could not be correlated with nutrient variations, except during periods of extreme starvation. The decline in glycosylation with time during exponential growth appears to be unrelated to external glucose and amino acid concentrations. The fed-batch experiments could not rule out the possibility that other factors such as growth factors may influence central carbon metabolism with time. Changes in culture environment could have altered carbon

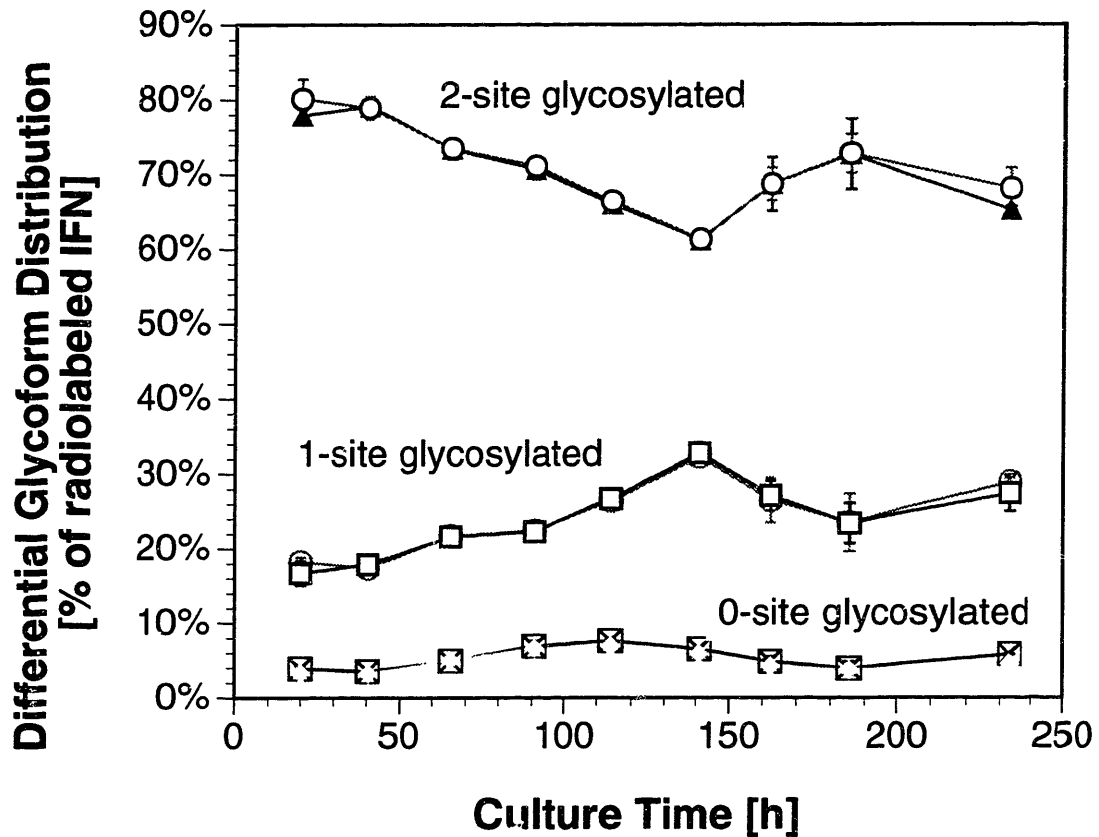


Figure 4-14. Differentially produced IFN- γ glycosylation site occupancy monitored with pulse radiolabeling in fed-batch culture of γ -CHO cells transfected with the Bcl-2 anti-death gene and control transfected γ -CHO cells. Glycosylation was monitored between feeding times with four hour pulses of radioactive methionine.

metabolism and hence the intracellular availability of activated sugar precursors. Chapter 5 examines the relationship between central carbon metabolism and glycosylation in more detail. The influence that central carbon metabolism has on glycosylation during exponential growth is then revisited in Chapter 6.

5. Central Carbon Metabolism and Glycosylation: Continuous Culture Experiments

To investigate the relationship between central carbon metabolism and glycosylation site occupancy, we studied the glycosylation of recombinant human interferon- γ (IFN- γ) produced in continuous culture (chemostat) experiments. Chemostat experiments were the preferred method for studying metabolic effects on glycosylation, because the accuracy of metabolite rate measurements is improved, and cell physiology can be studied under well-defined, steady state conditions. Intracellular nucleotide sugar levels and IFN- γ glycosylation were measured at different steady states, which were characterized by central carbon metabolic fluxes estimated by material balances and extracellular metabolite rate measurements.

Glycosylation site occupancy of IFN- γ produced in glucose and glutamine limited chemostat cultures was found to correlate with intracellular nucleotide sugar concentrations. From data obtained in glucose limited chemostats, we found that glycosylation site occupancy also correlated with TCA cycle activity but not glycolytic activity. Since the TCA cycle would be expected to influence precursors for nucleoside triphosphate synthesis, these findings led to the hypothesis that site occupancy was limited by nucleotide sugar formation, which was influenced primarily by nucleoside triphosphate availability. A glutamine limited chemostat illustrated that amino sugar formation can also limit the formation of the nucleotide sugar UDP-N-acetylglucosamine. Nucleotide and nucleotide sugar measurements from chemostat, batch and fed-batch experiments confirmed that the primary determinants of UDP-sugar concentrations during exponential growth are UTP levels and amino sugar formation. The chemostat experiments demonstrated that during periods of glucose or glutamine starvation, nucleotide sugar availability can limit glycosylation site occupancy.

5.1 Glycosylation Site Occupancy in Continuous Culture

5.1.1 Glycosylation at Steady State

Glycosylation site occupancy of recombinant IFN- γ was monitored in chemostat cultures of γ -CHO cells. One glutamine limited and four glucose limited continuous cultures resulted in the steady states described in Table 5-1. Dilution rates ranged from 0.0125 to 0.0248 1/h, which represents a range of 38% to 75% of the typical maximum growth rate observed in batch culture (batch culture $\mu_{\max} \sim 0.033$ 1/h). Significant cell death was observed at low dilution rates, and this death increased as the dilution rate was decreased. Since only viable cells can divide, the growth rate can deviate significantly from the

Table 5-1. Glucose and glutamine limited steady states achieved in continuous culture.

	Glucose Limited 1	Glucose Limited 2	Glucose Limited 3	Glucose Limited 4	Glutamine Limited
Dilution rate, D (1/h)	0.0227	0.0176	0.0141	0.0125	0.0248
Growth rate, μ (1/h)	0.0238	0.0186	0.0163	0.0165	0.0254
Biomass, DCW (g/l)	0.533 \pm 0.010	0.650 \pm 0.013	0.691 \pm 0.002	0.617 \pm 0.021	0.782 \pm 0.009
Viability (%)	95.4	94.5	86.4	75.8	97.5
Product Titer (mg/l)	–	1.26 \pm 0.12	2.27 \pm 0.25	2.27 \pm 0.23	2.72 \pm 0.17
CO ₂ evolution, CER (mmol/l/h)	0.353 \pm 0.024	0.467 \pm 0.024	0.408 \pm 0.019	0.330 \pm 0.016	0.608 \pm 0.027
O ₂ uptake, OUR (mmol/l/h)	0.456 \pm 0.022	0.420 \pm 0.027	0.396 \pm 0.019	0.326 \pm 0.022	0.522 \pm 0.028
Respiration Quotient, RQ	0.774 \pm 0.065	1.110 \pm 0.090	1.028 \pm 0.067	1.010 \pm 0.084	1.166 \pm 0.082

dilution rate at low dilutions ($\mu = D/\text{viability}$). Increasing death with decreasing dilution rate has been observed before with CHO cell chemostats (Hayter et al., 1993).

Glycosylation site occupancy at these steady states was analyzed using micellar electrokinetic capillary chromatography (MECC) of immunoprecipitated samples, and the results are presented in Table 5-2. Immunoprecipitations were performed in duplicate, and each immunoprecipitated sample was injected 2–3 times in MECC. Although growth rates and viabilities varied significantly at the different steady states, glycosylation site occupancy was found to vary over a rather narrow range. No obvious correlations were evident between site occupancy and growth rate.

Table 5-2. Glycosylation site occupancy for four glucose limited and one glutamine limited steady state cultures.

	Dilution rate, D (1/h)	Growth rate, μ (1/h)	Glycosylation Sites Occupied (%)		
			2-sites	1-site	0-sites
Glucose Limited 1	0.0227	0.0238	69.8 \pm 1.1	25.1 \pm 0.4	5.0 \pm 0.8
Glucose Limited 2	0.0176	0.0186	66.3 \pm 0.4	26.9 \pm 0.2	6.7 \pm 0.2
Glucose Limited 3	0.0141	0.0163	68.3 \pm 0.8	25.0 \pm 0.6	6.6 \pm 0.6
Glucose Limited 4	0.0125	0.0165	65.2 \pm 1.2	28.0 \pm 1.0	6.7 \pm 0.8
Glutamine Limited	0.0248	0.0254	61.7 \pm 0.8	30.0 \pm 0.6	8.2 \pm 0.4

5.1.2 Glycosylation Site Occupancy and Nucleotide Sugars

Nucleotide sugar concentrations were analyzed to determine whether their availability may have been responsible for the observed variations in glycosylation site occupancy. Perchloric acid cell extracts were collected for the glutamine limited chemostat and for three of the four glucose limited chemostats, and the extracts were analyzed with ion-pair reverse phase HPLC as described in Materials and Methods. The measured nucleotide concentrations are reported in Table 5-3 as $\mu\text{mole}/(\text{g viable dry cell weight})$. Results are expressed on a dry cell weight rather than cell number basis to account for variations in cell size, and because extensive cell aggregation (clumping) at low dilution rates made cell number determination difficult. Perchloric acid extracts of non-viable (trypan blue permeable) cells were found to contain negligible concentrations of nucleotides and nucleotide sugars (data not shown). This result was not surprising, since loss of membrane integrity, as measured by trypan blue permeability, was expected to increase free nucleotide permeability. Hence, nucleotide concentration results are considered on a viable dry cell weight basis.

As the glycosylation site occupancy decreased, there was a corresponding decrease in intracellular UDP-N-acetylglucosamine + UDP-N-acetylgalactosamine (the nucleotide sugars co-eluted in HPLC as discussed in Materials and Methods; the sum will be referred to as UDP-GNAc). Figure 5-1 shows the percentage of IFN- γ glycosylated at both potential sites against the intracellular UDP-GNAc. A trend, consistent for all of the glucose and glutamine limited chemostats, is identified. For the glucose limited chemostats, the concentrations of all nucleotides and nucleotide sugars declined as UDP-GNAc declined, indicating that declining UDP-GNAc may have been related to an overall reduction in nucleotide levels (Table 5-3). In contrast, the glutamine limited culture had high levels of nucleoside triphosphates, but very low UDP-GNAc.

Table 5-3. Cell mass-specific nucleotide concentrations ($\mu\text{mole/g}$ viable dry cell weight) measured in perchloric acid extracts.

Nucleotide	Glucose Limited 1	Glucose Limited 2	Glucose Limited 4	Glutamine Limited
ATP	25.40 ± 0.19	21.68 ± 0.25	19.18 ± 0.43	25.07 ± 0.37
ADP	2.57 ± 0.36	2.18 ± 0.14	2.09 ± 0.27	1.58 ± 0.10
AMP	0.49 ± 0.03	0.43 ± 0.03	0.49 ± 0.06	0.25 ± 0.02
GTP	4.62 ± 0.07	3.96 ± 0.03	3.57 ± 0.07	4.87 ± 0.06
GDP	0.54 ± 0.06	0.41 ± 0.01	0.50 ± 0.08	0.31 ± 0.04
CTP	3.79 ± 0.19	3.34 ± 0.01	2.82 ± 0.06	4.17 ± 0.11
UTP	7.81 ± 0.21	6.72 ± 0.01	4.87 ± 0.05	9.66 ± 0.05
UDP	0.75 ± 0.19	0.56 ± 0.03	0.63 ± 0.11	0.82 ± 0.04
UDP-Gal	0.64 ± 0.33	0.66 ± 0.16	0.50 ± 0.10	1.10 ± 0.03
UDP-Glc+ GDP-Man	2.16 ± 0.20	2.05 ± 0.06	2.00 ± 0.15	2.57 ± 0.12
UDP-GNAc	2.85 ± 0.02	2.30 ± 0.08	1.98 ± 0.08	1.70 ± 0.02

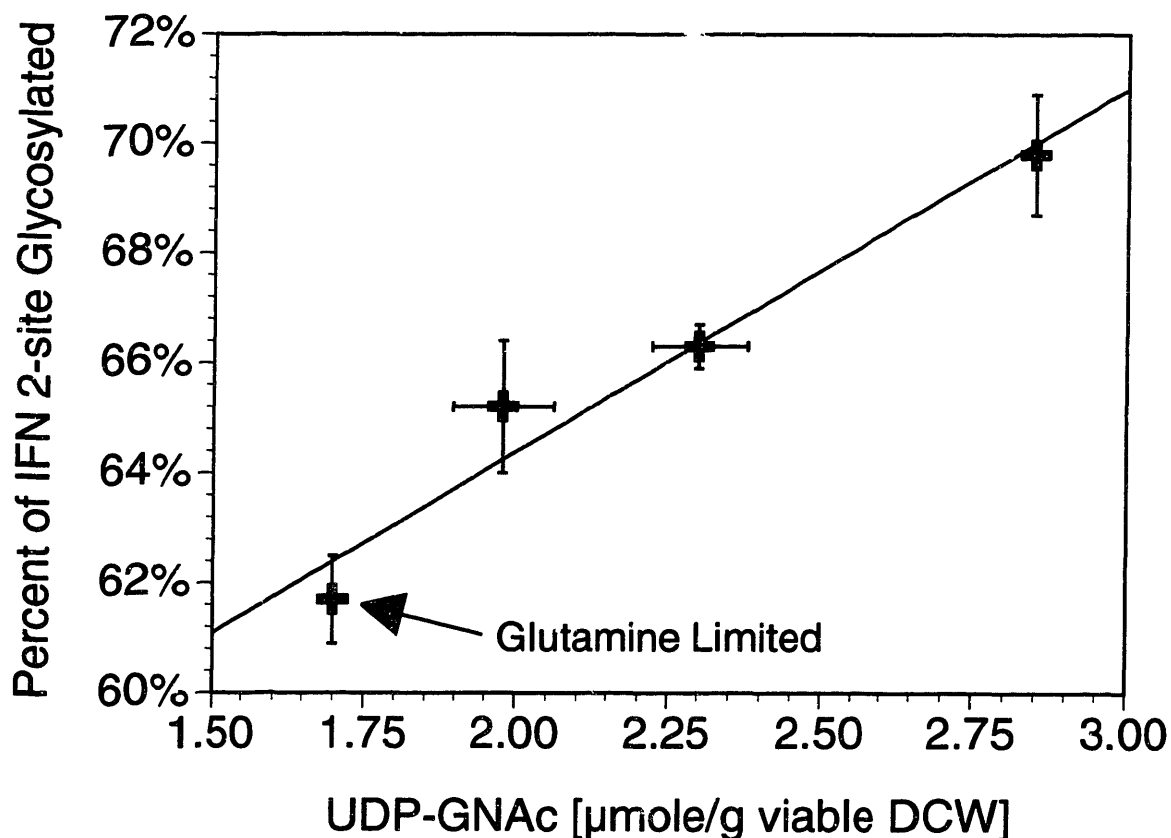


Figure 5-1. The relationship between glycosylation site occupancy and intracellular UDP-GNAc concentration in glucose and glutamine limited chemostat cultures.

5.2 Metabolic Flux Analysis

To determine whether changes in nucleotide sugars and glycosylation were related to metabolism, the fluxes of central carbon metabolism were estimated from material balances. Figure 5-2 depicts the metabolic network model used (see Materials and Methods). Accurate determination of metabolic fluxes using material balances requires that all significant material uptake be taken into account. Peptides represent a potentially substantial source of amino acids in our serum free medium, since the hydrolysate Primatone RL, which is present at 2.5 g/l, contains approximately 41% peptides by

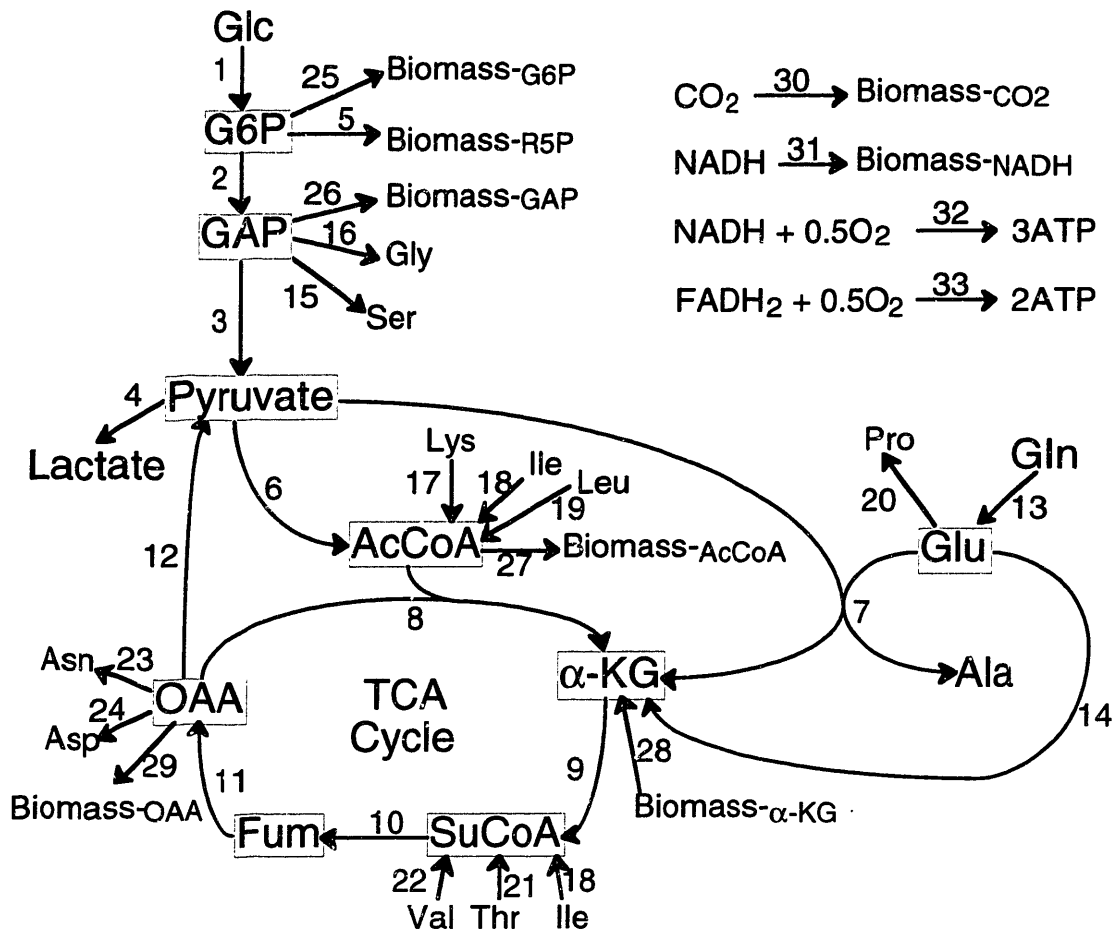


Figure 5-2. Schematic diagram of a simplified biochemical reaction network describing central carbon metabolism.

weight (from manufacturer specifications). Amino acids present in peptides were measured in the feed and steady state reactor samples to determine whether utilization of peptide amino acids occurred under these conditions.

We found that uptake of some peptide amino acids did occur. The amounts of peptide-bound alanine, aspartate, glycine, hydroxyproline, isoleucine, leucine, phenylalanine and valine were significantly lower in reactor effluents compared to the feed. Figure 5-3 compares the amounts of these peptide-bound amino acids in the feed to the amounts in the reactor effluent for glucose limited steady state 4; the difference represents a source of amino acids which may have been metabolized or accumulated in the medium. Other amino acids not shown in Figure 5-3 were present in equal amounts in the feed and reactor effluent within experimental error, which indicates that only selected amino acids were liberated from peptides in significant amounts. Table 5-4 shows the contribution that peptide derived amino acids made to measured metabolite production rates. Including peptide derived amino acids, the overall metabolite production rates for the steady states are listed in Table 5-5. The amino acid requirements for biosynthesis (i.e. protein, nucleotide and lipid synthesis) have already been subtracted from the data in Table 5-5, and so the data are net catabolic rates (Bonarius et al., 1996).

The consistency of the metabolite measurements and assumed biochemistry can be assessed by considering the reaction network depicted in Figure 5-2. The network includes 37 metabolites and 33 reactions (i.e. $m=37$ and $n=33$). The stoichiometric matrix, A , is 37×33 , with $\text{rank}(A)=33$ and a condition number $c(A)=69$ (see Materials and Methods for details). The number of redundant equations in the network is equal to $m - n$ - (the number of linearly dependent equations). Since the equations for NAD(P)^+ and NAD(P)H are linearly dependent as are the equations for FAD and FADH_2 , the number of redundant equations in the network is $2 (37 - 33 - 2)$. Hence there are two redundant measurements used in solving the network, and we can use these redundancies to determine the consistency of the metabolite measurements and assumed biochemistry.

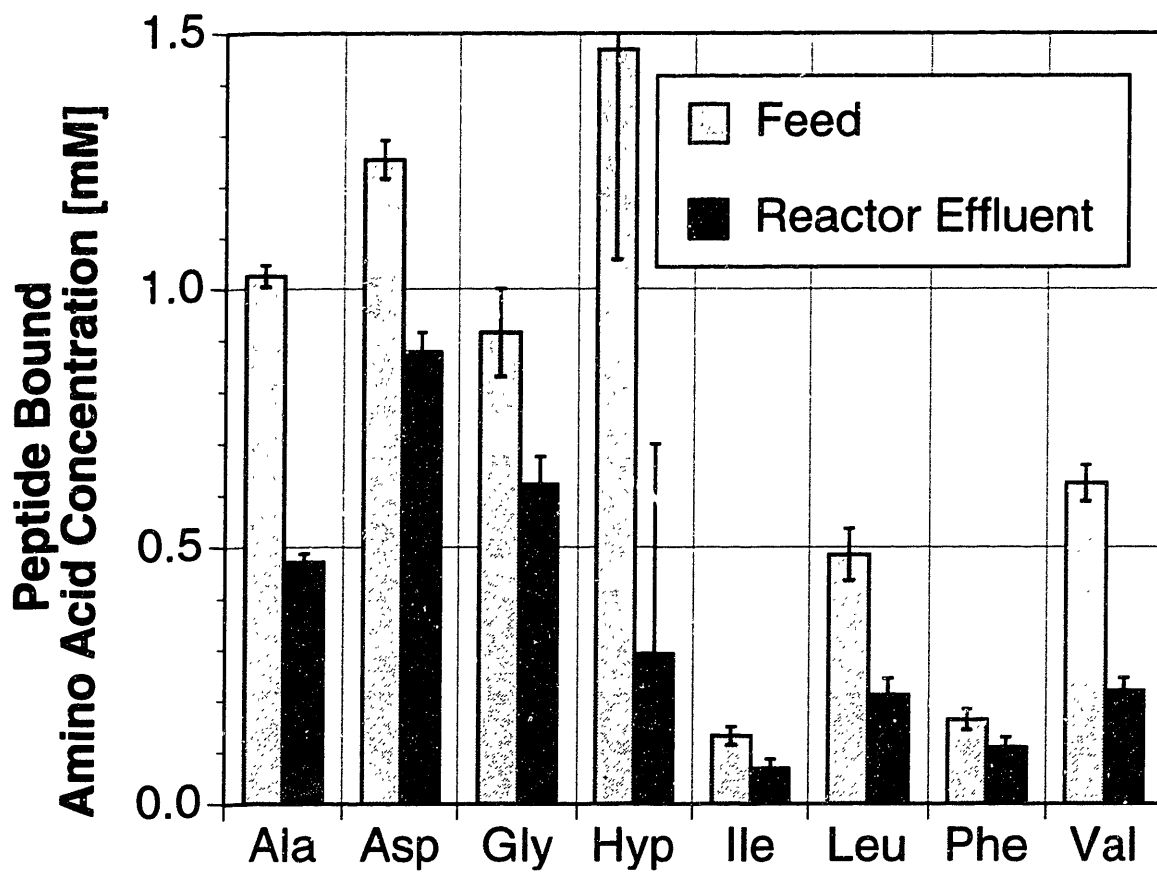


Figure 5-3. Peptide bound amino acids in the feed and reactor effluent for glucose limited steady state 4.

Table 5-4. Rates of peptide amino acid consumption in steady state chemostat cultures (mmol/g DCW/d).

	Glucose Limited 1	Glucose Limited 2	Glucose Limited 3	Glucose Limited 4	Glutamine Limited
Ala	0.204±0.031	0.288±0.009	0.242±0.018	0.269±0.013	0.268±0.027
Asn+ Asp	0.052±0.056	0.127±0.031	0.130±0.022	0.183±0.026	0.171±0.044
Gly	0.048±0.040	0.122±0.026	0.080±0.036	0.143±0.049	0.126±0.049
Ile	0.034±0.019	0.038±0.005	0.028±0.016	0.031±0.012	0.045±0.011
Leu	0.124±0.042	0.112±0.007	0.084±0.032	0.133±0.029	0.137±0.026
Pro	-0.100±0.060	-0.005±0.031	0.090±0.020	-0.002±0.064	0.070±0.078
Hyp	0.815±0.266	0.568±0.201	0.515±0.144	0.572±0.282	0.369±0.153
Val	0.146±0.040	0.205±0.014	0.197±0.028	0.196±0.021	0.191±0.018

Table 5-5. Measured metabolite production rates (r) for steady state chemostat cultures (mmol/g DCW/d). Amino acid production rates include peptide derived amino acids and are the net catabolic rates after accounting for biomass synthesis.

	Glucose Limited 1	Glucose Limited 2	Glucose Limited 3	Glucose Limited 4	Glutamine Limited
Glucose	-2.712±0.147	-1.711±0.098	-1.283±0.042	-1.271±0.062	-8.137±0.348
Lactate	0.869±0.351	0.218±0.085	0.036±0.106	-0.081±0.021	9.190±0.491
CO ₂	15.89±1.37	17.23±1.30	14.15±0.77	12.82±0.851	18.682±1.150
O ₂	-20.54±1.46	-15.52±1.30	-13.76±0.76	-12.70±1.039	-16.020±1.091
Ala	0.515±0.039	-0.172±0.019	-0.157±0.015	-0.224±0.020	0.071±0.028
Asn	-0.248±0.023	-0.228±0.030	-0.210±0.018	-0.194±0.020	-0.260±0.029
Asp	0.000±0.018	-0.056±0.021	0.001±0.019	-0.009±0.018	-0.191±0.026
Gln	-2.311±0.141	-1.674±0.095	-1.251±0.055	-1.179±0.070	-0.039±0.026
Glu	0.046±0.024	-0.016±0.013	0.076±0.018	0.102±0.014	-0.273±0.025
Gly	0.090±0.042	0.062±0.029	0.165±0.029	0.217±0.050	-0.052±0.041
Ile	-0.060±0.021	-0.107±0.015	-0.065±0.011	-0.068±0.013	-0.130±0.020
Leu	-0.148±0.025	-0.289±0.023	-0.206±0.014	-0.218±0.020	-0.342±0.030
Lys	0.007±0.107	0.060±0.050	-0.012±0.049	0.013±0.136	-0.041±0.052
Pro+ Hyp	0.266±0.026	0.085±0.032	0.041±0.018	0.041±0.065	0.017±0.060
Ser	0.361±0.029	0.190±0.017	0.154±0.024	0.147±0.017	0.064±0.042
Thr	0.048±0.019	0.042±0.014	0.064±0.018	0.079±0.013	0.036±0.019
Val	-0.011±0.042	-0.123±0.021	-0.067±0.022	-0.071±0.022	-0.128±0.023

5.2.1 Redundancy Analysis: Predictions of Oxygen Uptake and Carbon Dioxide Evolution

One method for determining the consistency of a data set is to use the minimum required information to solve the network, and then calculate the value of redundant measurements based upon the solved network. If the assumed biochemistry is correct and the measurement set is consistent, then the calculated values for redundant measurements should match the experimentally determined values. This technique can be applied to the

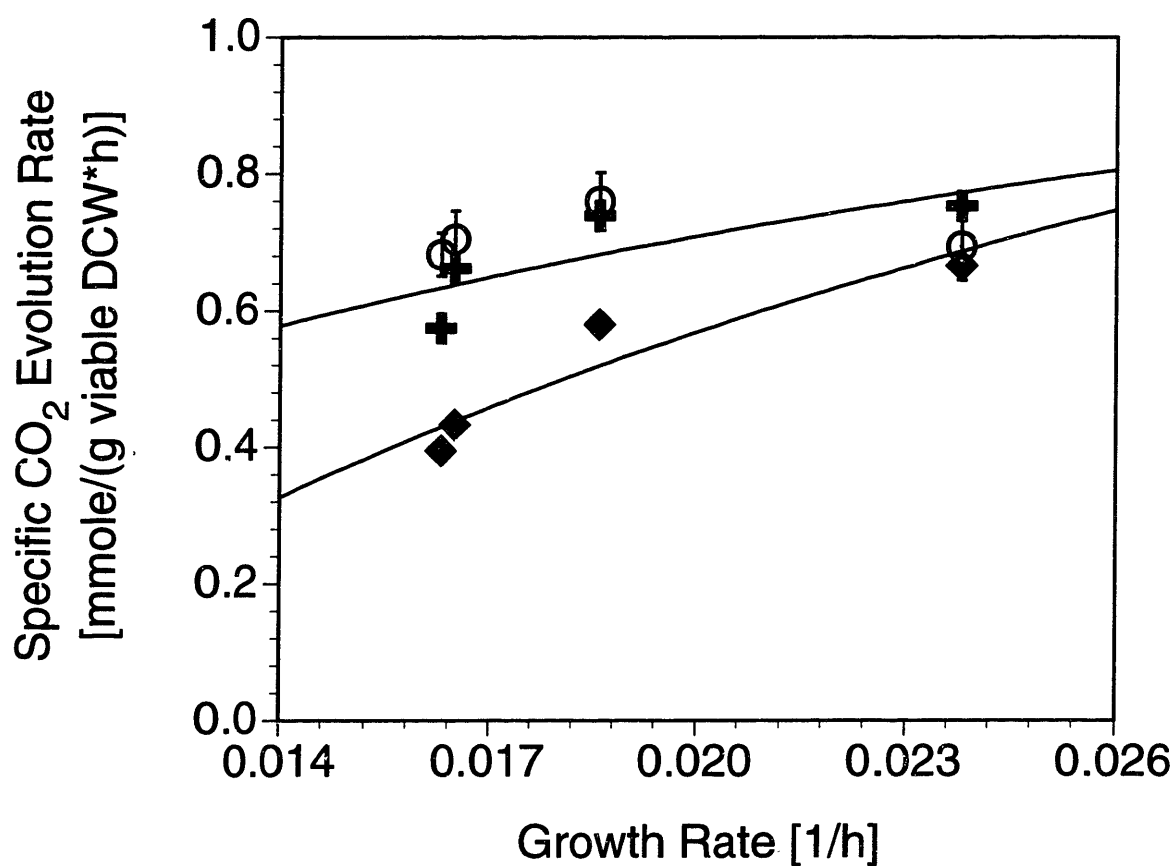


Figure 5-4. Measured specific carbon dioxide evolution rate in glucose limited chemostats (⊙) compared to calculated based upon free amino acid data only (◆) and calculated based upon total (peptide + free) amino acids (⊕).

network of Figure 5-2 by using the oxygen uptake and carbon dioxide evolution measurements as redundant data. Eliminating oxygen and carbon dioxide simplifies **A** to a 29×29 matrix \mathbf{A}_2 , with $\text{rank}(\mathbf{A}_2)=29$ and a condition number $c(\mathbf{A}_2)=79$. The network now includes zero redundant equations, and can be solved independently of oxygen and carbon dioxide. The calculated fluxes can then be used to predict oxygen uptake and carbon dioxide evolution.

Figure 5-4 compares the measured and calculated specific carbon dioxide evolution rates (CER) for the four glucose limited steady states. When calculations are based upon free amino acid data only, CER is underpredicted. Accounting for uptake of amino acids from peptides improves the prediction so that the calculated values agree with the experimental values within experimental error, except for glucose limited steady state 3, which is still somewhat underpredicted. Similarly, the calculated specific oxygen uptake rate (OUR) is underpredicted with free amino acid based data (Figure 5-5). Accounting for peptide amino acid uptake improves agreement, but the experimental OUR for steady state 1 is still significantly above the calculated value. In this case the experimental oxygen uptake value is likely in error. From Table 5-1 the respiration quotient ($\text{RQ} \equiv \text{CER}/\text{OUR}$) was 0.774 for this steady state, while it varied between 1.010 and 1.166 for the other steady states. A respiration quotient of 0.774 is highly unlikely. As discussed in Bonarius et al. (1996), the RQ is expected to be near unity, with fatty acid biosynthesis possibly increasing the RQ to slightly greater than one. When calculated from OUR and CER values predicted from the flux analysis, the RQ for steady state 1 is 1.172, which is more in line with expected values for RQ.

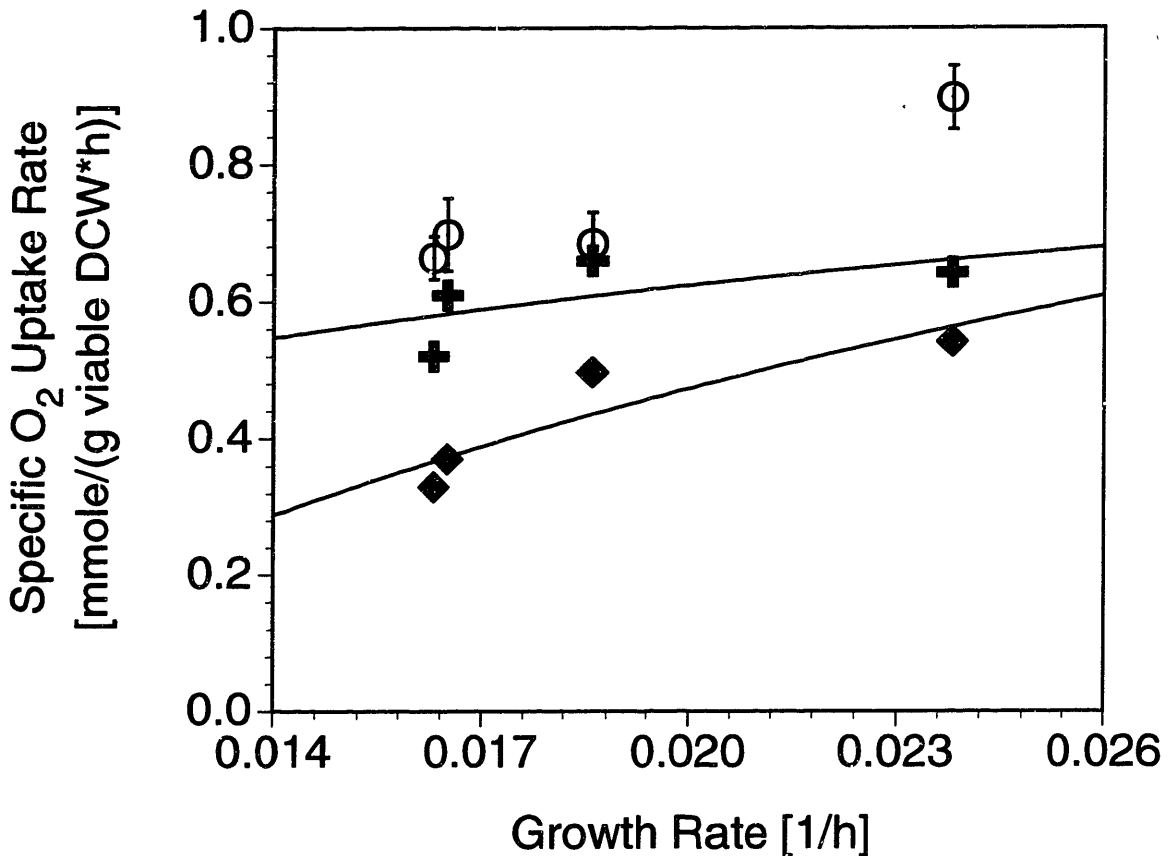


Figure 5-5. Measured specific oxygen uptake rate in glucose limited chemostats (○) compared to calculated based upon free amino acid data only (◆) and calculated based upon total (peptide + free) amino acids (⊕).

5.2.2 Redundancy Analysis using a Statistical Consistency Index

An alternative method for determining data consistency is to employ a statistical test based upon system redundancy. Using methods described in Chapter 3 (Materials and Methods), a consistency index, h , can be calculated to measure the extent to which redundancies are satisfied within expected experimental error. Large values of h indicate that the data are not consistent with the assumed biochemistry. Consistency indices were calculated for each of the steady states, and Table 5-6 tabulates the results. Calculations

Table 5-6. Consistency indices, h , for steady state data analyzed with a metabolic network including two redundant measurements. Glucose limited chemostat data were analyzed based upon either free amino acid measurements only or on total (free + peptide) amino acid measurements.

	h Free amino acids	h Total amino acids
Glucose Limited 1	54.603	22.044
Glucose Limited 2	72.616	0.023
Glucose Limited 3	131.516	13.842
Glucose Limited 4	93.589	1.312
Glutamine Limited	—	6.529

for the glucose limited steady states were performed on both the free amino acid based data and the total (free+peptide) amino acid based data. The data based only on free amino acids had higher h values than data which account for peptide uptake. These results, which indicate that accounting for peptide uptake results in more consistent data, agree with the qualitative results obtained above by predicting OUR and CER.

Table 5-6 reveals that the data from the glutamine limited steady state and the glucose limited steady states 1 and 3 still fail the 90% confidence level consistency check ($h > 4.604$), even when peptide-derived amino acids are taken into account. For these steady states, suspect measurements can be identified by eliminating measurements one at a time and recalculating h . If elimination of a particular measurement dramatically decreases h , then it is likely that either the measurement is in error, or the assumed biochemical

pathways involving the particular metabolite are incorrect. Eliminating the oxygen measurement for glucose limited steady state 1 reduces the consistency index from $h = 22.044$ ($h > \chi^2 = 4.61$, 90% confidence, 2 degrees of freedom) to $h = 0.595$ ($h < \chi^2 = 2.71$, 90% confidence, 1 degree of freedom). Thus the consistency analysis indicates that there is a greater than 90% chance that the oxygen measurement is in error. This result is consistent with the observation that the respiration quotient, RQ, is abnormally low for steady state 1, as was noted above.

Eliminating the leucine measurement for glucose limited steady state 3 reduces the consistency index from $h = 13.842$ ($h > \chi^2 = 4.61$, 90% confidence, 2 degrees of freedom) to $h = 0.027$ ($h < \chi^2 = 2.71$, 90% confidence, 1 degree of freedom). Similarly, the glutamine limited steady state's consistency index can be reduced from $h = 6.529$ to $h = 0.082$ by eliminating the leucine measurement. In both cases the high consistency indices are due to OUR and CER measurements which are not consistent with the remaining measurements and metabolic network. When leucine is converted to a dependent variable, material input into the TCA cycle can be altered to account for higher or lower OUR and CER measurements. The data inconsistencies are therefore either due to inaccurate estimations of TCA flux, or the experimental OUR and CER measurements are incorrect due to systematic errors such as inaccurate dilution rate measurements. The dilution rate is used to calculate both the OUR and CER, and therefore a dilution rate error would cause errors in these quantities.

5.2.3 Estimated Metabolic Fluxes

For consistent data sets, the final metabolic flux estimates were based upon a weighted least squares solution including all measurements. For the glucose limited steady state 1, the oxygen data was not included in the solution, because the data consistency analysis had identified the measurement as inconsistent. Likewise, the oxygen and carbon dioxide

data were not used in the weighted least squares solutions for the glucose limited steady state 3 and the glutamine limited steady state.

The final intracellular flux estimates obtained by material balancing are presented in Table 5-7. Fluxes were normalized by the growth rate, μ , instead of the uptake rate of a particular nutrient to facilitate comparisons of flux distributions at different steady states and different nutrient limitations. Normalizing by the growth rate allows direct comparison of the reaction yields (mmole/g dry cell weight), which are measures of reaction pathway activities per cell mass produced.

5.3 Nucleotide Sugars, Glycosylation and Metabolism

5.3.1 Reaction Yields Correlated with Glycosylation Site Occupancy

For the glucose limited chemostats, glycosylation site occupancy correlated strongly with citric acid (TCA) cycle activity. The percentage of IFN- γ glycosylated at both potential sites was linearly related to TCA cycle reaction yields. Figure 5-6 shows these relationships for the pyruvate to acetyl CoA reaction ($R^2 = 0.997$), the α -ketoglutarate to succinyl CoA reaction ($R^2 = 0.990$) and the oxaloacetate to α -ketoglutarate reaction ($R^2 = 0.965$). In contrast, no correlation was observed between glycosylation site occupancy and the reactions of glycolysis. This was somewhat surprising, since the hexose donor in nucleotide sugar formation is derived from isomerization of glucose-6-P, an intermediate in glycolysis. The results suggest that hexose availability was not the limiting factor for nucleotide sugar formation.

Table 5-7. Estimated central carbon metabolism reaction yields (mmole/g viable dry cell weight) for chemostat steady state cultures.

Reaction	Glucose Limited 1	Glucose Limited 2	Glucose Limited 3	Glucose Limited 4	Glutamine Limited
1 Glc → G6P	4.96	4.05	3.80	4.26	13.67
2 G6P → 2 GAP	4.52	3.62	3.37	3.82	13.24
3 GAP → Pyr	7.98	6.42	5.56	6.23	26.22
4 Pyr → Lac	1.89	0.51	0.11	-0.27	15.44
5 G6P → Biomass_R5P + CO ₂	0.19	0.19	0.19	0.19	0.19
6 Pyr → AcCoA + CO ₂	9.53	11.50	10.37	11.95	12.55
7 Pyr + Glu ↔ α-KG + Ala	0.95	-0.41	-0.47	-0.75	0.12
8 Oaa + AcCoA → α-KG + CO ₂	6.03	9.24	8.17	10.68	10.33
9 α-KG → SuCoA + CO ₂	10.02	13.40	11.88	14.58	11.18
10 SuCoA → Fum	10.05	13.85	12.08	14.79	11.55
11 Fum → Oaa	10.05	13.85	12.08	14.79	11.55
12 Oaa → Pyr + CO ₂	4.38	5.18	4.44	4.70	1.89
13 Gln → Glu	4.67	4.51	4.33	4.60	0.50
14 Glu → α-KG	2.31	4.29	3.50	3.78	1.12
15 GAP + Glu → Ser + α-KG	0.66	0.45	0.46	0.49	0.11
16 GAP + Glu → Gly + α-KG	0.17	0.15	0.49	0.70	-0.09
17 Lys → 2 AcCoA + 2 CO ₂	-0.05	-0.14	0.04	0.30	0.07
18 Ile → AcCoA + SuCoA	0.11	0.25	0.19	0.23	0.22
19 Leu → 3 AcCoA	0.27	0.69	0.61	0.73	0.57
20 Glu → Pro	0.49	0.20	0.12	0.08	0.03
21 Thr → SuCoA	-0.09	-0.10	-0.19	-0.26	-0.06
22 Val → SuCoA + CO ₂	0.01	0.29	0.20	0.24	0.21
23 Oaa + Gln → Asn + α-KG	-0.45	-0.54	-0.62	-0.65	-0.44
24 Oaa + Glu → Asp + α-KG	0.00	-0.13	0.00	-0.03	-0.32
25 G6P → Biomass_G6P	0.25	0.25	0.25	0.25	0.25
26 GAP → Biomass_GAP	0.23	0.23	0.23	0.23	0.23
27 AcCoA → Biomass_AcCoA	4.31	4.29	4.30	4.28	4.30
28 Biomass_AKG → α-KG	0.35	0.35	0.35	0.35	0.35
29 Oaa → Biomass_OAA	0.09	0.09	0.09	0.09	0.09
30 CO ₂ → Biomass_CO ₂	-0.22	-0.22	-0.22	-0.22	-0.22
31 NADH → Biomass_NADH	5.38	5.38	5.38	5.37	5.38
32 0.5 O ₂ + 3 ADP + NADH → 3 ATP + NAD ⁺	40.40	56.32	50.43	63.56	55.09
33 0.5 O ₂ + 2 ADP + FADH ₂ → 2 ATP + FAD	10.39	14.94	13.12	16.29	12.63

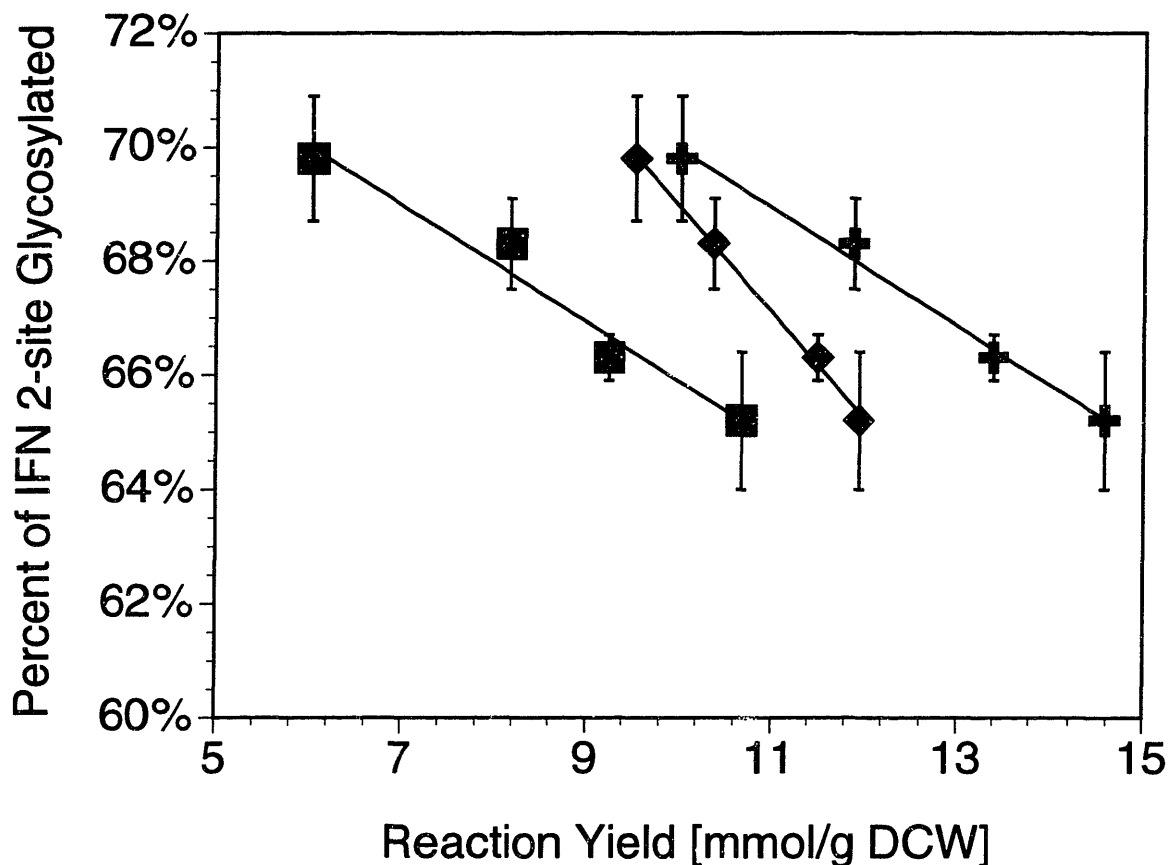


Figure 5-6. Reaction yields correlated to glycosylation site occupancy heterogeneity in glucose limited chemostat cultures. Site occupancy correlated with the yield of the pyruvate to acetyl CoA reaction (◆) and the reactions of the TCA cycle such as oxaloacetate to α -ketoglutarate (■) and α -ketoglutarate to succinyl CoA (⊕).

5.3.2 Nucleoside Triphosphates and Nucleotide Sugars in Chemostat Cultures

The correlation between glycosylation and the TCA cycle implicates nucleoside triphosphates as the main factor influencing nucleotide sugar levels. The reactions of the TCA cycle impact nucleotide synthesis, because potential TCA metabolites, such as aspartate and glutamine, are important intermediates in pyrimidine and purine base synthesis (Stryer, 1988). When the TCA cycle is producing more energy and fewer byproducts, the yield of TCA cycle reactions increases and nucleotide synthesis declines. In such cases available carbon is used to generate energy, and less carbon is available for biosynthesis. The observation from the glucose limited chemostats that declining nucleotide sugars correlated with declining total nucleotide levels supports the hypothesis that nucleoside triphosphate levels were impacting nucleotide sugar concentrations. Figure 5-7 shows the relationship between UDP-GNAc and UTP. For glucose limited chemostats, UDP-GNAc levels declined as UTP declined.

It is noted that the glutamine limited chemostat did not follow the same trends regarding TCA cycle activity, nucleoside triphosphates and nucleotide sugars. Although glycosylation site occupancy in the glutamine limited chemostat did correlate with UDP-GNAc, the low levels of UDP-GNAc did not appear to be related to UTP concentration or the TCA cycle. UTP was actually in excess compared to the concentration of UDP-GNAc (Figure 5-7). A likely cause of the low UDP-GNAc concentration in this case is limitation of the N-acetylglucosamine-1-P precursor. The committed step in the formation of this amino sugar is conversion of fructose-6-P to glucosamine-6-P, which is catalyzed by the enzyme glutamine:fructose-6-P amidotransferase (GFAT). GFAT uses glutamine as an ammonia donor, and hence glutamine limitation would be expected to inhibit amino sugar synthesis.

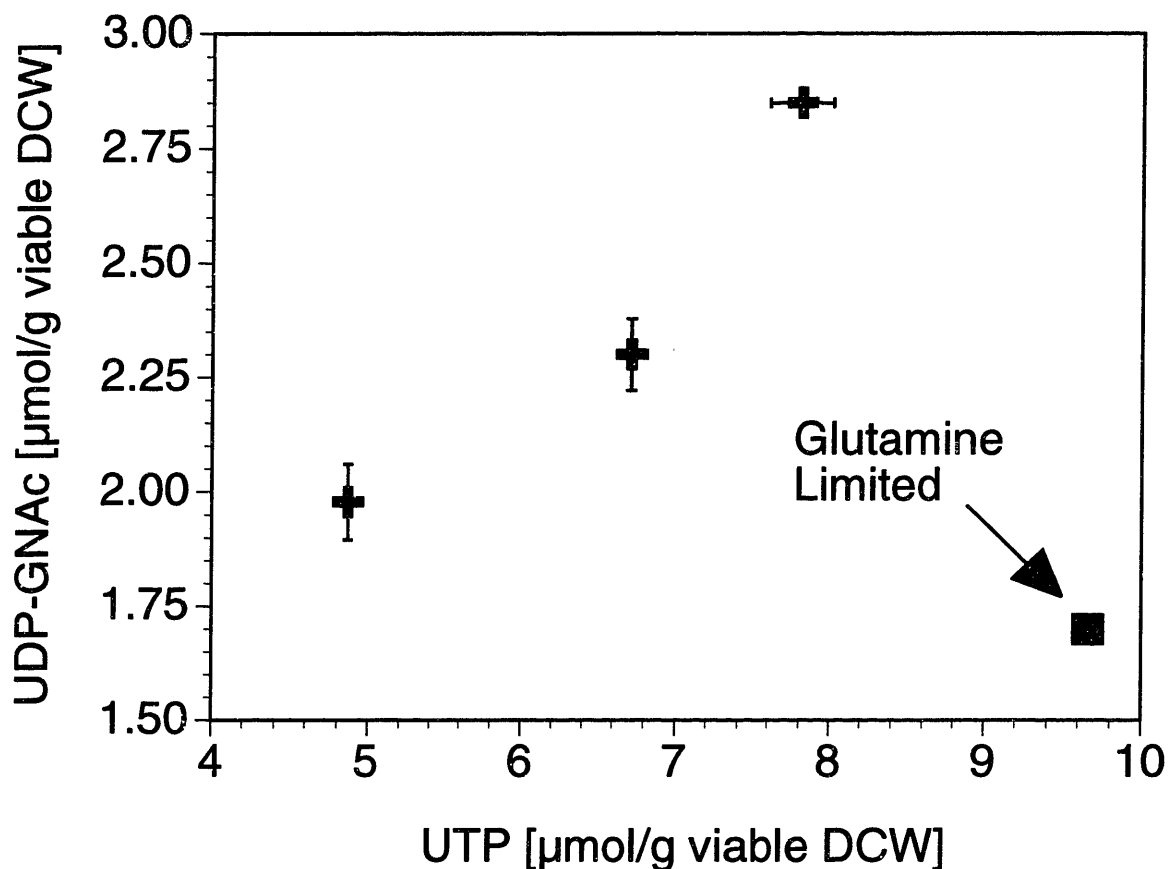


Figure 5-7. The relationship between intracellular UDP-GNac concentration and UTP in glucose and glutamine limited chemostat cultures.

5.3.3 Nucleoside Triphosphates and Nucleotide Sugars in Batch and Fed-Batch Cultures

Examination of nucleotide levels in batch and fed-batch cultures supports the hypothesis that nucleoside triphosphates are the primary determinants of nucleotide sugar concentrations in the absence of glutamine limitation. Figure 5-8 shows UDP-GNac vs. UTP during exponential growth in batch, fed-batch and chemostat cultures. Intracellular UTP levels varied between 5 and 10 $\mu\text{mole/g viable dry cell weight}$ over the course of a

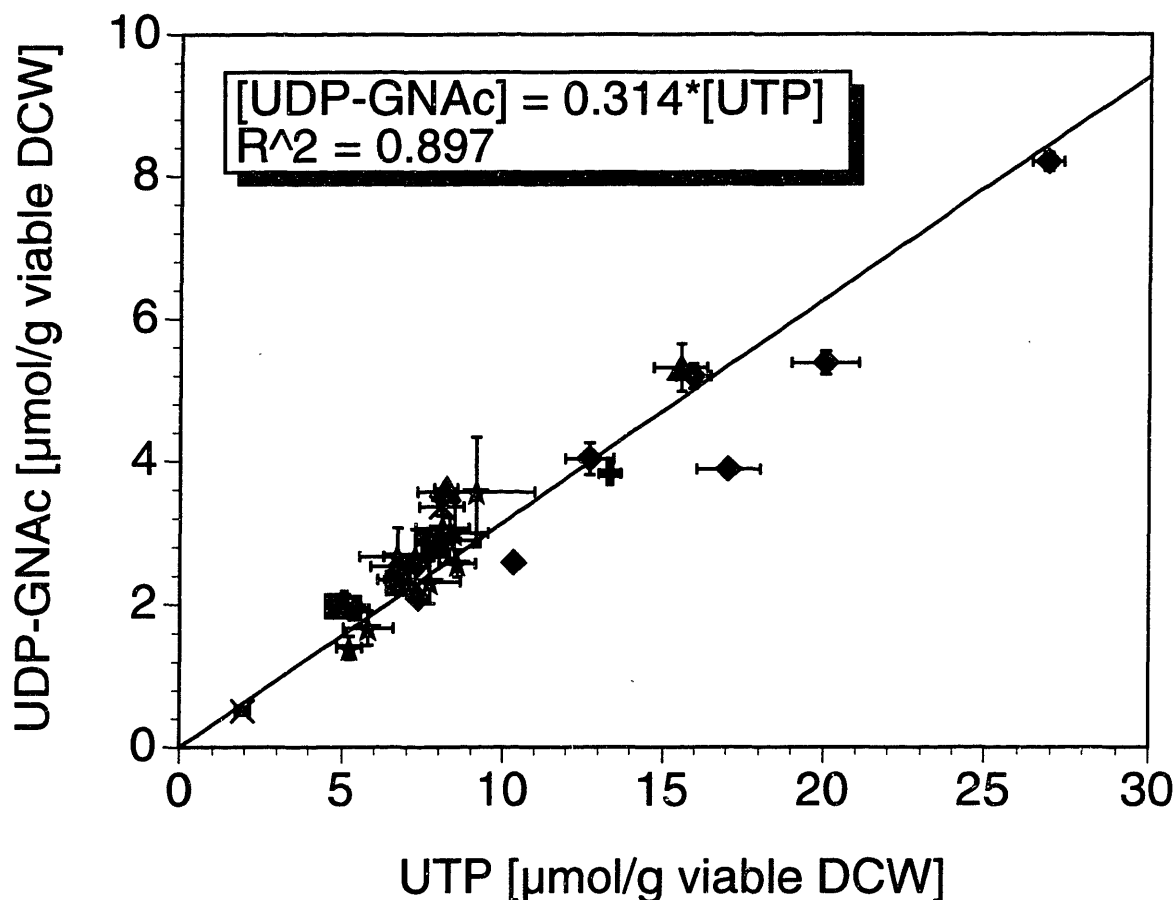


Figure 5-8. The correlation between intracellular UDP-GNac and UTP during exponential growth in batch, fed-batch and chemostat cultures. Symbols indicate results from various independent experiments.

fed-batch culture. Higher concentrations of UTP were obtained by feeding the nucleotide precursor uridine (up to 10 mM), while lower concentrations were observed during glucose starvation at the end of batch culture. Figure 5-8 demonstrates that UDP-GNac was linearly correlated with UTP over a 10-fold range in UTP (from 2.5 to 25 μmole/g vDCW). Similar correlations were found for UDP-Gal and UDP-Glc (data not shown), indicating that in general UDP-sugar levels are regulated by nucleoside triphosphate concentrations. This data is in agreement with the data of Pels Rijcken et al. (1995a), who

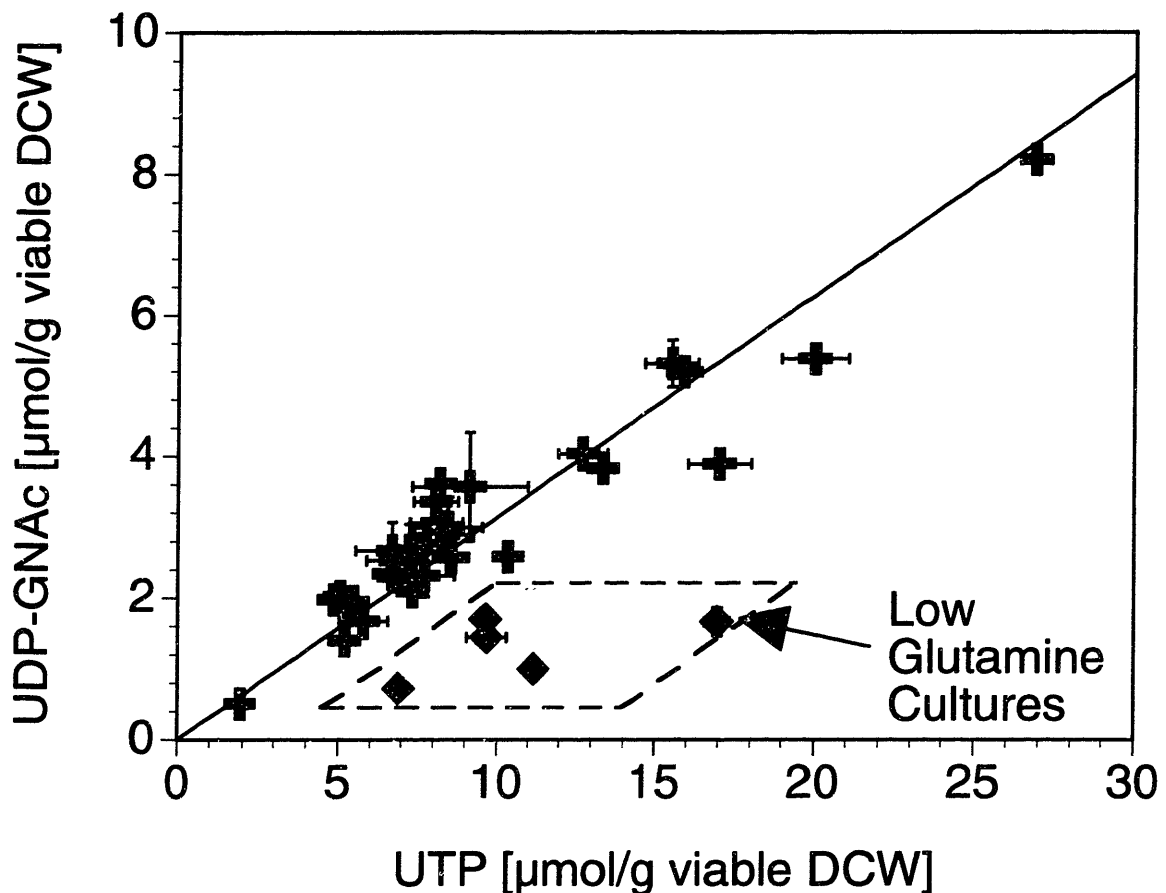


Figure 5-9. Reduced UDP-GNac formation under glutamine limitation: the relationship between UDP-GNac and UTP during glutamine limitation (◆) compared to exponential growth in batch, fed-batch and chemostat cultures (⊕).

found that rat hepatocytes fed 0.5 mM uridine for 40 hours increased the pools of UTP, UDP-Hexose and UDP-GNac 6.7-, 3.8- and 4.6-fold, respectively.

Nucleoside triphosphates are not the only regulators of UDP-sugar synthesis, however, as the glutamine limited chemostat demonstrates. In this case amino sugar formation appears to limit UDP-GNac synthesis. Figure 5-9 re-plots the data from Figure 5-8 along with additional data from glutamine limited cultures (the glutamine limited

chemostat and cells starved for glutamine in batch and fed-batch culture). The data from glutamine limited cultures fall below the exponential growth data, indicating an excess of UTP compared to UDP-GNAc. The glutamine starvation effect was specific to amino sugars, since UDP-Glc and UDP-Gal still correlated with UTP (data not shown). Thus amino sugar formation most likely limits UDP-GNAc synthesis during glutamine starvation.

5.4 Discussion

Glycosylation site occupancy of recombinant IFN- γ varied with intracellular UDP-GNAc (the combined UDP-GlcNAc and UDP-GalNAc pool) for the glucose and glutamine limited steady states analyzed. Based upon analysis of nucleotide levels and estimates of central carbon metabolic fluxes, we propose the model in Figure 5-10 to explain the effects of glucose and glutamine limitation. During glucose limitation available carbon is preferentially used for energy production, causing reduced nucleotide biosynthesis. Because they are continually consumed for RNA synthesis, nucleoside triphosphates such as UTP become depleted. Lower nucleoside triphosphate pools in turn cause lower nucleotide sugar pools and lower glycosylation site occupancy. During glutamine deprivation, amino sugar formation limits UDP-GNAc synthesis, since glutamine is the ammonia donor in this reaction.

While it has been known for some time that glucose starvation decreases glycosylation efficiency (Baumann and Jahreis, 1983; Chapman and Calhoun, 1988; Gershman and Robbins, 1981; Rearick et al., 1981; Stark and Heath, 1979; Turco, 1980), the exact mechanism of this effect has remained unresolved. Glucose starved cells synthesize truncated lipid-linked oligosaccharide precursors, which are transferred to protein with a much lower efficiency than the normal precursor (see Chapter 2). Nucleotide sugar depletion has also been observed in glucose starved cultures (Chapman and Calhoun, 1988; Ullrey and Kalckar, 1979), and it is often cited as the likely cause of truncated

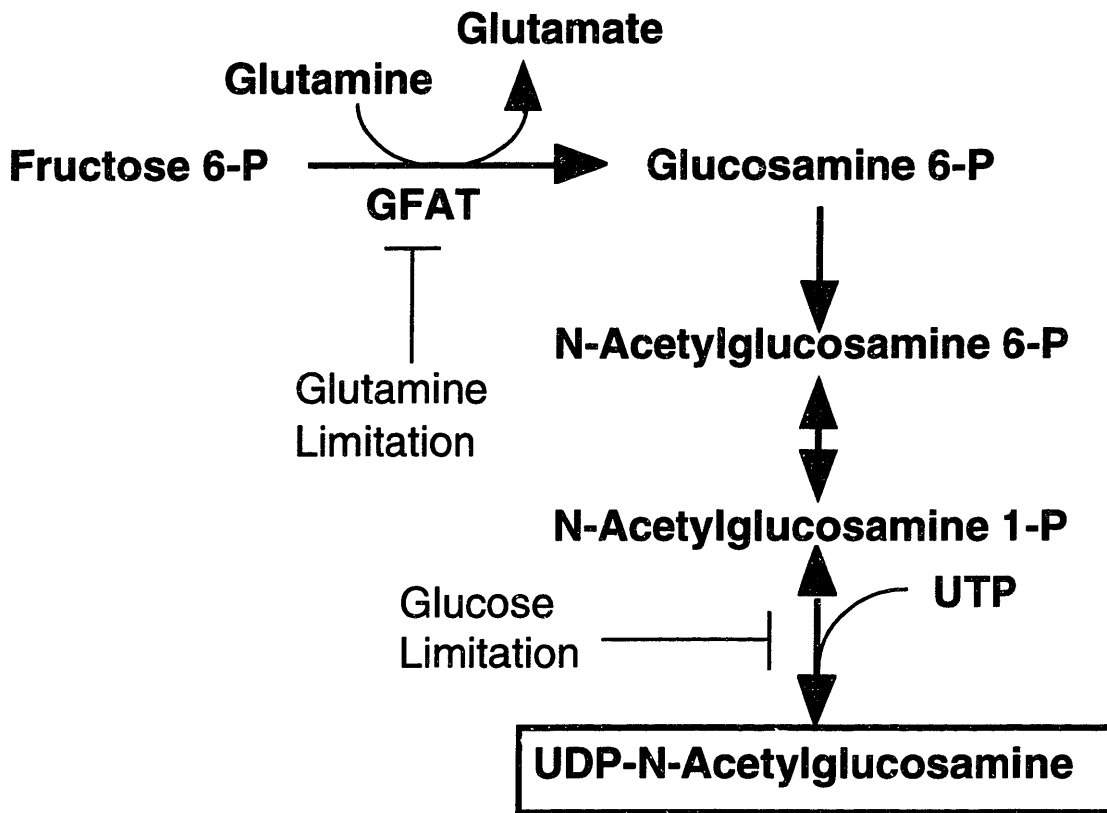


Figure 5-10. Synthesis of UDP-GlcNAc under glucose and glutamine limitation. During glucose starvation, nucleoside triphosphates including UTP are depleted, which limits nucleotide sugar formation. In contrast, glutamine starvation limits UDP-GlcNAc synthesis by preventing amino sugar formation.

precursor synthesis. Proposed explanations for nucleotide sugar depletion during glucose starvation have generally focused on supply of hexose phosphates, but little work has been done to investigate these hypotheses. This chapter presents evidence that nucleoside triphosphate depletion is the cause of reduced intracellular nucleotide sugar concentrations during glucose starvation.

Evidence from the literature supports our hypothesis that glucose starvation affects glycosylation by causing depletion of nucleoside triphosphates. Nucleoside triphosphate depletion during glucose starvation has been observed in the past (Kaminskas, 1979; Rapaport et al., 1979). Declines in nucleoside triphosphates were not explained by increases in nucleoside mono- and diphosphates, indicating that the nucleosides were being depleted. Treatment with cycloheximide, which inhibits protein and RNA synthesis, was found to prevent the decline in ribonucleotide pools during glucose starvation. This result suggests that RNA synthesis plays a role in ribonucleotide depletion during glucose starvation. Interestingly, other experiments have shown that cycloheximide treatment allows glucose starved cells to synthesize the normal $\text{Glc}_3\text{Man}_9\text{GlcNAc}_2\text{-P-P-Dol}$ precursor oligosaccharide (Chapman and Calhoun, 1988). Hence under glucose-starved conditions which do not lead to depletion of nucleoside triphosphates, glycosylation appears normal. This may also explain the results of Lanks et al. (1988), who found that feeding nucleosides was more effective on a molar basis than feeding glucose to suppress glucose regulated protein synthesis in glucose starved murine L929 cells. When glycosylation efficiency is impaired, synthesis of glucose regulated proteins such as BiP (GRP78) is induced, presumably because the underglycosylated proteins mis-fold and accumulate (Kozutsumi et al., 1988; Lee, 1987; Wooden et al., 1991). The finding that uridine feeding can suppress GRP synthesis in glucose starved cultures strongly suggests that uridine fed cells are able to maintain normal glycosylation patterns.

Additional evidence linking glycosylation deterioration to nucleotide depletion during glucose starvation is that the kinetics of the phenomena are very similar. The kinetics of nucleotide depletion are quite rapid; Kaminskas (1979) reported that ribonucleoside triphosphate pools decreased by 66–90% within 15 minutes of glucose starvation in exponentially growing Erlich ascites tumor cells. Within 1 hour of glucose re-feeding, nucleotide levels increased to at or above pre-starvation levels. These kinetics agree with the rapid changes in lipid-linked oligosaccharides observed during glucose starvation (Gershman and Robbins, 1981) and with the rapid changes in glycosylation site occupancy we have observed with periodically starved cells in fed-batch culture (see Chapter 4).

Altered nucleotide levels in non-starved cultures have also been found to influence nucleotide sugars and glycosylation. Treatment of glucose fed Ehrlich ascites tumor cells with cycloheximide was found to increase nucleoside triphosphate pools (Kaminskas, 1979), and this treatment has been shown to increase glycosylation site occupancy of recombinant human prolactin produced in C127 cells (Shelikoff et al., 1994). Shelikoff et al. (1994) found that other protein synthesis inhibitors did not improve glycosylation, and so the effect may have been linked to cycloheximide's ability to inhibit RNA formation and increase nucleotide levels. Pels Rijcken et al. (1995b) demonstrated that nucleotide levels can also be increased by feeding precursors such as uridine, and variations in UDP-sugars were sufficient to cause alterations in glycosylation patterns. Uridine feeding increased the incorporation of N-acetylhexosamine into macromolecules, while sialylation decreased. The authors suggested that elevated UDP-sugar concentrations may have impaired transport of CMP-NeuAc into the Golgi, causing decreased sialylation. Experiments with nucleotide antimetabolites provide further evidence that altered nucleotide levels can influence glycosylation. For example inhibition of purine biosynthesis in HL-60 leukemia cells with 3 μ M 6-methylmercaptapurine ribonucleoside resulted in reduced GTP levels (21% of control) and reduced mannose

incorporation into proteins and oligosaccharides (40% of control) (Sokoloski and Sartorelli, 1987).

For the glucose limited chemostat experiments described here, nucleotide concentrations appeared to vary in response to changes in metabolism. The reactions of the citric acid (TCA) cycle in particular were found to correlate with nucleotide levels and glycosylation in glucose limited chemostats (see Figure 5-6). Metabolism could impact nucleotide biosynthesis by altering the availability of important precursor metabolites such as aspartate, glutamine, serine, glycine and ribose-5-P. Of these precursor metabolites, the TCA cycle is most likely to impact aspartate. The importance of the TCA cycle in providing aspartate for nucleotide synthesis was demonstrated in a respiration deficient Chinese hamster lung fibroblast cell line which had an almost complete shutdown of TCA cycle reactions (DeFrancesco et al., 1976). While the cells were able to grow when 3 mM asparagine was added to the medium, the amount of ^{14}C labeled ATP was reduced by 70% compared to control cells, and UDP-glucose was reduced by 50%. Exogenous aspartate would not even support growth, apparently because it was less readily taken up by the cells. The data suggest that exogenous asparagine can only partially satisfy the demand for intracellular aspartate, and normal nucleotide synthesis relies on the TCA cycle for aspartate supply.

Aspartate is synthesized by the enzyme aspartate aminotransferase, which catalyzes the transfer of a glutamine ammonia group to oxaloacetate. Oxaloacetate is a TCA cycle intermediate which can also react with acetyl CoA to form citrate by the citrate synthase enzyme. Eigenbrodt et al. (1985) cited evidence that oxaloacetate availability is a primary regulator of aspartate formation, and the citrate synthase and aspartate aminotransferase reactions can compete for available oxaloacetate. High concentrations of acetyl CoA favor consumption of oxaloacetate for citrate synthesis, and so increased pyruvate oxidation leads to consumption of oxaloacetate in the TCA cycle and lower aspartate production. Interestingly, we found that increased pyruvate oxidation in glucose limited chemostats

led to lower glycosylation site occupancy (Figure 5-6). Thus when carbon utilization patterns favored consumption of oxaloacetate for citrate synthesis, nucleotide levels and glycosylation site occupancy declined. The data are consistent with the hypothesis that oxaloacetate availability for aspartate synthesis influenced nucleotide synthesis, which in turn influenced nucleotide sugars and glycosylation site occupancy. Glycosylation was best when pyruvate was converted to byproducts such as lactate and alanine, while the worst glycosylation occurred when both lactate and alanine were consumed and more pyruvate was oxidized.

The glutamine limited chemostat demonstrated that, although nucleoside triphosphates play an important role in determining nucleotide sugar concentrations, they are clearly not the only factor. Amino sugar formation can also determine the supply of UDP-GNAc. The glutamine:fructose-6-P amidotransferase (GFAT) enzyme responsible for amino sugar formation transfers an ammonia group from glutamine to fructose-6-P to form glucosamine-6-P. The rate of this reaction depends upon the concentration of glutamine and fructose-6-P, among other factors. Traxinger and Marshall (1991) reported GFAT's glutamine K_m values measured in adipose, liver and other tissues ranged from 0.4 to 1.6 mM. The steady-state concentration of glutamine in the glutamine limited chemostat was 0.022 mM. While the intracellular glutamine concentration most likely differed from the extracellular concentration, one would expect intracellular glutamine was in short supply as well. Limited glutamine supply for amino sugar formation could explain low UDP-GNAc and high UTP concentrations under glutamine limitation (Figure 5-9).

Further evidence implicating amino sugar formation as a regulator of UDP-GNAc synthesis is that feeding amino sugars such as glucosamine or galactosamine leads to accumulation of UDP-GNAc (Kornfeld and Ginsburg, 1966; Pels Rijcken et al., 1995a). Following their entry into the cell, amino sugars are converted into hexosamine phosphates, acetylated, and reacted with UTP to make UDP-GNAc. Since the reaction catalyzed by GFAT is essentially not reversible, glucosamine-6-P is not converted to

fructose-6-P, and the majority of the hexosamine accumulates as nucleotide sugars. The UDP-GNAc expansion can be severe enough to cause UTP depletion and cell death. Such excessive accumulation demonstrates that amino sugar levels can play a key role in UDP-GNAc synthesis. Under normal conditions amino sugar formation must be tightly regulated to maintain sufficient supply of glucosamine-6-P, without over-stimulating nucleotide sugar formation. However, UDP-GNAc concentrations cannot be the only source of feedback regulation, since amino sugar formation does not limit UDP-GNAc expansion when UTP is increased by feeding uridine. This data seem to implicate hexosamine phosphates as regulators of the GFAT reaction.

5.5 Conclusions

Continuous culture experiments allowed us to analyze central carbon metabolism under conditions which led to varied product glycosylation site occupancy. Although site occupancy varied over a narrow range, we found that differences correlated with the intracellular UDP-GNAc concentration. Measured nucleotide levels and estimates of central carbon metabolic fluxes point to nucleoside triphosphate depletion as the cause of decreased site occupancy during glucose limitation. Subsequent experiments in batch and fed-batch culture have confirmed that UDP-sugar concentrations are correlated with UTP levels in the absence of glutamine limitation. Glutamine limitation appears to influence glycosylation by reducing amino sugar formation and hence UDP-GNAc concentrations.

It should be emphasized that continuous culture experiments are used to study cells under nutrient limitation. We found that under glucose or glutamine limitation, nucleotide sugar formation can be responsible for observed changes in glycosylation site occupancy. Under non-limiting conditions, nucleotide sugars may or may not play an important role in regulating glycosylation site occupancy. The relatively modest change in site occupancy (from 70% to 62% 2-site glycosylated protein) for a 40% reduction in UDP-GNAc tends to suggest that nucleotide sugar concentrations can vary over a fairly wide

range without having major impact on glycosylation site occupancy. Nucleotide sugar concentrations may only be critical during extreme starvation. The influence of nucleotide sugars on glycosylation site occupancy during normal exponential growth is explored in Chapter 6.

6. The Influence of Nucleotide Sugars on IFN- γ Glycosylation Site Occupancy

The experiments described in the previous chapter established that the primary determinants of nucleotide sugar concentrations during exponential growth were nucleoside triphosphate concentrations and amino sugar formation. Under conditions of glucose or glutamine limitation, nucleotide sugars limited glycosylation site occupancy. However, it was not clear from the results in Chapter 5 to what extent nucleotide sugars influence glycosylation in cultures which are not nutrient limited. Can increasing nucleotide sugar concentrations improve glycosylation site occupancy in non-starved cultures? Do nucleotide sugar variations during normal batch and fed-batch culture explain the changes in glycosylation site occupancy described in Chapter 4?

The experiments described in this chapter were designed to answer these questions. The influence of nucleotide sugars on glycosylation site occupancy was investigated by feeding nucleotide sugar precursors. Alterations in nucleotide sugar concentrations were monitored and related to glycosylation site occupancy. Nucleotide sugar concentrations and glycosylation site occupancy were also monitored with time during fed-batch culture. The results indicate that nucleotide sugars primarily influence glycosylation site occupancy during periods of starvation; increased nucleotide sugar concentrations led to only modest improvement in glycosylation. Furthermore the gradual decline in glycosylation site occupancy observed during exponential growth (Chapter 4) is caused by a step downstream of nucleotide sugar formation, as nucleotide sugar concentrations actually increased during this time.

6.1 Sugar Precursor Feeding

6.1.1 Alternative Carbon Sources

According to the results from Chapter 5, nucleoside triphosphates and amino sugar formation are the primary determinants of nucleotide sugar concentrations in glucose fed cultures. Hexose phosphates did not appear limiting, despite the demand placed on hexose phosphates by glycolysis and the pentose phosphate cycle. To further examine the role of hexose carbon in glycosylation, a series of sugar feeding experiments were performed in serum-free, suspension culture. Sugars which enter carbon metabolism at various reactions (Figure 6-1) were fed and glycosylation was monitored with radiolabeling after two days. Galactose, fructose, mannose and glucosamine were chosen based upon literature information about uptake and utilization (Schachter, 1978; Yurchenco et al., 1978).

Glycosylation after a two day exposure to the sugars fed is shown in Figure 6-2. The data illustrate that glycosylation was minimally affected by hexose feeding, while a dramatic decline in glycosylation was observed upon feeding the amino sugar glucosamine. To insure that the sugars were indeed transported to and utilized by the cells, sugar concentrations were monitored over a three day batch. Measurable consumption of sugars occurred, with mannose most readily utilized. In addition, cells were adapted to growth in the presence of mannose alone (i.e. without glucose), or mannose plus galactose (the cells would not grow well with galactose or fructose as the sole carbon source). Maximal glycosylation with the various sugar sources was found to be similar in all cases, although end of batch starvation behavior varied as the sugars were exhausted at different times (results not shown). The data are consistent with the hypothesis that hexose phosphates are not the primary regulators of nucleotide sugar formation and glycosylation. Amino sugars can be important, however, as the glucosamine-fed flask demonstrated.

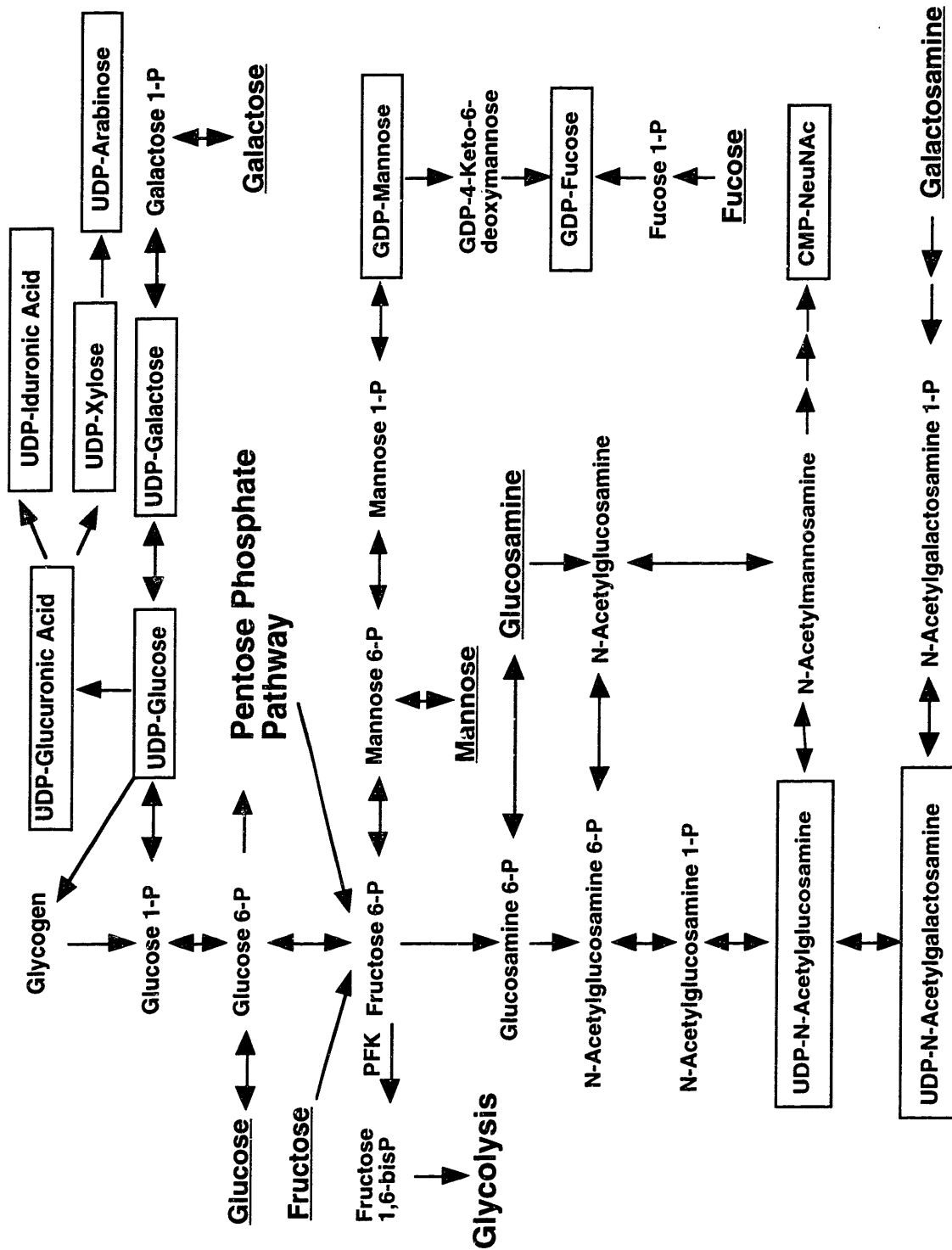


Figure 6-1. Biosynthesis of common nucleotide sugars from various carbon sources (Schachter, 1978).

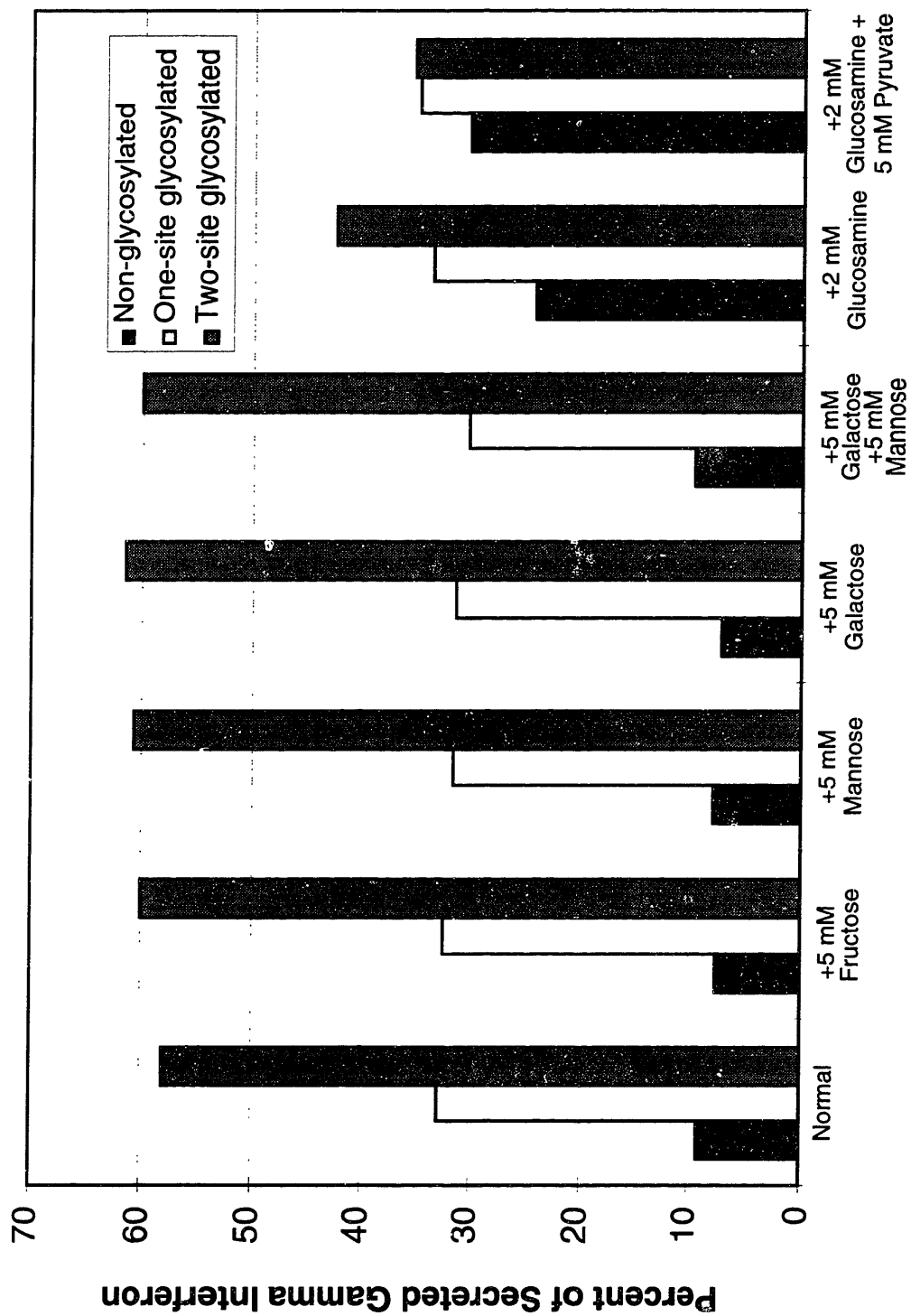


Figure 6-2. Glycosylation site occupancy of IFN- γ produced in the presence of various sugars.

6.1.2 The Influence of Glucosamine On Nucleotide Sugars and Glycosylation Site Occupancy

The most interesting result from the sugar feeding experiments was the decline in glycosylation observed with glucosamine feeding. A dose-response experiment was performed to see if the decline would occur in a dose-dependent manner. The results shown in Figure 6-3 indicate that as the glucosamine concentration was increased, glycosylation decreased. In addition to its impact on glycosylation, glucosamine is known to cause accumulation of UDP-GlcNAc and UDP-GalNAc (the sum is referred to as UDP-GNAc) (Kornfeld and Ginsburg, 1966). Glucosamine feeding causes accumulation of UDP-GNAc, because glucosamine is not freely converted to other sugars and metabolized. As discussed in the Literature Review, this is because amino sugar formation is not normally reversible, and so glucosamine-6-P is not readily converted to fructose-6-P.

In order to explain the decline in glycosylation with glucosamine feeding, several hypotheses can be suggested: (1) accumulation of UDP-GNAc could deplete the cellular UTP needed for UDP-Glc synthesis, (2) accumulation of UDP-GlcNAc may elevate GlcNAc-P-P-dolichol, depleting the dolichol which is also necessary for Glc-P-dolichol and Man-P-dolichol and (3) glucosamine itself may inhibit glycosylation reactions. The first hypothesis seemed plausible, since depletion of UTP with galactosamine feeding had been reported in the literature (Pels Rijcken et al., 1995a). Moreover, feeding pyruvate with glucosamine led to even worse glycosylation (Figure 6-2), and pyruvate would be expected to worsen UTP depletion, since pyruvate oxidation was correlated to decreased nucleoside triphosphate levels in chemostat cultures (Chapter 5).

To investigate the hypothesis that glucosamine affects glycosylation by depleting UTP, nucleotide levels and glycosylation site occupancy were monitored when γ -CHO cells were fed glucosamine alone or in combination with uridine. Table 6-1 presents the intracellular nucleotide concentrations for untreated (control) cells, cells treated with 2

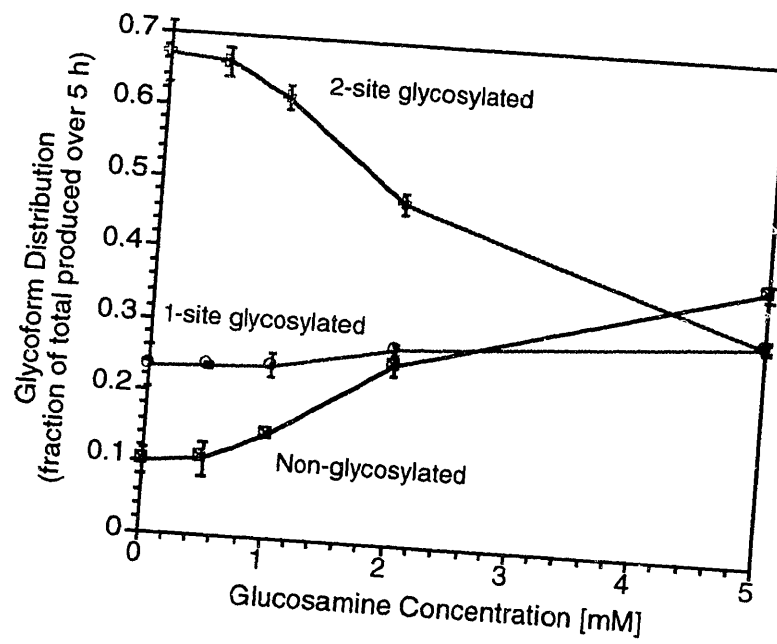
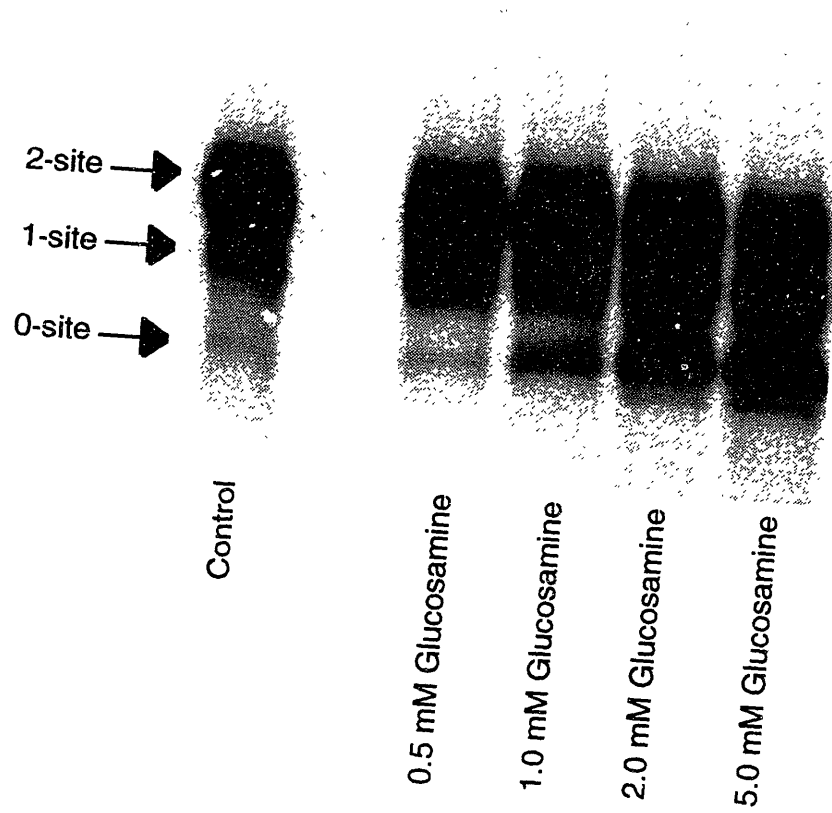


Figure 6-3. The influence of glucosamine on IFN- γ glycosylation site occupancy.

Table 6-1. The effects of uridine (5 mM) and glucosamine (2 mM) on intracellular nucleotide levels ($\mu\text{mol/g}$ viable dry cell weight).

Nucleotide	Control	+glucosamine	+uridine	+glucosamine +uridine
ATP	21.95 \pm 0.42	23.28 \pm 0.88	18.38 \pm 0.91	19.69 \pm 0.09
ADP	1.64 \pm 0.05	1.49 \pm 0.05	1.63 \pm 0.17	1.40 \pm 0.08
GTP	4.82 \pm 0.21	4.45 \pm 0.11	4.51 \pm 0.21	4.30 \pm 0.08
GDP	0.34 \pm 0.00	0.32 \pm 0.01	0.32 \pm 0.02	0.33 \pm 0.03
CTP	4.73 \pm 0.11	3.53 \pm 0.19	7.18 \pm 0.34	4.41 \pm 0.33
UTP	8.21 \pm 0.36	5.38 \pm 0.20	15.53 \pm 0.84	9.43 \pm 0.23
UDP	0.86 \pm 0.20	1.17 \pm 0.15	1.31 \pm 0.16	1.95 \pm 0.08
UDP-GNAc	3.61 \pm 0.02	38.56 \pm 0.41	5.31 \pm 0.33	49.53 \pm 0.94
UDP-Glc+ GDP-Man	2.19 \pm 0.04	1.69 \pm 0.05	3.14 \pm 0.14	2.34 \pm 0.10
UDP-Gal	0.96 \pm 0.02	0.79 \pm 0.03	1.38 \pm 0.06	0.95 \pm 0.04

mM glucosamine, cells treated with 5 mM uridine and cells treated with both 2 mM glucosamine and 5 mM uridine. Accumulation of UDP-GNAc due to glucosamine feeding did appear to cause some depletion of UTP and other UDP-sugars. Feeding 2 mM glucosamine led to a 10-fold increase in intracellular UDP-GNAc, and decreases in UDP-Gal (18% decrease), UDP-Glc+GDP-Man (23% decrease) and UTP (35% decrease). The UTP depletion could be reversed by feeding uridine. Feeding 5 mM uridine in addition to 2 mM glucosamine recovered UDP-sugar and UTP concentrations to at or above control concentrations, and led to even higher UDP-GNAc concentrations.

The relationship between glycosylation site occupancy and UDP-GNac during glucosamine and uridine feeding is shown in Figure 6-4. As the UDP-GNac concentration increased, glycosylation site occupancy decreased. The effect was not due to UDP-Glc depletion, since the uridine+glucosamine culture had a UDP-Glc+GDP-Man concentration slightly higher than the control, and yet glycosylation site occupancy was even worse than with glucosamine alone. Worse glycosylation with uridine+glucosamine implicates excessive UDP-GNac as the cause of poor glycosylation, rather than inhibition of glycosylation by glucosamine itself.

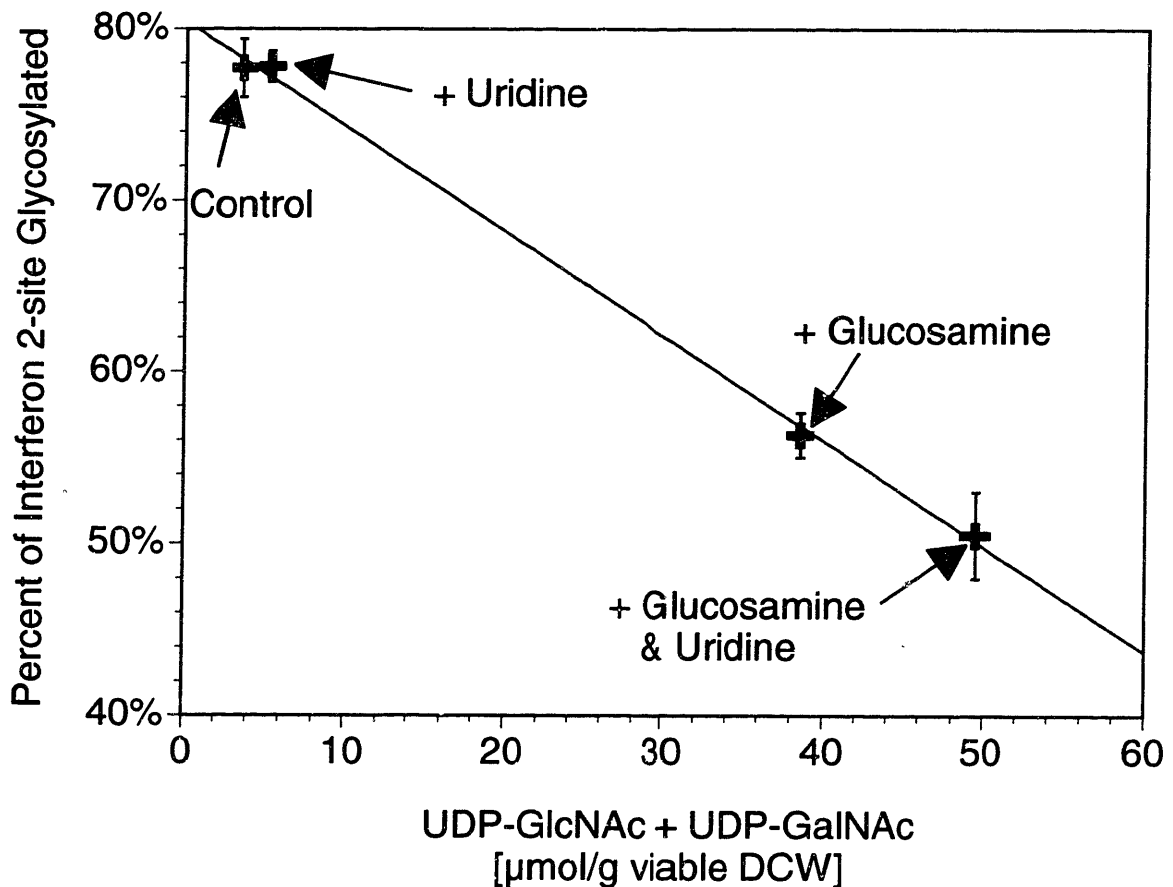


Figure 6-4. The relationship between IFN- γ glycosylation site occupancy and intracellular UDP-GNac with glucosamine and uridine feeding.

6.1.3 Discussion

Previous investigators have also found that glucosamine feeding causes a reduction in glycosylation (Datema and Schwarz, 1979; Elbein, 1987; Koch et al., 1979; Pan and Elbein, 1982). In our glucosamine and uridine feeding experiments, we observed an inverse correlation between intracellular UDP-GNAc and glycosylation site occupancy. The evidence did not support the hypotheses that glucosamine itself inhibits glycosylation or that UTP depletion inhibits glycosylation. An inverse correlation between UDP-GNAc and glycosylation may seem contradictory to the positive correlation reported in Chapter 5. However, the range of UDP-GNAc concentrations is quite different in each case. The highest concentration of UDP-GNAc observed during normal exponential growth is $\sim 4 \mu\text{mol/g}$ viable DCW, while glucosamine feeding results in concentrations ten times higher. Furthermore, in normal cultures the UDP-GNAc concentration fluctuates with the UTP concentration, and so UDP-GNAc remains in balance with UDP-Glc. With glucosamine feeding, UDP-GNAc pools expand dramatically out of proportion compared with UDP-Glc. Such lopsided, excessive accumulation of one nucleotide sugar may be detrimental to glycosylation.

A possible mechanism for glucosamine's negative impact on glycosylation site occupancy is that accumulation of UDP-GlcNAc may cause accumulation of GlcNAc-P-P-dolichol, depleting the dolichol which is also necessary to make Glc-P-dolichol and Man-P-dolichol. The proposed mechanism is similar to the effect of UDP-GlcNAc:dolichol-P GlcNAc-1-P transferase (GPT) overexpression discussed in the Literature Review. GPT catalyzes the formation of GlcNAc-P-P-dolichol, and overexpression of this enzyme leads to formation of truncated oligosaccharide precursors and a decrease in glycosylation site occupancy (Waldman et al., 1987; Zhu et al., 1992). The dolichol linked sugars mannose-P-Dol and glucose-P-Dol were depleted in cells overexpressing GPT, due to excessive accumulation of oligosaccharide-P-P-Dol (primarily $\text{Man}_5\text{GlcNAc}_2\text{-P-P-Dol}$) (Rosenwald et al., 1990). The truncated $\text{Man}_5\text{GlcNAc}_2\text{-P-P-Dol}$ precursor is synthesized

directly from nucleotide sugars; the four mannoses and three glucoses which are normally added to complete the precursor are added from dolichol linked sugars. The enzymes catalyzing dolichol sugar formation (Man-P-Dol synthase and Glc-P-Dol synthase) compete with GPT for a common pool of dolichol-P, and overexpression of GPT depletes the dolichol-P needed for dolichol sugar formation. Excessive accumulation of UDP-GlcNAc may mimic GPT overexpression by stimulating the synthesis of GlcNAc-P-P-dolichol.

Although an attractive hypothesis, some evidence seems to contradict dolichol-P depletion as the mechanism for glucosamine's negative impact on glycosylation. Galactosamine feeding was found to cause accumulation of UDP-GNAc similar to glucosamine feeding, but glycosylation was actually slightly enhanced (Pels Rijcken et al., 1995a). Furthermore, 5 mM glucosamine caused truncated precursor oligosaccharide synthesis in MDCK cells, while the same concentration of galactosamine did not influence precursor synthesis or glycosylation (Pan and Elbein, 1982). Pels Rijcken et al. (1995) suggest that such apparent contradictions may be caused by compartmentation of separate pools of UDP-GNAc, with glucosamine-derived and galactosamine-derived pools of UDP-GNAc maintained separately. Such compartmentation need not arise from membrane barriers, but may be caused by multienzyme channeling of metabolites or distinct cellular localization of related enzymes. An alternative explanation is that glucosamine itself may inhibit glycosylation, rather than UDP-GlcNAc (Koch et al., 1979). The finding that uridine enhances glucosamine's negative impact on glycosylation implicates UDP-GlcNAc as the inhibitory compound, but it cannot be ruled out that uridine may also cause higher intracellular glucosamine concentrations via an indirect mechanism.

The sugar precursor feeding experiments confirmed that amino sugar formation plays an important role in nucleotide sugar synthesis and glycosylation. In contrast, altering

hexose carbon sources had little impact on glycosylation site occupancy. Hexose phosphates do not appear to normally limit nucleotide sugar synthesis or glycosylation.

6.2 Nucleotide Precursor Feeding

Since nucleoside triphosphates were implicated as regulators of nucleotide sugar synthesis, nucleotide precursors were used as tools to manipulate nucleotide sugar concentrations. Such experiments allowed us to examine the impact of nucleotide sugar concentrations on glycosylation in non-starved cultures. The nucleotide sugars with the greatest impact on glycosylation site occupancy are UDP-GlcNAc, GDP-Man and UDP-Glc, since they are involved in the synthesis of the lipid-linked oligosaccharide precursor. Therefore the nucleoside triphosphates most likely to impact site occupancy are UTP and GTP.

6.2.1 Altered Nucleotide Levels and Glycosylation Site Occupancy with Exposure to Nucleotide Precursors

The influence of nucleotide precursors on nucleotide sugar concentrations and glycosylation site occupancy was analyzed by feeding γ -CHO cells 1 mM each of orotic acid, uridine, adenosine and guanosine. Orotic acid is an intermediate in the *de novo* synthesis of pyrimidine nucleotides such as UTP and CTP, and orotic acid feeding has been shown to increase pyrimidine pools in rat hepatocytes (Pels Rijcken et al., 1993). Uridine can also be used to synthesize pyrimidine nucleotides, although through salvage pathways rather than the *de novo* pathway (Pels Rijcken et al., 1993). Similarly, adenosine and guanosine can be utilized via salvage pathways to make purine nucleotides (Cory, 1992). After a two day exposure to the various precursors in serum-free, suspension culture, glycosylation was monitored with radiolabeling and perchloric acid extracts were collected for nucleotide analysis.

The impact of nucleotide precursors on intracellular nucleotide sugar concentrations is shown in Table 6-2. Although orotic acid exposure led to elevated pyrimidine nucleotide pools in rat hepatocytes (Pels Rijcken et al., 1993), we observed no increases in pyrimidines with orotic acid feeding in our γ -CHO cells. In contrast, exposure to 1 mM uridine led to doubling of intracellular UTP and an 80% increase in CTP. It is not surprising that CTP levels were affected by uridine feeding, since CTP is synthesized directly from UTP (Cory, 1992). As expected, UDP-sugar concentrations increased in response to the elevated UTP concentration, with UDP-GNac increasing 63%, UDP-Glc+GDP-Man increasing 129% and UDP-Gal increasing 135%.

Table 6-2. The effects of various nucleotide precursors on intracellular nucleotide levels ($\mu\text{mol/g}$ viable dry cell weight).

	Control	+1 mM orotic acid	+1 mM uridine	+1 mM adenosine	+1 mM guanosine
ATP	27.00 \pm 1.28	20.10 \pm 0.14	21.95 \pm 0.13	34.98 \pm 0.05	19.64 \pm 0.05
ADP	1.91 \pm 0.04	1.22 \pm 0.17	1.44 \pm 0.08	1.98 \pm 0.00	1.37 \pm 0.04
AMP	0.37 \pm 0.05	0.17 \pm 0.00	0.33 \pm 0.01	0.41 \pm 0.03	0.37 \pm 0.01
GTP	4.38 \pm 0.32	3.35 \pm 0.12	4.49 \pm 0.35	5.14 \pm 0.02	19.25 \pm 0.32
GDP	0.40 \pm 0.01	0.24 \pm 0.01	0.31 \pm 0.01	0.43 \pm 0.05	1.03 \pm 0.19
CTP	2.63 \pm 0.39	1.96 \pm 0.01	4.73 \pm 0.37	1.37 \pm 0.03	2.51 \pm 0.35
UTP	6.67 \pm 0.58	5.30 \pm 0.15	13.35 \pm 0.35	3.36 \pm 0.08	4.40 \pm 0.06
UDP	0.90 \pm 0.04	0.44 \pm 0.02	0.95 \pm 0.06	0.46 \pm 0.01	0.84 \pm 0.18
UDP-GNac	2.35 \pm 0.14	1.95 \pm 0.02	3.83 \pm 0.01	2.20 \pm 0.14	2.33 \pm 0.00
UDP-Glc + GDP-Man	0.68 \pm 0.05	0.74 \pm 0.01	1.56 \pm 0.00	0.99 \pm 0.16	1.08 \pm 0.03
UDP-Gal	0.31 \pm 0.03	0.35 \pm 0.01	0.73 \pm 0.01	0.40 \pm 0.13	0.39 \pm 0.01

Adenosine caused an increase in purine nucleotides, but to a lesser degree than the pyrimidine expansion observed with uridine feeding. ATP increased by 30% and GTP by 17% in cells fed 1 mM adenosine. The purine nucleotides ATP and GTP can be interconverted through an inosine monophosphate (IMP) intermediate, which explains why both ATP and GTP levels increased (Cory, 1992). Interestingly, adenosine also caused a 50% reduction in UTP levels; the reason for this reduction is unclear. The combined UDP-Glc+GDP-Man pool increased by 46% in response to adenosine feeding, probably due to expansion of GDP-Man pools. Cells fed 1 mM guanosine had a remarkable 340% increase in GTP concentration. Surprisingly, ATP concentrations did not increase, which indicates that the purine nucleotides are not always kept in balance. Guanosine feeding resulted in a 59% increase in the UDP-Glc+GDP-Man pool. Similar to adenosine, guanosine caused a slight decline in UTP concentration, but the effect was less pronounced.

The glycosylation site occupancy of IFN- γ produced in the presence of the various nucleotide precursors is tabulated in Table 6-3. Orotic acid had no effect on glycosylation site occupancy, which was not surprising since nucleotide sugar concentrations were not affected either. Uridine appeared to improve site occupancy slightly, although the improvement was minor in comparison to the large increases in the UDP-GNAc and UDP-Glc+GDP-Man pools (63% and 129% increases, respectively). Likewise, guanosine improved slightly glycosylation site occupancy, probably as the result of a 59% increase in the UDP-Glc+GDP-Man pool. Despite a 46% increase in the UDP-Glc+GDP-Man pool, adenosine negatively impacted glycosylation site occupancy. Depletion of UDP-sugars does not appear to explain the poor glycosylation, since UDP-GNAc concentrations were similar in adenosine fed and control cultures. The reason for adenosine's negative impact on glycosylation remains unclear.

Table 6-3. The effects of various nucleotide precursors on secreted IFN- γ glycosylation site occupancy.

	Glycosylation Sites Occupied (%)		
	2-sites	1-site	0-sites
Control	76.7 \pm 1.5	20.4 \pm 1.2	2.8 \pm 0.5
+1 mM orotic acid	75.9 \pm 1.3	21.4 \pm 0.9	2.7 \pm 0.7
+1 mM uridine	78.6 \pm 1.3	18.1 \pm 1.1	3.3 \pm 0.5
+1 mM adenosine	71.4 \pm 0.8	25.5 \pm 0.4	3.1 \pm 0.5
+1 mM guanosine	79.2 \pm 1.0	18.1 \pm 0.7	2.8 \pm 0.4

6.2.2 Uridine Feeding in Fed-Batch Culture

The nucleotide precursor feeding experiment suggested that an increase in nucleotide sugar concentrations can have a small positive impact on glycosylation site occupancy. However, the experiment was conducted after a brief two day exposure to nucleotide precursors, and glycosylation was not monitored with time. To understand how nucleotide sugars influence glycosylation at various stages during fed-batch culture, a nucleotide precursor-fed culture was monitored over an entire culture span. Uridine was chosen as the nucleotide precursor, so that nucleotide sugar effects could be clearly separated from cell growth effects. Over the course of a two day experiment, 1 mM uridine did not affect cell growth or viability. In contrast, 1 mM adenosine and 1 mM guanosine reduced cell growth by 25% over the two days. Subsequent experiments confirmed that 1 mM guanosine negatively impacts γ -CHO growth and viability, while uridine up to 10 mM has little impact on cell growth.

Fed-batch cultures were analyzed with initial uridine concentrations of 2.5 and 10 mM. At 75 hours an additional 1 mM uridine was added to account for consumption. Two

control flasks were also analyzed: a non-fed batch and a fed-batch, both without added uridine. The feeding strategy was performed according to the stoichiometric fed-batch technique with a modified RPMI-SFM initial medium as described in Materials and Methods (Chapter 3). Differential product glycosylation was monitored daily with pulse-radiolabeling, and perchloric acid extracts were collected for nucleotide analysis. Extracts were collected during the four hour radiolabeling period so that observed glycosylation patterns could be directly compared with measured nucleotide sugar concentrations.

The differentially measured glycosylation site occupancy in the fed batch cultures is shown in Figure 6-5. For most of the culture, the percentage of protein glycosylated at both potential sites was about 4% higher than the control for the 10 mM uridine fed cultures and about 2% higher for the 2.5 mM fed cultures (Figure 6-6 replots only the 2-site glycosylated data to show this more clearly). As seen in Figure 6-7, cell growth was minimally affected by the uridine treatment (regressed growth rates were 0.0176 1/h for the control, 0.0194 1/h for the 2.5 mM uridine flask and 0.0174 1/h for the 10 mM uridine flask). Figure 6-8 shows that gamma interferon productivities were also identical at 1.4 pg/cell/day. Thus the improvement in product quality did not come at the expense of product titer.

As in previous fed batch studies (see Chapter 4), glycosylation site occupancy declined during the growth phase, with each of the fed batch cultures declining in parallel. Figure 6-9 and Figure 6-10 show that during this time nucleotide sugar concentrations were increasing. The fact that nucleotide sugar concentrations increased while glycosylation site occupancy decreased suggests that a step downstream of nucleotide sugar formation caused the decline.

The fed batch experiments also confirmed the starvation behavior suggested in Chapter 5 based upon chemostat results. The batch control flask exhibited a classic glucose

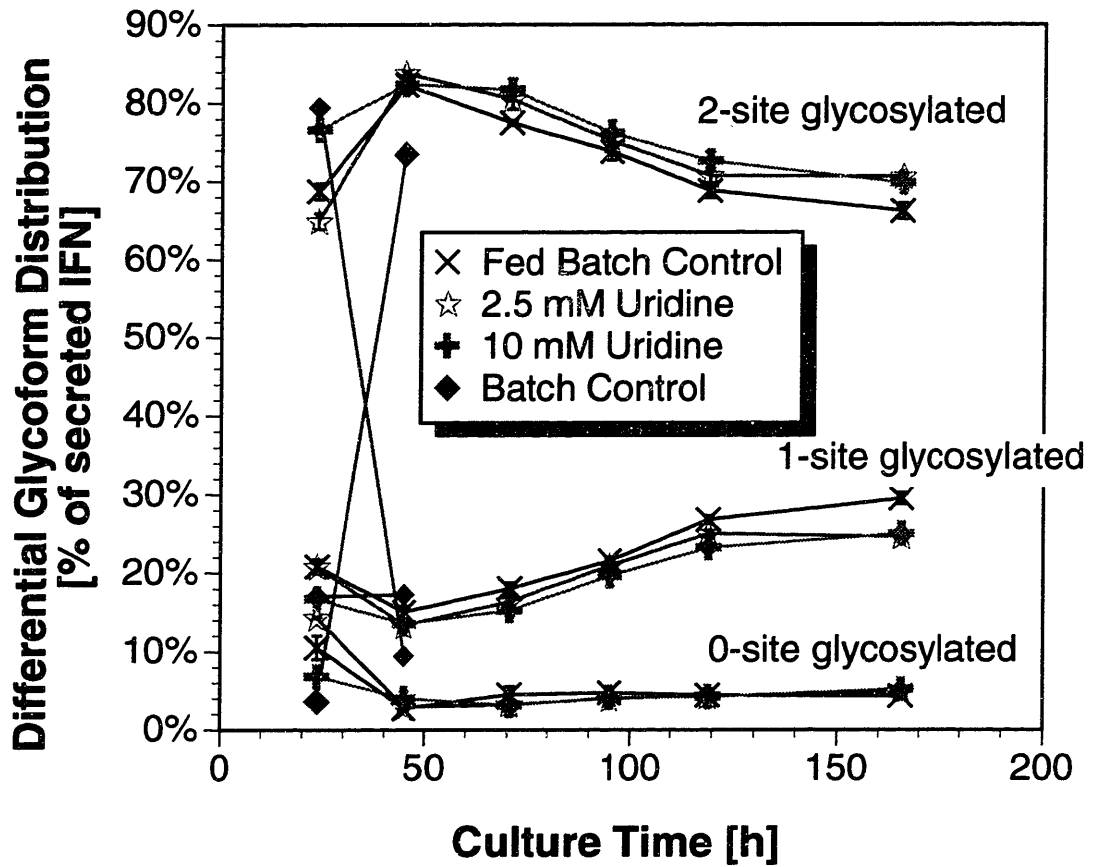


Figure 6-5. Differentially produced IFN- γ glycosylation site occupancy monitored with pulse radiolabeling in fed-batch culture of γ -CHO cells with and without uridine supplementation.

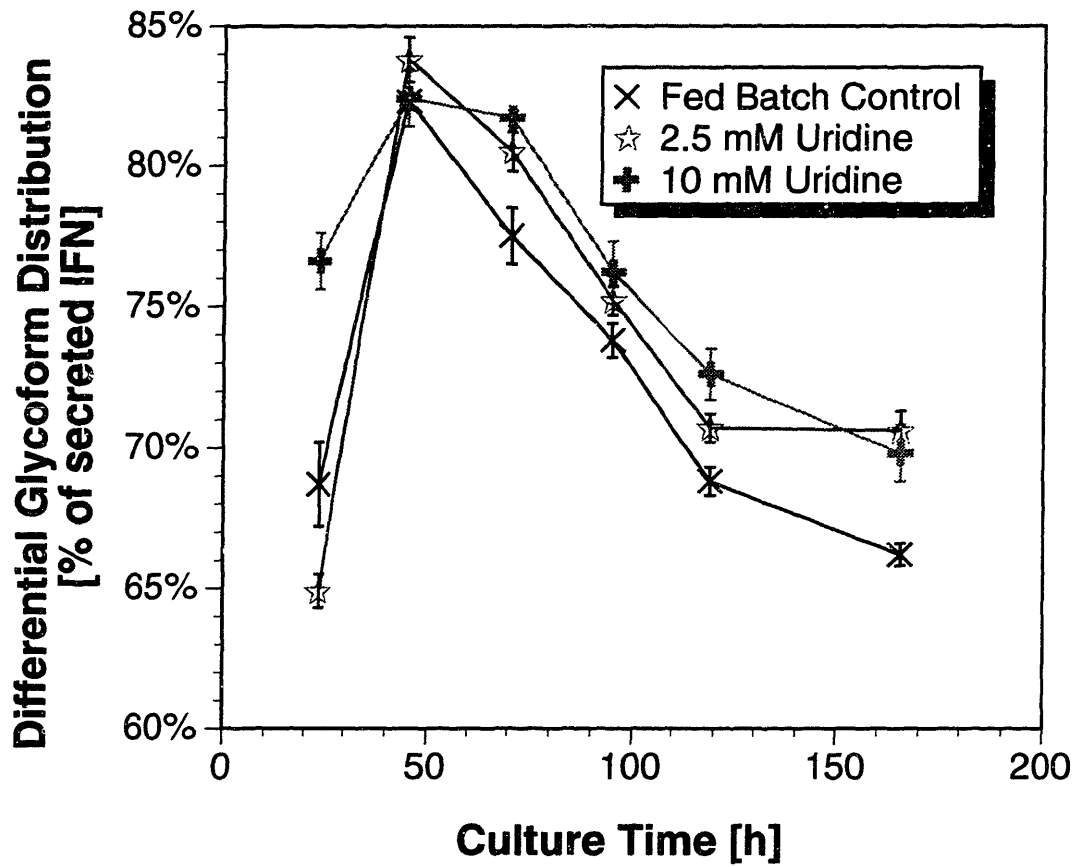


Figure 6-6. Percentage of IFN- γ two-site glycosylated (monitored with pulse radiolabeling) during fed-batch culture of γ -CHO cells with and without uridine supplementation.

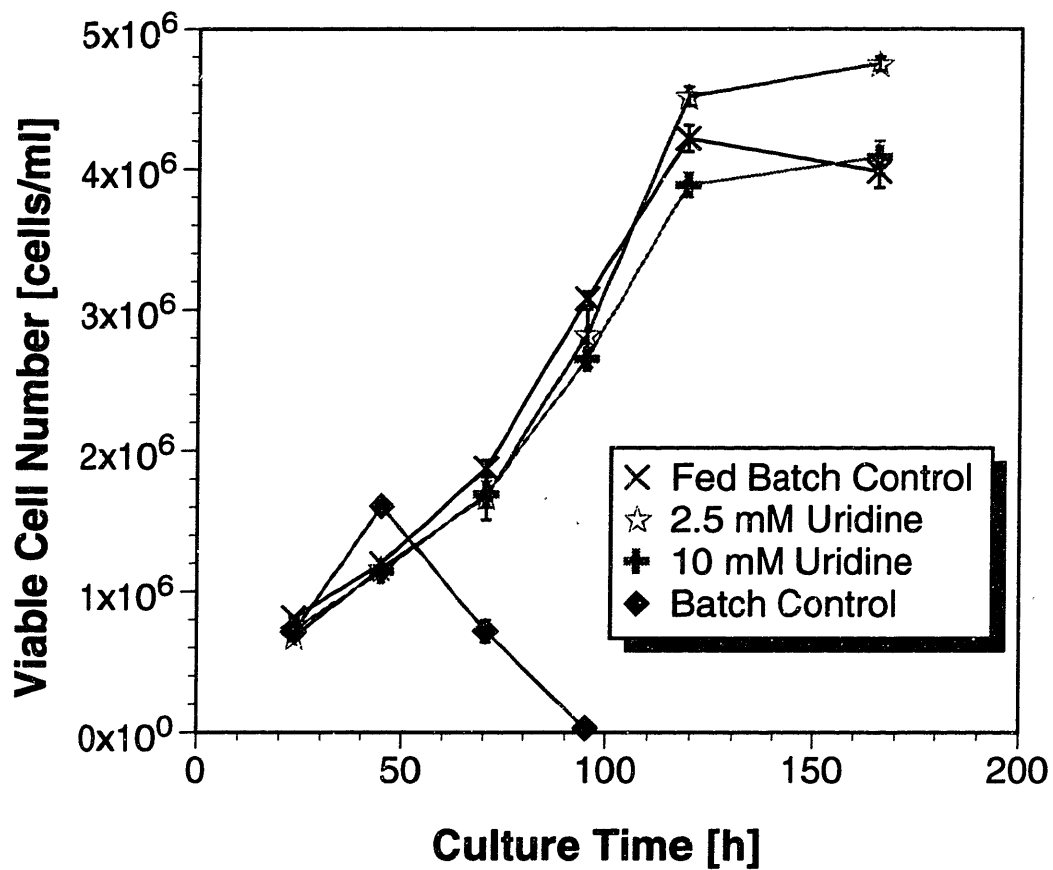


Figure 6-7. Viable γ -CHO cell densities during fed-batch culture with and without uridine supplementation.

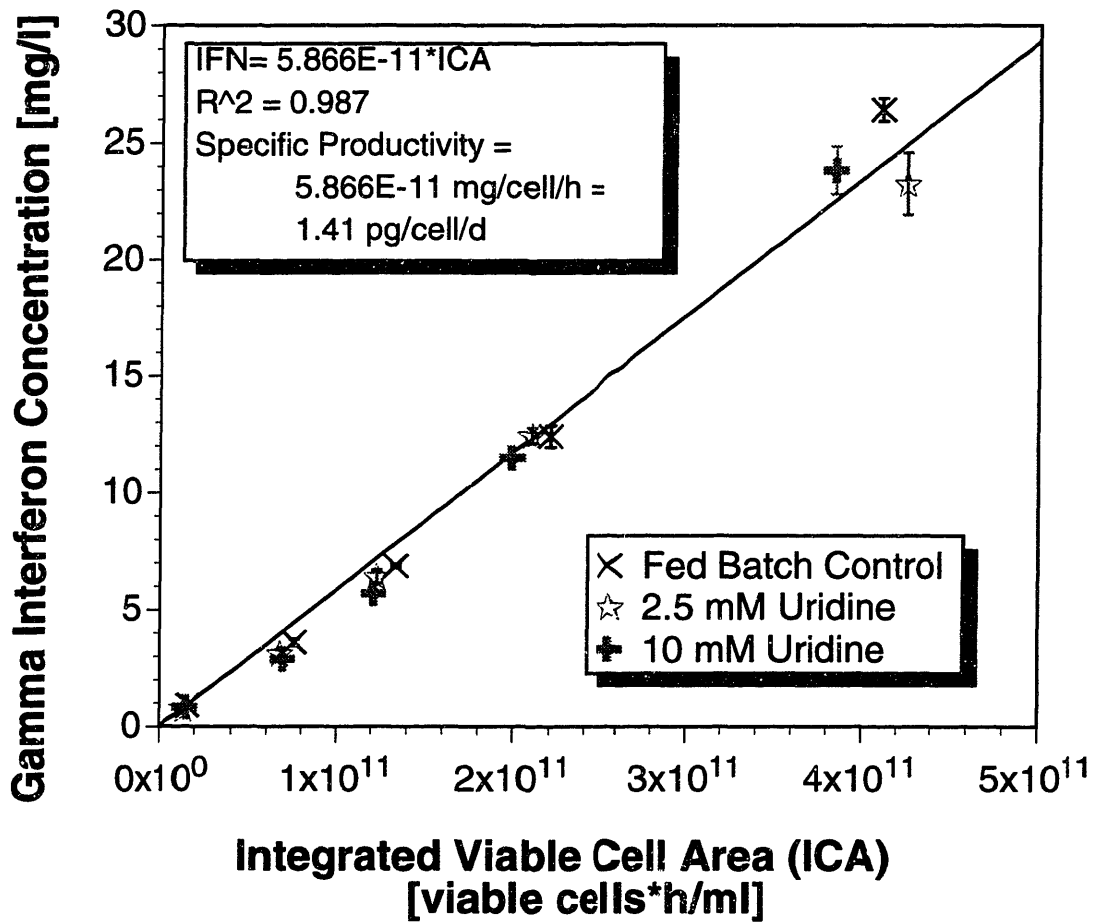


Figure 6-8. Gamma interferon productivity during fed-batch culture of γ -CHO cells with and without uridine supplementation.

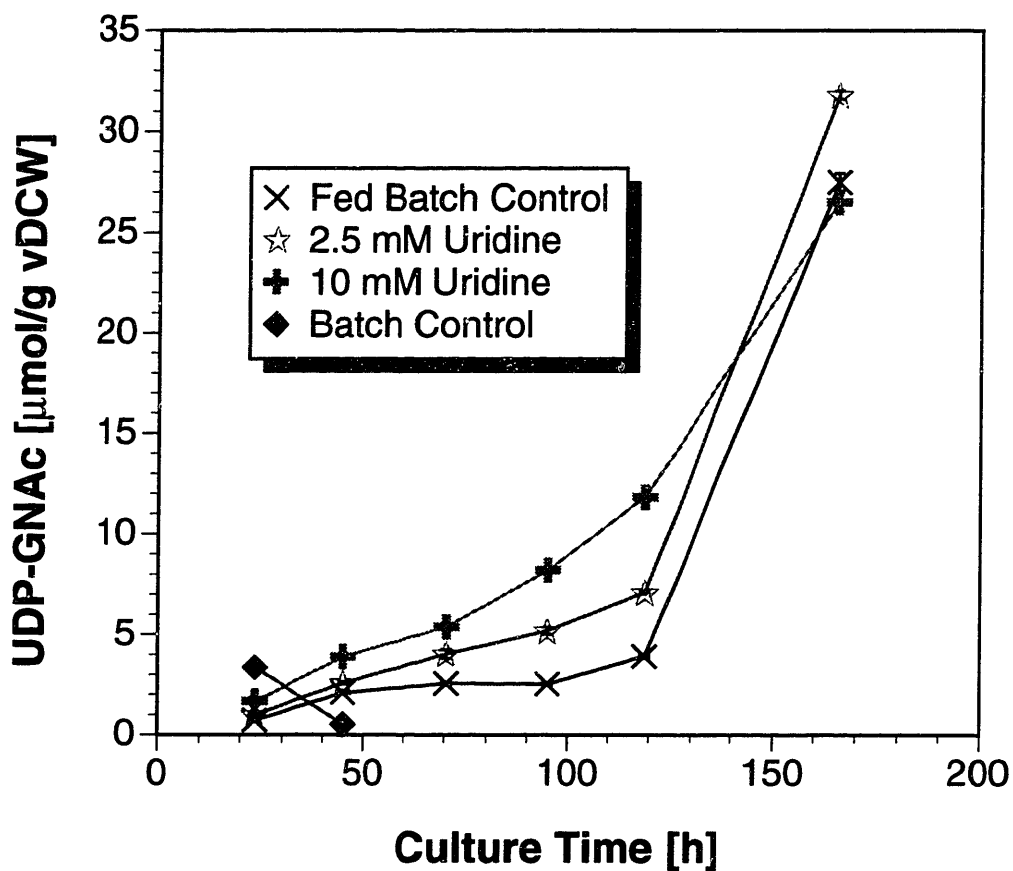


Figure 6-9. Changes in intracellular UDP-GNac concentration during fed-batch culture of γ -CHO cells with and without uridine supplementation.

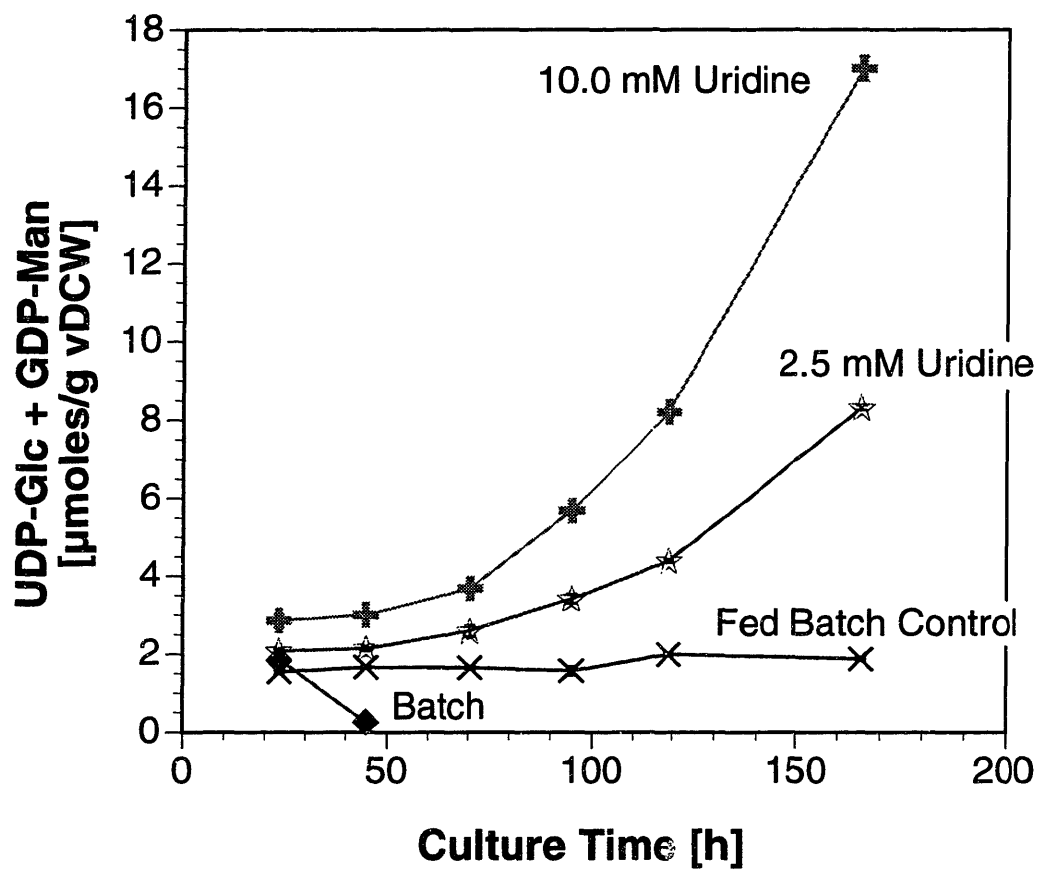


Figure 6-10. Changes in intracellular UDP-Glc+GDP-Man concentration during fed-batch culture of γ -CHO cells with and without uridine supplementation.

limitation, as is shown in the plot of glucose vs. time in Figure 6-11. At 45 hours the cells were still 98% viable, but the secreted interferon was 73% non glycosylated (Figure 6-5). At this time nucleotide and nucleotide sugar levels were much lower than normal (Figure 6-9 and Figure 6-10). The data confirm that intracellular nucleotide concentrations decrease during glucose starvation, and this decrease is probably the cause of decreased nucleotide sugars and poor glycosylation. The results in Chapter 5 also indicated that during glutamine limitation the formation of amino sugars limits UDP-GlcNAc formation and glycosylation. HPLC amino acid analysis indicated that the first samples of the fed batch cultures were glutamine limited as a result of underfeeding (Figure 6-12). Despite high UTP concentrations, the UDP-GlcNAc concentrations were low and glycosylation was lower than expected for these samples, consistent with amino sugar formation limiting UDP-GlcNAc synthesis.

In addition to affecting glycosylation site occupancy, nucleotide sugars may influence the structure and composition of the attached oligosaccharides (glycosylation microheterogeneity). The microheterogeneity of the accumulated IFN- γ produced during the first 144 hours of the fed-batch cultures was analyzed by Dr. Jifeng Zhang using chromatography and matrix-assisted laser-desorption ionization/time-of-flight (MALDI/TOF) mass spectrometry (Gu et al., 1997; Harmon et al., 1996). The site-specific oligosaccharide heterogeneity at Asn-25 and Asn-97 are presented in Table 6-4. As the concentration of uridine increased, the antennarity and sialylation of oligosaccharides at both Asn-25 and Asn-97 decreased. Because the fed-batches all had high viabilities and similar growth kinetics, the changes in microheterogeneity were attributed to altered nucleotide sugar concentrations.

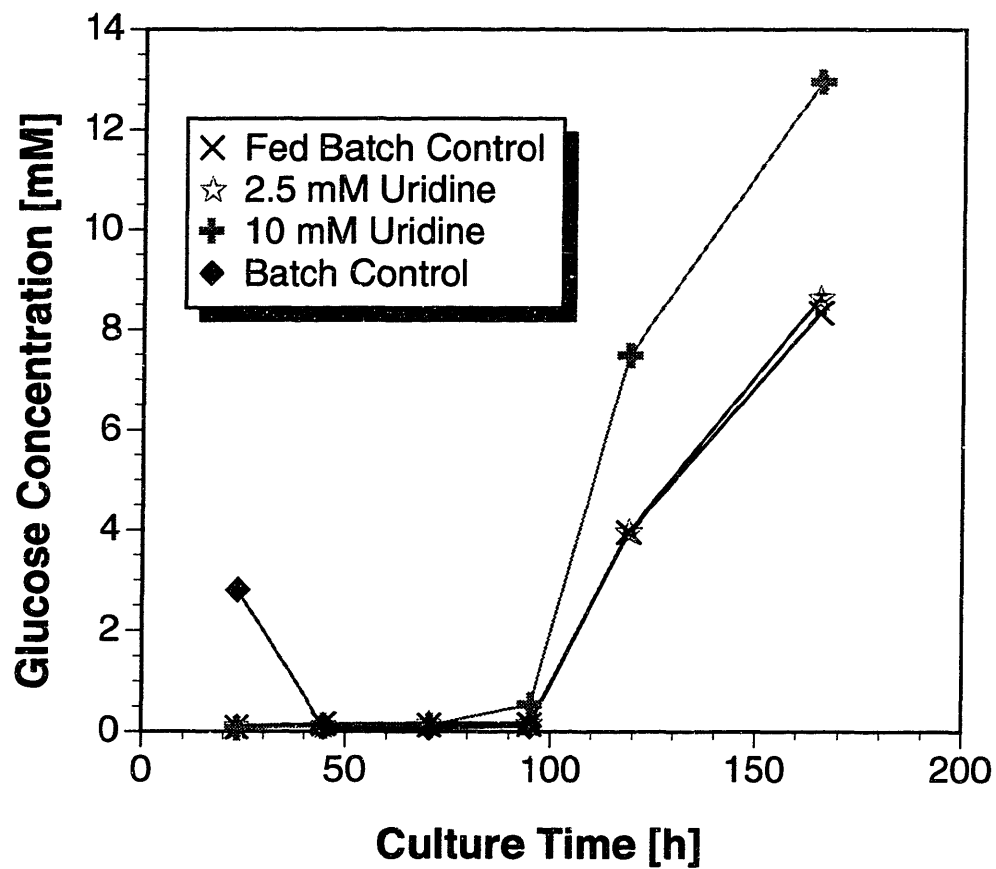


Figure 6-11. Glucose concentration during fed-batch culture of γ -CHO cells with and without uridine supplementation.

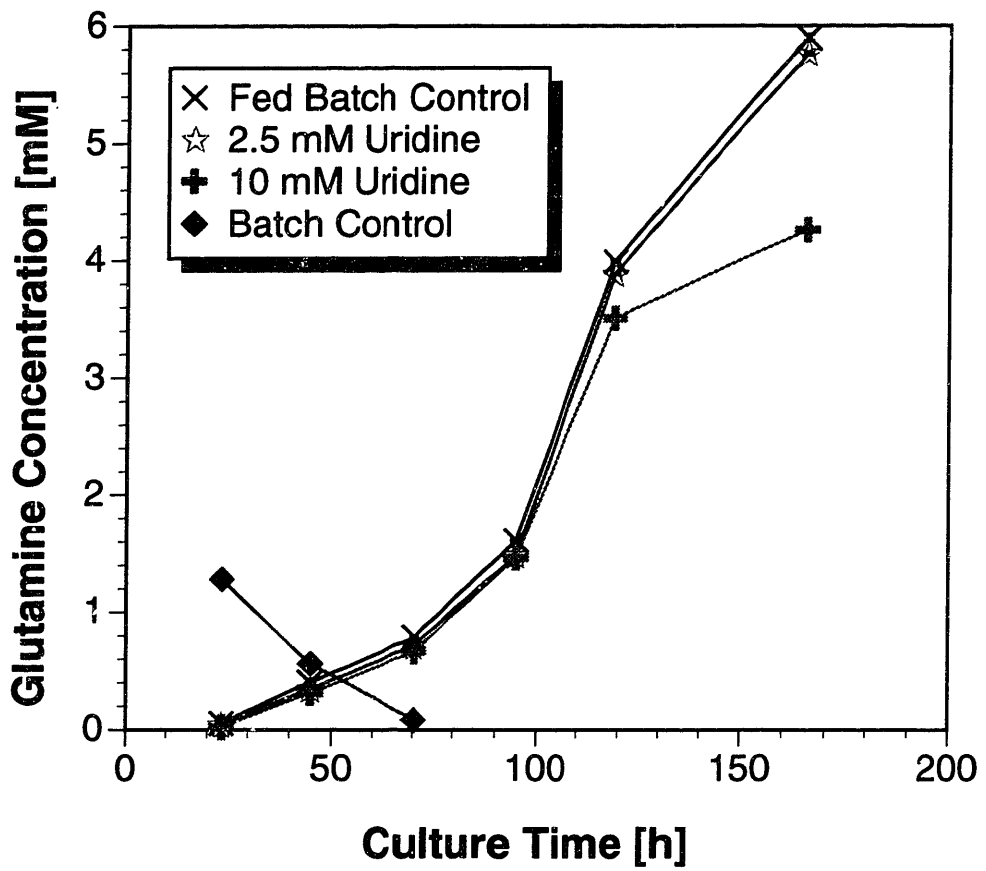


Figure 6-12. Glutamine concentration during fed-batch culture of γ -CHO cells with and without uridine supplementation.

Table 6-4. Site-specific oligosaccharide microheterogeneity of IFN- γ secreted during fed-batch culture of γ -CHO cells with and without uridine supplementation.

	Uridine [mM]	IFN- γ oligosaccharide microheterogeneity			
		tetraantennary	triantennary	biantennary	sialylation
Asn-25:	0.0	19.4%	24.3%	56.3%	94.3%
	2.5	14.7%	22.4%	62.9%	92.3%
	10.0	8.89%	18.7%	72.4%	88.1%
Asn-97:	0.0	3.89%	14.4%	81.7%	78.7%
	2.5	2.47%	7.80%	89.7%	72.5%
	10.0	0.00%	4.30%	95.8%	67.6%

6.2.3 Discussion

Nucleotide sugar availability is one of several factors which may influence glycosylation site occupancy. As discussed in Chapter 2, site occupancy can also be affected by dolichol availability, glycosyltransferase activities, oligosaccharyltransferase activity, and competition with protein folding. Understanding how nucleotide sugars influence glycosylation requires an understanding of how nucleotide sugar levels interact with other factors influencing glycosylation.

Figure 6-13 presents a “tank and valve” analogy to help visualize how nucleotide sugar levels are related to glycosylation site occupancy. In this analogy the intracellular nucleotide sugar concentration is represented as a liquid level in a tank. The nucleotide sugars influence the glycosylation flux to protein through a series of “valves” which

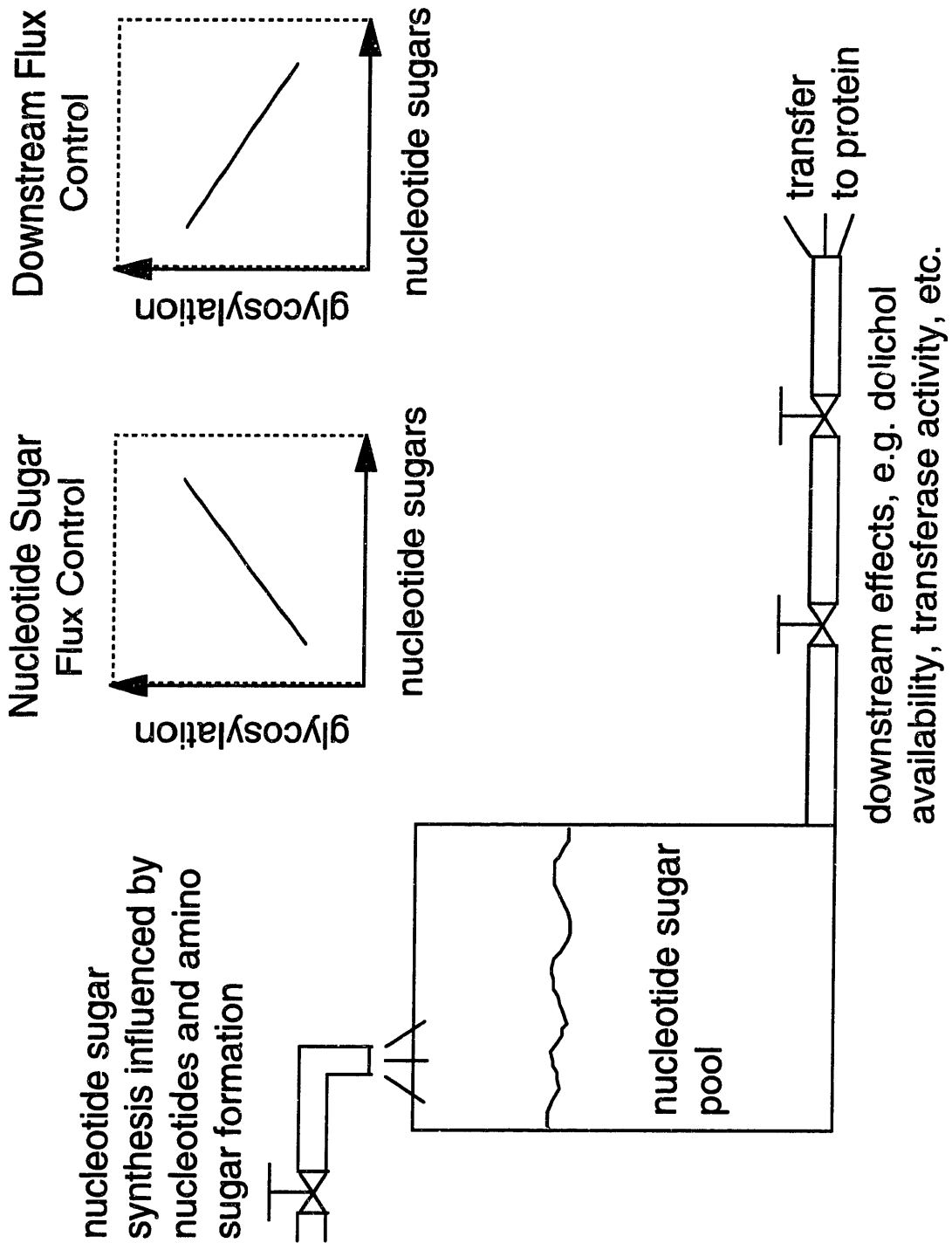


Figure 6-13. Conceptual schematic of the initial N-linked glycosylation steps.

The nucleotide sugar pool is considered as a liquid in a tank, with the height corresponding to the nucleotide sugar concentration.

represent downstream step(s) influencing glycosylation, such as dolichol availability, oligosaccharyltransferase activity, etc. If the “valve positions” remain constant, then the liquid level (nucleotide sugar concentration) represents a driving force which should influence the flow rate (glycosylation flux), assuming the tank is not “overflowing.” Thus for given valve settings, increasing the liquid level (e.g. feeding uridine to increase UDP-sugars) should lead to an increase in flow (glycosylation flux). For the uridine fed-batch experiment, the case of constant downstream limitations can be considered by comparing cultures with different uridine concentrations at the same culture time. Each time point should represent similar downstream limitations for each culture, since cell growth and product formation were essentially identical. Figure 6-14 shows that for a given set of downstream limitations there is a weak positive correlation between nucleotide sugar concentrations and glycosylation site occupancy. Increasing nucleotide sugars for a given set of downstream limitations can lead to modest improvement in glycosylation.

In the tank and valve analogy, changes in downstream limitations are represented as changes in valve settings. As valve settings change, the flow rate will change, causing changes in the tank’s liquid level. For example, when a valve is slowly closed (when downstream factors limit glycosylation), the out-flow (glycosylation flux) is reduced and the tank liquid level (nucleotide sugar concentration) will increase since out-flow is reduced, while in-flow remains the same. In this manner the liquid level will rise, working to counteract changes in flow caused downstream. Thus if factors downstream of nucleotide sugar formation are dominating glycosylation flux, then glycosylation should vary inversely with nucleotide sugar concentrations. We found this to be the case as glycosylation site occupancy changed with time during fed-batch culture (Figure 6-15). Therefore the decline in site occupancy with time during exponential growth is due to steps downstream of nucleotide sugar formation.

In addition to affecting glycosylation site occupancy, uridine feeding influenced the structure and composition of the attached oligosaccharides (glycosylation

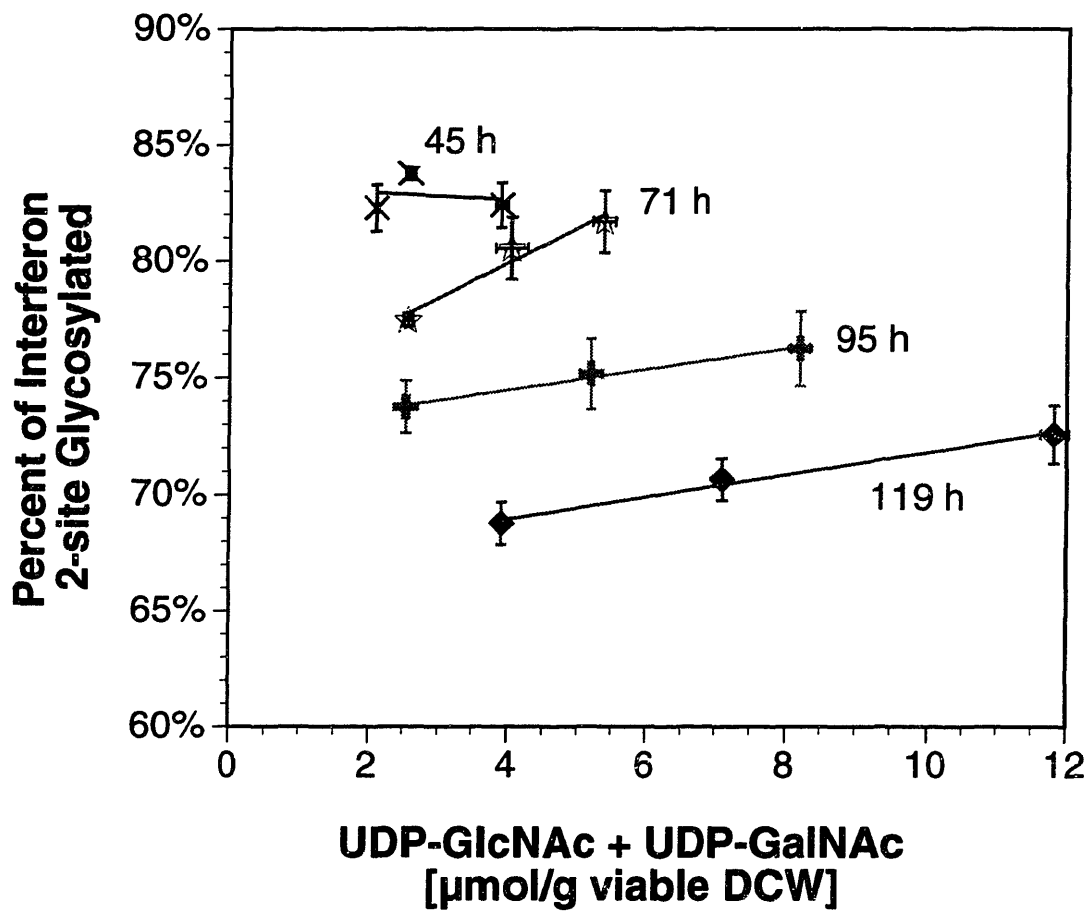


Figure 6-14. The relationship between glycosylation site occupancy and intracellular UDP-GNac concentration during fed-batch exponential growth of γ -CHO cells with and without uridine supplementation. Data is grouped by sample time.

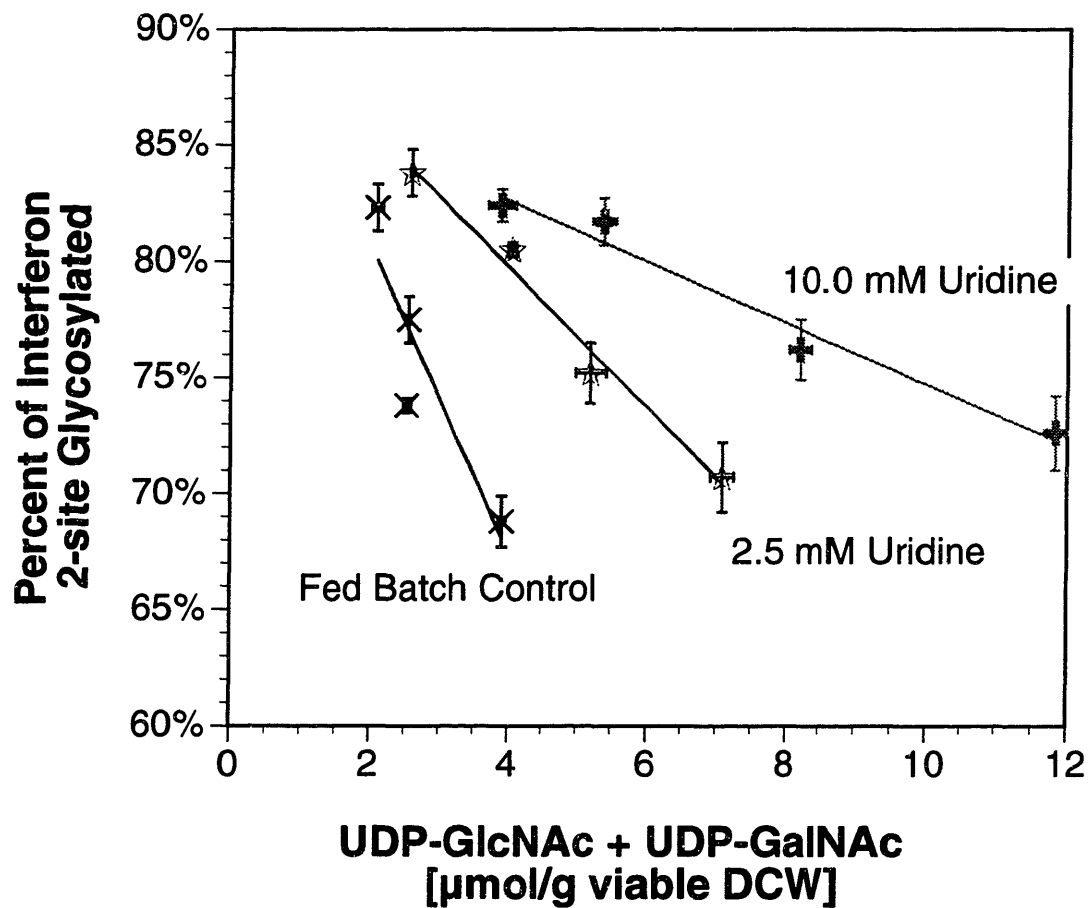


Figure 6-15. The relationship between glycosylation site occupancy and intracellular UDP-GNac concentration during fed-batch exponential growth of γ -CHO cells with and without uridine supplementation. Data is grouped by supplemental uridine concentration.

microheterogeneity). As the uridine concentration increased, terminal sialylation and branching of the attached oligosaccharides decreased. Pels Rijcken et al. (1995b) observed decreased glycoconjugate sialylation with uridine feeding of rat hepatocytes, and they suggested that accumulation of UDP-sugars such as UDP-GNAc and UDP-Glc may interfere with transport of CMP-NeuNAc across the Golgi membrane. This hypothesis was based upon the observation that UDP-sugars inhibit CMP-NeuNAc transport in isolated mouse liver microsomes (Carey et al., 1980).

The decreased oligosaccharide branching observed with uridine feeding is more difficult to explain. The GlcNAc-transferases control branching (Schachter, 1986; Umaña and Bailey, 1997), and one might expect an elevated UDP-GlcNAc concentration to increase branching during uridine exposure. However, uridine feeding also elevates the intracellular UDP-Gal concentration, and once a galactose residue is transferred to an oligosaccharide it is no longer a substrate for GlcNAc-transferases (Schachter, 1986). The galactosyltransferase (GalT) enzyme is mainly localized in the trans Golgi, while GlcNAc-transferase is in the medial Golgi, and so these enzymes do not normally compete for substrate. Branching is typically determined before the glycoprotein encounters the GalT in the trans Golgi. It is possible, nevertheless, that small amounts of GalT in the medial Golgi are active, and that an elevated UDP-Gal concentration results in premature oligosaccharide galactosylation.

6.3 Conclusions

The influence of nucleotide sugars on glycosylation site occupancy was investigated by feeding nucleotide sugar precursors. Consistent with the hypothesis that hexose phosphates are not normally limiting for nucleotide sugar formation or glycosylation, feeding various hexoses did not alter glycosylation site occupancy. Feeding the amino sugar glucosamine, on the other hand, led to accumulation of UDP-GNAc and alterations in glycosylation. Glucosamine feeding experiments confirmed that amino sugar formation

is an important regulatory step in UDP-GNAC synthesis. Excessive accumulation of UDP-GNAC with glucosamine feeding led to lower glycosylation site occupancy, possibly due to dolichol phosphate depletion.

Nucleotide sugar concentrations were also altered by feeding nucleotide precursors. Uridine and guanosine both increased nucleotide sugar concentrations and glycosylation site occupancy, but guanosine was also slightly toxic to the cells. Uridine feeding increased UTP and UDP-sugar concentrations without impacting cell growth or productivity. A fed-batch experiment demonstrated that feeding 10 mM uridine can slightly increase site occupancy. However, a three-fold increase in UDP-GNAC led to only a 4% increase in the percentage of interferon that was two site glycosylated, indicating that nucleotide sugars have a small impact on glycosylation site occupancy in non-starved cultures. Finally, the gradual decline in glycosylation site occupancy observed during exponential growth (Chapter 4) is caused by a step downstream of nucleotide sugar formation, as nucleotide sugar concentrations actually increased during this time.

7. Quality Control of Secreted Glycoproteins via Molecular Chaperones

Previous chapters focused on how metabolism affects the fraction of potential glycosylation sites which receives oligosaccharide. By understanding how metabolism influences the availability of sugar donors, we hoped to devise strategies to increase the concentration of oligosaccharide precursors, thereby increasing the extent of the oligosaccharyltransferase reaction. Rather than improving the efficiency of the initial glycosylation reaction, an alternative strategy for improving product quality is to manipulate the cell's normal "quality control" mechanisms. The quality of the secreted product could be improved by preventing the secretion of non-glycosylated product. A quality control mechanism based upon the rate of protein folding is in place in the endoplasmic reticulum which may allow underglycosylated proteins to be selectively identified and retained for degradation.

Quality control mechanisms in the endoplasmic reticulum prevent the secretion of improperly folded proteins. When a protein folds too slowly, chaperone proteins, which normally prevent aggregation and non-productive folding pathways by binding to unfolded polypeptides, remain bound until the protein is eventually degraded. Typically, proteins that are underglycosylated have more trouble folding than their fully glycosylated counterparts (see Chapter 2). Underglycosylated proteins are therefore more likely to be complexed to chaperones and degraded. Chaperone proteins may thus provide a method for identifying and retaining underglycosylated proteins. Increasing the concentration of chaperone protein should result in more chaperone/unfolded protein complexes with a corresponding increase in protein degradation. Because slowly folding species would be more susceptible to chaperone complexing, underglycosylated proteins

should be complexed and degraded to a larger extent than their fully glycosylated counterparts. Hence the secreted product will have a higher percentage of glycosylation.

In order to examine the implications of this hypothesis further, it is helpful to develop a mathematical model for protein secretion from the endoplasmic reticulum. This chapter presents a model for the chaperone BiP and its role in mediating the secretion of glycoproteins. The model is used to study the feasibility of overexpressing BiP to influence protein quality.

7.1 Background

BiP, also known as GRP78, is one of the most abundant and intensively studied chaperone proteins in the endoplasmic reticulum (other ER chaperones include GRP94 and calnexin). BiP derives its name from the fact that it was initially identified as the immunoglobulin heavy chain binding protein (Haas and Wabl, 1983). Subsequent investigation found that BiP was identical to the glucose regulated protein 78 (GRP78), a member of a family of stress related proteins which also includes heat shock proteins (HSPs). Stress proteins were identified based upon their induction under a variety of cellular stresses, including heat shock (HSPs), exposure to amino acid analogues (HSPs), anoxia (GRPs followed by HSPs upon reoxygenation) and glucose starvation (GRPs followed by HSPs upon glucose addition) (Beckmann et al., 1990; Sciandra and Subject, 1983). BiP has also been observed in association with non-glycosylated proteins in CHO cells treated with tunicamycin, an inhibitor of N-linked glycosylation (Dorner et al., 1987).

A common theme of induction is the accumulation of misfolded or partially denatured proteins (Hartl et al., 1992). BiP has been observed in association with misfolded proteins under such conditions (Gething et al., 1986; Kassenbrock et al., 1988). Peptide binding experiments have shown that BiP binds preferentially to stretches of hydrophobic residues in an environment that appears to be energetically equivalent to the

interior of a folded protein (Flynn et al., 1991). Recent work has identified a BiP binding motif consisting of three or four hydrophobic residues in alternating positions (Blond-Elguindi et al., 1993a; Flynn et al., 1991; Gething et al., 1994). BiP is believed to interact transiently with all proteins as they enter the ER, aiding the folding process by preventing inappropriate interactions between hydrophobic regions of unfolded polypeptide. BiP does not accelerate folding, but prevents non-productive folding and aggregation (Puig and Gilbert, 1994). BiP may also play a role in oligomer formation, as it seems to associate with regions that form subunit interfaces (Gething and Sambrook, 1992). ATP hydrolysis is necessary for BiP to release the polypeptide, allowing it to either fold or oligomerize into a more energetically favorable conformation. BiP binds more permanently to misfolded proteins or aggregates by binding to exposed hydrophobic regions.

Proteins which remain associated with BiP for an extended period are ultimately targeted for degradation (Knittler et al., 1995; Schmitz et al., 1995). Such proteins are typically folding mutants or underglycosylated proteins which do not fold effectively. Extent of association with BiP has been correlated to secretion efficiency for several recombinant proteins (Dorner et al., 1993). Studies with separate CHO cell lines producing three different proteins (tPA, factor VIII and von Willebrand factor) correlated under utilization of N-linked glycosylation sites to increased association with BiP and decreased secretion efficiency (Dorner et al., 1987). Subsequent studies indicated that when levels of BiP were decreased by co-expressing an antisense BiP gene, secretion of nonglycosylated tPA increased proportionally (Dorner et al., 1988). Overexpression of BiP, on the other hand, lead to selective retention of proteins which normally transiently associated with BiP (factor VIII and von Willebrand factor) (Dorner et al., 1992). Secretion of M-CSF, which was not detected in association with BiP, was not affected by BiP overexpression. The influence of the ER BiP concentration on protein secretion correlated with the stability of the BiP-nascent protein complex. As discussed above, the stability of the BiP-protein complex is a function of the protein folding rate. Since underglycosylated proteins

typically fold more slowly and therefore associate with BiP to a greater extent, secretion of underglycosylated proteins is more likely to be affected by altered BiP concentrations.

Normally, the concentration of BiP in the ER is tightly regulated. The fact that accumulation of misfolded proteins stimulates BiP expression suggests a homeostatic mechanism of regulation similar to that proposed for HSP70 (Beckmann et al., 1990; Blond-Elguindi et al., 1993b; Craig and Gross, 1991; DiDomencio et al., 1982). In this model the amount of unbound BiP determines the rate of gene expression. The mechanism for sensing the amount of unbound BiP may be related to the extent of modification of BiP. BiP exists *in vivo* as an interconvertible pool of phosphorylated and adenylated oligomers and unmodified monomers (Freiden et al., 1992). Only unmodified monomers are found in complexes with unfolded proteins (Hendershot et al., 1988), and binding of peptide results in the conversion of modified oligomers to unmodified monomers (Blond-Elguindi et al., 1993b). Blond-Elguindi et al. (1993b) have proposed that the modified oligomers may represent a storage pool, and that the amount of unbound BiP is monitored by monitoring the size of this pool relative to the unmodified monomers. Under conditions where many misfolded proteins are present, gene expression is stimulated in order to maintain an adequate storage pool of modified oligomers.

7.2 Model Development

7.2.1 Model Structure

A successful model for protein secretion from the ER must incorporate information from the experimental evidence discussed above. Figure 7-1 presents a schematic illustration for a model describing the interaction of BiP with a single folding species. In this model a newly synthesized polypeptide (P) can either fold productively to form an active species (F), be complexed to BiP (BP) or form an aggregate (A). BiP complexed proteins may be released with the simultaneous hydrolysis of ATP or they may be degraded (D) at a set

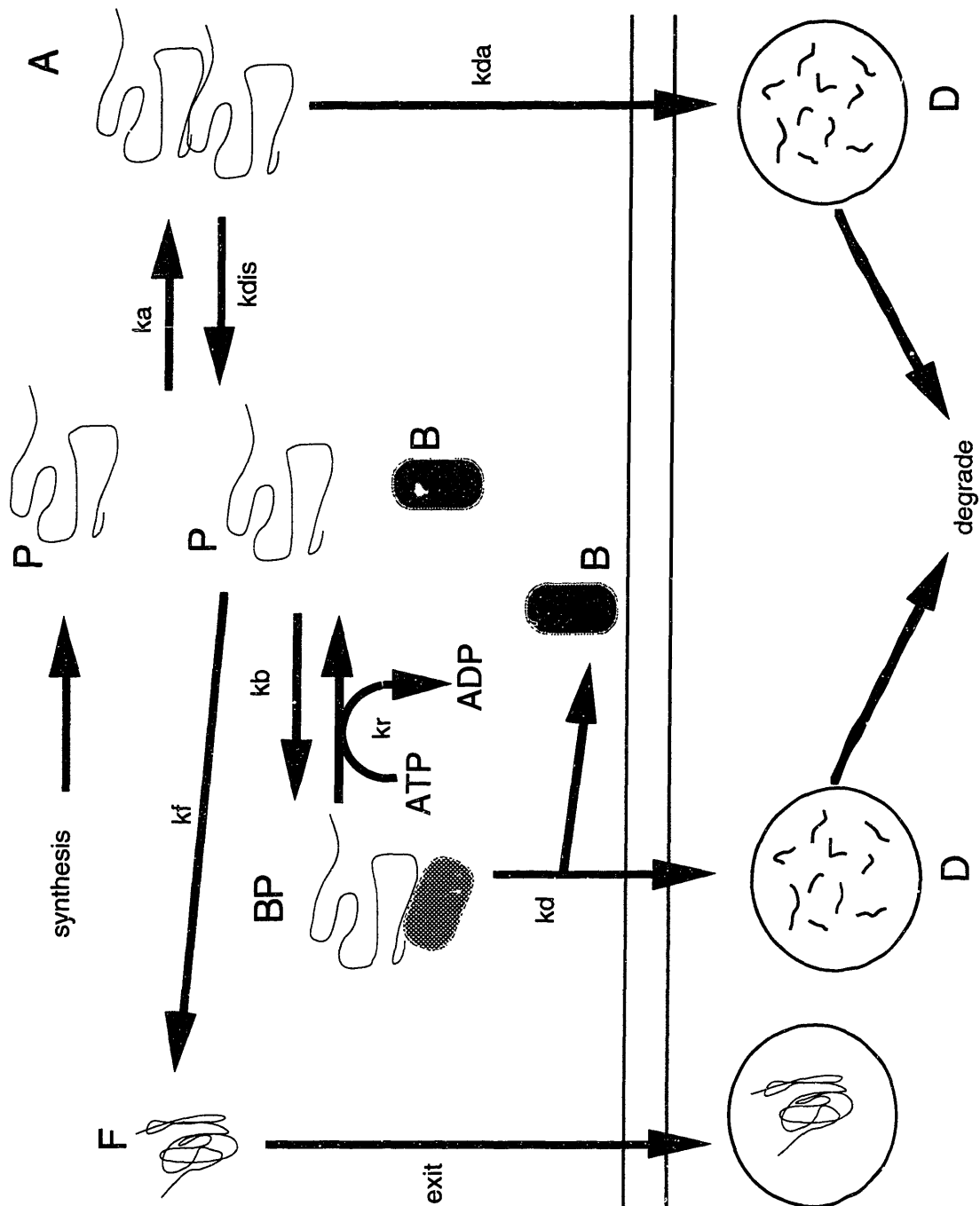
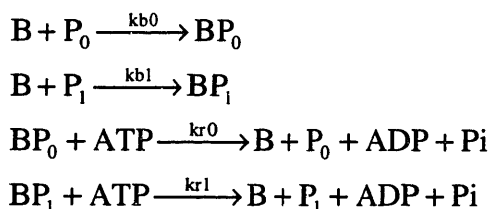


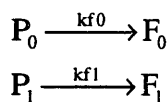
Figure 7-1. Schematic of a single species model for BiP mediated protein folding, secretion and degradation (B = BiP; P = unfolded polypeptide; BP = BiP/unfolded polypeptide complex; F = folded polypeptide; A = unfolded polypeptide aggregates; D = degradation products).

rate. Experimental observations indicate that a large percentage of BiP is recycled when the bound polypeptide is slated for degradation (Freiden et al., 1992). This model assumes complete recycling of BiP for simplicity. It is apparent from this model that unfolded polypeptides can undergo a series of binding and release by BiP, and that the extent to which the protein folds productively will depend upon the relative rate of folding compared to the rates of aggregate formation and BiP mediated degradation. Another assumption implicit in the model is that once the protein assumes its correctly folded structure, it will no longer associate with BiP and will be secreted.

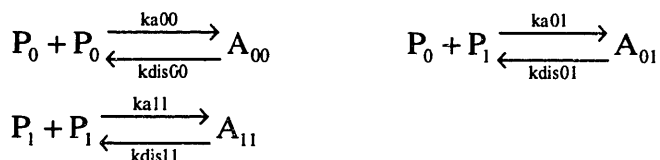
Extension of this model to account for multiple folding species is conceptually straightforward. The same basic reactions illustrated in Figure 7-1 are assumed possible, but now we must keep track of multiple folding species. For the case of a single protein with one glycosylation site that is variably occupied there are two folding species. In the following discussion the subscript 0 represents the nonglycosylated form, while 1 represents the glycosylated form. The unfolded protein complex formation and disruption reactions are now:



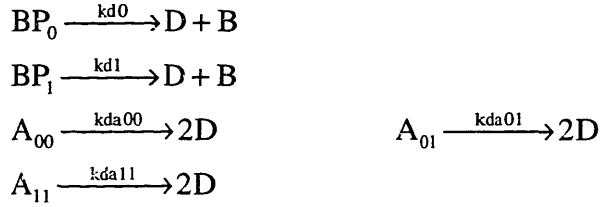
where Pi represents the phosphate released during the hydrolysis of ATP to ADP. The protein folding reactions are:



Aggregation is accounted for through the following expressions:



Finally, degradation of proteins is considered through the following reactions:



In order to put the model reactions presented above into a mathematical framework, species balances can be performed. An overall BiP balance yields:

$$(i) \quad [\text{B}]_{\text{total}} = [\text{B}] + [\text{BP}_0] + [\text{BP}_1]$$

Species balances for the remaining species gives:

$$(ii) \quad \frac{d[\text{P}_0]}{dt} = \text{synthesis}_0 + \text{kr}0 [\text{BP}_0] [\text{ATP}] - \text{kb}0 [\text{B}] [\text{P}_0] - \text{kf}0 [\text{P}_0] - 2\text{ka}00 [\text{P}_0]^2 + 2\text{kdis}00 [\text{A}_{00}] - \text{ka}01 [\text{P}_0] [\text{P}_1] + \text{kdis}01 [\text{A}_{01}]$$

$$(iii) \quad \frac{d[\text{P}_1]}{dt} = \text{synthesis}_1 + \text{kr}1 [\text{BP}_1] [\text{ATP}] - \text{kb}1 [\text{B}] [\text{P}_1] - \text{kf}1 [\text{P}_1] - 2\text{ka}11 [\text{P}_1]^2 + 2\text{kdis}11 [\text{A}_{11}] - \text{ka}01 [\text{P}_0] [\text{P}_1] + \text{kdis}01 [\text{A}_{01}]$$

$$(iv) \quad \frac{d[\text{BP}_0]}{dt} = \text{kb}0 [\text{B}] [\text{P}_0] - \text{kr}0 [\text{BP}_0] [\text{ATP}] - \text{kd}0 [\text{BP}_0]$$

$$(v) \quad \frac{d[\text{BP}_1]}{dt} = \text{kb}1 [\text{B}] [\text{P}_1] - \text{kr}1 [\text{BP}_1] [\text{ATP}] - \text{kd}1 [\text{BP}_1]$$

$$(vi) \quad \frac{d[\text{F}_0]}{dt} = \text{kf}0 [\text{P}_0] - \text{exit}_0$$

$$(vii) \quad \frac{d[\text{F}_1]}{dt} = \text{kf}1 [\text{P}_1] - \text{exit}_1$$

$$(viii) \quad \frac{d[\text{A}_{00}]}{dt} = \text{ka}00 [\text{P}_0]^2 - \text{kdis}00 [\text{A}_{00}] - \text{kda}00 [\text{A}_{00}]$$

$$(ix) \quad \frac{d[\text{A}_{01}]}{dt} = \text{ka}01 [\text{P}_0] [\text{P}_1] - \text{kdis}01 [\text{A}_{01}] - \text{kda}01 [\text{A}_{01}]$$

$$(x) \quad \frac{d[\text{A}_{11}]}{dt} = \text{ka}11 [\text{P}_1]^2 - \text{kdis}11 [\text{A}_{11}] - \text{kda}11 [\text{A}_{11}]$$

$$(xi) \quad \frac{d[\text{D}]}{dt} = \text{kd}0 [\text{BP}_0] + \text{kd}1 [\text{BP}_1] + 2\text{kda}00 [\text{A}_{00}] + 2\text{kda}01 [\text{A}_{01}] + 2\text{kda}11 [\text{A}_{11}] - \text{degrade}$$

Given appropriate initial conditions equations (i) through (xi) could in principle be solved to obtain a solution for protein secretion ($exit_0$ and $exit_1$) with time. In this analysis, however, the steady-state solution is obtained by setting all of the time derivatives to zero. Equations (i) and (iv) through (x) allow all of the independent variables to be solved in terms of $exit_0$ and $exit_1$. Equations (ii) and (iii) are then solved simultaneously to determine $exit_0$ and $exit_1$.

Solving the model for the steady state solution also requires an assumption to be made concerning the concentration of BiP. As discussed above, there is accumulating evidence to support a homeostatic mechanism of BiP regulation. The evidence suggests that cells will alter gene expression to maintain a relatively constant supply of BiP not complexed to nascent polypeptides. Thus for wild-type cells the level of uncomplexed BiP ($[B]$) is specified and the total BiP ($[B]_{total}$) is solved for as an unknown using equation (i).

In contrast to wild-type cells, cells overexpressing BiP from a plasmid would be expected to have overcome the homeostatic regulation mechanism. One would expect that the cells would shut down endogenous BiP synthesis due to the negative feedback from having excess free BiP in the ER from plasmid expression. Experimental evidence suggests that this is indeed the case: overexpression of BiP mitigates the stress induction of BiP in CHO cells (Dorner et al., 1992). In this case the total BiP concentration will be specified ($[B]_{total}$) by the level of plasmid expression, and the uncomplexed BiP ($[B]$) is solved for as an unknown using equation (i). Both wild-type expression and overexpression from a plasmid will be considered in the following sections.

7.2.2 Parameter Estimation

Solving the above equations requires estimates for the kinetic rate constants. Estimates for some parameters can be obtained from *in vitro* studies, while for others only very crude estimates are available. In practice the oligosaccharide of a glycoprotein may affect

several of the kinetic rate constants including the BiP complexing reaction (k_b), the aggregate formation reactions (k_a) and the protein folding reaction (k_f). In order to limit the current study to the relationship between protein folding rate and secretion, however, only the folding rate constants are assumed to vary between the glycosylated species. All other kinetic parameters are assumed identical.

The rate of BiP/polypeptide complex formation (k_b) is an important parameter for which there is unfortunately very little experimental data. Studies of BiP/polypeptide complexing ordinarily use ATP hydrolysis as an endpoint. The ATP hydrolysis step is generally considered to be limiting as opposed to the initial BP complex formation. Thus the quantity being measured in these studies is the rate of ATP hydrolysis, k_r . Complex formation should have kinetics similar to second order aggregation kinetics. As a crude estimate, complex formation is assumed to occur at $10^6 \text{ M}^{-1}\text{s}^{-1}$ which is of the order of magnitude of *in vitro* aggregation for lactic dehydrogenase (Zettlmeissl et al., 1979).

The rate of ATP hydrolysis is found to be saturable with respect to ATP concentration. The K_m for ATP is on the order of $10 \mu\text{M}$ (Flynn et al., 1989). The intracellular ATP concentration in batch hybridoma culture was found to be constant at 4.2 mM (Sonderhoff et al., 1992). Similarly, the ATP concentration in our γ -CHO cells is typically fairly constant around $23 \mu\text{mol/g}$ viable dry cell weight (6.0 mM intracellular concentration). ATP is transported into the ER via a protein mediated translocation mechanism which can concentrate ATP in the lumen of isolated vesicles up to 30 times (Clairmont et al., 1992). Thus the concentration of ATP in the ER should be saturating (it should be in the mM range while the K_m is in the μM range), and the rate of ATP hydrolysis by BP complexes should be at V_{max} . For short peptides k_{cat} is found in *in vitro* studies to be $0.16 \text{ (mol ATP)/(mol BiP)/min}$ (Blond-Elguindi et al., 1993b; Flynn et al., 1989), and an *in vitro* study with denatured lysozyme found $k_{\text{cat}} = 0.35 \text{ (mol}$

ATP)/(mol BiP)/min (Puig and Gilbert, 1994). Thus the quantity $kr_0 [ATP] = kr_1 [ATP]$ is taken to be 0.35 (mol ATP)/(mol BiP)/min.

The protein folding rate (k_f) will vary extensively from one protein to another. The dominant time constant for protein folding has been reported to vary from 1-1000 s (Ptitsyn and Semisotnov, 1991). The refolding of lysozyme had a rate constant of $k_f = 0.039$ 1/min uncatalyzed and $k_f = 0.31$ 1/min when catalyzed by PDI (Puig and Gilbert, 1994). In order to reflect the difficulty underglycosylated proteins face in folding, k_{f0} was set to 0.1 1/min, while k_{f1} for the glycosylated species was set at 10 1/min.

As discussed previously, an *in vitro* example of protein aggregation was found to have a second order rate constant on the order of $10^6 \text{ M}^{-1}\text{s}^{-1}$ (Zettlmeissl et al., 1979). As Robinson and Lauffenburger (1996) point out, the *in vivo* rate of aggregation is likely to be significantly less. The presence of chaperones other than BiP (e.g. GRP94, calnexin, PDI, etc.) should serve to reduce the *in vivo* aggregation significantly. For the purpose of the model $ka_{00} = ka_{01} = ka_{11} = 10^2 \text{ M}^{-1}\text{s}^{-1}$. The aggregate formation is assumed to be only slightly reversible, with $k_{dis} = 0.001$ 1/min.

An estimate for the rate of protein degradation can be obtained from literature reports on the *in vivo* degradation kinetics of secretion incompetent proteins. Ig heavy chains were degraded with a half time of about 6 hours in Ag8(8) cells not producing light chains (Freiden et al., 1992). Similarly, light chains in NS1 cells not producing heavy chains were degraded with half lives varying from 1 to 4 hours (Knittler et al., 1995). In CHO cells overexpressing BiP, the half-life of retained von Willebrand factor was more than 6 hours (Dorner et al., 1992). Based upon these literature estimates, the first order degradation constant was taken as $k_d = 0.002$ 1/min (half life of 5.8 hours). The degradation of aggregated protein (k_{da}) was assumed to occur at this same rate.

Additional parameters which must be estimated in order to solve the model include the protein synthesis rate and the concentration of BiP in the ER. The overall synthesis rate

for proteins in the ER can be estimated based upon the number of ribosomes bound to the rough endoplasmic reticulum (Flynn et al., 1989). The average number of bound ribosomes in a rat hepatocyte was found to be 13×10^6 , and the volume of the ER was calculated as 470×10^{-15} liters (Weibel et al., 1969). Given that each bound ribosome contributes one nascent polypeptide chain, the concentration of nascent polypeptide in the ER is approximately 50 μM . If an average secretory protein is 400 amino acids (Robinson and Lauffenburger, 1996) and protein translation in eukaryotes occurs at approximately 6 amino acids/second (Haschemeyer, 1976), then protein synthesis will take about 1 minute on average. Thus the nascent protein synthesis rate is approximately 50 $\mu\text{M}/\text{min}$.

Literature estimates for the amount of BiP in the ER range between 5 and 10% of the luminal content of the ER (Gething and Sambrook, 1992; Mori et al., 1992). We have estimated the BiP concentration in our γ -CHO cells as approximately 2–7% of total protein based upon quantitative Western blots (the absolute BiP concentration could not be determined unambiguously, because the assay was found to vary depending upon the antibodies used in the Western blot). The average total protein for this cell line is 350 pg/cell and the volume of the ER can be estimated at between 250×10^{-15} liters (for BHK cells (Griffiths et al., 1984)) and 470×10^{-15} liters (for hepatocytes (Weibel et al., 1969)). If BiP is assumed to account for 2% of cellular protein, this provides an estimate of between 0.19 and 0.36 mM BiP. A similar estimate is obtained for yeast cells if one assumes BiP comprises 1% of total cellular protein and an average yeast contains 6 pg protein/cell (Robinson and Lauffenburger, 1996). The volume of a yeast ER can be estimated as $\sim 10\%$ of the total yeast volume, where a typical yeast volume is 40×10^{-15} liters. This estimate yields 0.19 mM BiP. A value of 0.2 mM was used as a total BiP concentration in the simulations.

7.3 Model Results

Quantitative predictions of protein secretion are not feasible given the uncertainty involved in many of the parameter estimations. The model may be used effectively, however, to study qualitative predictions concerning the relationship between glycosylation (i.e. protein folding rates) and protein secretion. When studying the effects of glycosylation it will be helpful to define the oligosaccharyltransferase (OST) efficiency:

$$\text{OST Efficiency} = \frac{\text{Glycosylated Product Synthesis Rate}}{\text{Total Product Synthesis Rate}}$$

The OST efficiency refers to the efficiency of the transfer of precursor oligosaccharides to a potential glycosylation site during protein synthesis (i.e. the efficiency of the oligosaccharyltransferase reaction). An efficiency of 1 means the glycosylation site is always occupied, while 0 indicates that the protein is not glycosylated. In terms of the mathematical model, $\text{synthesis}_1 = (\text{OST efficiency}) \times (\text{total protein synthesis})$ and $\text{synthesis}_0 = (1 - \text{OST efficiency}) \times (\text{total protein synthesis})$.

Figure 7-2 illustrates the predicted relationship between OST efficiency and total BiP concentration for a wild-type cell (recall that a wild-type cell will maintain a constant amount of uncomplexed BiP by varying the total BiP concentration). This figure illustrates that as OST efficiency decreases, more BiP is complexed to protein and hence synthesis of BiP is induced. This trend is supported by experimental data where the OST efficiency is decreased by adding the glycosylation inhibitor tunicamycin (Figure 7-3). Tunicamycin inhibits the formation of the lipid-bound oligosaccharide precursor, and hence inhibits glycosylation. Figure 7-3 demonstrates that BiP is synthesized in response to glycosylation inhibitor treatment. Similarly, we found that BiP synthesis was induced at the end of batch culture when glycosylation site occupancy deteriorated due to glucose starvation (see Chapter 4). The model correctly accounts for changes in BiP concentration in response to changes in glycosylation.

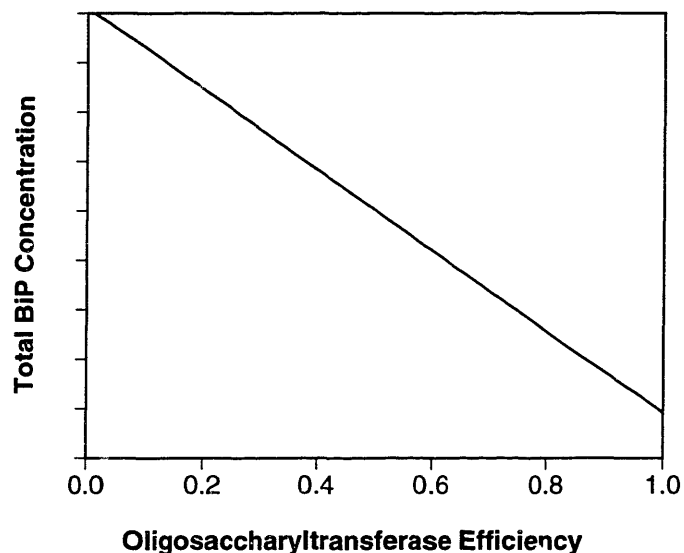


Figure 7-2. Model simulation of total BiP concentration versus oligosaccharyltransferase (OST) efficiency in a wild-type cell maintaining a constant level of uncomplexed BiP.

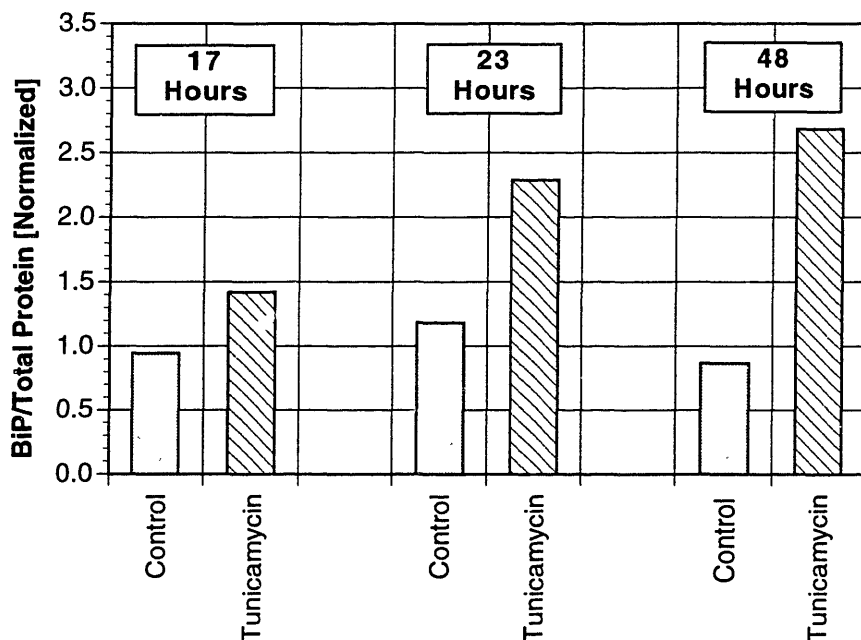


Figure 7-3. Experimental data for the induction of BiP synthesis in γ -CHO cells in the presence of the glycosylation inhibitor tunicamycin (10 μ g/ml).

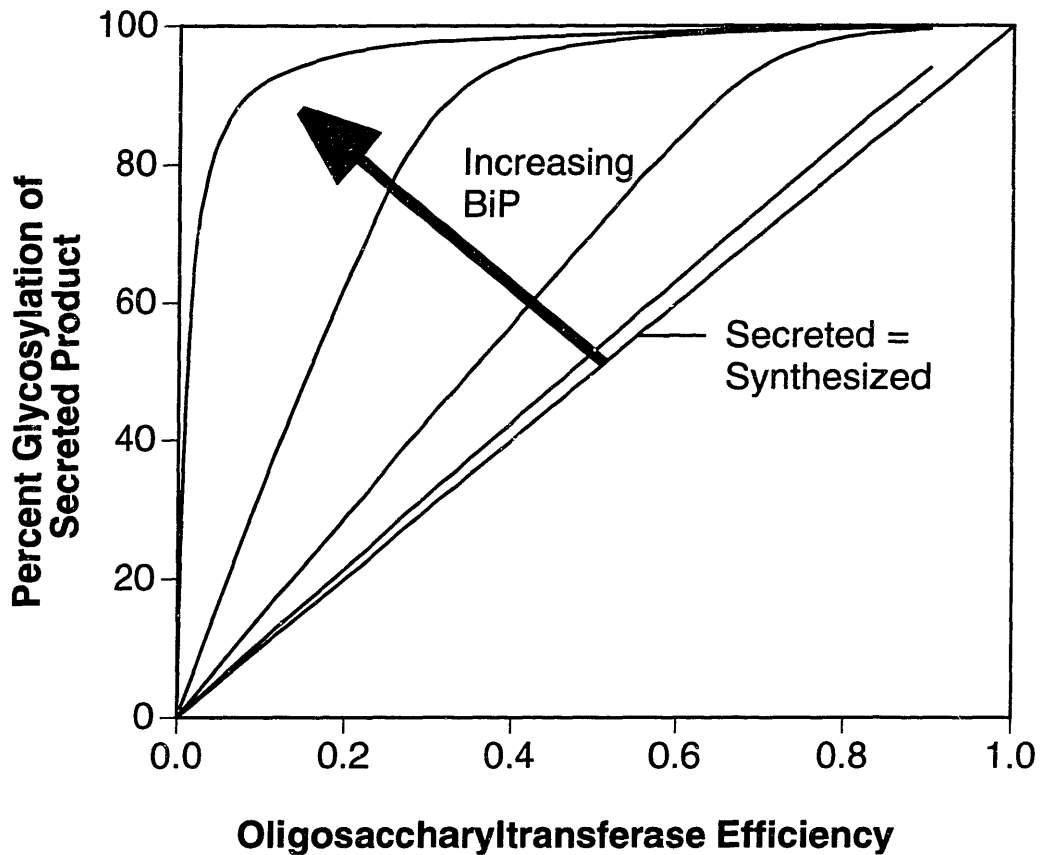


Figure 7-4. Model simulation of BiP overexpression: secreted product glycosylation vs. oligosaccharyltransferase (OST) efficiency with varying total BiP concentrations.

The model can also be used to predict the consequences of overproducing BiP. Figure 7-4 shows the relationship between the OST efficiency and the glycosylation characteristics of the secreted product. As the concentration of total BiP is increased, the secreted product has a higher percentage of glycosylation. The secreted product's glycosylation pattern is also less sensitive to changes in OST efficiency. The secreted product glycosylation can remain at high levels despite shifts in the efficiency of the oligosaccharyltransferase reaction, because the underglycosylated protein is selectively retained and degraded.

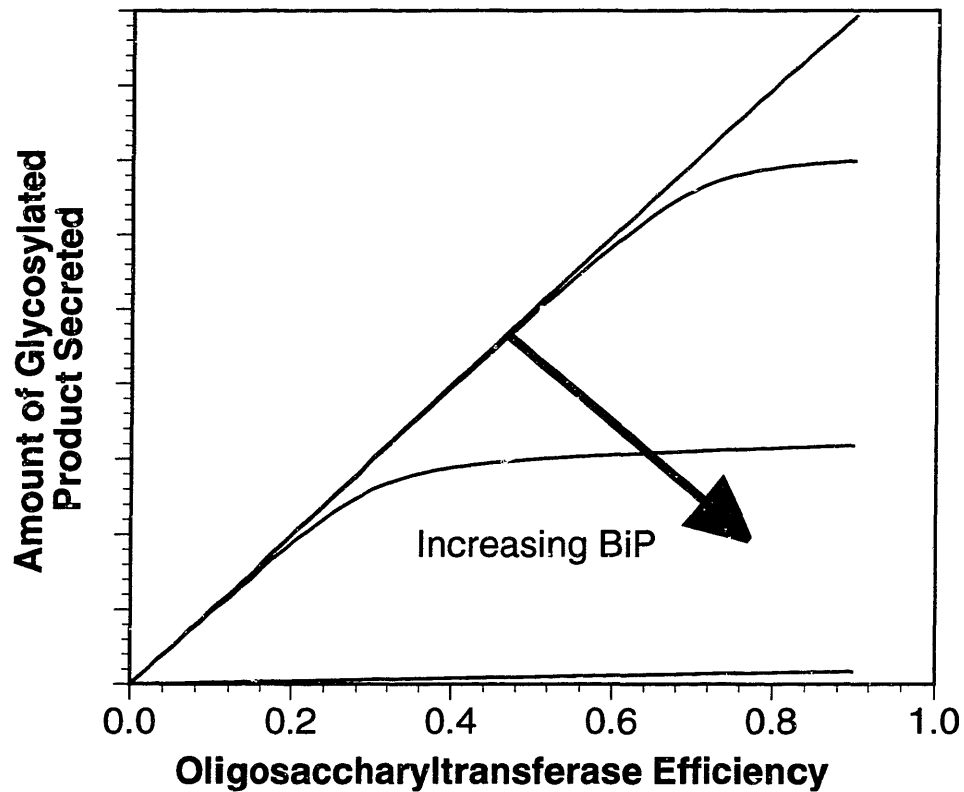


Figure 7-5. Model simulation of BiP overexpression: amount of glycosylated product secreted vs. oligosaccharyltransferase (OST) efficiency with varying total BiP concentrations. As the total concentration of BiP increases, more of the desired product is degraded along with the underglycosylated species.

The improvement in product quality with overproduction of BiP does not come without a price, however. Figure 7-5 illustrates that the total amount of glycosylated protein secreted decreases with increasing BiP. Increased BiP leads to an increase in BiP complexing of unfolded proteins and a subsequent increase in the amount of protein that gets degraded. The slower folding species are preferentially retained, but Figure 7-5 shows that significant amounts of the desired product may also be degraded.

7.4 Discussion

This chapter proposes a mathematical model for BiP mediated folding and secretion from the endoplasmic reticulum. In this model a newly synthesized polypeptide can either fold productively to form an active species, be complexed to BiP or form an aggregate. BiP complexed proteins may be released with the simultaneous hydrolysis of ATP or they may be degraded at a set rate. In order to explore how glycosylation might influence protein secretion the model was solved for two species. The species were considered identical except that the underglycosylated protein was assigned a slower folding rate than its fully glycosylated counterpart.

As expected, the model was able to predict the wild-type behavior that as the OST efficiency decreases, the level of total BiP increases. The model was designed under the assumption that cells will regulate BiP expression to maintain a constant amount of BiP uncomplexed to protein. A more slowly folding protein will lead to an increase in BiP complexes because BiP will have a longer opportunity to bind the nascent chain before it folds. Thus, increasing the percentage of slowly folding protein is sufficient to produce the expected rise in the level of total BiP.

The model also shows that secreted product glycosylation site occupancy heterogeneity can be influenced by BiP concentration if the folding rates between the glycosylated species varies significantly. However the model also highlights a trade-off: as BiP concentration increases and secreted product quality improves, the rate of secretion of the desired product will decrease. The exact nature of this trade-off will depend upon the ratio of the folding rates between the two species. As the difference in folding rates becomes larger, secreted product percent glycosylation can be improved with less of a decline in secretion of glycosylated product.

An assumption implicit in the above analysis is that the only difference between the variably glycosylated species lies in the folding rate (k_f). It is in fact a distinct possibility

that other kinetic parameters will be altered as a result of glycosylation. The attached oligosaccharide may reduce the BiP/polypeptide binding rate (k_{b1}) by shielding the protein from the chaperone. Analogously the aggregation of glycosylated proteins (k_{a01} and k_{a11}) may be decreased as a result of enhanced solubility afforded by the polar oligosaccharide. In fact, enhanced solubility of glycoproteins compared to their underglycosylated counterparts is observed (Cumming, 1991). Accounting for these changes would lead to an increase in the extent of BiP complexing with the underglycosylated species compared to the glycosylated species. The increase in complexing will increase the selective degradation of underglycosylated protein, improving upon the trade-off described earlier. Product quality improvement could be achieved with less of a reduction in glycosylated product secretion.

Another complication arises from the fact that overexpression of BiP may influence the oligosaccharyltransferase (OST) reaction efficiency. Kinetic competition between the oligosaccharide transfer reaction and folding of the nascent polypeptide is commonly proposed as an explanation for observed glycosylation site-occupancy heterogeneity (Bulleid et al., 1992; Savvidou et al., 1981; Shelikoff et al., 1996). Interaction of the translocating polypeptide with BiP would be expected to decrease the extent of premature folding. Even though the folding rate of the free polypeptide (k_f) would not change, complexing with BiP will decrease the amount of time during which folding may occur and hence it will take longer for a given polypeptide to fold. Evidence supporting the interaction of BiP with translocating nascent polypeptides comes primarily from studies that show yeast require BiP in order to translocate nascent polypeptides into the ER (Nguyen et al., 1991; Vogel et al., 1990). Although the exact role of BiP in translocation is not clear, direct interaction with nascent chains seems probable. Recent work shows that BiP can be crosslinked to secretory proteins trapped during translocation into the ER, further suggesting that BiP interacts directly with nascent chains co-translationally (Sanders et al., 1992). Overexpression of BiP may increase the

efficiency of the oligosaccharyltransferase reaction by preventing premature folding of the polypeptide.

7.5 The Feasibility of Improving IFN- γ Quality Through BiP Overexpression in γ -CHO Cells

The mathematical model described above demonstrated that overexpression of BiP has the potential to alter secreted product glycosylation if the folding rates differ significantly between the glycosylated and non-glycosylated species. There is experimental evidence that *in vivo* folding and dimerization of IFN- γ is dependent upon glycosylation. When the Asn-25 glycosylation site was eliminated through site directed mutagenesis, dimerization was less efficient and protein secretion dropped by more than 90% (Sareneva et al., 1994). IFN- γ was observed in insoluble aggregates which were hypothesized to be misfolded material tightly bound to chaperone proteins. IFN- γ therefore appears to be a good candidate for quality improvement through BiP overexpression.

In order to determine the feasibility of BiP overexpression in our γ -CHO cell line, initial studies compared the BiP levels in our recombinant cells with BiP concentrations in non-transfected CHO cell lines. It was of interest to determine whether BiP was already induced in the γ -CHO cells due to expression of IFN- γ . BiP levels were found to be the same for a CHO-K1 wild-type line, a dehydrofolate reductase deficient cell line and our recombinant γ -CHO cell line. Since stable overexpression of BiP has been achieved in a dehydrofolate reductase deficient CHO cell line (Dorner et al., 1992), overexpression of BiP in the γ -CHO cell line should be possible.

7.6 Conclusions

Even if changes in glycosylation site occupancy during batch culture could be eliminated, a significant fraction of under-glycosylated protein would continue to be produced.

Incomplete glycosylation of proteins would still be caused by factors such as competition with protein folding and variable effectiveness of acceptor amino acid sequences (see Chapter 2). Improvement in quality beyond such limits might be possible if a quality control mechanism could prevent secretion of underglycosylated protein. This chapter explored the feasibility of limiting the secretion of underglycosylated proteins by overexpressing the chaperone BiP. A mathematical model suggests that overexpression of BiP has the potential to alter secreted product glycosylation if the folding rates differ significantly between the glycosylated and non-glycosylated species. Unfortunately protein folding is not always influenced by glycosylation, and so the effectiveness of BiP overexpression would be protein specific. Another potential disadvantage is that secretion of the desired glycosylated product could be negatively impacted as well. Despite these drawbacks, overexpression of BiP has potential as a tool to improve product quality.

8. Conclusions and Recommendations

8.1 Conclusions

The goal of this thesis was to understand the causes of N-linked glycosylation site occupancy heterogeneity. Of particular interest was the role of central carbon metabolism in determining the availability of the nucleotide sugar precursors used in glycosylation. The relationship between metabolism, nucleotide sugars and glycosylation was studied in continuous culture experiments. Based upon these chemostat experiments, metabolic factors which influence nucleotide sugar availability were identified. The extent to which nucleotide sugars influence glycosylation site occupancy was then determined by manipulating and monitoring nucleotide sugar concentrations in fed-batch culture.

Nucleotide sugars were found to influence glycosylation site occupancy primarily during periods of nutrient limitation. Under starvation conditions, nucleotide sugar levels decreased, and glycosylation site occupancy also decreased. The primary determinants of intracellular nucleotide sugar concentrations during exponential growth were nucleoside triphosphates, although amino sugar formation was also limiting for the synthesis of UDP-N-acetylglucosamine (UDP-GlcNAc). During glucose limitation, nucleoside triphosphates and nucleotide sugars were depleted. Analysis of central carbon metabolic fluxes suggests that nucleotide synthesis was reduced during glucose limitation, because available carbon was consumed in the TCA cycle. Potential TCA metabolites, such as aspartate and glutamine, are important intermediates in pyrimidine and purine base synthesis, and these metabolites were consumed for energy production during glucose limitation. Thus, during glucose limitation nucleoside triphosphates were depleted, causing depletion of nucleotide sugars and reduced glycosylation. Glutamine starvation was also found to decrease glycosylation site occupancy. Since glutamine is the ammonia donor in amino sugar formation, glutamine limitation reduced the formation of the amino sugars which are required to synthesize UDP-GlcNAc.

The influence of nucleotide sugars on glycosylation site occupancy in non-starved cultures was analyzed by feeding nucleotide sugar precursors. Consistent with the hypothesis that hexose phosphates are not normally limiting for nucleotide sugar formation or glycosylation, feeding various hexoses did not alter glycosylation site occupancy. Feeding the amino sugar glucosamine, on the other hand, led to accumulation of UDP-GlcNAc and alterations in glycosylation. Glucosamine feeding experiments confirmed that amino sugar formation is an important regulatory step in UDP-GlcNAc synthesis. Excessive accumulation of UDP-GlcNAc with glucosamine feeding led to lower glycosylation site occupancy, possibly due to depletion of dolichol phosphate.

Nucleotide sugar concentrations were also altered by feeding nucleotide precursors. Uridine feeding increased UTP and UDP-sugar concentrations without impacting cell growth or productivity. A fed-batch experiment demonstrated that feeding 10 mM uridine can slightly increase site occupancy. However, a three-fold increase in UDP-GlcNAc lead to only a 4% increase in the percentage of interferon that was two site glycosylated, indicating that nucleotide sugars have a small impact on glycosylation site occupancy in non-starved cultures. Furthermore, glycosylation site occupancy declined during exponential growth in both uridine-fed and control cultures. The decreases in site occupancy were characteristic of the changes routinely observed in batch and fed-batch cultures. By the end of the exponential growth phase, the percentage of IFN- γ being synthesized with both potential glycosylation sites occupied was typically 10-20% lower than it had been initially. At the onset of the stationary phase, glycosylation site occupancy quickly improved back to nearly the initial levels. Analysis of nucleotide sugar levels revealed that the decreases in site occupancy during exponential growth were caused by a step downstream of nucleotide sugar formation, as nucleotide sugar concentrations actually increased during this time.

Figure 8-1 summarizes the interactions between metabolism, nucleotide sugar synthesis and glycosylation site occupancy that were deduced in this thesis. Sugar phosphates

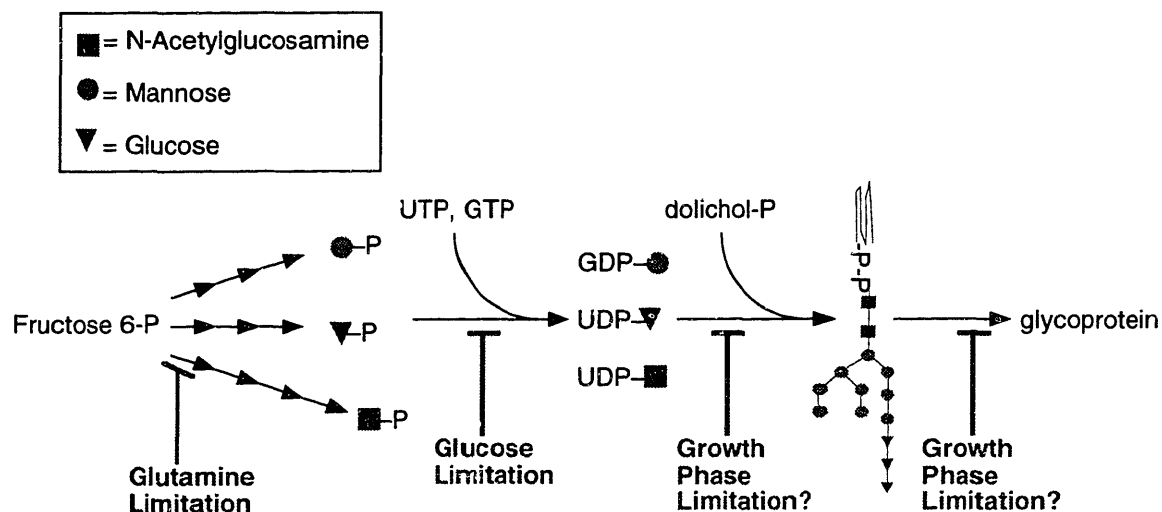


Figure 8-1. Interactions between metabolism, nucleotide sugar formation and glycosylation site occupancy.

generally are not limiting for glycosylation site occupancy, except for amino sugars such as N-acetylglucosamine-1-P, which can be limiting under glutamine restriction. Alterations in nucleoside triphosphate levels will affect nucleotide sugar concentrations. During glucose starvation, nucleoside triphosphates are depleted, and nucleotide sugars can limit glycosylation. The decline in glycosylation site occupancy during normal exponential growth in batch culture cannot be attributed to nucleotide sugars. Downstream factors which might cause such a decline include availability of dolichol-P, the activities of glycosyltransferase enzymes or the activity of the oligosaccharyltransferase enzyme.

Rather than improving the efficiency of the initial glycosylation reaction, an alternative strategy for improving product quality is to manipulate the cell's normal "quality control" mechanisms. The quality of the secreted product could be improved by preventing the secretion of non-glycosylated product. A quality control mechanism designed to eliminate slowly folding proteins exists in the endoplasmic reticulum.

Because underglycosylated proteins typically have more trouble folding than their fully glycosylated counterparts, this quality control may allow underglycosylated proteins to be selectively identified and retained for degradation. A mathematical model was used to explore the feasibility of limiting the secretion of underglycosylated proteins by overexpressing the chaperone BiP. Model simulations suggest that overexpression of BiP has the potential to alter secreted product glycosylation if the folding rates differ significantly between the glycosylated and non-glycosylated species. Unfortunately, protein folding is not always influenced by glycosylation, and so the effectiveness of BiP overexpression would be protein specific. Another potential disadvantage is that secretion of the desired glycosylated product could be negatively impacted as well. Despite these drawbacks, overexpression of BiP has potential as a tool to improve product quality.

8.2 Recommendations

The finding that nucleotide sugars do not normally limit glycosylation site occupancy during exponential growth narrows the list of possible glycosylation bottlenecks. In the past, sugar availability was often hypothesized to be responsible for changes in site occupancy during exponential growth. Future efforts to explain the decrease in site occupancy during exponential growth should focus on downstream factors. A good starting point might be to investigate the effects of lipids on site occupancy. Lipid supplements have been shown to influence glycosylation site occupancy of IFN- γ produced by CHO cells with time during batch culture (Jenkins et al., 1994). Lipids could be expected to influence glycosylation site occupancy through at least two mechanisms. Lipid supplements could alter the activity of the oligosaccharyltransferase (OST) enzyme due to changes in the composition of the endoplasmic reticulum membrane. As discussed in Chapter 2, there is evidence that OST activity may be affected by the phosphatidylcholine content of the ER membrane (Chalifour and Spiro, 1988; Chan and Wolf, 1987; Oda-Tamai et al., 1985). Alternatively, the lipid

supplements may influence the availability of dolichol phosphate, thereby changing the amount of precursor oligosaccharide. Dolichol phosphate availability has been shown to modulate N-glycosylation capacity in several cell types (Crick et al., 1994; Crick and Waechter, 1994; Fukushima et al., 1997).

Other potential bottlenecks for site occupancy include the activities of the glycosyltransferase enzymes which synthesize the lipid-linked precursor oligosaccharide. In order to differentiate between changes in site occupancy due to altered OST activity versus changes in oligosaccharide precursor availability, it may be necessary to quantify the dolichol-sugar species involved in N-glycosylation. Changes in the distribution of the dolichol species may aid in the identification of limiting reaction steps.

Even if the exponential growth phase limitation is not identified, the site occupancy of recombinant IFN- γ could probably be increased through other means. A simple practical suggestion would be to alter the amino acid sequence of the Asn-97 glycosylation sequon. The Asn-Tyr-Ser acceptor sequence could be improved by replacing the serine residue with threonine, which is a more effective hydroxy amino acid in the Asn-Xxx-Ser/Thr glycosylation sequon (Kasturi et al., 1995). In addition, bulky aromatic amino acids such as Tyr in the Xxx position generally reduce the effectiveness of the glycosylation sequon (Shakin-Eshleman et al., 1996). Alterations in the acceptor sequon are admittedly of more practical interest than academic interest, since such improvements have been documented in the past with other glycoproteins.

Quality control via the molecular chaperone BiP (Chapter 7) is a more innovative method for attempting to improve site occupancy. With innovation comes added risk, however, and there is no guarantee that BiP overexpression will work as intended. In order for the method to be successful, the non-glycosylated protein must fold significantly more slowly than the fully glycosylated protein. While there is some literature evidence suggesting that IFN- γ requires glycosylation at Asn-25 for efficient folding (Sareneva et

al., 1994), we have not observed any correlation between site occupancy and IFN- γ secretion. Overexpression of BiP may apply added selective pressure, but the possibility remains that non-glycosylated protein will continue to be secreted. BiP overexpression is also less likely to impact the relative secretion of one-site versus two-site glycosylated IFN- γ , and this difference constitutes the majority of IFN- γ underglycosylation. Furthermore, BiP overexpression could negatively impact secretion of the desired product in addition to the undesired products. Even if BiP does not alter IFN- γ secretion, glycosylation site occupancy might be improved if BiP reduces the competition between protein folding and glycosylation. Potential improvement of the oligosaccharyltransferase reaction may offset some of the risk involved in attempting to implement the quality control hypothesis.

A final suggestion for improving glycosylation site occupancy is to produce the product primarily during the stationary phase or during limited cell growth. At the onset of the stationary phase, we observed rapid increases in glycosylation site occupancy (Chapter 4). We hypothesized that the rapid improvement in site occupancy was due to reduced biosynthesis of cellular glycoproteins. When fewer glycoproteins were being synthesized, more oligosaccharide was available for the recombinant product. If the product were to be produced during the stationary phase, it would be expected to be of higher quality. Unfortunately, the γ -CHO cell line had very low IFN- γ productivity during the stationary phase. Cell cycle dependent protein secretion has been observed for other cell lines and products, and it has been suggested that the promoter might be partially responsible for such dependencies (Gu et al., 1993; Gu et al., 1994; Gu et al., 1996). Thus, producing high quality product during the stationary phase would require developing a cell line that would maintain high productivity in this phase. Alternatively, the cell growth could be artificially reduced, for example by limiting an essential amino acid. By slowly feeding the limiting amino acid, the growth rate could be controlled. Glycosylation site occupancy would be expected to be high under such conditions, since glycoprotein biosynthesis would be limited without limiting oligosaccharide formation.

References

- Abeijon, C. and C. B. Hirschberg (1990). Topography of Initiation of N-glycosylation Reactions. Journal of Biological Chemistry, **265**: 14691–14695.
- Abeijon, C. and C. B. Hirschberg (1992). Topography of Glycosylation Reactions in the Endoplasmic Reticulum. TIBS, **17**: 32–36.
- Allen, S., H. Y. Naim and N. J. Bulleid (1995). Intracellular Folding of Tissue-type Plasminogen Activator: Effects of Disulfide Bond Formation on N-Linked Glycosylation and Secretion. The Journal of Biological Chemistry, **270**: 4797–4804.
- Anderson, D. C. and C. F. Goochee (1995). The Effect of Ammonia on the O-linked Glycosylation of Granulocyte Colony-Stimulating Factor Produced by Chinese Hamster Ovary Cells. Biotechnology and Bioengineering, **47**: 96–105.
- Anfinsen, C. B. (1973). Principles That Govern the Folding of Protein Chains. Science, **181**: 223-230.
- Arakawa, T., N. K. Alton and Y.-R. Hsu (1985). Preparation and Characterization of Recombinant DNA-derived Human Interferon- γ . The Journal of Biological Chemistry, **260**: 14435–14439.
- Arakawa, T. and Y. R. Hsu (1987). Acid Unfolding and Self-Association of Recombinant *Escherichia coli* Derived Human Interferon γ . Biochemistry, **26**: 5428-5432.
- Avanov, A. Y. (1991). Conformational Aspects of Glycosylation. Molekulyarnaya Biologiya, **25**: 293–308.
- Baumann, H. and G. P. Jahreis (1983). Glucose Starvation Leads in Rat Hepatoma Cells to Partially N-Glycosylated Glycoproteins Including α 1-Acid Glycoproteins. The Journal of Biological Chemistry, **258**: 3942-3949.
- Bause, E. and G. Legler (1981). The Role of the Hydroxy Amino Acid in the Triplet Sequence Asn-Xaa-Thr(Ser) for the N-glycosylation Step During Glycoprotein Biosynthesis. Biochem. J., **195**: 639–644.
- Beckmann, R. P., L. A. Mizzen and W. J. Welch (1990). Interaction of Hsp70 with Newly Synthesized Proteins: Implications for Protein Folding and Assembly. Science, **248**: 850-854.
- Beeley, J. G. (1985). Glycoprotein and Proteoglycan Techniques. Elsevier, New York.

- Berg, D. T., P. J. Burck, D. H. Berg and B. W. Grinnell (1993). Kringle Glycosylation in a Modified Human Tissue Plasminogen Activator Improves Functional Properties. Blood, **81**: 1312–1322.
- Blond-Elguindi, S., S. E. Cwirla, W. J. Dower, R. J. Lipshutz, S. R. Sprang, J. F. Sambrook and M.-J. Gething (1993a). Affinity Panning of a Library of Peptides Displayed on Bacteriophages Reveals the Binding Specificity of BiP. Cell, **75**: 717-728.
- Blond-Elguindi, S., A. M. Fourie, J. F. Sambrook and M. J. H. Gething (1993b). Peptide-dependent Stimulation of the ATPase Activity of the Molecular Chaperone BiP Is the Result of Conversion of Oligomers to Active Monomers. Journal of Biological Chemistry, **268**: 12730-12735.
- Bocci, V., A. Pacini, G. P. Pessina, L. Paulesu, M. Muscettola and G. Lunghetti (1985). Catabolic Sites of Human Interferon- γ . J. Gen. Virol., **66**: 887–891.
- Bonarius, H. P. J., C. D. de Gooijer, J. Tramper and G. Schmid (1995). Determination of the Respiration Quotient in Mammalian Cell Culture in Bicarbonate Buffered Media. Biotechnology and Bioengineering, **45**: 524–535.
- Bonarius, H. P. J., V. Hatzimanikatis, K. P. H. Meesters, C. D. deGooijer, G. Schmid and J. Tramper (1996). Metabolic Flux Analysis of Hybridoma Cells in Different Culture Media Using Mass Balances. Biotechnology and Bioengineering, **50**: 299–318.
- Borys, M. C., D. I. H. Linzer and E. T. Papoutsakis (1993). Culture pH Affects Expression Rates and Glycosylation of Recombinant Mouse Placental Lactogen Proteins by Chinese Hamster Ovary (CHO) Cells. Bio/Technology, **11**: 720-724.
- Borys, M. C., D. I. H. Linzer and E. T. Papoutsakis (1994a). Ammonia Affects the Glycosylation Patterns of Recombinant Mouse Placental Lactogen-I by Chinese Hamster Ovary Cells in a pH-Dependent Manner. Biotechnology and Bioengineering, **43**: 505–514.
- Borys, M. C., D. I. H. Linzer and E. T. Papoutsakis (1994b). Cell Aggregation in a Chinese Hamster Ovary Cell Microcarrier Culture Affects the Expression Rate and N-linked Glycosylation of Recombinant Mouse Placental Lactogen-1. Annals of the New York Academy of Sciences, **745**: 360–371.
- Brändli, A. W. (1991). Mammalian Glycosylation Mutants as Tools for the Analysis and Reconstitution of Protein Transport. Biochem. J., **276**: 1–12.

- Bulleid, N. J., R. S. Bassel-Duby, R. B. Freedmen, J. F. Sambrook and M. J. H. Gething (1992). Cell-Free Synthesis of Enzymatically Active Tissue-Type Plasminogen Activator. Biochemical Journal, **286**: 275-280.
- Carey, D. J., L. W. Sommers and C. B. Hirschberg (1980). CMP-N-Acetylneuraminic Acid: Isolation from and Penetration into Mouse Liver Microsomes. Cell, **19**: 597-605.
- Carlberg, M., A. Dricu, H. Blegen, M. Wang, M. Hjertman, P. Zickert, A. Höög and O. Larsson (1996). Mevalonic Acid Is Limiting for N-Linked Glycosylation and Translocation of the Insulin-like Growth Factor-1 Receptor to the Cell Surface. The Journal of Biological Chemistry, **271**: 17453-17462.
- Chalifour, R. J. and R. G. Spiro (1988). Effect of Phospholipids on Thyroid Oligosaccharyltransferase Activity and Orientation: Evaluation of Structural Determinants for Stimulation of N-Glycosylation. The Journal of Biological Chemistry, **263**: 15673-15680.
- Chan, V. T. and G. Wolf (1987). The Role of Vitamin A in the Glycosylation Reactions of Glycoprotein Synthesis in an '*in vitro*' System. Biochemical Journal, **247**: 53-62.
- Chapman, A. E. and J. C. Calhoun (1988). Effects of Glucose Starvation and Puromycin Treatment on Lipid-Linked Oligosaccharide Precursors and Biosynthetic Enzymes in Chinese Hamster Ovary Cells *in Vivo* and *in Vitro*. Archives of Biochemistry and Biophysics, **260**: 320-333.
- Chen, W., J. Helenius, I. Braakman and A. Helenius (1995). Cotranslational Folding and Calnexin Binding During Glycoprotein Synthesis. Proc. Natl. Acad. Sci. USA, **92**: 6229-6233.
- Chiou, S.-H. and K.-T. Wang (1988). Simplified Protein Hydrolysis With Methanesulphonic Acid at Elevated Temperature for the Complete Amino Acid Analysis of Proteins. Journal of Chromatography, **448**: 404-410.
- Chiou, S.-H. and K.-T. Wang (1989). Peptide and Protein Hydrolysis by Microwave Irradiation. Journal of Chromatography, **491**: 424-431.
- Clairmont, C. A., A. De Maio and C. B. Hirschberg (1992). Translocation of ATP into the Lumen of Rough Endoplasmic Reticulum-derived Vesicles and Its Binding to Luminal Proteins Including BiP (GRP 78) and GRP 94. Journal of Biological Chemistry, **267**: 3983-3990.

- Coppen, S. R., R. Newsam, A. T. Bull and A. J. Baines (1995). Heterogeneity Within Populations of Recombinant Chinese Hamster Ovary Cells Expressing Human Interferon- γ . Biotechnology and Bioengineering, **46**: 147–158.
- Cory, J. G. (1992). Purine and Pyrimidine Nucleotide Metabolism. In: T. M. Devlin, Textbook of Biochemistry with Clinical Correlations, Third Edition. Wiley-Liss, New York.
- Craig, E. A. and C. A. Gross (1991). Is Hsp70 the Cellular Thermometer? Trends in Biochemical Science, **16**: 135-140.
- Crick, D. C., J. R. Scocca, J. S. Rush, D. W. Frank, S. S. Krag and C. J. Waechter (1994). Induction of Dolichyl-Saccharide Intermediate Biosynthesis Corresponds to Increased Long Chain *cis*-Isoprenyltransferase Activity during the Mitogenic Response in Mouse B Cells. The Journal of Biological Chemistry, **269**: 10559–10565.
- Crick, D. C. and C. J. Waechter (1994). Long-Chain *cis*-Isoprenyltransferase Activity Is Induced Early in the Developmental Program for Protein N-Glycosylation in Embryonic Rat Brain Cells. Journal of Neurochemistry, **62**: 247–256.
- Cumming, D. A. (1991). Glycosylation of Recombinant Protein Therapeutics: Control and Functional Implications. **1**: 115-130.
- Curling, E. M. A., P. M. Hayter, A. J. Baines, A. T. Bull, K. Gull, P. G. Strange and N. Jenkins (1990). Recombinant Human Interferon- γ : Differences in Glycosylation and Proteolytic Processing Lead to Heterogeneity in Batch Culture. **272**: 333-337.
- Dan, N. and M. A. Lehrman (1997). Oligomerization of Hamster UDP-GlcNAc:Dolichol-P GlcNAc-1-P Transferase, an Enzyme with Multiple Transmembrane Spans. The Journal of Biological Chemistry, **272**: 14214–14219.
- Darnell, J., H. Lodish and D. Baltimore (1990). Molecular Cell Biology. Second Edition. Scientific American Books, New York.
- Datema, R. and R. T. Schwarz (1979). Interference with Glycosylation of Glycoproteins: Inhibition of Formation of Lipid-linked Oligosaccharides *In Vivo*. Biochem. J., **184**: 113–123.
- DeFrancesco, L., I. E. Scheffler and M. J. Bissell (1976). A Respiration-deficient Chinese Hamster Cell Line with a Defect in NADH-Coenzyme Q Reductase. The Journal of Biological Chemistry, **251**: 4588–4595.

- Devos, R., H. Cheroutre, Y. Taya, W. Degrave, H. Van Heuverswyn and W. Fiers (1982). Molecular Cloning of Human Immune Interferon cDNA and its Expression in Eukaryotic Cells. Nucleic Acids Research, **10**: 2487-2501.
- DiDomencio, B., G. Bugaisky and S. Lindquist (1982). Cell, **31**: 593-603.
- Dordal, M. S., F. F. Wang and E. Goldwasser (1985). The Role of Carbohydrate in Erythropoietin Action. Endocrinology, **116**: 2293-2299.
- Dorner, A. J., D. G. Bole and R. J. Kaufman (1987). The Relationship of N-linked Glycosylation and Heavy Chain-binding Protein Association with the Secretion of Glycoproteins. Journal of Cell Biology, **105**: 2665-2674.
- Dorner, A. J., M. G. Krane and R. J. Kaufman (1988). Reduction of Endogenous GRP78 Levels Improves Secretion of a Heterologous Protein in CHO Cells. Molecular and Cellular Biology, **8**: 4063-4070.
- Dorner, A. J., L. C. Wasley and R. J. Kaufman (1992). Overexpression of GRP78 Mitigates Stress Induction of Glucose Regulated Proteins and Blocks Secretion of Selective Proteins in Chinese Hamster Ovary Cells. The EMBO Journal, **11**: 1563-1571.
- Dorner, A. J., L. C. Wasley, M. G. Krane and R. J. Kaufman (1993). Protein Retention in the Endoplasmic Reticulum Mediated by GRP78. In: M. S. Oka and R. G. Rupp, Cell Biology and Biotechnology: Novel Approaches to Increased Cellular Productivity, Springer-Verlag, New York.
- Dudich, I. V., V. P. Zav'yalov, V.-A. V. Bumyalis and D. V. Paulauskas (1992). A Study of the Structural Properties of Recombinant γ -Interferon with the Aid of Circular Dichroism and Scanning Differential Microcalorimetry. Molekulyarnaya Biologiya, **26**: 441-451.
- Ealick, S. E., W. J. Cook, S. Vijay-Kumar, M. Carson, T. L. Nagabhushan, P. P. Trotta and C. E. Bugg (1991). Three-Dimensional Structure of Recombinant Human Interferon- γ . Science, **252**: 698-702.
- Eigenbrodt, E., P. Fister and M. Reinacher (1985). New Perspectives on Carbohydrate Metabolism in Tumor Cells. In: R. Beitner, Regulation of Carbohydrate Metabolism, CRC Press, Inc., Boca Raton, Florida.
- Elbein, A. D. (1987). Inhibitors of the Biosynthesis and Processing of N-linked Oligosaccharide Chains. Annual Review of Biochemistry, **56**: 497-534.

- Ezekowitz, R. A. B. and P. D. Stahl (1988). The Structure and Function of Vertebrate Mannose Lectin-like Proteins. In: S. Gordon, Macrophage Plasma Membrane Receptors: Structure and Function, The Company of Biologists Limited, Cambridge.
- Farrar, M. A. and R. D. Schreiber (1993). The Molecular Cell Biology of Interferon- γ and Its Receptor. Annual Reviews in Immunology, **11**: 571–611.
- Fedorov, A. N. and T. O. Baldwin (1995). Contribution of Cotranslational Folding to the Rate of Formation of Native Protein Structure. Proc. Natl. Acad. Sci. USA, **92**: 1227–1231.
- Fielder, K. and K. Simons (1995). The Role of N-Glycans in the Secretory Pathway. Cell, **81**: 309–312.
- Fischer, T., B. Thoma, P. Scheurich and K. Pfizenmaier (1990). Glycosylation of the Human Interferon- γ Receptor. N-linked Carbohydrates Contribute to Structural Heterogeneity and are Required for Ligand Binding. The Journal of Biological Chemistry, **265**: 1710–1717.
- Flesher, A. R., J. Marzowski, W.-C. Wang and H. V. Raff (1995). Fluorophore-Labeled Carbohydrate Analysis of Immunoglobulin Fusion Proteins: Correlation of Oligosaccharide Content with In Vivo Clearance Profile. Biotechnology and Bioengineering, **46**: 399–407.
- Flynn, G. C., T. G. Chappell and J. E. Rothman (1989). Peptide Binding and Release by Proteins Implicated as Catalysts of Protein Assembly. Science, **245**: 385-390.
- Flynn, G. C., J. Pohl, M. T. Flocco and J. E. Rothman (1991). Peptide-binding Specificity of the Molecular Chaperone BiP. Nature, **353**: 726-730.
- Freiden, P. J., J. R. Gaut and L. M. Hendershot (1992). Interconversion of Three Differentially Modified and Assembled Forms of BiP. EMBO Journal, **11**: 63-70.
- Fukushima, K., T. Ohkura and K. Yamashita (1997). Synthesis of Lipid-Linked Oligosaccharides Is Dependent on the Cell Cycle in Rat 3Y1 Cells. Journal of Biochemistry, **121**: 415–418.
- Gallagher, P. J., J. M. Henneberry, J. F. Sambrook and M.-J. Gething (1992). Glycosylation Requirements for Intracellular Transport and Function of the Hemagglutinin of Influenza Virus. J. Virol., **66**: 7136–7145.
- Gavel, Y. and G. von Heijne (1990). Sequence Differences Between Glycosylated and Non-glycosylated Asn-X-Thr/Ser Acceptor Sites: Implications for Protein Engineering. Protein Engineering, **3**: 433–442.

- Gawlitzeck, M., U. Valley, M. Nimtz, R. Wagner and H. S. Conradt (1995a). Characterization of Changes in the Glycosylation Pattern of Recombinant Proteins from BHK-21 Cells Due to Different Culture Conditions. Journal of Biotechnology, **42**: 117–131.
- Gawlitzeck, M., U. Valley, M. Nimtz, R. Wagner and H. S. Conradt (1995b). Effects of Ammonia and Glucosamine on the Glycosylation Pattern of Recombinant Proteins Expressed from BHK-21 Cells. In: E. C. Beuvery, J. B. Griffiths and W. P. Zeijlemaker, Animal Cell Technology: Developments Towards the 21st Century, Kluwer Academic Publishers, Dordrecht, The Netherlands.
- Gerald, C. F. and P. O. Wheatley (1994). Applied Numerical Analysis. Fifth Edition. Addison-Wesley Publishing Co., Reading, MA.
- Gershman, H. and P. W. Robbins (1981). Transitory Effects of Glucose Starvation on the Synthesis of Dolichol-linked Oligosaccharides in Mammalian Cells. Journal of Biological Chemistry, **256**: 7774-7780.
- Gething, M.-J., S. Blond-Elguindi, K. Mori and J. F. Sambrook (1994). Structure, Function, and Regulation of the Endoplasmic Reticulum Chaperone, BiP. In: R. I. Morimoto, A. Tissières and C. Georgopoulos, The Biology of Heat Shock Proteins and Molecular Chaperones, Cold Spring Harbor Laboratory Press, Plainview, NY.
- Gething, M. J., K. McCammon and J. Sambrook (1986). Expression of Wild-Type and Mutant Forms of Influenza Hemagglutinin: The role of Folding in Intracellular Transport. Cell, **46**: 939-950.
- Gething, M. J. and J. Sambrook (1992). Protein Folding in the Cell. Nature, **355**: 33-45.
- Glabe, C. G., J. A. Hanover and W. J. Lennarz (1980). Glycosylation of Ovalbumin Nascent Chains: The Spatial Relationship Between Translation and Glycosylation. The Journal of Biological Chemistry, **255**: 9236–9242.
- Goochee, C. F., M. J. Gramer, D. C. Anderson and J. B. Bahr (1991). The Oligosaccharides of Glycoproteins: Bioprocess Factors Affecting Oligosaccharide Structure and Their Effect on Glycoprotein Properties. Bio/Technology, **9**: 1347–1355.
- Goochee, C. F., M. J. Gramer, D. C. Anderson and J. B. Bahr (1992). The Oligosaccharides of Glycoproteins: Factors Affecting their Synthesis and their Influence on Glycoprotein Properties. In: P. Todd, S. K. Sikdar and M. Bier, Frontiers in Bioprocessing II, American Chemical Society, Washington, D.C.

- Goochee, C. F. and T. Monica (1990). Environmental Effects on Protein Glycosylation. **8**: 421-427.
- Goswami, J., A. J. Sinskey, H. Steller, G. N. Stephanopoulos and D. I. C. Wang (1998). Apoptosis in Batch Cultures of Chinese Hamster Ovary Cells. Biotechnology and Bioengineering (Submitted).
- Griffiths, G., G. Warren, P. Quinn, O. Mathieu-Costello and H. Hoppeler (1984). Density of Newly Synthesized Plasma Membrane Proteins in Intracellular Membranes. I. Stereological Studies. Journal of Cell Biology, **98**: 2133-2141.
- Gross, V., P. C. Heinrich, D. vom Berg, K. Steube, T. Andus, T.-A. Tran-Thi, K. Decker and W. Gerok (1988). Involvement of Various Organs in the Initial Plasma Clearance of Differently Glycosylated Rat Liver Secretory Proteins. European Journal of Biochemistry, **173**: 653-659.
- Gross, V., K. Steube, T.-A. Tran-Thi, W. Gerok and P. C. Heinrich (1989). Role of N-glycosylation for the Plasma Clearance of Rat Liver Secretory Glycoproteins. Biochemical Society Transactions, **17**: 21-23.
- Gu, M. B., P. Todd and D. S. Kompala (1993). Foreign Gene Expression (β -Galactosidase) During the Cell Cycle Phases in Recombinant CHO Cells. Biotechnology and Bioengineering, **42**: 1113-1123.
- Gu, M. B., P. Todd and D. S. Kompala (1994). Analysis of Foreign Protein Overproduction in Recombinant CHO Cells. Annals of N.Y. Acad. Sci., **721**: 194-207.
- Gu, M. B., P. Todd and D. S. Kompala (1996). Cell Cycle Analysis of Foreign Gene (β -Galactosidase) Expression in Recombinant Mouse Cells under Control of Mouse Mammary Tumor Virus Promoter. Biotechnology and Bioengineering, **50**: 229-237.
- Gu, X. (1997). Characterization and Improvement of Interferon- γ Glycosylation in Chinese Hamster Ovary Cell Culture. Ph.D. Massachusetts Institute of Technology.
- Gu, X., B. J. Harmon and D. I. C. Wang (1997). Site- and Branch-Specific Sialylation of Recombinant Human Interferon- γ in Chinese Hamster Ovary Cell Culture. Biotechnology and Bioengineering, **55**: 390-398.
- Haas, I. G. and M. Wabl (1983). Immunoglobulin Heavy Chain Binding Protein. Nature, **306**: 387-389.

- Hamilton, W. G. and R. G. Ham (1977). Clonal growth of Chinese Hamster Cell lines in protein-free media. In Vitro, **13**: 537-547.
- Harlow, E. and D. Lane (1988). Antibodies: A Laboratory Manual. Cold Spring Harbor Laboratory,
- Harmon, B. J., X. Gu and D. I. C. Wang (1996). Rapid Monitoring of Site-Specific Glycosylation Microheterogeneity of Recombinant Human Interferon- γ . Analytical Chemistry, **68**: 1465–1473.
- Hartl, F. U., J. Martin and W. Neupert (1992). Protein Folding in the Cell: The Role of Molecular Chaperones Hsp70 and Hsp60. Annual Rev. Biophys. Biomol. Struct., **21**: 293-322.
- Haschemeyer, A. E. V. (1976). Kinetics of Protein Synthesis in Higher Organisms *In Vivo*. Trends Biochem. Sci., **1**: 133.
- Hayter, P. M., E. M. A. Curling, A. J. Baines, N. Jenkins, I. Salmon, P. G. Strange, J. M. Tong and A. T. Bull (1992). Glucose-Limited Chemostat Culture of Chinese Hamster Ovary Cells Producing Recombinant Human Interferon- γ . Biotechnology and Bioengineering, **39**: 327-335.
- Hayter, P. M., E. M. A. Curling, M. L. Gould, A. J. Baines, N. Jenkins, I. Salmon, P. G. Strange and A. T. Bull (1993). The Effect of the Dilution Rate on CHO Cell Physiology and Recombinant Interferon- γ Production in Glucose-Limited Chemostat Culture. Biotechnology and Bioengineering, **42**: 1077–1085.
- Helenius, A. (1994). How N-linked Oligosaccharides Affect Glycoprotein Folding in the Endoplasmic Reticulum. Molecular Biology of the Cell, **5**: 253-265.
- Hendershot, L. M., J. Ting and A. S. Lee (1988). Identity of the Immunoglobulin Heavy-chain -binding Protein with the 78,000-dalton Glucose-regulated Protein and the Role of Posttranslational Modifications in Its Binding Function. Molecular and Cellular Biology, **8**: 4250-4256.
- Hirschberg, C. B. and M. D. Snider (1987). Topography of Glycosylation in the Rough Endoplasmic Reticulum and Golgi Apparatus. Annual Review of Biochemistry, **56**: 63-87.
- Holst, B., A. W. Bruun, M. C. Kielland-Brandt and J. R. Winther (1996). Competition Between Folding and Glycosylation in the Endoplasmic Reticulum. The EMBO Journal, **15**: 3538–3546.

- Imperiali, B., K. L. Shannon and K. W. Rickert (1992a). Role of Peptide Conformation in Asparagine-Linked Glycosylation. Journal of the American Chemical Society, **114**: 7942–7944.
- Imperiali, B., K. L. Shannon, M. Unno and K. W. Rickert (1992b). A Mechanistic Proposal for Asparagine-Linked Glycosylation. Journal of the American Chemical Society, **114**: 7944–7945.
- James, D. C., R. B. Freedman, M. Hoare and N. Jenkins (1994). High-Resolution Separation of Recombinant Human Interferon- γ Glycoforms by Micellar Electrokinetic Capillary Chromatography. Analytical Biochemistry, **222**: 315–322.
- James, D. C., R. B. Freedman, M. Hoare, O. W. Ogonah, B. C. Rooney, O. A. Larionov, V. N. Dobrovolsky, O. V. Lagutin and N. Jenkins (1995). N-Glycosylation of Recombinant Human Interferon- γ Produced in Different Animal Expression Systems. Bio/Technology, **13**: 592–596.
- Jenkins, N. (1991). Growth Factors. In: M. Butler, Mammalian Cell Biotechnology: A Practical Approach, Oxford University Press,
- Jenkins, N., P. Castro, S. Menon, A. Ison and A. Bull (1994). Effect of Lipid Supplements on the Production and Glycosylation of Recombinant Interferon- γ Expressed in CHO Cells. Cytotechnology, **15**: 209–215.
- Jenkins, N. and E. M. A. Curling (1994). Glycosylation of Recombinant Proteins: Problems and Prospects. Enzyme Microb. Technol., **16**: 354–364.
- Jenkins, N., R. B. Parekh and D. C. James (1996). Getting the Glycosylation Right: Implications for the Biotechnology Industry. Nature Biotechnology, **14**: 975–981.
- Kaiden, A. and S. S. Krag (1992). Dolichol Metabolism in Chinese Hamster Ovary Cells. Biochem. Cell Biol., **70**: 385–389.
- Kaminskas, E. (1979). Ribonucleotide Depletion in Glucose-Deprived Tumor Cells: The Role of RNA Synthesis. Biochemical and Biophysical Research Communications, **88**: 1391–1397.
- Kanwar, Y. S. (1984). Biology of Disease: Biophysiology of Glomerular Filtration and Proteinuria. Laboratory Investigation, **51**: 7–21.
- Kaplan, H. A., J. K. Welply and W. J. Lennarz (1987). Oligosaccharyl Transferase: The Central Enzyme in the Pathway of Glycoprotein Assembly. Biochimica et Biophysica Acta, **906**: 161–173.

- Kassenbrock, C. K., P. D. Garcia, P. Walter and R. B. Kelly (1988). Heavy-chain Binding Protein Recognizes Aberrant Polypeptides Translocated *in-vitro*. Nature, **333**: 90-93.
- Kasturi, L., J. R. Eshleman, W. H. Wunner and S. H. Shakin-Eshleman (1995). The Hydroxy Amino Acid in an Asn-X-Ser/Thr Sequon Can Influence N-linked Core Glycosylation Efficiency and the Level of Expression of a Cell Surface Glycoprotein. The Journal of Biological Chemistry, **270**: 14756–14761.
- Kaufman, R. J. and P. A. Sharp (1982). Amplification and Expression of Sequences Cotransfected with a Modular Dihydrofolate Reductase Complementary DNA Gene. Journal of Molecular Biology, **159**: 601–621.
- Kean, E. L. (1991a). Studies on the Activation by Dolichol-P-mannose of the Biosynthesis of GlcNAc-P-P-dolichol and the Topography of the GlcNAc-transferases Concerned with the Synthesis of GlcNAc-P-P-dolichol and (GlcNAc)₂-P-P-dolichol: A Review. Biochem. Cell Biol., **70**: 413–421.
- Kean, E. L. (1991b). Topographical Orientation in Microsomal Vesicles of the N-acetylglucosaminyltransferases Which Catalyze the Biosynthesis of N-acetylglucosaminylpyrophosphoryldolichol and N-acetylglucosaminyl-N-acetylglucosaminylpyrophosphoryl-dolichol. Journal of Biological Chemistry, **266**: 942–946.
- Keen, M. J. and N. T. Rapson (1995). Development of a Serum-free Culture Medium for the Large Scale Production of Recombinant Protein from a Chinese Hamster Ovary Cell Line. Cytotechnology, **17**: 153–163.
- Kelleher, D. J., G. Kreibich and R. Gilmore (1992). Oligosaccharyltransferase Activity Is Associated with a Protein Complex Composed of Ribophorins I and II and a 48 kd Protein. Cell, **69**: 55–65.
- Kern, G., M. Schmidt, J. Buchner and R. Jaenicke (1992). Glycosylation Inhibits the Interaction of Invertase with the Chaperone GroEL. FEBS Letters, **305**: 203–205.
- Kitagawa, Y., Y. Sano, M. Ueda, K. Higashio, H. Narita, M. Okano, S.-I. Matsumoto and R. Sasaki (1994). N-Glycosylation of Erythropoietin Is Critical for Apical Secretion by Madin-Darby Canine Kidney Cells. Experimental Cell Research, **213**: 449–457.

- Knittler, M. R., S. Dirks and I. G. Haas (1995). Molecular Chaperones Involved in Protein Degradation in the Endoplasmic Reticulum: Quantitative Interaction of the Heat Shock Cognate Protein BiP with Partially Folded Immunoglobulin Light Chains That Are Degraded in the Endoplasmic Reticulum. Proc. Natl. Acad. Sci. USA, **92**: 1764–1768.
- Koch, H. U., R. T. Schwarz and C. Scholtissek (1979). Glucosamine Itself Mediates Reversible Inhibition of Protein Glycosylation. European Journal of Biochemistry, **94**: 515–522.
- Konrad, M. and W. E. Merz (1994). Regulation of N-Glycosylation: Long Term Effect of Cyclic AMP Mediates Enhanced Synthesis of the Dolichol Pyrophosphate Core Oligosaccharide. Journal of Biological Chemistry, **269**: 8659-8666.
- Kopp, K., W. Noé, M. Schlüter, R. Werner and F. Götz (1995). The Role of Physiological Cell Parameters and Culture Conditions on Product Consistency and Glycosylation Pattern of Recombinant CHO Expressed Glycoproteins - Interferon Omega and Tissue Plasminogen Activator. In: E. C. Beuvery, J. B. Griffiths and W. P. Zeijlemaker, Animal Cell Technology: Developments Towards the 21st Century, Kluwer Academic Publishers, Dordrecht, The Netherlands.
- Kornfeld, R. and S. Kornfeld (1985). Assembly of Asparagine-linked Oligosaccharides. **54**: 631-664.
- Kornfeld, S. and V. Ginsburg (1966). The Metabolism of Glucosamine by Tissue Culture Cells. Experimental Cell Research, **41**: 592–600.
- Kornfeld, S. and I. Mellman (1989). The Biogenesis of Lysosomes. Annual Reviews in Cell Biology, **5**: 483–525.
- Kozutsumi, Y., M. Segal, K. Normington, M.-J. Gething and J. Sambrook (1988). The Presence of Malfolded Proteins in the Endoplasmic Reticulum Signals the Induction of Glucose-Regulated Proteins. Nature, **332**: 462–464.
- Krebs, H., F. X. Schmid and R. Jaenicke (1983). Folding of Homologous Proteins: The Refolding of Different Ribonucleases is Independent of Sequence Variations, Proline Content and Glycosylation. The Journal of Molecular Biology, **169**: 619–635.
- Langer, B. G., J. W. Weisel, P. A. Dinauer, C. Nagaswami and W. R. Bell (1988). Deglycosylation of Fibrinogen Accelerates Polymerization and Increases Lateral Aggregation of Fibrin Fibers. Journal of Biological Chemistry, **263**: 15056–15063.

- Lanks, K. W., J.-P. Gao and E. J. Kasambalides (1988). Nucleoside Restoration of Heat Resistance and Suppression of Glucose-regulated Protein Synthesis by Glucose-deprived L929 Cells. Cancer Research, **48**: 1442–1445.
- Lee, A. S. (1987). Coordinated Regulation of a Set of Genes by Glucose and Calcium Ionophores in Mammalian Cells. TIBS, **12**: 20–23.
- Lehrman, M. A. and Y. Zeng (1989). Pleiotropic Resistance to Glycoprotein Processing Inhibitors in Chinese Hamster Ovary Cells. The Journal of Biological Chemistry, **264**: 1584–1593.
- Lennon, K., R. Pretel, J. Kesselheim, S. te Hessen and M. A. Kukuruzinska (1995). Proliferation-Dependent Differential Regulation of the Dolichol Pathway Genes in *Saccharomyces cerevisiae*. Glycobiology, **5**: 633–642.
- Lodish, H. F., N. Hong, M. Snider and G. J. Strous (1983). Hepatoma Secretory Proteins Migrate from Rough Endoplasmic Reticulum to Golgi at Characteristic Rates. Nature, **304**: 80–83.
- Ma, J., H. Saito, T. Oka and I. K. Vijay (1996). Negative Regulatory Element Involved in the Hormonal Regulation of GlcNAc-1-P Transferase Gene in Mouse Mammary Gland. The Journal of Biological Chemistry, **271**: 11197–11203.
- Marcantonio, E. E., A. Amar-Costesec and G. Kreibich (1984). Segregation of the Polypeptide Translocation Apparatus to Regions of the Endoplasmic Reticulum Containing Ribophorins and Ribosomes. II. Rat Liver Microsomal Subfractions Contain Equimolar Amounts of Ribophorins and Ribosomes. The Journal of Cell Biology, **99**: 2254–2259.
- Maron, M. J. and R. J. Lopez (1991). Numerical Analysis: A Practical Approach. Wadsworth Publishing Company, Belmont, CA.
- Marshall, R. D. (1972). Glycoproteins. Annual Reviews in Biochemistry, **41**: 673–702.
- Misaizu, T., S. Matsuki, T. W. Strickland, M. Takeuchi, A. Kobata and S. Takasaki (1995). Role of Antennary Structure of N-linked Sugar Chains in Renal Handling of Recombinant Human Erythropoietin. Blood, **86**: 4097–4104.
- Monroe, R. S. and B. E. Huber (1994). The Major Form of the Murine Asialoglycoprotein Receptor: cDNA Sequence and Expression in Liver, Testis and Epididymis. Gene, **148**: 237–244.
- Mori, K., A. Sant, K. Kohno, K. Normington, M. J. Gething and J. F. Sambrook (1992). A 22 bp *Cis*-acting Element is Necessary and Sufficient for the Induction of the Yeast KAR2 (BiP) Gene by Unfolded Proteins. EMBO Journal, **11**: 2583–2593.

- Mørtz, E., T. Sareneva, I. Julkunen and P. Roepstorff (1996). Does Matrix-assisted Laser Desorption/Ionization Mass Spectrometry Allow Analysis of Carbohydrate Heterogeneity in Glycoproteins? A Study of Natural Human Interferon- γ . Journal of Mass Spectrometry, **31**: 1109–1118.
- Mota, O. M., G. T. Huang and M. A. Kukuruzinska (1994). Developmental Regulation and Tissue-Specific Expression of Hamster Dolichol-P-Dependent N-Acetylglucosamine-1-P Transferase (GPT). Biochemical and Biophysical Research Communications, **204**: 284–291.
- Mutsaers, J. H. G. M., J. P. Kamerling, R. Devos, Y. Guisez, W. Fiers and J. F. G. Vliegthart (1986). Structural Studies of the Carbohydrate Chains of Human γ -interferon. **156**: 651-654.
- Nguyen, T. H., D. T. S. Law and D. B. Williams (1991). Binding Protein BiP is Required for Translocation of Secretory Proteins into the Endoplasmic Reticulum in *Saccharomyces cerevisiae*. Proceedings of the National Academy of Sciences of the United States of America, **88**: 1565-1569.
- Nilsson, I. M. and G. von Heijne (1993). Determination of the Distance Between the Oligosaccharyltransferase Active Site and the Endoplasmic Reticulum Membrane. Journal of Biological Chemistry (?), **268**: 5798-5801.
- Oda-Tamai, S., S. Kato, S. Hara and N. Akamatsu (1985). Decreased Transfer of Oligosaccharide from Oligosaccharide-Lipid to Protein Acceptors in Regenerating Rat Liver. The Journal of Biological Chemistry, **260**: 57–63.
- Ohkura, T., K. Fukushima, A. Kurisaki, H. Sagami, K. Ogura, K. Ohno, S. Hara-Kuge and K. Yamashita (1997). A Partial Deficiency of Dehydrodolichol Reduction Is a Cause of Carbohydrate-deficient Glycoprotein Syndrome Type I. The Journal of Biological Chemistry, **272**: 6868–6875.
- Orlean, P. (1992). Enzymes That Recognize Dolichols Participate in Three Glycosylation Pathways and Are Required for Protein Secretion. Biochem. Cell Biol., **70**: 438–447.
- Pan, Y.-T. and A. D. Elbein (1982). The Formation of Lipid-linked Oligosaccharides in Madin-Darby Canine Kidney Cells. The Journal of Biological Chemistry, **257**: 2795–2801.
- Pels Rijcken, W. R., W. Ferwerda, D. H. Van den Eijnden and B. Overdijk (1995a). Influence of D-Galactosamine on the Synthesis of Sugar Nucleotides and Glycoconjugates in Rat Hepatocytes. Glycobiology, **5**: 495–502.

- Pels Rijcken, W. R., B. Overdijk, D. H. van den Eijnden and W. Ferwerda (1993). Pyrimidine Nucleotide Metabolism in Rat Hepatocytes: Evidence for Compartmentation of Nucleotide Pools. Biochem. J., **293**: 207–213.
- Pels Rijcken, W. R., B. Overdijk, D. H. Van Den Eijnden and W. Ferwerda (1995b). The Effect of Increasing Nucleotide-Sugar Concentrations on the Incorporation of Sugars into Glycoconjugates in Rat Hepatocytes. Biochemistry Journal, **305**: 865–870.
- Popov, M., L. Y. Tam, J. Li and R. A. F. Reithmeier (1997). Mapping the Ends of Transmembrane Segments in a Polytopic Membrane Protein: Scanning N-Glycosylation Mutagenesis of Extracytosolic Loops in the Anion Exchanger, Band 3. The Journal of Biological Chemistry, **272**: 18325–18332.
- Ptitsyn, O. B. and G. V. Semisotnov (1991). In: B. T. Nall and K. A. Dill, Conformations and Forces in Protein Folding, AAAS, Washington, D.C.
- Puig, A. and H. F. Gilbert (1994). Anti-chaperone Behavior of BiP during the Protein Disulfide Isomerase-catalyzed Refolding of Reduced Denatured Lysosyme. Journal of Biological Chemistry, **269**: 25889-25896.
- Putnam, R. and A. Roos (1991). Which Value for the First Dissociation Constant of Carbonic Acid Should Be Used in Biological Work? American Journal of Physiology, **260**: C1113–C1116.
- Rademacher, T. W., R. B. Parekh and R. A. Dwek (1988). Glycobiology. Annual Reviews in Biochemistry, **57**: 785–838.
- Rapaport, E., C. W. Christopher, S. K. Svihovec, D. Ullrey and H. M. Kalckar (1979). Selective High Metabolic Lability of Uridine, Guanosine and Cytosine Triphosphates in Response to Glucose Deprivation and Refeeding of Untransformed and Polyoma Virus-transformed Hamster Fibroblasts. Journal of Cellular Physiology, **101**: 229–236.
- Rearick, J. I., A. Chapman and S. Kornfeld (1981). Glucose Starvation Alters Lipid-linked Oligosaccharide Biosynthesis in Chinese Hamster Ovary Cells. Journal of Biological Chemistry, **256**: 6255-6261.
- Riederer, M. A. and A. Hinnen (1991). Removal of N-Glycosylation Sites of the Yeast Acid Phosphatase Severely Affects Protein Folding. Journal of Bacteriology, **173**: 3539–3546.
- Rinderknecht, E., B. H. O'Conner and H. Rodriques (1984). Natural Human Interferon- γ : Complete Amino Acid Sequence and Determination of Sites of Glycosylation. Journal of Biological Chemistry, **259**: 6790-6797.

- Robinson, A. S. and D. A. Lauffenburger (1996). Model for ER Chaperone Dynamics and Secretary Protein Interactions. *AIChE Journal*, **42**: 1443–1453.
- Robinson, D. K., C. P. Chan, C. Yu Ip, P. K. Tsai, J. Tung, T. C. Seamans, A. B. Lenny, D. K. Lee, J. Irwin and M. Silberklang (1994). Characterization of a Recombinant Antibody Produced in the Course of a High Yield Fed-Batch Process. *Biotechnology and Bioengineering*, **44**: 727–735.
- Romagnoli, J. A. and G. Stephanopoulos (1981). Rectification of Process Measurement Data in the Presence of Gross Errors. *Chemical Engineering Science*, **36**: 1849–1863.
- Rosenwald, A. G., J. Stoll and S. S. Krag (1990). Regulation of Glycosylation: Three Enzymes Compete for a Common Pool of Dolichyl Phosphate *In Vivo*. *The Journal of Biological Chemistry*, **265**: 14544–14553.
- Rothman, J. E. and H. F. Lodish (1977). Synchronised Transmembrane Insertion and Glycosylation of a Nascent Membrane Protein. *Nature*, **269**: 775–780.
- Ryll, T., U. Valley and R. Wagner (1994). Biochemistry of Growth Inhibition by Ammonium Ions in Mammalian Cells. *Biotechnology and Bioengineering*, **44**: 184–193.
- Ryll, T. and R. Wagner (1991). Improved Ion-Pair High-Performance Liquid Chromatographic Method for the Quantification of a Wide Variety of Nucleotides and Sugar-Nucleotides in Animal Cells. *Journal of Chromatography*, **570**: 77–88.
- Sagami, H., Y. Igarashi, S. Tateyama, K. Ogura, J. Roos and W. J. Lennarz (1996). Enzymatic Formation of Dehydrodolichal and Dolichal, New Products Related to Yeast Dolichol Biosynthesis. *The Journal of Biological Chemistry*, **271**: 9560–9566.
- Sagami, H., A. Kurisaki and K. Ogura (1993). Formation of Dolichol from Dehydrodolichol Is Catalyzed by NADPH-dependent Reductase Localized in Microsomes of Rat Liver. *The Journal of Biological Chemistry*, **268**: 10109–10113.
- Sanders, S. L., K. M. Whitfield, J. P. Vogel, M. D. Rose and R. W. Schekman (1992). Sec61p and BiP Directly Facilitate Polypeptide Translocation into the ER. *Cell*, **69**: 353–365.
- Sareneva, T., K. Cantell, L. Pyhälä, J. Pirhonen and I. Julkunen (1993). Effect of Carbohydrates on the Pharmacokinetics of Human Interferon- γ . *Journal of Interferon Research*, **13**: 267–269.

- Sareneva, T., J. Pirhonen, K. Cantell and I. Julkunen (1995). N-glycosylation of Human Interferon- γ : Glycans at Asn-25 Are Critical for Protease Resistance. Biochem. J., **308**: 9–14.
- Sareneva, T., J. Pirhonen, K. Cantell, N. Kalkkinen and I. Julkunen (1994). Role of N-Glycosylation in the Synthesis, Dimerization and Secretion of Human Interferon- γ . Biochem. J., **303**: 831–840.
- Savinell, J. M. and B. O. Palsson (1992). Network Analysis of Intermediary Metabolism using Linear Optimization. I. Development of Mathematical Formalism. Journal of Theoretical Biology, **154**: 421–454.
- Savvidou, G., M. Klein, C. Horne, T. Hofmann and K. J. Dorrington (1981). A Monoclonal Immunoglobulin G1 in which Some Molecules Possess Glycosylated Light Chains—I. Site of Glycosylation. Molec. Immun., **18**: 793-805.
- Scahill, S. J., R. Devos, J. Van der Heyden and W. Fiers (1983). Expression and Characterization of the Product of a Human Immune Interferon cDNA Gene in Chinese Hamster Ovary Cells. **80**: 4654-4658.
- Schachter, H. (1978). Glycoprotein Biosynthesis. In: M. I. Horowitz and W. Pigman, The Glycoconjugates. Volume II: Mammalian Glycoproteins, Glycolipids, and Proteoglycans, Academic Press, New York.
- Schachter, H. (1986). Biosynthetic Controls that Determine the Branching and Microheterogeneity of Protein-Bound Oligosaccharides. Biochem. Cell Biol., **64**: 163–181.
- Schmitz, A., M. Maintz, T. Kehle and V. Herzog (1995). *In Vivo* Iodination of a Misfolded Proinsulin Reveals Co-localization Signals for BiP Binding and for Degradation in the ER. The EMBO Journal, **14**: 1091–1098.
- Schülke, N. and F. X. Schmid (1988). Effect of Glycosylation on the Mechanism of Renaturation of Invertase from Yeast. The Journal of Biological Chemistry, **263**: 8832–8837.
- Schumpe, A., G. Quicker and W. D. Deckwer (1982). Gas Solubilities in Microbial Culture Media. Advances in Biochemical Engineering, **24**: 1–38.
- Schumpp, B. and E. J. Schlaeger (1990). Optimization of Culture Conditions for High Cell Density Proliferation of HL-60 Human Promyelocytic Leukemia Cells. Journal of Cell Science, **97**: 639–647.

- Sciandra, J. J. and J. R. Subjeck (1983). The Effects of Glucose on Protein Synthesis and Thermosensitivity in Chinese Hamster Ovary Cells. The Journal of Biological Chemistry, **258**: 12091-12093.
- Severinghaus, J. W. (1965). Chapter 61: Blood Gas Concentrations. In: W. O. Fenn and H. Rahn, Hanbook of Physiology Section 3: Respiration, American Physiological Society, Washington, D.C.
- Shakin-Eshleman, S. H., S. L. Spitalnik and L. Kasturi (1996). The Amino Acid at the X Position of an Asn-X-Ser Sequon Is an Important Determinant of N-Linked Core-glycosylation Efficiency. The Journal of Biological Chemistry, **271**: 6363–6366.
- Shelikoff, M., A. J. Sinskey and G. Stephanopoulos (1994). The Effect of Protein Synthesis Inhibitors on the Glycosylation Site Occupancy of Recombinant Human Prolactin. Cytotechnology, **12**: 1–14.
- Shelikoff, M., A. J. Sinskey and G. Stephanopoulos (1996). A Modeling Framework for the Study of Protein Glycosylation. Biotechnology and Bioengineering, **50**: 73–90.
- Silberstein, S. and R. Gilmore (1996). Biochemistry, Molecular Biology, and Genetics of the Oligosaccharyltransferase. FASEB J., **10**: 849–858.
- Silberstein, S., D. J. Kelleher and R. Gilmore (1992). The 48-kDa Subunit of the Mammalian Oligosaccharyltransferase Complex Is Homologous to the Essential Yeast Protein WBP1. The Journal of Biological Chemistry, **267**: 23658–23663.
- Sokoloski, J. A. and A. C. Sartorelli (1987). Inhibition of the Synthesis of Glycoproteins and Induction of the Differentiation of HL-60 Promyelocytic Leukemia Cells by 6-Methylmercaptapurine Ribonucleoside. Cancer Research, **47**: 6283–6287.
- Sonderhoff, S. A., D. G. Kilburn and J. M. Piret (1992). Analysis of Mammalian Viable Cell Biomass Based on Cellular ATP. Biotechnology and Bioengineering, **39**: 859–864.
- Sousa, M. C., M. A. Ferrero-Garcia and A. J. Parodi (1992). Recognition of the Oligosaccharide and Protein Moities of Glucoproteins by the UDP-Glc:glycoprotein Glucosyltransferase. Biochem., **31**: 97–105.
- Spiro, R. G., Q. Zhu, V. Bhojroo and H.-D. Söling (1996). Definition of the Lectin-like Properties of the Molecular Chaperone, Calreticulin, and Demonstration of Its Copurification with Endomannosidase from Rat Liver Golgi. The Journal of Biological Chemistry, **271**: 11588–11594.

- Spivak, J. L. and B. B. Hogans (1989). The *In vivo* Metabolism of Recombinant Human Erythropoietin in the Rat. Blood, **73**: 90–99.
- Stanley, P. (1983). Selection of Lectin-Resistant Mutants of Animal Cells. Methods in Enzymology, **96**: 157–185.
- Stark, N. J. and E. C. Heath (1979). Glucose-Dependent Glycosylation of Secretory Glycoprotein in Mouse Myeloma Cells. Archives of Biochemistry and Biophysics, **192**: 599-609.
- Stoll, J. and S. S. Krag (1988). A Mutant of Chinese Hamster Ovary Cells with a Reduction in Levels of Dolichyl Phosphate Available for Glycosylation. The Journal of Biological Chemistry, **263**: 10766–10773.
- Stoll, J., A. G. Rosenwald and S. S. Krag (1988). A Chinese Hamster Ovary Cell Mutant F2A8 Utilized Polyprenol Rather Than Dolichol for Its Lipid-dependent Asparagine-linked Glycosylation Reactions. The Journal of Biological Chemistry, **263**: 10774–10782.
- Strang, G. (1988). Linear Algebra and Its Applications. Third Edition. Harcourt Brace Jovanovich, Inc., San Diego.
- Strickland, T. W., A. R. Thomason, J. H. Nilson and J. G. Pierce (1985). The Common α Subunit of Bovine Glycoprotein Hormones: Limited Formation of Native Structure by the Totally Nonglycosylated Polypeptide Chain. Journal of Cellular Biochemistry, **29**: 225–237.
- Stryer, L. (1988). Biochemistry. Third Edition. W. H. Freeman and Company, New York.
- Tatu, U. and A. Helenius (1997). Interactions Between Newly Synthesized Glycoproteins, Calnexin and a Network of Resident Chaperones in the Endoplasmic Reticulum. J. Cell Biol., **136**: 555–565.
- te Heesen, S., B. Janetzky, L. Lehle and M. Aebi (1992). The Yeast WBP1 Is Essential for Oligosaccharyl Transferase Activity *in vivo* and *in vitro*. The EMBO Journal, **11**: 2071–2075.
- Thorens, B. and P. Vassalli (1986). Chloroquine and Ammonium Chloride Prevent Terminal Glycosylation of Immunoglobulins in Plasma Cells without Affecting Secretion. Nature, **321**: 618–620.
- Traxinger, R. R. and S. Marshall (1991). Coordinated Regulation of Glutamine:Fructose-6-phosphate Amidotransferase Activity by Insulin, Glucose, and Glutamine. The Journal of Biological Chemistry, **266**: 10148–10154.

- Turco, S. J. (1980). Modification of Oligosaccharide-Lipid Synthesis and Protein Glycosylation in Glucose-Deprived Cells. Archives of Biochemistry and Biophysics, **205**: 330-339.
- Ullrey, D. B. and H. M. Kalckar (1979). Methods for Specific Characterization of Trace Amounts of Uridine Nucleotides in Animal Cell Cultures. Analytical Biochemistry, **95**: 245-249.
- Umaña, P. and J. E. Bailey (1997). A Mathematical Model of N-Linked Glycoform Biosynthesis. Biotechnology and Bioengineering, **55**: 890-908.
- Vallino, J. J. and G. Stephanopoulos (1990). Flux Determination in Cellular Bioreaction Networks: Applications to Lysine Fermentations. In: S. K. Sikdar, M. Bier and P. Todd, Frontiers in Bioprocessing, CRC Press, Boca Raton, FL.
- Velez, D., S. Reuveny, L. Miller and J. D. Macmillan (1986). Kinetics of Monoclonal Antibody Production in Low Serum Growth Medium. Journal of Immunological Methods, **86**: 45-52.
- Vogel, J. P., L. M. Misra and M. D. Rose (1990). Loss of BiP/GRP78 Function Blocks Translocation of Secretory Proteins in Yeast. Journal of Cell Biology, **110**: 1885-1895.
- Waldman, B. C., C. Oliver and S. S. Krag (1987). A Clonal Derivative of Tunicamycin-Resistant Chinese Hamster Ovary Cells With Increased N-Acetylglucosamine-Phosphate Transferase Activity Has Altered Asparagine-Linked Glycosylation. Journal of Cellular Physiology, **131**: 302-317.
- Wang, F.-F. C. and C. H. W. Hirs (1977). Influence of the Heterosaccharides in Porcine Pancreatic Ribonuclease on the Conformation and Stability of the Protein. The Journal of Biological Chemistry, **252**: 8358-8364.
- Wang, N. S. and G. Stephanopoulos (1983). Application of Macroscopic Balances to the Identification of Gross Measurement Errors. Biotechnology and Bioengineering, **25**: 2177-2208.
- Ware, F. E., A. Vassilakos, P. A. Peterson, M. R. Jackson, M. A. Lehrman and D. B. Williams (1995). The Molecular Chaperone Calnexin Binds Glc₁Man₉GlcNAc₂ Oligosaccharide as an Initial Step in Recognizing Unfolded Glycoproteins. The Journal of Biological Chemistry, **270**: 4697-4704.
- Weibel, E. R., W. Staubli, H. R. Gnagi and F. A. Hess (1969). Correlated Morphometric and Biochemical Studies on the Liver Cell. I. Morphometric Model, Stereologic Methods and Normal Morphometric Data for Rat Liver. Journal of Cell Biology, **42**: 68-91.

- Weiss, P. and G. Ashwell (1989). The Asialoglycoprotein Receptor: Properties and Modulation by Ligand. In: P. Baumann, C. B. Eap, W. E. Müller and J.-P. Tillement, Alpha₁-Acid Glycoprotein: Genetics, Biochemistry, Physiological Functions, and Pharmacology, Alan R. Liss, Inc., New York.
- Wittwer, A. J. and S. C. Howard (1990). Glycosylation at Asn-184 Inhibits the Conversion of Single-Chain to Two-Chain Tissue-Type Plasminogen Activator by Plasmin. Biochemistry, **29**: 4175–4180.
- Wooden, S. K., L.-J. Li, D. Navarro, I. Qadri, L. Pereira and A. S. Lee (1991). Transactivation of the *grp78* Promoter by Malfolded Proteins, Glycosylation Block, and Calcium Ionophore Is Mediated through a Proximal Region Containing a CCAAT Motif Which Interacts with CTF/NF- κ B. Molecular and Cellular Biology, **11**: 5612–5623.
- Xie, L., G. Nyberg, X. Gu, H. Li, F. Möllborn and D. I. C. Wang (1997). Gamma-Interferon Production and Quality in Stoichiometric Fed-Batch Cultures of Chinese Hamster Ovary (CHO) Cells Under Serum-Free Conditions. Biotechnology and Bioengineering, **56**: 577–582.
- Xie, L. and D. I. C. Wang (1994a). Applications of Improved Stoichiometric Model in Medium Design and Fed-Batch Cultivation of Animal Cells in Bioreactor. Cytotechnology, **15**: 17–29.
- Xie, L. and D. I. C. Wang (1994b). Fed-Batch Cultivation of Animal Cells Using Different Medium Design Concepts and Feeding Strategies. Biotechnology and Bioengineering, **43**: 1175–1189.
- Xie, L. and D. I. C. Wang (1994c). Stoichiometric Analysis of Animal Cell Growth and Its Application in Medium Design. Biotechnology and Bioengineering, **43**: 1164–1174.
- Xie, L. and D. I. C. Wang (1996a). High Cell Density and High Monoclonal Antibody Production Through Medium Design and Rational Control in a Bioreactor. Biotechnology and Bioengineering, **51**: 725–729.
- Xie, L. and D. I. C. Wang (1996b). Material Balance Studies on Animal Cell Metabolism Using a Stoichiometrically Based Reaction Network. Biotechnology and Bioengineering, **52**: 579–590.
- Yu, Y., D. D. Sabatini and G. Kreibich (1990). Antiribophorin Antibodies Inhibit the Targeting to the ER Membrane of Ribosomes Containing Nascent Secretory Polypeptides. The Journal of Cell Biology, **111**: 1335–1342.

- Yurchenco, P. D., C. Ceccarini and P. H. Atkinson (1978). Labeling Complex Carbohydrates of Animal Cells with Monosaccharides. In: V. Ginsburg, Complex Carbohydrates, Part C, Academic Press, New York.
- Zettlmeissl, G., R. Rudolph and R. Jaenicke (1979). Reconstitution of Lactic Dehydrogenase. Noncovalent Aggregation vs. Reactivation. 1. Physical Properties and Kinetics of Aggregation. Biochemistry, **18**: 5567-5571.
- Zhang, Z., K.-T. Tong, M. Belew, T. Pettersson and J.-C. Janson (1992). Production, Purification and Characterization of Recombinant Human Interferon γ . Journal of Chromatography, **604**: 143-155.
- Zhu, X., Y. Zeng and M. A. Lehrman (1992). Evidence That the Hamster Tunicamycin Resistance Gene Encodes UDP-GlcNAc:Dolichol Phosphate N-Acetylglucosamine-1-phosphate Transferase. The Journal of Biological Chemistry, **267**: 8895-8902.
- Zupke, C. and G. Stephanopoulos (1995). Intracellular Flux Analysis in Hybridomas Using Mass Balances and In Vitro ^{13}C NMR. Biotechnology and Bioengineering, **45**: 292-303.

THESIS PROCESSING SLIP

FIXED FIELD: ill. _____ name _____

index _____ biblio _____

► COPIES: Archives Aero Dewey Eng Hum
Lindgren Music Rotch Science

TITLE VARIES ► _____

NAME VARIES: ► Bartell

IMPRINT: (COPYRIGHT) _____

► COLLATION: 236p

► ADD. DEGREE: _____ ► DEPT.: _____

SUPERVISORS: _____

NOTES:

cat'r: _____ date: _____

► DEPT: Chem Eng page: N177
► YEAR: 1998 ► DEGREE: Ph.D.
► NAME: NYBERG, Gregg B.